# THE *STAPHYLOCOCCUS AUREUS* REDOXOME: CHARACTERIZATION OF ENZYMES INVOLVED IN OXIDATIVE STRESS RESISTANCE AND SURVIVAL

**Blake Howard Balcomb**

Dissertation presented for the degree of Doctor of
Philosophy (Biochemistry) in the
Faculty of Natural Sciences at
Stellenbosch University

Supervisor: Prof. Erick Strauss

December 2019

# Declaration

By submitting this dissertation electronically, I declare that the entirety of the work contained therein is my own, original work, that I am the sole author thereof (save to the extent explicitly otherwise stated), that reproduction and publication thereof by Stellenbosch University will not infringe any third party rights and that I have not previously in its entirety or in part submitted it for obtaining any qualification.

December 2019

# Abstract

The prevalence of antibiotic resistance is increasing at an alarming rate in South Africa, as well as globally. In particular, multi-drug resistant pathogens such as *Staphylococcus aureus* (MRSA) are a significant health concern, as these are responsible for the majority of hospital- and community-acquired infections. The human innate immune system is the first line of defense against such pathogens. An important component of these defenses is the chemical attacks lodged by various white blood cells; these attacks include the release of oxidising reagents such as hydrogen peroxide ($H_2O_2$) and hypochlorous acid (HOCl), the latter also being the active component of domestic bleach. In order to protect itself against these attacks *S. aureus* uses a network of redox enzymes and low molecular weight (LMW) thiols, many of which have been shown to play crucial roles in defending against reactive oxygen species. However, the manner in which the effects of HOCl is counteracted is not as well understood. This project set out to characterize enzymes of unknown function that appear to be involved in oxidative stress resistance. In addition, the mechanism by which selected LMW thiols protect a key metabolic enzyme in *S. aureus* from oxidative damage was also investigated.

The results of the study uncover for the first time the activity of a previously uncharacterized enzyme that is conserved in several pathogenic bacteria, and identify it as a key actor in *S. aureus*'s defence mechanisms against HOCl, as well as the reactive chlorine species that form in the human body when it is released by neutrophils. Furthermore, a small collection of compounds were synthesized and examined as potential mechanism-based inhibitors of this enzyme. Considering the enzyme's importance as a bacterial defense mechanism at the human-microbe interface, this discovery provides an exciting opportunity for novel drug development focused on the host-pathogen interaction.

The results of this study also demonstrate for the first time the moonlighting role of coenzyme A (CoA) — usually a central metabolic cofactor — in protecting enzymes under oxidative stress conditions. In addition, a novel function of *S. aureus* CoA disulfide reductase was proposed. Finally, the mechanism whereby the LMW thiol bacillithiol is recycled in *S. aureus* was also explored.

Taken together, the results of this study demonstrate the importance of understanding basic molecular mechanisms at the host-pathogen interface that may provide new insight and avenues for novel drug development.

# Opsomming

Die voorkoms van antibiotiese weerstandbiedendheid in Suid-Afrika, sowel as wêreldwyd, styg teen 'n kommerwekkende tempo. In die besonder, multi-dwelm weerstandbiedende patogene soos *Staphylococcus aureus* (MRSA) is 'n belangrike gesondheidsorg, aangesien dit verantwoordelik is vir die meeste hospitaal- en gemeenskapverworwe infeksies. Die menslike aangebore immuunstelsel is die eerste lyn van verdediging teen sulke patogene. 'N Belangrike komponent van hierdie verdediging is die gebruik van chemiese aanvalle deur verskeie witbloedselle; hierdie aanvalle sluit in die vrystelling van oksideermiddels soos waterstofperoksied ($H_2O_2$) en hipochloorsuur (HOCl), die aktiewe komponent van huishoudelike bleikmiddel. Ten einde homself te beskerm teen hierdie aanvalle, produseer *S. aureus* 'n netwerk van ensieme en lae molekulêre gewig (LMW) thiols, waarvan baie gewys word om belangrike rol te speel in die verdediging van reaktiewe suurstofspesies. Die manier waarop HOCl verset word, is egter nie so goed verstaan nie. Hierdie projek het betrekking op ensieme van onbekende funksie wat blykbaar by oksidatiewe stresweerstand betrokke is. Daarbenewens is die meganisme waardeur geselekteerde LMW-tiole 'n belangrike metaboliese ensiem *S. aureus* van oksidatiewe skade beskerm, ook ondersoek.

Die resultate van die studie onthul vir die eerste keer die aktiwiteit van 'n voorheen ongekarakteriseerde ensiem wat in verskeie patogene bakterieë bewaar word, en identifiseer dit as 'n sleutelaktor in *S. aureus* se verdedigingsmeganismes teen HOCl en die reaktiewe chloorspesies wat in die menslike liggaam vorm wanneer dit deur neutrofiele vrygestel word. Verder is 'n klein versameling verbindings gesintetiseer en ondersoek as potensiële meganisme gebaseerde inhibeerders. Met inagneming van die belangrikheid van hierdie ensiem as 'n bakteriese verdedigingsmeganisme by die mens-mikrobe-koppelvlak, bied dit 'n opwindende geleentheid vir nuwe geneesmiddelontwikkeling, sowel as die vergroting van die begrip van hoe HOCl en reaktiewe chloorspesies moontlik in *S. aureus* verwerk kan word.

Die resultate van hierdie studie toon ook vir die eerste keer die maanliggingsrol van koënsiem A (CoA) — gewoonlik 'n sentrale metaboliese kofaktor — in die beskerming van ensieme onder oksidatiewe stres toestande. Daarbenewens is 'n nuwe funksie van *S. aureus* CoA disulfide reduktase voorgestel.

Ten slotte word die meganisme waarvolgens die LMW-thiolbacillithiol herwin word, *S. aureus* ondersoek. Saam met mekaar, die resultate van hierdie studie demonstreer die

belangrikheid van die verstaan van basiese molekulêre meganismes by die gasheer-patogeen koppelvlak wat nuwe insig en weë vir nuwe geneesmiddelontwikkeling kan bied.

# Acknowledgements

The mammoth task of completing a PhD study is no easy feat and I could not have done it without the support of a number of people along the way. First and foremost, I would like to thank my supervisor Prof. Erick Strauss. Erick, thank you for taking a chance on me and allowing me to join your lab. I truly appreciate your continuous guidance, patience and support over the past three years. Thank you for allowing me to take on a challenging project that certainly contributed towards my growth as a scientist as well as a person. I am also grateful for your commitment and devotion in helping your students' to persevere and succeed. I also enjoyed learning from your chemistry based thought process in approaching biological questions.

I would also like to thank Dr Marianne De Villiers for her supportive comments and encouragement during my studies. I truly appreciate all the realistic advice you gave me during the writing process.

To our lab manager, Dr Helba Bredell – you are truly an asset to the lab. Thank you for ensuring that the daily operations of the lab and instruments ran smoothly. I am grateful for our coffee chats as well as the genuine care you show for students and of course your sense of humor.

To all the Strauss-lab members, past and present, thank you for all the support and encouragement along the way. It was a pleasure to work alongside you all. In particular, my thanks go to Konrad – it was a pleasure being your lab bench neighbor over the past few years. I would also like to thank Deon for all his help and expertise relating to the microbiology experiments done in this study.

To all my friends and family, thank you for your support, encouragement and interest in my scientific endeavors. Lastly, I want to thank Jaco for his love, support and for putting up with me during these past few years – especially during the writing of my dissertation!

# Additional Acknowledgements


- Stellenbosch University and the Department of Biochemistry for creating a wonderful environment in which to study.
- Financial assistance from the Wilhelm Frank Scholarship and Prof. Erick Strauss.
- Dr. D.J. Brand and Ms. E. Malherbe of the NMR-unit of the Central Analytical Facility of Stellenbosch University.
- Dr. Maré Vlok of the MS Unit (Proteomics laboratory) of the Central Analytical Facility of Stellenbosch University.

# Table of Contents

# Abbreviations

| | |
|---|---|
| ABTS | 2,2'-azino-bis |
| Ahp | Alkylhydroperoxide |
| AHR | Alkyl hydroperoxide reductase |
| ADR | Adrenodoxin reductase |
| AHR | Alkylhydroperoxide reductase |
| Brx | Bacilliredoxin |
| BSH | Bacillithiol |
| BSSB | Bacillithiol disulfide (oxidised BSH) |
| CD | Circular dichroism |
| CFU | Colony forming units |
| CoA | Coenzyme A |
| $(CoAS)_2$ | CoA disulfide (oxidised CoA) |
| CoADR | CoA disulfide reductase |
| Cys | Cysteine |
| DCR | 2,4-dienoyl CoA reductase |
| DCM | Dichloromethane |
| DHLA | Dihydrolipoic acid/ dihydrolipoamide |
| DMF | *N*,*N*-Dimethylformamide |
| DMSO | Dimethyl sulfoxide |
| DSR | Disulfide reductase |
| DTNB | 5,5-Dithiobis-(2-nitrobenzoic acid) |
| DTT | Dithiothreitol |
| Ec | *Escherichia coli* (also *E.coli*) |
| Enz | Enzyme |
| ESH | Ergothioneine |
| Eox | Enzyme (oxidized) |
| FAD | Flavin adenine dinucleotide |
| $FADH_2$ | Flavin adenine dinucleotide (reduced) |
| FDR | Flavoprotein disulfide reductases |
| GAPDH | Glyceraldehyde-3-phosphate dehydrogenase |

| | |
|---|---|
| GMS | Glutamate synthase |
| Gpx | Glutathione peroxidase |
| GR | Glutathione reductase (also Gor) |
| Grx | Glutaredoxin |
| GSH | Glutathione |
| GSSG | Glutathione disulfide |
| GST | Glutathione-S-transferase |
| Hmp | Flavohemoglobin |
| HRP | Horseradish peroxidase |
| IMAC | Immobilized Metal Affinity Chromatography |
| IOA | Iodacetamide |
| IPTG | Isopropyl β-D-1-thiogalactopyranoside |
| KatA | Catalase |
| kDa | Kilodalton |
| LB | Luria Bertani |
| LipDH | Lipoamide dehydrogenase (Also LPD or LipA) |
| LMW | Low molecular weight thiol |
| MAL | Malate |
| MerA | Mercuric ion reductase |
| MOX | Monooxygenase |
| MPOs | myeloperoxidases |
| MRSA | Methicillin resistant *Staphylococcus aureus* |
| MSH | Mycothiol |
| MTBE | Methyl tertiary-butyl ether |
| MW | Molecular weight |
| NADH | Nicotinamide adenine dinucleotide (reduced) |
| NADPH | Nicotinamide adenine dinucleotide phosphate (reduced) |
| NCT | N-chlorotaurine |
| NDCT | *N*,*N*-dichlorotaurine |
| NDH | NADH dehydrogenase |
| NEM | N-Ethylmaleimide |

| | |
|---|---|
| NFR | NADH ferredoxin reductase |
| NMR | Nuclear Magnetic Resonance Spectroscopy |
| NO● | Nitric oxide radical |
| $NO^{3-}$ | Peroxynitrite |
| NOX | NADPH-dependent oxidase |
| $O_2^-$ | Superoxide |
| OD | Optical density |
| OH● | Hydroxyl radical |
| OSH | Ovothiol |
| Pa | *Pseudomonas aeruginosa* |
| PBS | Phosphate buffered saline |
| PCR | Polymerase chain reaction |
| PMNs | Polymorphonuclear leukocytes |
| POR | NADH peroxidase/oxidase and CoA-disulfide reductase |
| Prx | Peroxiredoxin |
| QRSA | Quinolone resistant *Staphylococcus aureus* |
| ROS | Reactive oxygen species |
| RCS | Reactive chlorine species |
| RNS | Reactive nitrogen species |
| RNR | Ribonucleotide reductase |
| Sa | *Staphylococcus aureus* (also *S.aureus*) |
| SDS PAGE | Sodium dodecyl sulphate polyacrylamide gel electrophoresis |
| SOD | Superoxide dismutase |
| SOH | Sulfenic acid |
| $SO_2H$ | Sulfinic acid |
| $SO_3H$ | Sulfonic acid |
| tDBDF | Two- dinucleotide binding domains flavoprotein |
| TFP | Thioredoxin fold protein |
| TR | Trypanothione reductase |
| $T(SH)_2$ | Trypanothione |
| Trx | Thioredoxin (also TrxA) |

| | |
|---|---|
| TrxR | Thioredoxin Reductase |
| TLC | Thin Layer Chromatography |
| TRIS | Tris (hydroxymethyl)aminomethane |
| VRSA | Vancomycin resistant *Staphylococcus aureus* |
| WT | Wild-type |

*Chapter 1*

# INTRODUCTION

## 1.1 Antimicrobial resistance – A global health concern

One of the most pressing medical problems facing mankind is the exponential rise of antimicrobial resistant organisms and the lack of novel classes of antibiotics. Since the first discovery of the "wonder drug" penicillin in the 1940's, antibiotics have proven to be very useful in saving many lives. Figure 1.1 shows antibiotic discovery and the emergence of antibiotic resistance over the past few decades.

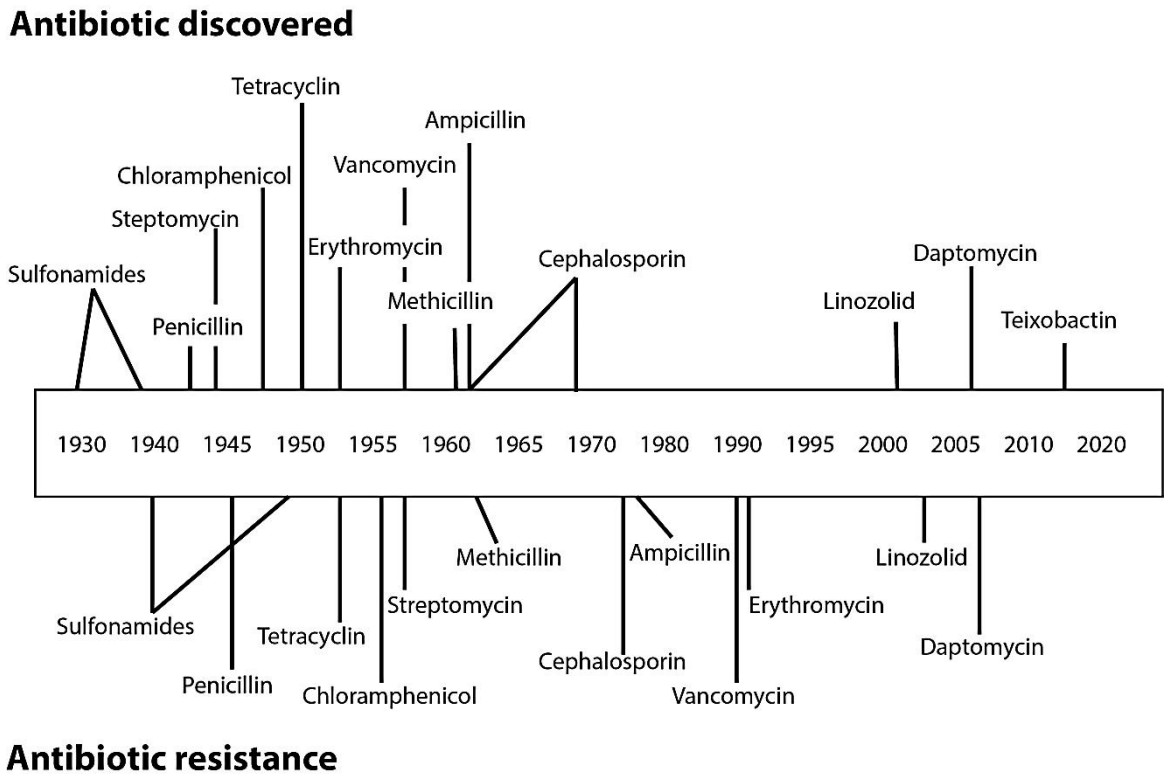


**Figure 1.1 Timeline of antibiotic discovery and resistance. Redrawn and adapted from [1, 2].**

According to the *WHO 2014 AMR Global Report on Surveillance*, the BRICS (Brazil, Russia, India, China and South Africa) countries have seen the greatest rise in occurrence of antimicrobial resistance. In addition, it is predicted that by the year 2050 the major cause of human deaths globally will be due to antimicrobial resistant pathogens [3].

One of the leading factors contributing to antibiotic resistance is the inappropriate use of antibiotics in both human disease and in agricultural practices. Furthermore the lack of regulation or proper control of antibiotic usage in many countries is also a global concern [4].

Antibiotics either kill or stop a pathogen's growth. However, some bacteria develop the ability to survive exposure to antibiotics [5-8]. The known molecular mechanisms that allow survival include reducing cell membrane permeability to antibiotics, chemical/structural changes of drug targets, antibiotic efflux and inactivation [9, 10]. Broadly speaking, the major classes of antibiotics primarily target bacterial protein synthesis, cell wall biosynthesis, DNA/RNA replication and folate related pathways [8, 11]. Over the past 50 years, despite the development of new antibiotics through chemically modified derivatives of existing scaffolds, inevitably antibiotic resistance towards these next generation antibiotics still occurs [12, 13]. Furthermore, many pharmaceutical companies have abandoned their research and development into antibiotics mainly due to the low returns when compared to chronic medications or lifestyle drugs [1, 14, 15]. In the past 10 years, less than 10 new antibiotics have been FDA approved against the difficult to treat human pathogens also known as the "ESKAPE" pathogens (*Enterococcus faecium*, *Staphylococcus aureus*, *Klebsiella pneumoniae*, *Acinetobacter baumannii*, *Pseudomonas aeruginosa*, and *Enterobacter* species). Many of these antibiotics are in fact not new classes of antibiotics and target existing bacterial target components [12, 16-22].

Although efforts have been made in developing "new" antibiotics there is an urgent need to identify novel molecular targets in the development of new classes of antibiotics. In particular, understanding bacterial defense mechanisms at the human-microbe interface may provide unique insight and opportunity for novel drug development. An example of an attractive treatment option that takes advantage of the interplay between the human host and the bacterial pathogen entails either augmenting the host's own immune response, or compromising the pathogen's defenses against the human immune system to such an extent that the infection is cleared by the host.

It is within this context that current study finds its main aim and objectives. First, it focusses on a conserved enzyme which has been shown to be upregulated in the important human pathogen *S. aureus* when it is challenged with neutrophils, one of the white blood cells that is crucial to the innate immune response. However, the function of the enzyme remains unknown, and its potential for being exploited for the treatment of bacterial infections remain unexplored. Second, the study explores the mechanisms by which low molecular weight (LMW) thiols are recycled in *S. aureus* as it fends of the oxidative stress that result from the

attack by the innate immune system. LMW thiols form a crucial part of the bacterial defense mechanisms against oxidative stress, but must be efficiently recycled to remain effective. Currently, our understanding of how this is achieved in *S. aureus* remains limited.

To provide a broader context for this study, the remainder of this introductory chapter focusses on the host-pathogen interface with particular focus on the mechanisms by which the consequences of oxidative stress are averted and neutralized.

## 1.2 The human pathogen *S. aureus* and antistaphylococcal agents

Described as the “Killer Bug” by Fortune and Time Magazines, *S. aureus* is perhaps one of the most dangerous human pathogens of our time [23, 24]. In addition to the emergence of multi-drug resistance strains, the high prevalence and spread of *S. aureus* is attributed to the fact that 30% of the global population are asymptomatic carriers of the organism [25]. *S. aureus* is also notorious for its ability to adapt to changes in environmental condition [26]. It is now the leading cause of hospital- and community-acquired infections — a particularly alarming situation in developing countries where poor sanitation, overpopulated towns and comorbidities with viral infections (AIDS and/or SARS) is rife [27, 28].

*S. aureus* is a Gram-positive organism that forms part of the *Micrococcaceae* family. It is the cause of “minor” skin infections, as well as more serious life-threatening infections causing septicemia and pneumonia. It is visually unique from many others in the *Micrococcaceae* family due to the presence of the pigment staphyloxanthin that imparts the characteristic gold hue in colony formation [26, 29-31]. Under the microscope in Gram’s stain, they appear as clusters of micrococci.

Currently a meagre 10% of *S. aureus* strains remain susceptible to penicillin while many other isolates show increasing resistance to methicillin, vancomycin, and quinolones [32]. The current treatment strategies include the mono- or mixed- use of β-lactams, rifampins, glycopeptides & glycosides, -cyclines, fluoroquinolones and the fairly newer classes such as oxazolidinones, streptogramins, current generation lipopeptides, glycopeptides, sulfonamides and cephalosporins [7, 11, 33, 34]. These classes of antibiotics and their general mechanism of action towards *S. aureus* are shown in Table 1.

**Table 1: General antibiotic classification and mechanism**

| Antibiotic Class | Mechanism of Action / Target |
|---|---|
| β-lactams | Cell wall - Disruption of peptidoglycan synthesis |
| Fluoroquinolones | DNA replication – DNA gyrase |
| Glycopeptides | Cell wall - Disruption of peptidoglycan synthesis |
| Glycosides | Protein synthesis |
| Lipopeptides | Cell membrane depolarization |
| Oxazolidinones | Protein synthesis |
| Rifampin | RNA polymerase |
| Sulfonamides | Folate synthesis |
| Cyclines | Protein synthesis |

Many bacteria, including *S. aureus*, rely on a number of mechanisms to counteract the effect of antibiotics upon treatment. These mechanisms include: acquisition of resistance genes, genomic mutations rendering altered or inactive protein targets, production of enzymes that either alter specific chemical groups on the antibiotic to prevent binding of the target, or which destroy it completely, mutations on specific enzyme targets abolishing antibiotic binding, bypass of the target through overproduction of enzymes that overwhelm antibiotic binding, changes in cell wall composition and increased permeability and efflux of antibiotics [32, 35].

Resistant *S. aureus* strains that have appeared more regularly in the clinical and community-acquired setting are quinolone-, methicillin- and vancomycin-resistant *S. aureus* (QRSA, MRSA and VRSA, respectively). Quinolones bind to DNA gyrase inhibiting further DNA replication. With *S. aureus*, quinolone resistance occurs through point mutations in *grlA*, the gene encoding the GyrA subunit of the gyrase, thereby preventing the binding of quinolones. *S. aureus* also upregulates NorA which is a known multidrug efflux pump [36, 37]. Methicillin and vancomycin were once treatments of last resort, but are now becoming the norm to combat resistant strains. With MRSA, the organism has acquired the *mecA* gene through horizontal gene transfer which encodes for penicillin binding protein 2a (PBP2a) which is different to other PBP's and hence can continue to synthesize peptidoglycan in the presence

of antibiotics [7]. VRSA on the other hand occasionally has the *mecA* gene but also has acquired a transposon encoding the vancomycin resistance gene *vanA*. The *vanA* gene originated from vancomycin-resistant *Enterococci* which have been shown to transfer this to *S. aureus*. The characteristics of VRSA is the over-thickening of the cell wall and hence reducing permeability of many antibiotics, including vancomycin [38].

It is these types of resistant mechanisms that allow *S. aureus* to persist even when challenged with antimicrobial treatment, and has made many common antibiotics ineffective.

## 1.3 It takes two to tango - the immune system & *Staphylococcus aureus*

### 1.3.1 The immune response

Although mankind has discovered and developed many useful compounds in an attempt to treat bacterial infections, the human body has its own natural way of defending against infections – the immune system.

The immune system is the primary host defense mechanism that is activated upon encountering pathogens. The immune system can be divided into the quick acting innate immune response and the slower developed adaptive immune response [39, 40]. When *S. aureus* invades the host cells the first line of defense is the innate immune response, which specifically entails the recruitment of polymorphonuclear leukocytes (PMNs), also known as neutrophils. This highly specialized type of white blood cell accounts for the majority of white blood cells circulating in the blood. It is these neutrophils that are adapted to quickly detect and engulf (phagocytose) pathogens such as *S. aureus* (Figure 1.2).

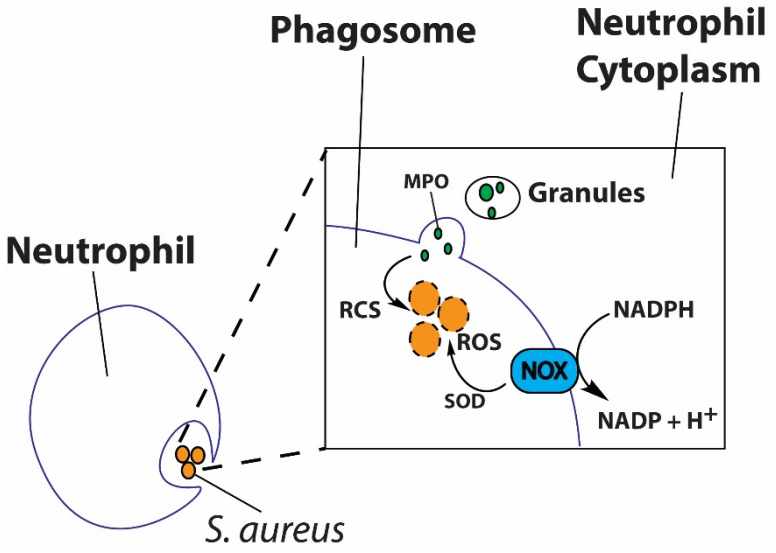


**Figure 1.2 Phagocytosis and enveloping of S. aureus into the phagolysosome vesicle. This is followed by the oxidative burst involving the formation of major reactive oxygen species (ROS), namely superoxide and hydrogen peroxide by neutrophils' membrane-bound NADPH-dependent oxidase (NOX) and superoxide dismutase (SOD) respectively. Further oxidation is provided by myeloperoxidase-containing granules that oxidise chloride ions to form reactive chlorine species (RCI), the major component being HOCl which is released into the phagolysosome. Image adapted and redrawn from [41].**

The engulfed bacteria are then retained in a phagosome, a vesicle which fuses with cytoplasmic granules to form a protected destructive compartment called a phagolysosome [40, 42, 43]. There are four types of granule vesicles that together contain myeloperoxidases, antibiotic proteins, proteases, NADPH-dependent oxidases and other signaling molecules that modulate the immune response. In addition to granules, it has been shown through studies involving *S. aureus* that the neutrophil produces interesting chromatin-based structures called neutrophil extracellular traps (NETs) which play a role in bacterial entrapment and neutrophil killing mechanisms in a wide range of engulfed pathogens [41, 44].

The formation of the phagolysosome initiates the first step in neutrophil killing mechanisms, namely the oxidative burst (respiratory burst). This is followed by a series of non-oxidative killing mechanisms.

### 1.3.2 Neutrophil killing mechanism - the oxidative burst

The respiratory burst starts with the multicomponent membrane-bound NADPH oxidase (NOX). Although there are a number of forms of NOX, NOX-1/2 appears the most crucial in producing the variety of oxidants in the phagolysosome [41]. The importance of NOX in the host defense mechanism is clearly evident in Chronic Granulomatous Disease patients

whose ability to clear common infections is severely impaired due to multiple mutations in the enzyme [45].

NOX is the major initiator of reactive intermediates that together constitute the oxidative burst produced by the neutrophil. As shown in Figure 1.3, NOX-2 catalyzes one one-electron reduction of oxygen to form reactive species such as superoxide anion ($O_2^{\bullet -}$). Finally the dismutation of superoxide results in the formation of $H_2O_2$ which constitutes the major oxidative species produced by these cells.

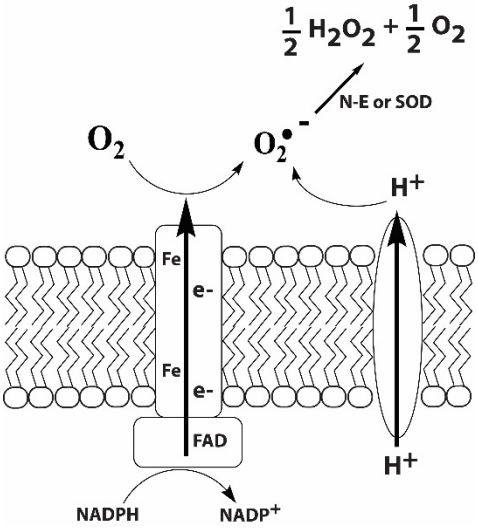


**Figure 1.3 Membrane associated NOX showing the generation of oxygen radicals and ultimately $H_2O_2$. The NOX-2 catalyzed reduction of oxygen results in the formation of superoxide which inturn dismutates either non-enzymatically (N-E) or via the action of SOD to ultimately form $H_2O_2$. Adapted and redrawn from [41].**

From activated (Flavin adenosine dinucleotide-containing) NOX-1/2, these reactive species pass into the phagolysosome which then react with the heme-containing protein myeloperoxidase (MPOs). MPOs are relatively abundant, accounting for 25% of the protein in the phagolysosome [46]. MPO's are able to form a number of complex intermediates (I-III) which allows the oxidation of a variety of biological substrates and perform a number of different radical and non-radical reactions. The reactions of MPOs include the oxidation of chloride, organic substrates (using $H_2O_2$) and superoxide formation [41, 42, 47-49]. However the major product of MPO-catalyzed reactions is the formation of HOCl (hypochlorous acid). This is not unexpected considering that the amount of chloride in the neutrophil is in the mM range [50-54]. Although there are also other halogens such as bromide and thiocyanate ions in the neutrophil that may form HOBr or HOSCN respectively, they are minor components when compared to chloride ions [41, 55].

The HOCl formed in this manner is an extremely strong oxidant and reacts with nearly all compounds within its proximity in some manner. It is a very short-lived oxidant, is membrane-permeable and predominantly targets the sulphur atoms of cysteine, methionine and the amino functional groups of amino acids and nucleotides [41, 56, 57].

Another oxidant product of the neutrophil is nitric oxide (NO) and its derivative peroxynitrite (formed from the reaction of nitric oxide with superoxide). The formation of the NO and peroxynitrite are plausible reactive nitrogen species (RNS) that have been implicated in a number of disease states, signaling pathways, cardiovascular system and inflammation [58]. The formation of RNS is also complicated by the fact that they can also occur in consort with the NOX system [58]. Out of the many RNS, peroxynitrite is shown to have strong oxidant and antimicrobial properties. The potential antimicrobial effects of peroxynitrite and NO range from reactions with metalloproteins [59], bacterial respiration [60, 61], inactivation of ribonucleotide reductase [62], nitration of tyrosine and DNA damage [63, 64]. In the last decade there is growing evidence that the formation of RNS appears to play a more prominent role in antimicrobial defense, whether alone or in combination with ROS, than previously thought.

### 1.3.3 Non-oxidative neutrophil killing mechanisms

Other than the abovementioned oxidative killing mechanisms, the non-oxidative killing mechanisms executed by neutrophils depend mainly on the effects exerted by released small peptides and larger proteins. These include short antimicrobial peptides, proteases, defensins, cathelicidines, collagenases, gelatinases, lysozymes and lactoferrins [42, 48, 65-67]. These biomolecules are known to elicit longer acting effects when compared to the short-lived quick reacting oxidants produced by NOX and MPOs [41, 48]. As the molecular targets and consequences of non-oxidative killing mechanisms are not the focus of this study they will not be discussed further here.

### 1.3.4 Neutrophil-derived oxidants – $H_2O_2$ and HOCl

In the context of neutrophils killing the bacterial pathogens that they have engulfed, it is clear that $H_2O_2$ and ultimately HOCl are crucial in antimicrobial defense. Both HOCl and $H_2O_2$ are shown to pass through the bacterial cell membrane. The targets of $H_2O_2$ and/or superoxide include oxidation of Fe-S clusters that would generate radical species via Fenton/Haber-Weiss chemistry (Figure 1.4) and in turn ultimately cause damage to bacterial DNA as well as intracellular proteins [41, 48, 68-70].

**Haber-Weiss Reaction**

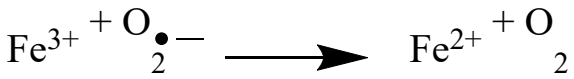


**Fenton Reaction**


**Figure 1.4 Oxidation of $Fe^{3+}/Fe^{2+}$ via Haber-Weiss/Fenton reactions [70].**

HOCl is known to chlorinate bacterial proteins, specifically causing side chain oxidation and protein unfolding [71-75]. Moreover, Fe-S clusters are also vulnerable to HOCl-mediated oxidation [71, 76]. However, due to its unstable nature and reactivity towards molecules in the immediate vicinity (such as cysteine, methionine and amines), it is unlikely that all the HOCl produced by the neutrophil will enter into the bacterium. It is more likely that HOCl would react with molecules on the bacterial outer membrane leaflet, or with compounds in the phagolysosome. The products of these secondary reactions would then enter the bacterium to elicit their combined antibacterial effects in the cytoplasm [41].

While HOCl has significant antibacterial activity as outlined above, it has also been shown to have negative impacts on the neutrophil itself. It has been shown in a number of studies that amino acids within the phagolysosome as well as components of the phagolysosome membrane itself are chlorinated by HOCl, supporting the notion that it reacts with molecules in its immediate surroundings [41, 67, 77, 78]. While self-chlorination may seem counterproductive (and possibly even detrimental) to the neutrophil, it appears that some chlorination of phagolysosomal components may result in the formation of signaling molecules that modulate the immune response as well as the overall fate of the neutrophil [51, 52].

### 1.3.5 HOCl and protein damage

There are a number of molecules with thiol groups present within the neutrophil as well as the engulfed pathogen that may react with HOCl. These include low molecular weight (LMW) thiols as well as cysteine and amine functional groups on proteins. Depending on the extent of thiol oxidization, it may be a reversible or irreversible process [49, 55, 79]. When oxidized to form sulfenyl chlorides, Cys residue can react with amines to form sulfonamides (Figure

1.5A). The sulfenyl chlorides may also react with LMW thiols either directly, or after having undergone hydrolysis to form sulfenic acids. This leads to intra- or inter molecular disulfide formation. The sulfenic acids can be oxidized further to sulfinic acids and finally sulfonic acids, the last step being irreversible (green boxed species).

Met residues can also undergo oxidation to sulfoxides or sulfones (Figure 1.5B). There is also evidence that HOCl oxidizes N-terminal methionine residues to irreversibly form dehydromethionine [80-82]. HOCl can also react with amines to form chloramines (Figure 1.5 C). The chloramines of α-amino acid are unstable and decompose to form aldehydes and ammonia which are also able to react with cellular components such as Fe-S clusters [56, 71, 83-88]. However, the chloramines of β-amino acids are much more stable, and these can mediate oxidative effects of their own as described below.

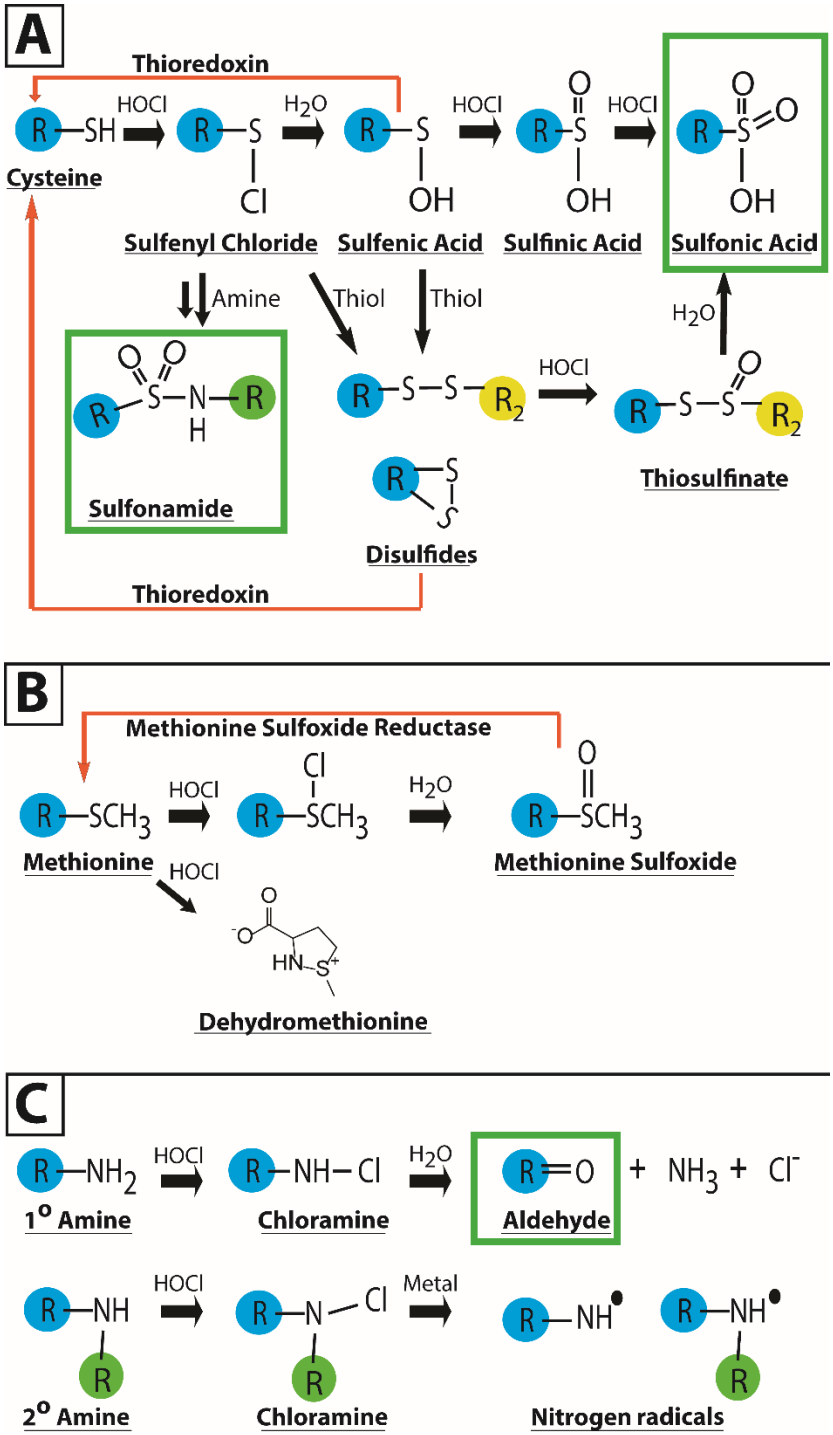


**Figure 1.5 Reactions of thiols and amines with HOCl. (A) Thiols are oxidized to varying degrees by HOCl. The formation of sulfonamides and sulfonic acids are irreversible (Green boxed species). Protein disulfides are regenerated by thioredoxin/thioredoxin reductase system (B) The oxidation of methionine predominantly results in the formation of methionine sulfoxide which can be repaired by methionine sulfoxide reductase. (C) The oxidation of amines results in the formation of chloramines. Amino acid generated chloramines are particularly unstable and degrade to form aldehydes [71].**

### 1.3.6 The role of taurine and its chloramine

In the context of the neutrophil environment, amino functional groups are far more abundant than cysteines or methionines [41]. One of the major amine-containing targets of HOCl is taurine, an abundant non-proteogenic sulfonated β-amino acid that is found in all types of human cells, with particularly high concentrations up to 20–50 mM being found in leukocytes such as neutrophils and eosinophils [89-94]. The physiological functions (both speculative and experimentally determined) of taurine include involvement in osmoregulation, calcium modulation, phospholipid and protein interactions, bile conjugation, antioxidant properties, inflammation and modulation of the immune response and signaling molecules [92, 95].

When HOCl reacts with taurine it forms a stable (compared to other chloramines) reactive chlorine species (RCS), *N*-chlorotaurine (NCT) (Figure 1.6).

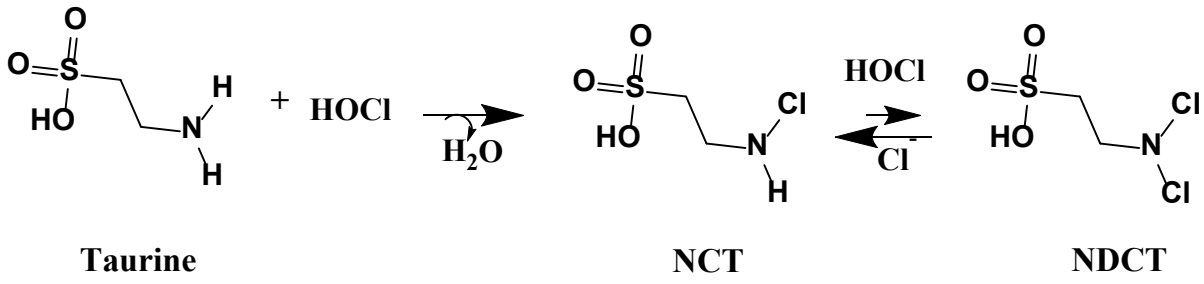


**Figure 1.6 Reaction of taurine with HOCl. NCT is the predominant product however a small amount of NCT can undergo further chlorination to form *N,N*-dichlorotaurine (NDCT). NDCT is unstable and quickly reverts back to NCT [96].**

NCT has been shown to have antimicrobial activity against a number of different pathogens [96-140]. NCT can react with thiols, amino acids and ascorbate but not amides nor alcohols [41, 71, 126]. Its antibacterial mode of action is proposed to act via the chlorination of components of energy metabolism, over-oxidation and chlorination of sensitive protein-based thiols, DNA damage and cell membrane disruption (ammonia chloramine) [41, 56, 57]. NCT also reacts with a number of neutrophil components (cytokines, chemokines, prostaglandin, tumor necrosis factor alpha, nitric oxide, interleukins, and collagenase) that downregulate the pro-inflammatory response [141-150].

In addition to mono-chlorinated taurine, a small amount of unstable di-chloro taurine species (NDCT) can also form [92] (Figure 1.6).

## 1.4 Mechanisms by which *S. aureus* directly counteract ROS and RCS

In light of the arsenal of ROS and RCS produced in the neutrophil, bacteria have developed a number of ways to resist and counteract the effects of oxidative stress. Figure 1.7 provides a graphical overview of mechanisms by which *S. aureus* avoids and neutralizes host-generated oxidative species, and counteracts their effects. The mechanisms are described in more detail in the following subsections.

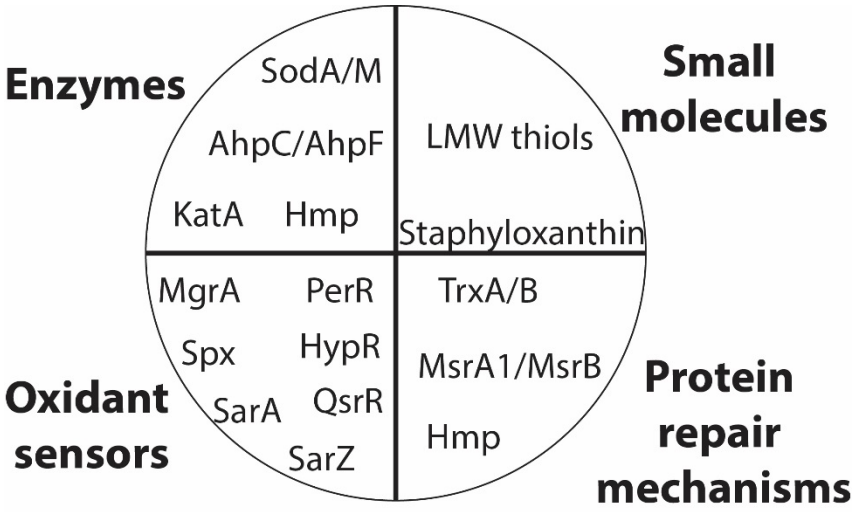


**Figure 1.7 Mechanisms by which *S. aureus* protections itself against oxidative damage from the oxidative burst.**

### 1.4.1 Direct elimination of ROS

In response to oxidative stress, *S. aureus* produces a number of enzymes that act directly on ROS. The first of these are two superoxide dismutases (SODs), SodA and SodM, which convert superoxide to $H_2O_2$ and $O_2$ (Figure 1.8) with the help of a manganese cofactor [151-155]. SodM and SodA not only protect *S. aureus* from superoxide damage but also prevent the indirect formation of hydroxyl radicals via $Fe^{3+}$-dependent Haber-Weiss reactions [156]. Superoxide is impermeable to most membranes and thus both SodA and SodM are present as extracellular membrane-bound or secreted proteins. The expression of SOD increases dramatically upon neutrophil phagocytosis (regardless of increase in $H_2O_2$ production) as well as during biofilm formation [157, 158]. The presence of SOD makes *S. aureus* more

resistant to oxidative stress, and when it is deleted or inactivated its pathogenicity and ability to colonize epidermal cells is decreased [151, 153, 159, 160].

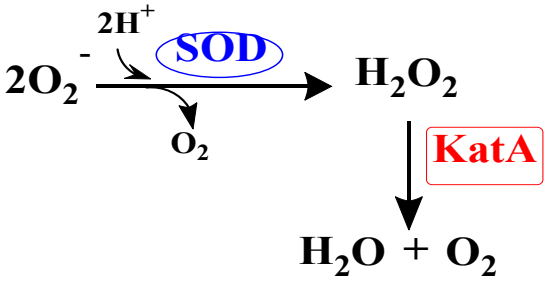


**Figure 1.8 Reactions involving superoxide dismutase (SOD) and catalase (KatA).**

The $H_2O_2$ resulting from SOD catalysis—if not removed—will result in further oxidative damage towards *S. aureus*. Thus KatA, a heme-containing catalase, is expressed that converts $H_2O_2$ to $H_2O$ and $O_2$ (Figure 1.8) [152, 161]. The reaction mechanism of KatA is a two-step reaction that involves the formation of an oxyferryl species which further combines with a second $H_2O_2$ molecule to generate $H_2O$ and $O_2$ [162]. KatA has extremely high tolerance for $H_2O_2$ and is only inactivated at $H_2O_2$ concentrations of ~400–500mM [162]. Like SOD, KatA is highly upregulated during neutrophil phagocytosis and the presence of $H_2O_2$ [152, 163]. Interestingly the inactivation of catalase in *S. aureus* causes increased sensitivity towards $H_2O_2$ only when competing bacteria are present such as streptococci found in nasal cavities [163, 164]. This is most likely due to the finding that alkyl hydroperoxide reductase (AhpC) can compensate for the lack of a KatA. Furthermore AhpC also plays a role in *S. aureus* pathogenesis [152, 164], and functions together with the help of protein partner AhpF, converting $H_2O_2$ to $H_2O$ or organic peroxide molecules to alcohols and $H_2O$ (Figure 1.9) [165].

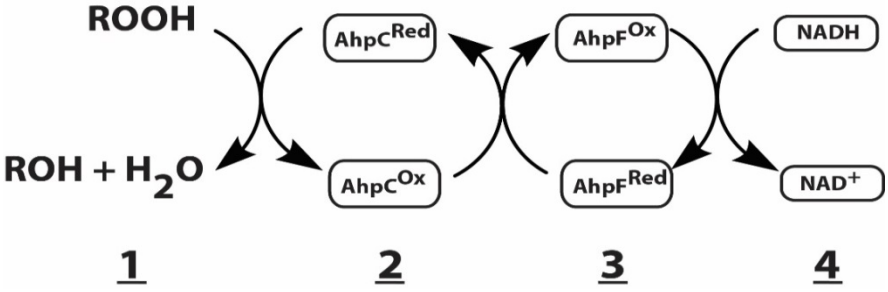


**Figure 1.9 General mechanism of alkyl hydroperoxidase AhpF/C. Organic peroxide molecules (1) are reduced by AhpC (2) which is reduced by FAD dependent AhpF (3,4).**

Unlike SOD or KatA, AhpF and AhpC makes use of cysteine residues as part of their mechanism to render oxidants ($H_2O_2$ or organic peroxide molecules) unreactive. The detailed catalytic mechanism (Figure 1.10) involves AhpF, a flavin adenosine dinucleotide (FAD)-dependent NADH disulfide reductase which reduces the disulfides of peroxiredoxin AhpC. Before AhpF reduces AhpC, a number of steps and domain rotations are involved, the details of which are described in Figure 1.10.

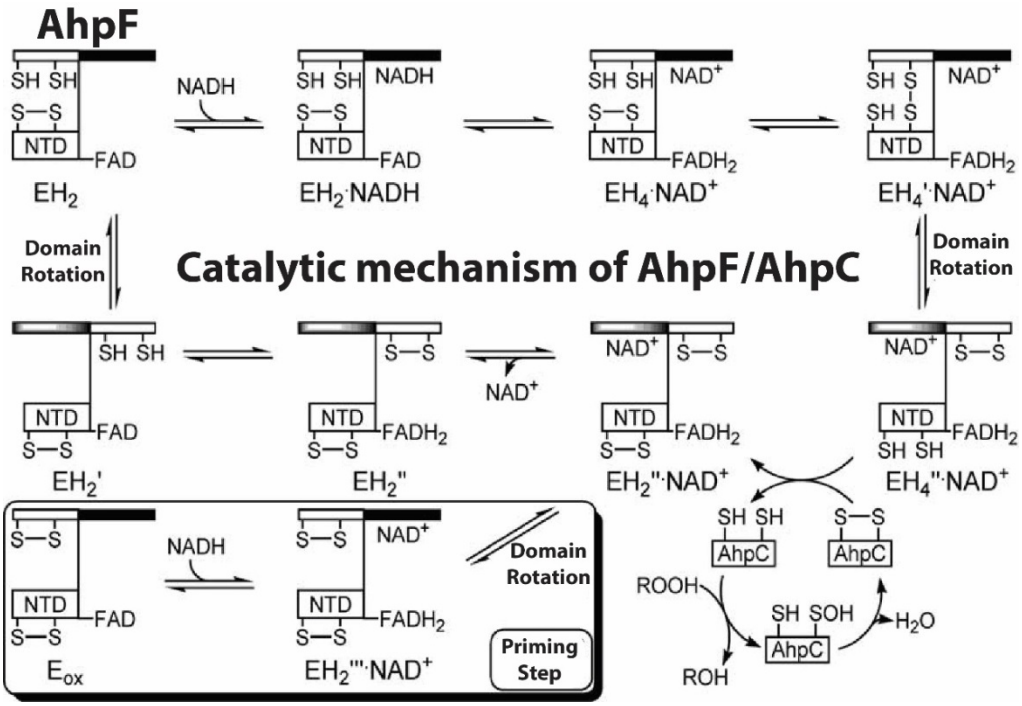


**Figure 1.10 Catalytic cycle of AhpF/AhpC. An initial priming reaction of AhpF initiates the cycle where by NADH reduces FAD followed by a domain rotation. Electrons are then transferred to AhpF C-terminal thiols followed by another domain rotation in the opposite direction. Further reduction of FAD by another round of NADH results in reducing the N-terminal domain (NTD) thiols. The C- and N- terminal domain thiols undergo dithiol-disulfide interchange followed by another domain rotation. This final rotation orientates the NTD thiols for interaction with AhpC which itself reacts with substrate (depicted as ROOH) [166].**

Poole and co-workers have shown in detail that an intrasubunit pathway occurs during the catalytic mechanism, affording the reduction of the appended N-terminal redox-active disulfide containing domain (NTD) of AhpF. This facilitates catalysis towards the incoming AhpC [167-172]. In addition, they also showed for the first time a high resolution view of the thiol-thiolate hydrogen bond which had for some time been speculated to play a role in catalysis, but for which experimental evidence was lacking [167].

Together AhpF/AhpC are up regulated in response to ROS [173]. In *E. coli* AhpFC shows a high degree of protection against oxidative killing by hydroperoxide species [174]. It is not

clear if RCS upregulates AhpF/AhpC or by what mechanism AhpF/AhpC protects *S. aureus* due to RCS-induced stress [71].

Another enzyme involved in ROS detoxification is flavohemoglobin (Hmp). As the name implies, Hmp contains both a heme and FAD cofactor that are involved in the de-oxygenation of NO to form nitrate [175]. Hmp are found in a number of bacteria, including *S. aureus* that are shown to detoxify RNS, ROS ($H_2O_2$) and organic peroxide molecules [175-179].

### 1.4.2 Direct elimination of RCS

The wealth of information that is available on bacterial responses to ROS stands in stark contrast to what is known regarding responses towards RCS. Most of the $H_2O_2$ produced in the neutrophil is used by MPOs to form one of its major products, the potent oxidant HOCl [46, 48, 57, 71-73, 77, 79, 152, 180]. As indicated previously, the primary targets of HOCl include sulfur-containing compounds and amine functional groups that subsequently form reactive aldehydes (Figure 1.5) [48, 71]. As part of their bacterial killing mechanism, HOCl and chloramines have also been shown to react with bacterial cell components such as membranes to form chlorinated lipid species [51, 181]. Specifically phosphatidylethanolamine is targeted in this manner. Moreover, the chlorination of nucleotides of DNA/RNA also occurs widely [182]. In response to HOCl-initiated lipid peroxidation and the formation of reactive aldehydes, bacteria upregulate a number of aldehyde dehydrogenases which are involved in their detoxification [183-189]. If not rendered inactive, the accumulation of aldehydes such as methylglyoxylate cause damage to bacterial cellular proteins, Fe-S clusters and DNA nucleotides [190-192]. To date no mechanism for the removal of HOCl or chloramines has been reported which is likely due to the chemical reactivity of these compounds.

Another mechanism that has shown to be protective against low doses of RCS is the pigment staphyloxanthin [29, 31, 180, 193, 194]. *Winterbourn* and co-workers have investigated the role staphyloxanthin and enterobactin (a siderophore found in Gram-negative bacteria) in the protective effects against exposure to HOCl and chloramines. Overall it was concluded that staphyloxanthin was able to protect some *S. aureus* strains against neutrophil killing; however enterobactin did not show significant protection against HOCl production.

It appears the majority of reactive chlorine species target multiple bacterial components simultaneously in order to elicit their antimicrobial effects. Clearly studies on RCS and their

exact targets, their mechanism of action and the bacterial repair systems that react in response to toxic chlorination events is an exciting area of research [48, 56, 71, 78].

## 1.5 Mechanisms that sense and repair oxidative damage to proteins

### 1.5.1 Repair mechanisms

*S. aureus* maintains several repair systems to counter the effects of oxidation on protein thiol groups. The first is the well-characterized thioredoxin (Trx)/thioredoxin reductase (TrxR) system. This system (Figure 1.11), which has been described in a number of extensive and pioneering studies by Holmgren and co-workers, is composed of a TrxR (designated as TrxB in *S. aureus*) and a thioredoxin-fold protein (Trx, designated as TrxA in *S. aureus*). TrxB is a flavoprotein disulfide reductase (FDR) enzyme that catalyzes the NADPH-dependent recycling of oxidized TrxA. In turn, TrxA is an oxidoreductase that reduces the disulfides that resulted from oxidation events in a variety of thiol-containing substrates [195-208]. TrxA is a member of the thioredoxin-fold superfamily that all have a thioredoxin (Trx) domain—four stranded beta sheets sandwiched between three alpha-helices—in common. So-called thioredoxin-fold proteins (TFPs) are found in all organisms and function in disulfide thiol interchange reactions, oxidative stress resistance, protein folding and removal of xenobiotics [199, 201, 207, 209, 210]. Thioredoxin proteins contain a characteristic CGPC motif that contains the two redox active cysteine residues that are involved in reducing disulfide-containing substrates via disulfide exchange; this results in oxidation of its own Cys residues [199, 201, 211]. The importance of the Trx/TrxR system as a defense mechanism against oxidative stress has been shown in studies involving TrxR-null mutants which are subsequently lethal [208]. Furthermore, a number of bacteria including *S. aureus* are sensitive to the well-known TrxR inhibitor ebselen [212-223].

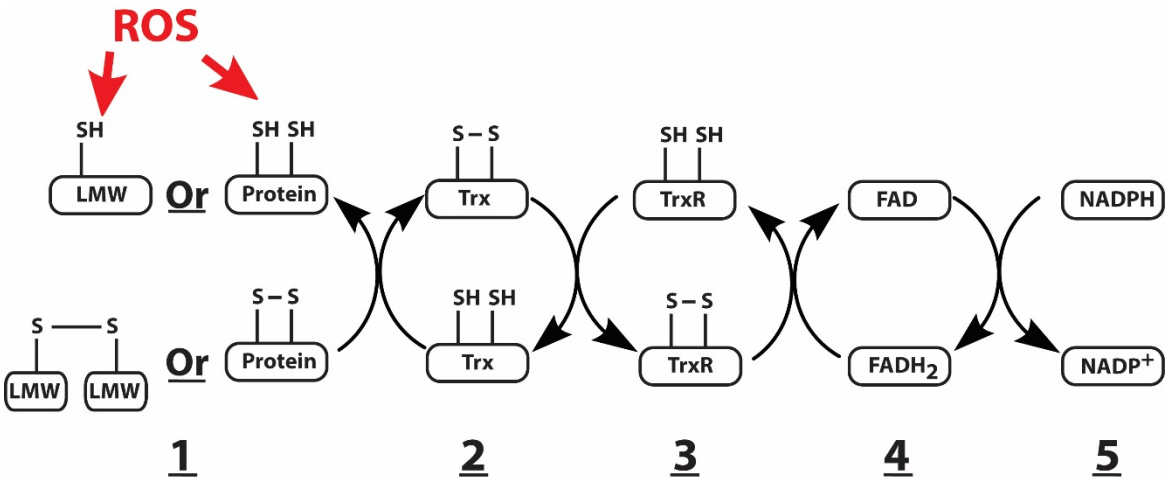


**Figure 1.11 Thiol disulfide interchange reactions of Trx/TrxR system. Trx (Step 2) can reduce disulfide substrates including LMW thiols or thiols on protein substrates (1). Oxidized Trx is recycled back to its reduced state via the NADPH-dependent TrxR reaction (Steps 3-5).**

Another important antioxidant enzyme involved in repairing damaged proteins is methionine sulfoxide reductase (Msr). Msr reverses the oxidation of methionine in proteins, i.e. it converts methionine sulfoxide residues back to methionine (Figure 1.5B) [80, 82, 224-227]. Methionine residues on protein surfaces have been hypothesized to act as oxidant scavengers; in such a scenario regeneration of these residues by Msr will allow for exposure to another round of oxidant [228, 229].

Another aspect of protein damage is the effect that oxidative stress has on protein folding. Specifically, RCS play a major role in protein denaturation when compared to ROS or RNS [45]. Jakob and co-workers, through a number of excellent studies and reviews, have described the effects of protein unfolding and aggregation due to RCS-mediated oxidative stress [71-73, 75, 230-234]. In regards to protein folding repair mechanisms in *S. aureus*, a number of stress-related chaperones from the ClpB family have been indicated to be involved in refolding and repair of protein damage due to oxidative stress [235].

Lastly, some enzymes require metal cofactors for catalysis (Mn, Cu, Co, Fe-S), thus as expected the oxidation of metals via Fenton/Haber-Weiss chemistry would result in the decrease of amount of available metals and the accumulation of toxic radicals species. The only known repair mechanism of *S. aureus* that relates directly on metals is the repair of Fe-S clusters. In *S. aureus* the *suf* system protects Fe-S cluster assembly during oxidative stress [236], as well as the MgrA and *scdA* system which sense and repair damage to Fe-S clusters [237-239].

### 1.5.2 Oxidative stress sensing and regulation mechanisms

A number of the above-mentioned repair mechanisms are recruited largely due to sensing and regulatory mechanisms of *S. aureus* that respond very specifically to the type of oxidant encountered [240]. Overall, the metabolic profile of *S. aureus* would also need to adjust to respond to the oxidative damage of Fe-S clusters, and free cysteine and methionine. In a number of bacteria, including *S. aureus*, the pathways associated with transcriptional regulation and metabolism of cysteine and methionine are upregulated upon exposure to chlorine-based oxidative stresses [241-246]. These transcriptional regulators largely share a similar mechanism in response to ROS. Instead of inactivation or damage by ROS, these regulators are in fact activated. Activation occurs via redox sensitive cysteines that form intramolecular disulfide bonds which facilitates cooperative binding of RNA polymerase to activate transcription of the genes involved in ROS detoxification and repair mechanisms [247]. A number of transcriptional regulators are upregulated in response to ROS and RCS; these include Fur (KatA) [66, 248], PerR (KatA, AhpC/F, Trx/TrxR) [71, 173, 249], MgrA (capsule and membrane biosynthesis, coagulase, αtoxin, autolysis, multidrug efflux pumps, infection progression) [250-255], SarZ (metabolism of amino acids, fatty acids, nucleotides and sugars, pyrimidine synthesis and gluconate catabolism) [256, 257], SarA (Sod, TrxR, biotin formation, entertoxin C, collagen and fibronectin binding, proteases and virulence factors) [258-260], Spx (Trx/TrxR) [261, 262], QsrR (Quinone reductase, nitroreductase, glyoxalase, dioxygenase), HrcA (transcriptional repressor of heat shock genes), HypR2-family (HOCl protection) and sigma B (infection progression and virulence) [263, 264].

Regulators that have been show to specifically respond to HOCl-mediated stress include PerR, QsrR, HrcA, HypR2 and sigma B [263, 264].

## 1.6 Oxidative stress resistance mediated by LMW Thiols and disulfide reductase enzymes

### 1.6.1 LMW thiols

In response to oxidative stress (ROS, RNS, RCS) and maintenance of redox balance, many organisms produce high concentrations of low molecular weight thiol compounds (Figure 1.12), of which the most extensively studied is glutathione (GSH) [55, 265-268].

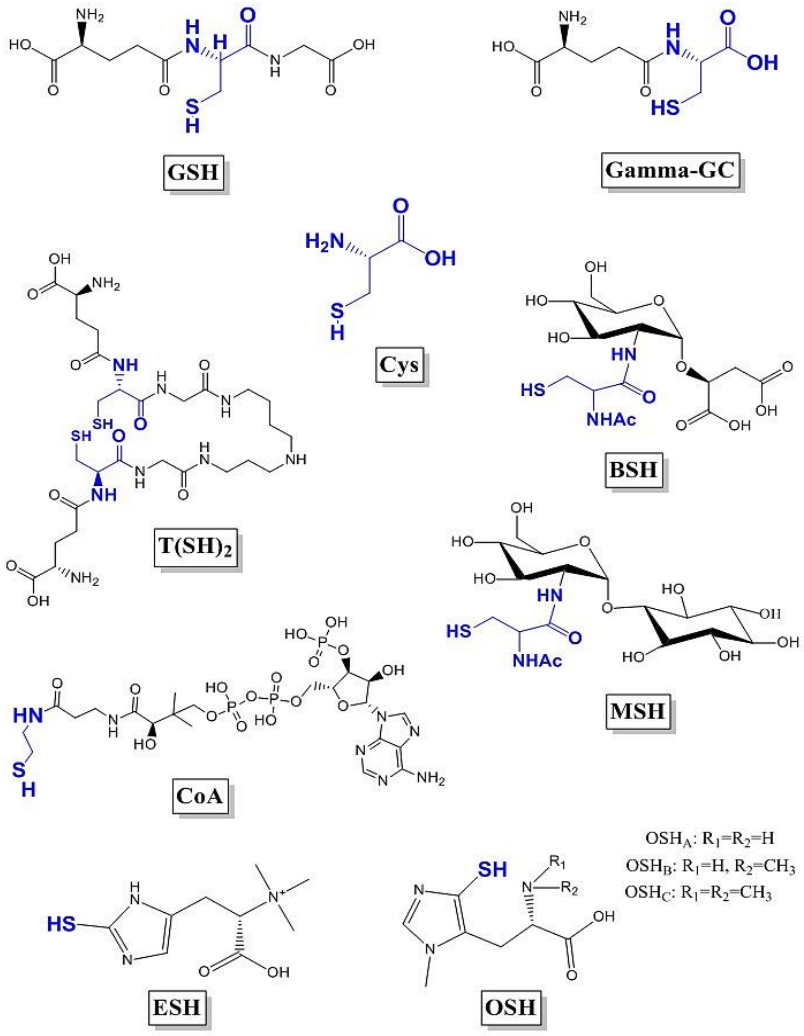


**Figure 1.12 Various LMW thiols implicated in oxidative stress responses. Glutatione (GSH, found in eukaryotes and Gram-negative bacteria), gamma-GlutamylCys (GGC, found in halobacteria, lactic acid bacteria), cysteine (Cys, found in all organisms), bacillithiol (BSH, found in *Firmicutes*), trypanothione ($T(SH)_2$, found in *Trypanosomes*), mycothiol (MSH, found in *Actinomycetes*), coenzyme A (CoA, found in all organisms), ergothioneine (ESH, found in fungi and *Mycobacteria*), and ovothiol (OSH, found in *Leishmania* and marine invertebrates).**

*S. aureus* does not produce GSH, instead relying on coenzyme A (CoA) and bacillithiol (BSH) as its major LMW thiols [192, 268-274]. When redox-sensitive cysteines within active sites of proteins are oxidized they have the potential to form sulfonic acids, an oxidation state which cannot be reversed. This would be problematic to cells if not prevented. In this context LMW thiols act as a protective mechanism that organisms use in which oxidized proteins are *S*-thiolated by these molecules in a reversible manner to protect and regulate enzyme functions [55, 211, 267, 268, 271, 273-277].

CoA is a ubiquitous cofactor found in many organisms, and plays a central role in metabolism. In addition to its well-defined involvement in metabolism, its potential role in

oxidative stress resistance by acting as a redox buffer is also apparent. In such a role, CoA would be sacrificially oxidized by ROS and RCS to its disulfide. Importantly, *S. aureus* possesses a dedicated CoA disulfide reductase that maintains CoA in its reduced state, thus replenishing the pool of free CoA [268-270, 278]. In addition, *S. aureus* was found to produce CoA in millimolar quantities [279]. In light of these facts, it was therefore not surprising that a recent study demonstrated that proteins in *S. aureus* undergo *S*-thiolation by CoA upon challenge with high concentrations of $H_2O_2$ and the stressor diamide, as well as low concentrations of NaOCl (100 µM) [280]. However, the relative importance of CoA to the oxidative stress resistance mechanisms of *S. aureus*, and the manner by which it reverses CoA-thiolation, remains unexplored.

Another major LMW thiol involved in oxidative stress of *S. aureus* is bacillithiol (BSH). It was discovered in 2009 and was found to be the α-glycoside of L-cysteinyl-D-glucosamine with L-malic acid [281]. It resembles the LMW thiol mycothiol (MSH) in that it contains the same cysteine moiety amide bonded to glucosamine [282]. However, MSH is linked to inositol, not malic acid, and mainly occurs in Actinomycetes.

*S. aureus* BSH mutants show increased sensitivity towards oxidative stress, metals and fosfomycin [274, 283]. *S. aureus* strains that are unable to produce BSH showed decreased viability in mouse macrophage models, but appeared to be only slightly compromised under oxidative stress [284]. This suggests that BSH in *S. aureus* might fulfil a non-essential role during oxidative stress resistance, or one that can be complemented/replaced by a secondary LMW thiol. Interestingly, the biosynthetic gene cluster for BSH production has been found upstream and co-directional to the *panBCD* operon responsible for pantothenate biosynthesis. However, the physiological relevance of this link is still to be uncovered [192].

Cysteine is unlikely to act as a redox buffer or play a role in redox homeostasis due to its toxicity at high concentrations. Furthermore it has been shown that cysteine undergoes $Cu^{2+}$ catalyzed auto-oxidation to form cystine and $H_2O_2$ which would result in further oxidative damage [269, 285, 286]

### 1.6.2 Disulfide reductase enzymes implicated in the recycling of LMW thiol disulfides in *S. aureus.*

The reliance on LMW thiols as redox buffers necessitates the presence of disulfide reductase enzymes that can recycle these compounds once they have been oxidized to their disulfide forms. Since *S. aureus* does not produce GSH, it also does not have a glutathione reductase enzyme. Instead, *S. aureus* only has two functionally characterized disulfide

reductases: CoA disulfide reductase (CoADR) and lipoamide dehydrogenase (LipDH, LPD or LipA) (Figure 1.13). Importantly, no enzyme has been described that is able to reduce the disulfide of BSH (BSSB). However, *S. aureus* does have two functionally uncharacterized enzymes belonging to the same superfamily; they will be discussed in the next subsection.

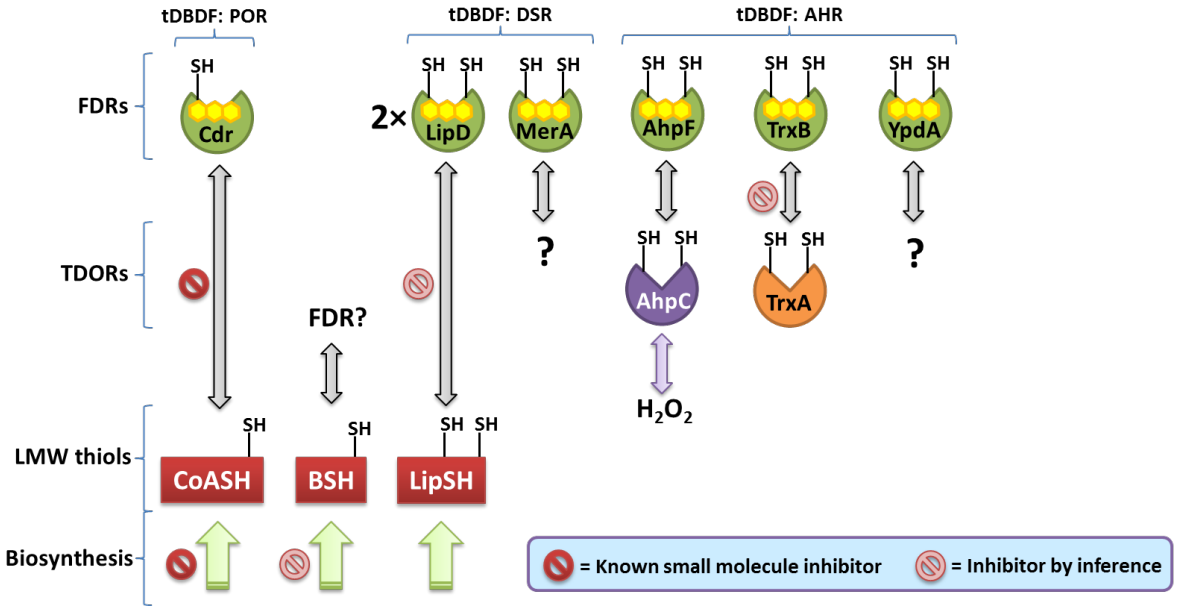


**Figure 1.13 Thiol redox network of *S. aureus*. The top tier of enzymes are labeled FDRs which form part of the larger tDBDF superfamily. The three subgroups NADH peroxidase/oxidase and CoA-disulfide reductase (POR), disulfide reductase (DSR) and alkylhydroperoxide reductase (AHR) relevant to this study are shown. The unknown information is indicated by question marks [287].**

Disulfide reductase enzymes are classified as FDRs, or more broadly belonging to the two dinucleotide binding domains flavoprotein (tDBDF) superfamily [166, 288]. As the name implies, tDBDFs contains two dinucleotide binding domains arranged in Rossman folds. Both domains are required for activity and bind the flavin cofactor, FAD (Flavin Adenosine Dinucleotide) and the second domain binds either NADH (Nicotinamide Adenine Dinucleotide, reduced) or NADPH (Nicotinamide Adenine Dinucleotide Phosphate, reduced).

The tDBDFs can be broadly classified into two major groups (Figure 1.14) which are further divided into nine subgroups based upon structure-based alignments [288].

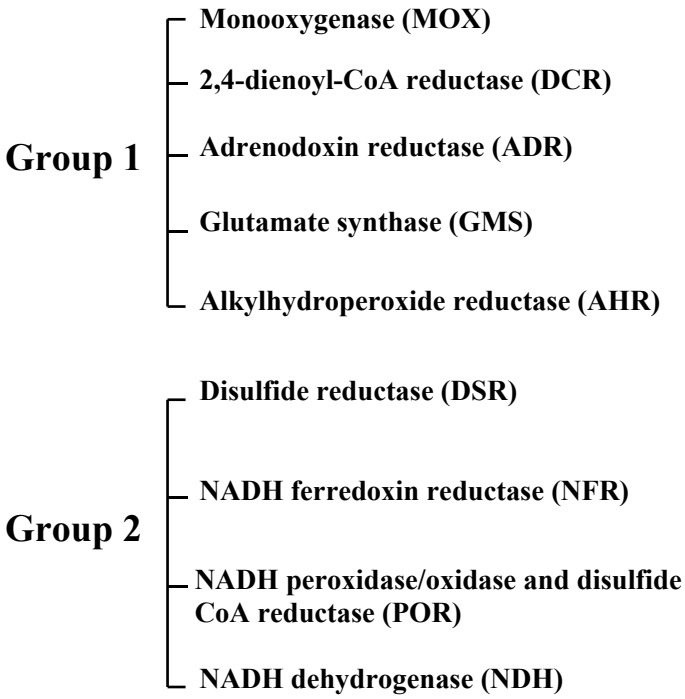


**Figure 1.14 Two dinucleotide binding domains flavoprotein (tDBDF) superfamily showing nine subgroups based on structure-sequence alignment [288].**

The first group include monooxygenases (MOX), 2,4-dienoyl CoA reductase (DCR), adrenodoxin reductase (ADR), glutamate synthase (GMS), and alkylhydroperoxide reductase (AHR). The second group includes disulfide reductase (DSR), NADH peroxidase/oxidase and CoA-disulfide reductase (POR), NADH ferredoxin reductase (NFR), and NADH dehydrogenase (NDH) [288]. In the context of disulfide reductase enzymes implicated in *S. aureus* redox homeostasis, only three subgroups—POR, DSR and AHR, representing CoADR, LipDH and two enzymes of unknown function—are relevant as shown in Figure 1.13.

CoADR is classified as a POR subgroup member and represents the only known tDBDF in *S. aureus* capable of reducing the disulfide form of the LMW thiol CoA [269, 278]. It is a dimeric flavoprotein and shares up to 50% sequence identitiy with many other tDBDFs with the highest identity found over the pyridine-binding and FAD domains. While it also shares some similarity in the vicinity of the active site, it crucially lacks the disulfide motif CxxxxC that is characteristic of other disulfide reductases. Instead, it has a single Cys in the active site that ensures its activity through the formation of a mixed disulfide with its substrate CoA [289]. Interestingly the single conserved Cys within CoADRs active site forms part of a SFxxC motif which is commonly seen in NADH peroxidase/oxidases and initially was thought to reduce $H_2O_2$ [269, 278, 290]. Its catalytic mechanism (Figure 1.15) involves the thiolate of

Cys43 which nucleophilically attacks one sulfur of the incoming CoA disulfide forming a mixed Cys43-CoA disulfide, whilst displacing one CoA molecule. The mixed disulfide state is the form in which it is usually isolated. The cycle continues with NADPH reducing the mixed disulfide via FAD, releasing another CoA molecule to regenerate the reduced form of the enzyme for another round of catalysis [269, 289, 291].

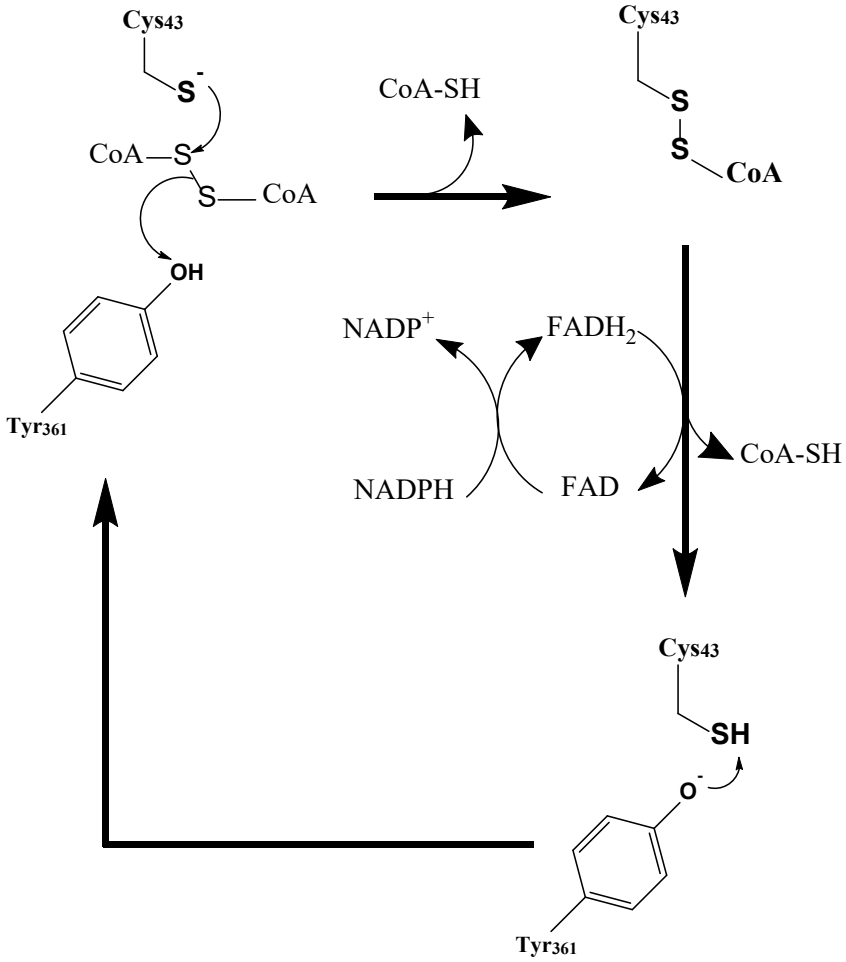


**Figure 1.15 Catalytic mechanism of CoADR. The thiolate from Cys43 attacks one of the sulfur atoms on the incoming CoA disulfide (releasing one CoA) forming an enzyme mixed Cys-CoA disulfide. The enzyme is regenerated through NADPH reduction via FAD cofactor (releasing the second CoA) [269].**

Since CoADR represents the only known enzyme with CoA disulfide reductase activity it has been targeted for the development of selective inhibitors to establish its relevance and importance to *S. aureus* growth and survival. The first CoADR inhibitors were synthesized by Van der Westhuyzen and Strauss and were shown to be competitive mechanistic inhibitors [292]. However, these inhibitors did not have any effect on *S. aureus* growth, in agreement with the finding that under normal growth conditions CoADR-encoding gene *cdr* is non-essential [293].

Lipoamide dehydrogenase (LipDH, LPD or LipA) from *S. aureus* was first cloned and purified in 1991. LipDH, which catalyzes the $NADP^+$-dependent oxidation of dihydrolipoamide, is classified as a DSR subgroup member and follows a similar mechanism (Figure 1.16) to that of other members of the DSR subgroup such as glutathione disulfide reductase.

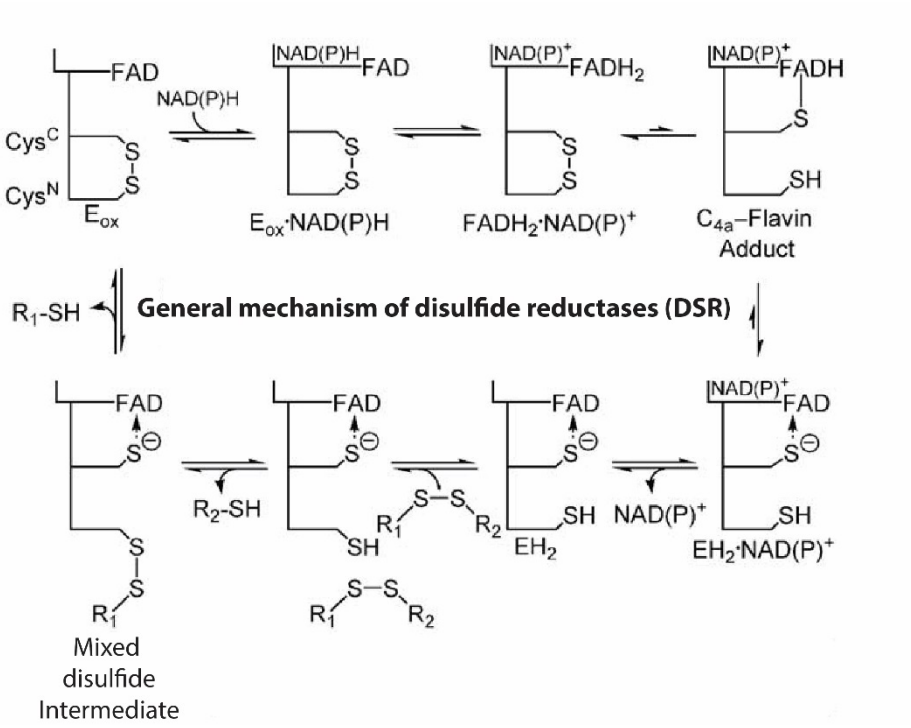


**Figure 1.16 General mechanism observed for disulfide reductase (DSR) subgroup. The top tier shows the oxidative half reaction and the bottom the reductive half reaction [166].**

The general mechanism is initiated by the binding of NADPH which reduces the FAD cofactor to form a stable intermediate [$FADH_2$●$NAD(P)^+$]. Electrons are then transferred to the redox active disulfides via a covalent C4a-adduct whilst $NAD(P)^+$ dissociates. The oxidative half reaction involves the N-terminal Cys forming a mixed disulfide intermediate. The final steps involve the C-terminal Cys thiolate attacking the sulfur of the mixed disulfide intermediate, releasing the reduced substrate and regenerating the oxidized enzyme for another round of catalysis [166, 294].

LipDH is found as a subunit of multi-enzyme systems of the pyruvate dehydrogenase (PDH) complex, 2-oxoglutarate dehydrogenase complex and branched chain 2-oxo acid dehydrogenase complex [295]. In *S. aureus*, it has been hypothesized as membrane bound subunit E3 of PDH. Experiments using LipDH in isolation proves to be unsuccessful owing to its association with other subunits of PDH, as well as the covalent attachment of its cofactor [296-299]. A separate study shows that lipoamide appears to function in immune

suppression, by lipoylating E2 of the PDH (lipoyl-E2-PDH) which is shown to be secreted by *S. aureus* that then inactivates neutrophil toll like receptors 1/2 thus suppressing the immune response towards *S. aureus* [300]. Considering its very specialized role in metabolism, it is unlikely that LipDH has a functional role in oxidative stress resistance in this organism.

### 1.6.3 Functionally uncharacterized tDBDF enzymes implicated in Oxidative Stress Resistance in *S. aureus*.

Apart from the enzymes described in the previous subsections, *S. aureus* also produces two enzymes—MerA and YpdA—that appear to play an important role in oxidative defense mechanisms yet remain functionally uncharacterized.

*Sa*MerA, based upon bioinformatics analysis, can be classified as a tDBDF of the DSR subgroup containing a CxxxxC motif within the active site and two pyridine nucleotide binding sites. *Sa*MerA shares highest sequence similarity to other DSR subgroup members such as mercuric ion reductases (MerA, from which it derives its name) and LipDHs. However, *Sa*MerA lacks critical auxiliary cysteines that have been shown to be important in the catalytic mechanism of true mercuric ion reductases [166], and it does not contain a lipoic acid cofactor. It is therefore unlikely to have a function related to that of either of its fellow DSR sub group members.

A study by Voyich *et al* showed that *Sa*MerA was upregulated more than 80-fold) when *S. aureus* was challenged with neutrophils [301]. In a separate study, the HypR operon containing the gene that encodes *Sa*MerA was found to be upregulated (~180-fold) under hypochlorite stress. The same study demonstrated that *S. aureus* in which the MerA-encoding gene was knocked out is more sensitive than the wild-type to hypochlorite stress and has reduced survival in macrophage infection models [264]. Importantly, the homologue of *Sa*MerA in *E. coli*, YkgC/RclA, is also significantly upregulated in response to hypochlorite stress [242]. In a separate study, the *E. coli* YkgC/RclA knockout mutant was shown to have increased sensitivity towards hypochlorite [76]. In light of these findings, the function of *Sa*MerA seems to be related to its defense against host-generated oxidative stress. Uncovering this function of this enzyme constitutes the first aim of this study as discussed in Chapter 2.

The other tDBDF of unknown function is YpdA, which shares closest homology to the TrxR family of proteins and is therefore classified as a member of the AHR subgroup. This

suggests that YpdA should have a TFP partner; however, it interestingly lacks the catalytically important CxxxxC motif found in all AHR enzymes and it is therefore unclear how this enzyme could act to reduce any disulfide without a disulfide motif. YpdA is found in all BSH producing bacteria and is proposed to play a role in bacillithiol dependent processes [211, 272, 281]. Using bioinformatics analysis as well as EMBL STRING, Gaballa *et al* showed that YpdA is associated with the biosynthesis of BSH [211]. These authors as well as a number of other authors have suggested that YpdA may function as a bacilliredoxin-like protein in reducing protein disulfides or may function in recycling bacillithiol disulfide (BSSB) analogous to CoADR [211, 246, 268, 272, 274, 281, 284, 302-304]. This enzyme and other select LMW thiols as a function of enzyme protection and regulation will be discussed further in Chapter 3.

## 1.7 Aim and objectives of this study

Oxidative stress is a crucially important component in the host-microbe interaction. Understanding the mechanisms by which pathogenic bacteria resist the oxidative attacks of the innate immune system can shed light onto the basic bacterial physiology as well as reveal new potential avenues by which the host's natural defenses against infections can be rendered more effective. Discovering ways in which the oxidative stress response can be modulated—particularly in bacteria such as *S. aureus* where antimicrobial resistant strains are becoming all too common—may prove to be a critical step in improving our treatment of bacterial infections.

In this context, this study set out to characterize enzymes putatively associated with oxidative stress resistance in *S. aureus*, as well as to clarify the respective roles of CoA and BSH in protecting enzyme activity in this organism under oxidative stress conditions.

As such, the specific aims of this study were:

(1) To characterize *Sa*MerA, an *S. aureus* Flavin Disulfide Reductase (FDR) relevant to redox homeostasis.
(2) To characterize the putative function of YpdA in the context of thiol/disulfide redox reactions involving bacillithiol (BSH).
(3) To study the relative importance of CoA and BSH in the reversal of protein-based thiol oxidation in *S. aureus*.

Taken together, the aims of this study were formulated to increase our knowledge and understanding of the oxidative stress resistance mechanisms that are unique to *S. aureus*, but which could also be more widely relevant—particularly in the context of the host-pathogen interface.

## 1.8 References

1. Walsh, C.T. and T.A. Wencewicz, *Prospects for new antibiotics: a molecule-centered perspective.* J Antibiot (Tokyo), 2014. **67**(1): p. 7-22.
2. Clatworthy, A.E., E. Pierson, and D.T. Hung, *Targeting virulence: a new paradigm for antimicrobial therapy.* Nat Chem Biol, 2007. **3**(9): p. 541-8.
3. Premanandh, J., B.S. Samara, and A.N. Mazen, *Race Against Antimicrobial Resistance Requires Coordinated Action - An Overview.* Front Microbiol, 2015. **6**: p. 1536.
4. Zaman, S.B., et al., *A Review on Antibiotic Resistance: Alarm Bells are Ringing.* Cureus, 2017. **9**(6): p. e1403.
5. Munita, J.M. and C.A. Arias, *Mechanisms of Antibiotic Resistance.* Microbiol Spectr, 2016. **4**(2).
6. Lin, J., et al., *Mechanisms of antibiotic resistance.* Front Microbiol, 2015. **6**: p. 34.
7. Gold, H.S. and S.K. Pillai, *Antistaphylococcal agents.* Infect Dis Clin North Am, 2009. **23**(1): p. 99-131.
8. Alanis, A.J., *Resistance to antibiotics: are we in the post-antibiotic era?* Arch Med Res, 2005. **36**(6): p. 697-705.
9. Davies, J. and D. Davies, *Origins and evolution of antibiotic resistance.* Microbiol Mol Biol Rev, 2010. **74**(3): p. 417-33.
10. Davies, J., *Origins and evolution of antibiotic resistance.* Microbiologia, 1996. **12**(1): p. 9-16.
11. Kohanski, M.A., D.J. Dwyer, and J.J. Collins, *How antibiotics kill bacteria: from targets to networks.* Nat Rev Microbiol, 2010. **8**(6): p. 423-35.
12. Fischbach, M.A. and C.T. Walsh, *Antibiotics for emerging pathogens.* Science, 2009. **325**(5944): p. 1089-93.
13. Nathan, C., *Antibiotics at the crossroads.* Nature, 2004. **431**(7011): p. 899-902.
14. Infectious Diseases Society of, A., et al., *Combating antimicrobial resistance: policy recommendations to save lives.* Clin Infect Dis, 2011. **52 Suppl 5**: p. S397-428.
15. Spellberg, B., et al., *The epidemic of antibiotic-resistant infections: a call to action for the medical community from the Infectious Diseases Society of America.* Clin Infect Dis, 2008. **46**(2): p. 155-64.
16. Kwon, J., et al., *A novel series of enoyl reductase inhibitors targeting the ESKAPE pathogens, Staphylococcus aureus and Acinetobacter baumannii.* Bioorg Med Chem, 2018. **26**(1): p. 65-76.
17. Karlowsky, J.A., et al., *Resistance among Gram-negative ESKAPE pathogens isolated from hospitalized patients with intra-abdominal and urinary tract infections in Latin American countries: SMART 2013-2015.* Braz J Infect Dis, 2017. **21**(3): p. 343-348.
18. Santajit, S. and N. Indrawattana, *Mechanisms of Antimicrobial Resistance in ESKAPE Pathogens.* Biomed Res Int, 2016. **2016**: p. 2475067.
19. Bassetti, M. and E. Righi, *Development of novel antibacterial drugs to combat multiple resistant organisms.* Langenbecks Arch Surg, 2015. **400**(2): p. 153-65.

20. Boucher, H.W., et al., *10 x '20 Progress--development of new drugs active against gram-negative bacilli: an update from the Infectious Diseases Society of America.* Clin Infect Dis, 2013. **56**(12): p. 1685-94.

21. Rice, L.B., *Progress and challenges in implementing the research on ESKAPE pathogens.* Infect Control Hosp Epidemiol, 2010. **31 Suppl 1**: p. S7-10.

22. Boucher, H.W., et al., *Bad bugs, no drugs: no ESKAPE! An update from the Infectious Diseases Society of America.* Clin Infect Dis, 2009. **48**(1): p. 1-12.

23. Shnayerson, M., *The killer bug.* Fortune, 2002. **146**(6): p. 149-50, 152, 154 passim.

24. Gorman, C., *Surviving the new killer bug.* Time, 2006. **167**(26): p. 52-3.

25. Chambers, H.F. and F.R. Deleo, *Waves of resistance: Staphylococcus aureus in the antibiotic era.* Nat Rev Microbiol, 2009. **7**(9): p. 629-41.

26. Lowy, F.D., *Staphylococcus aureus infections.* N Engl J Med, 1998. **339**(8): p. 520-32.

27. *National Nosocomial Infections Surveillance (NNIS) System Report, Data Summary from January 1992-June 2001, issued August 2001.* Am J Infect Control, 2001. **29**(6): p. 404-21.

28. National Nosocomial Infections Surveillance, S., *National Nosocomial Infections Surveillance (NNIS) System Report, data summary from January 1992 through June 2004, issued October 2004.* Am J Infect Control, 2004. **32**(8): p. 470-85.

29. Marshall, J.H. and G.J. Wilmoth, *Pigments of Staphylococcus aureus, a series of triterpenoid carotenoids.* J Bacteriol, 1981. **147**(3): p. 900-13.

30. Sasaki, T., *Chemical Analysis of Staphylococcus Aureus. I. Carotenoid Pigments of Staphylococcus Aureus.* J Biochem, 1964. **55**: p. 225-30.

31. Clauditz, A., et al., *Staphyloxanthin plays a role in the fitness of Staphylococcus aureus and its ability to cope with oxidative stress.* Infect Immun, 2006. **74**(8): p. 4950-3.

32. Lowy, F.D., *Antimicrobial resistance: the example of Staphylococcus aureus.* J Clin Invest, 2003. **111**(9): p. 1265-73.

33. Bal, A.M. and I.M. Gould, *Antibiotic resistance in Staphylococcus aureus and its relevance in therapy.* Expert Opin Pharmacother, 2005. **6**(13): p. 2257-69.

34. Bradley, J.S., *Newer antistaphylococcal agents.* Curr Opin Pediatr, 2005. **17**(1): p. 71-7.

35. Projan, S.J. and P.J. Youngman, *Antimicrobials: new solutions badly needed.* Curr Opin Microbiol, 2002. **5**(5): p. 463-5.

36. Hooper, D.C., *Emerging mechanisms of fluoroquinolone resistance.* Emerg Infect Dis, 2001. **7**(2): p. 337-41.

37. Hooper, D.C., *Fluoroquinolone resistance among Gram-positive cocci.* Lancet Infect Dis, 2002. **2**(9): p. 530-8.

38. Howden, B.P., et al., *Reduced vancomycin susceptibility in Staphylococcus aureus, including vancomycin-intermediate and heterogeneous vancomycin-intermediate strains: resistance mechanisms, laboratory detection, and clinical implications.* Clin Microbiol Rev, 2010. **23**(1): p. 99-139.

39. Bjotvedt, G., *The immune system: a practitioner's overview.* Vet Med Small Anim Clin, 1981. **76**(11): p. 1557-61.

40. Parkin, J. and B. Cohen, *An overview of the immune system.* Lancet, 2001. **357**(9270): p. 1777-89.

41. Winterbourn, C.C., A.J. Kettle, and M.B. Hampton, *Reactive Oxygen Species and Neutrophil Function.* Annu Rev Biochem, 2016. **85**: p. 765-92.

42. Witko-Sarsat, V., et al., *Neutrophils: molecules, functions and pathophysiological aspects.* Lab Invest, 2000. **80**(5): p. 617-53.

43. Segal, A.W., *How neutrophils kill microbes.* Annu Rev Immunol, 2005. **23**: p. 197-223.

44. Flannagan, R.S., B. Heit, and D.E. Heinrichs, *Antimicrobial Mechanisms of Macrophages and the Immune Evasion Strategies of Staphylococcus aureus.* Pathogens, 2015. **4**(4): p. 826-68.

45. Imlay, J.A., *Cellular defenses against superoxide and hydrogen peroxide.* Annu Rev Biochem, 2008. **77**: p. 755-76.

46. Klebanoff, S.J., *Myeloperoxidase: friend and foe.* J Leukoc Biol, 2005. **77**(5): p. 598-625.

47. Hurst, J.K., *What really happens in the neutrophil phagosome?* Free Radic Biol Med, 2012. **53**(3): p. 508-20.

48. Winterbourn, C.C. and A.J. Kettle, *Redox reactions and microbial killing in the neutrophil phagosome.* Antioxid Redox Signal, 2013. **18**(6): p. 642-60.

49. Paulsen, C.E. and K.S. Carroll, *Cysteine-mediated redox signaling: chemistry, biology, and tools for discovery.* Chem Rev, 2013. **113**(7): p. 4633-79.

50. Foote, C.S., T.E. Goyne, and R.I. Lehrer, *Assessment of chlorination by human neutrophils.* Nature, 1983. **301**(5902): p. 715-6.

51. Pattison, D.I. and M.J. Davies, *Reactions of myeloperoxidase-derived oxidants with biological substrates: gaining chemical insight into human inflammatory diseases.* Curr Med Chem, 2006. **13**(27): p. 3271-90.

52. Pattison, D.I., M.J. Davies, and C.L. Hawkins, *Reactions and reactivity of myeloperoxidase-derived oxidants: differential biological effects of hypochlorous and hypothiocyanous acids.* Free Radic Res, 2012. **46**(8): p. 975-95.

53. Weiss, S.J., *Tissue destruction by neutrophils.* N Engl J Med, 1989. **320**(6): p. 365-76.

54. Spickett, C.M., et al., *The reactions of hypochlorous acid, the reactive oxygen species produced by myeloperoxidase, with lipids.* Acta Biochim Pol, 2000. **47**(4): p. 889-99.

55. Poole, L.B., *The basics of thiols and cysteines in redox biology and chemistry.* Free Radic Biol Med, 2015. **80**: p. 148-57.

56. Winterbourn, C.C., *Neutrophil Oxidants: Production and Reactions*, in *Oxygen Radicals: systematic events and disease processes*, D.K. Das and W.B. Essman, Editors. 1990, Karger: Basel, N.Y. p. 31-70.

57. Hampton, M.B., A.J. Kettle, and C.C. Winterbourn, *Inside the neutrophil phagosome: Oxidants, myeloperoxidase, and bacterial killing.* Blood, 1998. **92**(9): p. 3007-3017.

58. Fang, F.C., *Antimicrobial reactive oxygen and nitrogen species: concepts and controversies.* Nat Rev Microbiol, 2004. **2**(10): p. 820-32.

59. Schapiro, J.M., S.J. Libby, and F.C. Fang, *Inhibition of bacterial DNA replication by zinc mobilization during nitrosative stress.* Proc Natl Acad Sci U S A, 2003. **100**(14): p. 8496-501.

60. Stevanin, T.M., et al., *Flavohemoglobin Hmp affords inducible protection for Escherichia coli respiration, catalyzed by cytochromes bo' or bd, from nitric oxide.* J Biol Chem, 2000. **275**(46): p. 35868-75.

61. Pacelli, R., et al., *Nitric oxide potentiates hydrogen peroxide-induced killing of Escherichia coli.* J Exp Med, 1995. **182**(5): p. 1469-79.

62. Lepoivre, M., et al., *Inactivation of ribonucleotide reductase by nitric oxide.* Biochem Biophys Res Commun, 1991. **179**(1): p. 442-8.

63. Evans, T.J., et al., *Cytokine-treated human neutrophils contain inducible nitric oxide synthase that produces nitration of ingested bacteria.* Proc Natl Acad Sci U S A, 1996. **93**(18): p. 9553-8.

64. Burney, S., et al., *The chemistry of DNA damage from nitric oxide and peroxynitrite.* Mutat Res, 1999. **424**(1-2): p. 37-49.

65. Borregaard, N. and J.B. Cowland, *Granules of the human neutrophilic polymorphonuclear leukocyte.* Blood, 1997. **89**(10): p. 3503-21.

66. Lehrer, R.I. and T. Ganz, *Antimicrobial polypeptides of human neutrophils.* Blood, 1990. **76**(11): p. 2169-81.

67. Nauseef, W.M., *How human neutrophils kill and degrade microbes: an integrated view.* Immunol Rev, 2007. **219**: p. 88-102.

68. Winterbourn, C.C., et al., *Modeling the reactions of superoxide and myeloperoxidase in the neutrophil phagosome: implications for microbial killing.* J Biol Chem, 2006. **281**(52): p. 39860-9.

69. Slauch, J.M., *How does the oxidative burst of macrophages kill bacteria? Still an open question.* Mol Microbiol, 2011. **80**(3): p. 580-3.

70. Wardman, P. and L.P. Candeias, *Fenton chemistry: an introduction.* Radiat Res, 1996. **145**(5): p. 523-31.

71. Gray, M.J., W.Y. Wholey, and U. Jakob, *Bacterial responses to reactive chlorine species.* Annu Rev Microbiol, 2013. **67**: p. 141-60.

72. Dahl, J.U., M.J. Gray, and U. Jakob, *Protein quality control under oxidative stress conditions.* J Mol Biol, 2015. **427**(7): p. 1549-63.

73. Reichmann, D., W. Voth, and U. Jakob, *Maintaining a Healthy Proteome during Oxidative Stress.* Mol Cell, 2018. **69**(2): p. 203-213.

74. Chapman, A.L., et al., *Characterization of non-covalent oligomers of proteins treated with hypochlorous acid.* Biochem J, 2003. **375**(Pt 1): p. 33-40.

75. Winter, J., et al., *Bleach activates a redox-regulated chaperone by oxidative protein unfolding.* Cell, 2008. **135**(4): p. 691-701.

76. Parker, B.W., et al., *The RclR protein is a reactive chlorine-specific transcription factor in Escherichia coli.* J Biol Chem, 2013. **288**(45): p. 32574-84.

77. Chapman, A.L., et al., *Chlorination of bacterial and neutrophil proteins during phagocytosis and killing of Staphylococcus aureus.* J Biol Chem, 2002. **277**(12): p. 9757-62.

78. Green, J.N., A.J. Kettle, and C.C. Winterbourn, *Protein chlorination in neutrophil phagosomes and correlation with bacterial killing.* Free Radic Biol Med, 2014. **77**: p. 49-56.

79. Ezraty, B., et al., *Oxidative stress, protein damage and repair in bacteria.* Nat Rev Microbiol, 2017. **15**(7): p. 385-396.

80. St John, G., et al., *Peptide methionine sulfoxide reductase from Escherichia coli and Mycobacterium tuberculosis protects bacteria against oxidative damage from reactive nitrogen intermediates.* Proc Natl Acad Sci U S A, 2001. **98**(17): p. 9901-6.

81. Peskin, A.V., et al., *Oxidation of methionine to dehydromethionine by reactive halogen species generated by neutrophils.* Biochemistry, 2009. **48**(42): p. 10175-82.

82. Boschi-Muller, S. and G. Branlant, *Methionine sulfoxide reductase: chemistry, substrate binding, recycling process and oxidase activity.* Bioorg Chem, 2014. **57**: p. 222-30.

83. Nweke, A. and F.E. Scully, *Stable N-Chloroaldimines and Other Products of the Chlorination of Isoleucine in Model Solutions and in a Wastewater.* Environ. Sci. Technol, 1989. **23**(8): p. 989-994.

84. Andres, J., et al., *Understanding the mechanism of base-assisted decomposition of (N-halo),N-alkylalcoholamines.* Org Biomol Chem, 2003. **1**(23): p. 4323-8.

85. How, Z.T., et al., *Organic chloramines in drinking water: An assessment of formation, stability, reactivity and risk.* Water Res, 2016. **93**: p. 65-73.

86. How, Z.T., et al., *Chlorination of Amino Acids: Reaction Pathways and Reaction Rates.* Environ Sci Technol, 2017. **51**(9): p. 4870-4876.

87. Zgliczynski, J.M. and T. Stelmaszynska, *Chlorinating ability of human phagocytosing leucocytes.* Eur J Biochem, 1975. **56**(1): p. 157-62.

88. Ostrowski, W., et al., *Chloramines as intermediates of oxidation reactions of amino acids by myeloperoxidase.* Biochemica et Biophysica Acta, 1971. **235**: p. 419-424.

89. Marcinkiewicz, J. and E. Kontny, *Taurine and inflammatory diseases.* Amino Acids, 2014. **46**(1): p. 7-20.

90. Chesney, R.W., *Taurine: its biological role and clinical implications.* Adv Pediatr, 1985. **32**: p. 1-42.

91. Fukuda, K., et al., *Free amino acid content of lymphocytes nd granulocytes compared.* Clin Chem, 1982. **28**(8): p. 1758-61.

92. Huxtable, R.J., *Physiological actions of taurine.* Physiol Rev, 1992. **72**(1): p. 101-63.

93. Learn, D.B., V.A. Fried, and E.L. Thomas, *Taurine and hypotaurine content of human leukocytes.* J Leukoc Biol, 1990. **48**(2): p. 174-82.

94. Thomas, E.L., *Myeloperoxidase-hydrogen peroxide-chloride antimicrobial system: effect of exogenous amines on antibacterial action against Escherichia coli.* Infect Immun, 1979. **25**(1): p. 110-6.

95. Niu, X., et al., *Protective effects of taurine against inflammation, apoptosis, and oxidative stress in brain injury.* Mol Med Rep, 2018. **18**(5): p. 4516-4522.

96. Gottardi, W. and M. Nagl, *Chemical properties of N-chlorotaurine sodium, a key compound in the human defence system.* Arch Pharm (Weinheim), 2002. **335**(9): p. 411-21.

97. Nagl, M., et al., *Bactericidal activity of micromolar N-chlorotaurine: evidence for its antimicrobial function in the human defense system.* Antimicrob Agents Chemother, 2000. **44**(9): p. 2507-13.

98. Nagl, M. and W. Gottardi, *Rapid killing of Mycobacterium terrae by N-chlorotaurine in the presence of ammonium is caused by the reaction product monochloramine.* J Pharm Pharmacol, 1998. **50**(11): p. 1317-20.

99. Nagl, M., et al., *Tolerance and bactericidal action of N-chlorotaurine in a urinary tract infection by an omniresistant Pseudomonas aeruginosa.* Zentralbl Bakteriol, 1998. **288**(2): p. 217-23.

100. Nagl, M., et al., *Tolerance of N-chlorotaurine, an endogenous antimicrobial agent, in the rabbit and human eye--a phase I clinical study.* J Ocul Pharmacol Ther, 1998. **14**(3): p. 283-90.

101. Nagl, M., C. Larcher, and W. Gottardi, *Activity of N-chlorotaurine against herpes simplex- and adenoviruses.* Antiviral Res, 1998. **38**(1): p. 25-30.

102. Nagl, M., et al., *The postantibiotic effect of N-chlorotaurine on Staphylococcus aureus. Application in the mouse peritonitis model.* J Antimicrob Chemother, 1999. **43**(6): p. 805-9.

103. Nagl, M., et al., *Tolerance of N-chlorotaurine, a new antimicrobial agent, in infectious conjunctivitis - a phase II pilot study.* Ophthalmologica, 2000. **214**(2): p. 111-4.

104. Nagl, M., et al., *Enhanced fungicidal activity of N-chlorotaurine in nasal secretion.* J Antimicrob Chemother, 2001. **47**(6): p. 871-4.

105. Gottardi, W., M. Hagleitner, and M. Nagl, *The influence of plasma on the disinfecting activity of the new antimicrobial agent N-chlorotaurine-sodium in comparison with chloramine T.* J Pharm Pharmacol, 2001. **53**(5): p. 689-97.

106. Neher, A., et al., *N-chlorotaurine, a novel endogenous antimicrobial agent: tolerability testing in a mouse model.* Arch Otolaryngol Head Neck Surg, 2001. **127**(5): p. 530-3.

107. Nagl, M., et al., *Impact of N-chlorotaurine on viability and production of secreted aspartyl proteinases of Candida spp.* Antimicrob Agents Chemother, 2002. **46**(6): p. 1996-9.

108. Gstottner, M., et al., *Refractory rhinosinusitis complicating immunosuppression: application of N-chlorotaurine, a novel endogenous antiseptic agent.* ORL J Otorhinolaryngol Relat Spec, 2003. **65**(5): p. 303-5.

109. Nagl, M., et al., *Tolerability and efficacy of N-chlorotaurine in comparison with chloramine T for the treatment of chronic leg ulcers with a purulent coating: a randomized phase II study.* Br J Dermatol, 2003. **149**(3): p. 590-7.

110. Hofer, E., et al., *In vitro study on the influence of N-chlorotaurine on the ciliary beat frequency of nasal mucosa.* Am J Rhinol, 2003. **17**(3): p. 149-52.

111. Neher, A., et al., *Acute otitis externa: efficacy and tolerability of N-chlorotaurine, a novel endogenous antiseptic agent.* Laryngoscope, 2004. **114**(5): p. 850-4.

112. Neher, A., et al., *Tolerability of N-chlorotaurine in the guinea pig middle ear: a pilot study using an improved application system.* Ann Otol Rhinol Laryngol, 2004. **113**(1): p. 76-81.

113. Neher, A., et al., *Tolerability of N-chlorotaurine in chronic rhinosinusitis applied via yamik catheter.* Auris Nasus Larynx, 2005. **32**(4): p. 359-64.

114. Teuchner, B., et al., *Tolerability and efficacy of N-chlorotaurine in epidemic keratoconjunctivitis--a double-blind, randomized, phase-2 clinical trial.* J Ocul Pharmacol Ther, 2005. **21**(2): p. 157-65.

115. Reeves, E.P., et al., *Effect of N-chlorotaurine on Aspergillus, with particular reference to destruction of secreted gliotoxin.* J Med Microbiol, 2006. **55**(Pt 7): p. 913-8.

116. Romanowski, E.G., et al., *N-chlorotaurine is an effective antiviral agent against adenovirus in vitro and in the Ad5/NZW rabbit ocular model.* Invest Ophthalmol Vis Sci, 2006. **47**(5): p. 2021-6.

117. Arnitz, R., et al., *A novel N-chlorotaurine-corticosteroid combination as a preservative-free local disinfectant: influence on the ciliary beat frequency in vitro.* Acta Otolaryngol, 2006. **126**(3): p. 291-4.

118. Arnitz, R., et al., *Protein sites of attack of N-chlorotaurine in Escherichia coli.* Proteomics, 2006. **6**(3): p. 865-9.

119. Gottardi, W., R. Arnitz, and M. Nagl, *N-Chlorotaurine and ammonium chloride: an antiseptic preparation with strong bactericidal activity.* Int J Pharm, 2007. **335**(1-2): p. 32-40.

120. Neher, A., et al., *N-chlorotaurine--a new safe substance for postoperative ear care.* Auris Nasus Larynx, 2007. **34**(1): p. 19-22.

121. Teuchner, B., et al., *Tolerability of N-chlorotaurine plus ammonium chloride in the rabbit and human eye--a phase 1 clinical study.* Graefes Arch Clin Exp Ophthalmol, 2008. **246**(12): p. 1723-30.

122. Neher, A., et al., *Antimicrobial activity of dexamethasone and its combination with N-chlorotaurine.* Arch Otolaryngol Head Neck Surg, 2008. **134**(6): p. 615-20.

123. Furnkranz, U., et al., *Cytotoxic activity of N-chlorotaurine on Acanthamoeba spp.* Antimicrob Agents Chemother, 2008. **52**(2): p. 470-6.

124. Geiger, R., et al., *Tolerability of inhaled N-chlorotaurine in the pig model.* BMC Pulm Med, 2009. **9**: p. 33.

125. Lorenz, K., et al., *Effect of N-chlorotaurine mouth rinses on plaque regrowth and plaque vitality.* Clin Oral Investig, 2009. **13**(1): p. 9-14.

126. Gottardi, W. and M. Nagl, *N-chlorotaurine, a natural antiseptic with outstanding tolerability.* J Antimicrob Chemother, 2010. **65**(3): p. 399-409.

127. Huemer, H.P., M. Nagl, and E.U. Irschick, *In vitro prevention of vaccinia and herpesvirus infection spread in explanted human corneas by N-chlorotaurine.* Ophthalmic Res, 2010. **43**(3): p. 145-52.

128. Schwienbacher, M., et al., *Tolerability of inhaled N-chlorotaurine in an acute pig streptococcal lower airway inflammation model.* BMC Infect Dis, 2011. **11**: p. 231.

129. Furnkranz, U., et al., *In vitro activity of N-chlorotaurine (NCT) in combination with NH4Cl against Trichomonas vaginalis.* Int J Antimicrob Agents, 2011. **37**(2): p. 171-3.

130. Eitzinger, C., et al., *N-chlorotaurine, a long-lived oxidant produced by human leukocytes, inactivates Shiga toxin of enterohemorrhagic Escherichia coli.* PLoS One, 2012. **7**(11): p. e47105.

131. Teuchner, B., et al., *N-chlorotaurine and its analogues N,N-dichloro-2,2-dimethyltaurine and N-monochloro-2,2-dimethyltaurine are safe and effective bactericidal agents in ex vivo corneal infection models.* Acta Ophthalmol, 2012. **90**(8): p. e632-7.

132. Martini, C., et al., *Antimicrobial and anticoagulant activities of N-chlorotaurine, N,N-dichloro-2,2-dimethyltaurine, and N-monochloro-2,2-dimethyltaurine in human blood.* Antimicrob Agents Chemother, 2012. **56**(4): p. 1979-84.

133. Ammann, C.G., et al., *Influence of poly-N-acetylglucosamine in the extracellular matrix on N-chlorotaurine mediated killing of Staphylococcus epidermidis.* New Microbiol, 2014. **37**(3): p. 383-6.

134. Coraca-Huber, D.C., et al., *Bactericidal activity of N-chlorotaurine against biofilm-forming bacteria grown on metal disks.* Antimicrob Agents Chemother, 2014. **58**(4): p. 2235-9.

135. Lackner, M., et al., *N-Chlorotaurine Exhibits Fungicidal Activity against Therapy-Refractory Scedosporium Species and Lomentospora prolificans.* Antimicrob Agents Chemother, 2015. **59**(10): p. 6454-62.

136. Mustedanagic, J., V.F. Ximenes, and M. Nagl, *Microbicidal activity of N-chlorotaurine in combination with hydrogen peroxide.* AMB Express, 2017. **7**(1): p. 102.

137. Gruber, M., et al., *Bactericidal and Fungicidal Activity of N-Chlorotaurine Is Enhanced in Cystic Fibrosis Sputum Medium.* Antimicrob Agents Chemother, 2017. **61**(5).

138. Bellmann-Weiler, R., et al., *The endogenous antiseptic N-chlorotaurine irreversibly inactivates Chlamydia pneumoniae and Chlamydia trachomatis.* J Med Microbiol, 2018. **67**(9): p. 1410-1415.

139. Arnitz, R., et al., *Tolerability of inhaled N-chlorotaurine in humans: a double-blind randomized phase I clinical study.* Ther Adv Respir Dis, 2018. **12**: p. 1753466618778955.

140. Nagl, M., R. Arnitz, and M. Lackner, *N-Chlorotaurine, a Promising Future Candidate for Topical Therapy of Fungal Infections.* Mycopathologia, 2018. **183**(1): p. 161-170.

141. Kim, J.W. and C. Kim, *Inhibition of LPS-induced NO production by taurine chloramine in macrophages is mediated though Ras-ERK-NF-kappaB.* Biochem Pharmacol, 2005. **70**(9): p. 1352-60.

142. Kim, C., H.S. Choi, and J.W. Kim, *Taurine chloramine inhibits the production of nitric oxide and superoxide anion by modulating specific mitogen-activated protein kinases.* Adv Exp Med Biol, 2006. **583**: p. 493-8.

143. Choi, H.S., Y.N. Cha, and C. Kim, *Taurine chloramine inhibits PMA-stimulated superoxide production in human neutrophils perhaps by inhibiting phosphorylation and translocation of p47(phox).* Int Immunopharmacol, 2006. **6**(9): p. 1431-40.

144. Kim, K.S., et al., *Taurine chloramine differentially inhibits matrix metalloproteinase 1 and 13 synthesis in interleukin-1beta stimulated fibroblast-like synoviocytes.* Arthritis Res Ther, 2007. **9**(4): p. R80.

145. Sun Jang, J., et al., *Taurine Chloramine Activates Nrf2, Increases HO-1 Expression and Protects Cells from Death Caused by Hydrogen Peroxide.* J Clin Biochem Nutr, 2009. **45**(1): p. 37-43.

146. Kim, C., et al., *Taurine chloramine induces heme oxygenase-1 expression via Nrf2 activation in murine macrophages.* Int Immunopharmacol, 2010. **10**(4): p. 440-6.

147. Kim, C. and Y.N. Cha, *Taurine chloramine produced from taurine under inflammation provides anti-inflammatory and cytoprotective effects.* Amino Acids, 2014. **46**(1): p. 89-100.

148. Kim, C. and I.S. Kang, *Taurine Chloramine, a Taurine Metabolite from Activated Neutrophils, Inhibits Osteoclastogenesis by Suppressing NFATc1 Expression.* Adv Exp Med Biol, 2015. **803**: p. 99-107.

149. Kim, W., et al., *Taurine Chloramine Stimulates Efferocytosis Through Upregulation of Nrf2-Mediated Heme Oxygenase-1 Expression in Murine Macrophages: Possible Involvement of Carbon Monoxide.* Antioxid Redox Signal, 2015. **23**(2): p. 163-77.

150. Joo, K., et al., *An anti-inflammatory mechanism of taurine conjugated 5-aminosalicylic acid against experimental colitis: taurine chloramine potentiates inhibitory effect of 5-aminosalicylic acid on IL-1beta-mediated NFkappaB activation.* Eur J Pharmacol, 2009. **618**(1-3): p. 91-7.

151. Karavolos, M.H., et al., *Role and regulation of the superoxide dismutases of Staphylococcus aureus.* Microbiology, 2003. **149**(Pt 10): p. 2749-58.

152. Beavers, W.N. and E.P. Skaar, *Neutrophil-generated oxidative stress and protein damage in Staphylococcus aureus.* Pathog Dis, 2016. **74**(6).

153. Clements, M.O., S.P. Watson, and S.J. Foster, *Characterization of the major superoxide dismutase of Staphylococcus aureus and its role in starvation survival, stress resistance, and pathogenicity.* J Bacteriol, 1999. **181**(13): p. 3898-903.

154. Valderas, M.W. and M.E. Hart, *Identification and characterization of a second superoxide dismutase gene (sodM) from Staphylococcus aureus.* J Bacteriol, 2001. **183**(11): p. 3399-407.

155. Winterbourn, C.C., *Reconciling the chemistry and biology of reactive oxygen species.* Nat Chem Biol, 2008. **4**(5): p. 278-86.

156. Halliwell, G., *Catalytic Decomposition of Cellulose under Biological Conditions.* Biochem J, 1965. **95**: p. 35-40.

157. Das, D., S.S. Saha, and B. Bishayi, *Intracellular survival of Staphylococcus aureus: correlating production of catalase and superoxide dismutase with levels of inflammatory cytokines.* Inflamm Res, 2008. **57**(7): p. 340-9.

158. Resch, A., et al., *Differential gene expression profiling of Staphylococcus aureus cultivated under biofilm and planktonic conditions.* Appl Environ Microbiol, 2005. **71**(5): p. 2663-76.

159. Hampton, M.B., A.J. Kettle, and C.C. Winterbourn, *Involvement of superoxide and myeloperoxidase in oxygen-dependent killing of Staphylococcus aureus by neutrophils.* Infect Immun, 1996. **64**(9): p. 3512-7.

160. Rosen, G.M. and B.A. Freeman, *Detection of superoxide generated by endothelial cells.* Proc Natl Acad Sci U S A, 1984. **81**(23): p. 7269-73.

161. Mandell, G.L., *Catalase, superoxide dismutase, and virulence of Staphylococcus aureus. In vitro and in vivo studies with emphasis on staphylococcal--leukocyte interaction.* J Clin Invest, 1975. **55**(3): p. 561-6.

162. Chelikani, P., I. Fita, and P.C. Loewen, *Diversity of structures and properties among catalases.* Cell Mol Life Sci, 2004. **61**(2): p. 192-208.

163. Park, B., V. Nizet, and G.Y. Liu, *Role of Staphylococcus aureus catalase in niche competition against Streptococcus pneumoniae.* J Bacteriol, 2008. **190**(7): p. 2275-8.

164. Cosgrove, K., et al., *Catalase (KatA) and alkyl hydroperoxide reductase (AhpC) have compensatory roles in peroxide stress resistance and are required for survival,*

*persistence, and nasal colonization in Staphylococcus aureus.* J Bacteriol, 2007. **189**(3): p. 1025-35.

165. Poole, L.B., *Bacterial defenses against oxidants: mechanistic features of cysteine-based peroxidases and their flavoprotein reductases.* Arch Biochem Biophys, 2005. **433**(1): p. 240-54.

166. Argyrou, A. and J.S. Blanchard, *Flavoprotein disulfide reductases: advances in chemistry and function.* Prog Nucleic Acid Res Mol Biol, 2004. **78**: p. 89-142.

167. Wood, Z.A., L.B. Poole, and P.A. Karplus, *Structure of intact AhpF reveals a mirrored thioredoxin-like active site and implies large domain rotations during catalysis.* Biochemistry, 2001. **40**(13): p. 3900-11.

168. Poole, L.B., et al., *AhpF can be dissected into two functional units: tandem repeats of two thioredoxin-like folds in the N-terminus mediate electron transfer from the thioredoxin reductase-like C-terminus to AhpC.* Biochemistry, 2000. **39**(22): p. 6602-15.

169. Poole, L.B. and H.R. Ellis, *Identification of cysteine sulfenic acid in AhpC of alkyl hydroperoxide reductase.* Methods Enzymol, 2002. **348**: p. 122-36.

170. Ellis, H.R. and L.B. Poole, *Roles for the two cysteine residues of AhpC in catalysis of peroxide reduction by alkyl hydroperoxide reductase from Salmonella typhimurium.* Biochemistry, 1997. **36**(43): p. 13349-56.

171. Jonsson, T.J., H.R. Ellis, and L.B. Poole, *Cysteine reactivity and thiol-disulfide interchange pathways in AhpF and AhpC of the bacterial alkyl hydroperoxide reductase system.* Biochemistry, 2007. **46**(19): p. 5709-21.

172. Hall, A., et al., *Redox-dependent dynamics of a dual thioredoxin fold protein: evolution of specialized folds.* Biochemistry, 2009. **48**(25): p. 5984-93.

173. Horsburgh, M.J., et al., *PerR controls oxidative stress resistance and iron storage proteins and is required for virulence in Staphylococcus aureus.* Infect Immun, 2001. **69**(6): p. 3744-54.

174. Poole, L.B. and H.R. Ellis, *Flavin-dependent alkyl hydroperoxide reductase from Salmonella typhimurium. 1. Purification and enzymatic activities of overexpressed AhpF and AhpC proteins.* Biochemistry, 1996. **35**(1): p. 56-64.

175. Forrester, M.T. and M.W. Foster, *Protection from nitrosative stress: a central role for microbial flavohemoglobin.* Free Radic Biol Med, 2012. **52**(9): p. 1620-33.

176. Goncalves, V.L., et al., *Flavohemoglobin requires microaerophilic conditions for nitrosative protection of Staphylococcus aureus.* FEBS Lett, 2006. **580**(7): p. 1817-21.

177. Bonamore, A. and A. Boffi, *Flavohemoglobin: structure and reactivity.* IUBMB Life, 2008. **60**(1): p. 19-28.

178. Richardson, A.R., P.M. Dunman, and F.C. Fang, *The nitrosative stress response of Staphylococcus aureus is required for resistance to innate immunity.* Mol Microbiol, 2006. **61**(4): p. 927-39.

179. Kinkel, T.L., et al., *The Staphylococcus aureus SrrAB two-component system promotes resistance to nitrosative stress and hypoxia.* MBio, 2013. **4**(6): p. e00696-13.

180. Coker, M.S., et al., *Interactions of staphyloxanthin and enterobactin with myeloperoxidase and reactive chlorine species.* Arch Biochem Biophys, 2018. **646**: p. 80-89.

181. Niki, E., *Lipid peroxidation: physiological levels and dual biological effects.* Free Radic Biol Med, 2009. **47**(5): p. 469-84.

182. Stanley, N.R., D.I. Pattison, and C.L. Hawkins, *Ability of hypochlorous acid and N-chloramines to chlorinate DNA and its constituents.* Chem Res Toxicol, 2010. **23**(7): p. 1293-302.

183. Cabiscol, E., J. Tamarit, and J. Ros, *Oxidative stress in bacteria and protein damage by reactive oxygen species.* Int Microbiol, 2000. **3**(1): p. 3-8.

184. Ahn, S., et al., *Role of Glyoxylate Shunt in Oxidative Stress Response.* J Biol Chem, 2016. **291**(22): p. 11928-38.

185. Grimsrud, P.A., et al., *Oxidative stress and covalent modification of protein with bioactive aldehydes.* J Biol Chem, 2008. **283**(32): p. 21837-41.

186. Perez, J.M., et al., *Escherichia coli YqhD exhibits aldehyde reductase activity and protects from the harmful effect of lipid peroxidation-derived aldehydes.* J Biol Chem, 2008. **283**(12): p. 7346-53.

187. Marnett, L.J., J.N. Riggins, and J.D. West, *Endogenous generation of reactive oxidants and electrophiles and their reactions with DNA and protein.* J Clin Invest, 2003. **111**(5): p. 583-93.

188. Singh, S., et al., *Aldehyde dehydrogenases in cellular responses to oxidative/electrophilic stress.* Free Radic Biol Med, 2013. **56**: p. 89-101.

189. Imber, M., et al., *The aldehyde dehydrogenase AldA contributes to the hypochlorite defense and is redox-controlled by protein S-bacillithiolation in Staphylococcus aureus.* Redox Biol, 2018. **15**: p. 557-568.

190. Ferguson, G.P., et al., *Methylglyoxal production in bacteria: suicide or survival?* Arch Microbiol, 1998. **170**(4): p. 209-18.

191. Booth, I.R., et al., *Bacterial production of methylglyoxal: a survival strategy or death by misadventure?* Biochem Soc Trans, 2003. **31**(Pt 6): p. 1406-8.

192. Chandrangsu, P., et al., *The Role of Bacillithiol in Gram-Positive Firmicutes.* Antioxid Redox Signal, 2018. **28**(6): p. 445-462.

193. Pelz, A., et al., *Structure and biosynthesis of staphyloxanthin from Staphylococcus aureus.* J Biol Chem, 2005. **280**(37): p. 32493-8.

194. Liu, G.Y., et al., *Staphylococcus aureus golden pigment impairs neutrophil killing and promotes virulence through its antioxidant activity.* J Exp Med, 2005. **202**(2): p. 209-15.

195. Holmgren, A., *Bovine thioredoxin system. Purification of thioredoxin reductase from calf liver and thymus and studies of its function in disulfide reduction.* J Biol Chem, 1977. **252**(13): p. 4600-6.

196. Uziel, O., et al., *Transcriptional regulation of the Staphylococcus aureus thioredoxin and thioredoxin reductase genes in response to oxygen and disulfide stress.* J Bacteriol, 2004. **186**(2): p. 326-34.

197. Liao, X., et al., *Targeting the Thioredoxin Reductase-Thioredoxin System from Staphylococcus aureus by Silver Ions.* Inorg Chem, 2017. **56**(24): p. 14823-14830.

198. Peng, H., et al., *Thioredoxin Profiling of Multiple Thioredoxin-Like Proteins in Staphylococcus aureus.* Front Microbiol, 2018. **9**: p. 2385.

199. Arner, E.S. and A. Holmgren, *Physiological functions of thioredoxin and thioredoxin reductase.* Eur J Biochem, 2000. **267**(20): p. 6102-9.

200. Stryer, L., A. Holmgren, and P. Reichard, *Thioredoxin. A localized conformational change accompanying reduction of the protein to the sulfhydryl form.* Biochemistry, 1967. **6**(4): p. 1016-20.

201. Lu, J. and A. Holmgren, *The thioredoxin superfamily in oxidative protein folding.* Antioxid Redox Signal, 2014. **21**(3): p. 457-70.

202. Holmgren, A., *Enzymatic reduction-oxidation of protein disulfides by thioredoxin.* Methods Enzymol, 1984. **107**: p. 295-300.

203. Arner, E.S., M. Bjornstedt, and A. Holmgren, *1-Chloro-2,4-dinitrobenzene is an irreversible inhibitor of human thioredoxin reductase. Loss of thioredoxin disulfide reductase activity is accompanied by a large increase in NADPH oxidase activity.* J Biol Chem, 1995. **270**(8): p. 3479-82.

204. Holmgren, A. and M. Bjornstedt, *Thioredoxin and thioredoxin reductase.* Methods Enzymol, 1995. **252**: p. 199-208.

205. Russel, M. and P. Model, *Sequence of thioredoxin reductase from Escherichia coli. Relationship to other flavoprotein disulfide oxidoreductases.* J Biol Chem, 1988. **263**(18): p. 9015-9.

206. Gleason, F.K. and A. Holmgren, *Thioredoxin and related proteins in procaryotes.* FEMS Microbiol Rev, 1988. **4**(4): p. 271-97.

207. Holmgren, A., *Thioredoxin.* Annu Rev Biochem, 1985. **54**: p. 237-71.

208. Prongay, A.J., D.R. Engelke, and C.H. Williams, Jr., *Characterization of two active site mutations of thioredoxin reductase from Escherichia coli.* J Biol Chem, 1989. **264**(5): p. 2656-64.

209. Atkinson, H.J. and P.C. Babbitt, *An atlas of the thioredoxin fold class reveals the complexity of function-enabling adaptations.* PLoS Comput Biol, 2009. **5**(10): p. e1000541.

210. Holmgren, A., *Thioredoxin structure and mechanism: conformational changes on oxidation of the active-site sulfhydryls to a disulfide.* Structure, 1995. **3**(3): p. 239-43.

211. Gaballa, A., et al., *Biosynthesis and functions of bacillithiol, a major low-molecular-weight thiol in Bacilli.* Proc Natl Acad Sci U S A, 2010. **107**(14): p. 6482-6.

212. Ren, X., et al., *Selenocysteine in mammalian thioredoxin reductase and application of ebselen as a therapeutic.* Free Radic Biol Med, 2018. **127**: p. 238-247.

213. Gustafsson, T.N., et al., *Ebselen and analogs as inhibitors of Bacillus anthracis thioredoxin reductase and bactericidal antibacterials targeting Bacillus species, Staphylococcus aureus and Mycobacterium tuberculosis.* Biochim Biophys Acta, 2016. **1860**(6): p. 1265-71.

214. Du, Y., et al., *Thioredoxin 1 is inactivated due to oxidation induced by peroxiredoxin under oxidative stress and reactivated by the glutaredoxin system.* J Biol Chem, 2013. **288**(45): p. 32241-7.

215. Lu, J., et al., *Inhibition of bacterial thioredoxin reductase: an antibiotic mechanism targeting bacteria lacking glutathione.* FASEB J, 2013. **27**(4): p. 1394-403.

216. Du, Y., et al., *Glutathione and glutaredoxin act as a backup of human thioredoxin reductase 1 to reduce thioredoxin 1 preventing cell death by aurothioglucose.* J Biol Chem, 2012. **287**(45): p. 38210-9.

217. Lu, J., C. Berndt, and A. Holmgren, *Metabolism of selenium compounds catalyzed by the mammalian selenoprotein thioredoxin reductase.* Biochim Biophys Acta, 2009. **1790**(11): p. 1513-9.

218. Fang, J., et al., *Ebselen: a thioredoxin reductase-dependent catalyst for alpha-tocopherol quinone reduction.* Toxicol Appl Pharmacol, 2005. **207**(2 Suppl): p. 103-9.

219. Zhao, R. and A. Holmgren, *Ebselen is a dehydroascorbate reductase mimic, facilitating the recycling of ascorbate via mammalian thioredoxin systems.* Antioxid Redox Signal, 2004. **6**(1): p. 99-104.

220. Zhao, R. and A. Holmgren, *A novel antioxidant mechanism of ebselen involving ebselen diselenide, a substrate of mammalian thioredoxin and thioredoxin reductase.* J Biol Chem, 2002. **277**(42): p. 39456-62.

221. Zhao, R., H. Masayasu, and A. Holmgren, *Ebselen: a substrate for human thioredoxin reductase strongly stimulating its hydroperoxide reductase activity and a superfast thioredoxin oxidant.* Proc Natl Acad Sci U S A, 2002. **99**(13): p. 8579-84.

222. Holmgren, A., *Antioxidant function of thioredoxin and glutaredoxin systems.* Antioxid Redox Signal, 2000. **2**(4): p. 811-20.

223. Hoffner, S., et al., *Bacterial thioredoxin reductase inhibitors and methods for use thereof*, WO, Editor. 2007.

224. Singh, V.K. and J. Moskovitz, *Multiple methionine sulfoxide reductase genes in Staphylococcus aureus: expression of activity and roles in tolerance of oxidative stress.* Microbiology, 2003. **149**(Pt 10): p. 2739-47.

225. Pang, Y.Y., et al., *Methionine sulfoxide reductases protect against oxidative stress in Staphylococcus aureus encountering exogenous oxidants and human neutrophils.* J Innate Immun, 2014. **6**(3): p. 353-64.

226. Singh, V.K., et al., *Significance of four methionine sulfoxide reductases in Staphylococcus aureus.* PLoS One, 2015. **10**(2): p. e0117594.

227. Singh, V.K., K. Singh, and K. Baum, *The Role of Methionine Sulfoxide Reductases in Oxidative Stress Tolerance and Virulence of Staphylococcus aureus and Other Bacteria.* Antioxidants (Basel), 2018. **7**(10).

228. Levine, R.L., et al., *Methionine residues as endogenous antioxidants in proteins.* Proc Natl Acad Sci U S A, 1996. **93**(26): p. 15036-40.

229. Sreekumar, P.G., D.R. Hinton, and R. Kannan, *Methionine sulfoxide reductase A: Structure, function and role in ocular pathology.* World J Biol Chem, 2011. **2**(8): p. 184-92.

230. Jakob, U., et al., *Chaperone activity with a redox switch.* Cell, 1999. **96**(3): p. 341-52.

231. Jakob, U., M. Eser, and J.C. Bardwell, *Redox switch of hsp33 has a novel zinc-binding motif.* J Biol Chem, 2000. **275**(49): p. 38302-10.

232. Ilbert, M., et al., *The redox-switch domain of Hsp33 functions as dual stress sensor.* Nat Struct Mol Biol, 2007. **14**(6): p. 556-63.

233. Wholey, W.Y. and U. Jakob, *Hsp33 confers bleach resistance by protecting elongation factor Tu against oxidative degradation in Vibrio cholerae.* Mol Microbiol, 2012. **83**(5): p. 981-91.

234. Voth, W., et al., *The protein targeting factor Get3 functions as ATP-independent chaperone under oxidative stress conditions.* Mol Cell, 2014. **56**(1): p. 116-27.

235. Matthews, T., R.G. Baumann, and T.L. Domanski, *Analysis and Characterization of Staphylococcus aureus ClpB and Associated Co-Chaperone Proteins dnaK, dnaJ and grpE.* American Society for Biochemistry and Molecular Biology, 2007. **21**(6).

236. Nachin, L., et al., *SufC: an unorthodox cytoplasmic ABC/ATPase required for [Fe-S] biogenesis under oxidative stress.* EMBO J, 2003. **22**(3): p. 427-37.

237. Overton, T.W., et al., *Widespread distribution in pathogenic bacteria of di-iron proteins that repair oxidative and nitrosative damage to iron-sulfur centers.* J Bacteriol, 2008. **190**(6): p. 2004-13.

238. Brunskill, E.W., B.L. de Jonge, and K.W. Bayles, *The Staphylococcus aureus scdA gene: a novel locus that affects cell division and morphogenesis.* Microbiology, 1997. **143 ( Pt 9)**: p. 2877-82.

239. Chang, W., et al., *Global transcriptome analysis of Staphylococcus aureus response to hydrogen peroxide.* J Bacteriol, 2006. **188**(4): p. 1648-59.

240. Wolf, C., et al., *Proteomic analysis of antioxidant strategies of Staphylococcus aureus: diverse responses to different oxidants.* Proteomics, 2008. **8**(15): p. 3139-53.

241. Gebendorfer, K.M., et al., *Identification of a hypochlorite-specific transcription factor from Escherichia coli.* J Biol Chem, 2012. **287**(9): p. 6892-903.

242. Wang, S., et al., *Transcriptomic response of Escherichia coli O157:H7 to oxidative stress.* Appl Environ Microbiol, 2009. **75**(19): p. 6110-23.

243. Peeters, E., et al., *Transcriptional response of Burkholderia cenocepacia J2315 sessile cells to treatments with high doses of hydrogen peroxide and sodium hypochlorite.* BMC Genomics, 2010. **11**: p. 90.

244. Small, D.A., et al., *Toxicogenomic analysis of sodium hypochlorite antimicrobial mechanisms in Pseudomonas aeruginosa.* Appl Microbiol Biotechnol, 2007. **74**(1): p. 176-85.

245. Wang, S., et al., *Transcriptomic responses of Salmonella enterica serovars Enteritidis and Typhimurium to chlorine-based oxidative stress.* Appl Environ Microbiol, 2010. **76**(15): p. 5013-24.

246. Chi, B.K., et al., *S-bacillithiolation protects against hypochlorite stress in Bacillus subtilis as revealed by transcriptomics and redox proteomics.* Mol Cell Proteomics, 2011. **10**(11): p. M111 009506.

247. Choi, H., et al., *Structural basis of the redox switch in the OxyR transcription factor.* Cell, 2001. **105**(1): p. 103-13.

248. Xiong, A., et al., *Molecular characterization of the ferric-uptake regulator, fur, from Staphylococcus aureus.* Microbiology, 2000. **146 ( Pt 3)**: p. 659-68.

249. Morrissey, J.A., et al., *The staphylococcal ferritins are differentially regulated in response to iron and manganese and via PerR and Fur.* Infect Immun, 2004. **72**(2): p. 972-9.

250. Gaupp, R., N. Ledala, and G.A. Somerville, *Staphylococcal response to oxidative stress.* Front Cell Infect Microbiol, 2012. **2**: p. 33.

251. Luong, T.T., et al., *Transcription Profiling of the mgrA Regulon in Staphylococcus aureus.* J Bacteriol, 2006. **188**(5): p. 1899-910.

252. Chen, P.R., et al., *An oxidation-sensing mechanism is used by the global regulator MgrA in Staphylococcus aureus.* Nat Chem Biol, 2006. **2**(11): p. 591-5.

253. Allard, M., et al., *Transcriptional modulation of some Staphylococcus aureus iron-regulated genes during growth in vitro and in a tissue cage model in vivo.* Microbes Infect, 2006. **8**(7): p. 1679-90.

254. Spiro, S. and B. D'Autreaux, *Non-heme iron sensors of reactive oxygen and nitrogen species.* Antioxid Redox Signal, 2012. **17**(9): p. 1264-76.

255. Chen, P.R., P. Brugarolas, and C. He, *Redox signaling in human pathogens.* Antioxid Redox Signal, 2011. **14**(6): p. 1107-18.

256. Chen, P.R., et al., *A new oxidative sensing and regulation pathway mediated by the MgrA homologue SarZ in Staphylococcus aureus.* Mol Microbiol, 2009. **71**(1): p. 198-211.

257. Ballal, A., B. Ray, and A.C. Manna, *sarZ, a sarA family gene, is transcriptionally activated by MgrA and is involved in the regulation of genes encoding exoproteins in Staphylococcus aureus.* J Bacteriol, 2009. **191**(5): p. 1656-65.

258. Ballal, A. and A.C. Manna, *Regulation of superoxide dismutase (sod) genes by SarA in Staphylococcus aureus.* J Bacteriol, 2009. **191**(10): p. 3301-10.

259. Ballal, A. and A.C. Manna, *Control of thioredoxin reductase gene (trxB) transcription by SarA in Staphylococcus aureus.* J Bacteriol, 2010. **192**(1): p. 336-45.

260. Ballal, A. and A.C. Manna, *Expression of the sarA family of genes in different strains of Staphylococcus aureus.* Microbiology, 2009. **155**(Pt 7): p. 2342-52.

261. Pamp, S.J., et al., *Spx is a global effector impacting stress tolerance and biofilm formation in Staphylococcus aureus.* J Bacteriol, 2006. **188**(13): p. 4861-70.

262. Jousselin, A., et al., *The Staphylococcus aureus thiol/oxidative stress global regulator Spx controls trfA, a gene implicated in cell wall antibiotic resistance.* Antimicrob Agents Chemother, 2013. **57**(7): p. 3283-92.

263. Hillion, M. and H. Antelmann, *Thiol-based redox switches in prokaryotes.* Biol Chem, 2015. **396**(5): p. 415-44.

264. Loi, V.V., et al., *Redox-Sensing Under Hypochlorite Stress and Infection Conditions by the Rrf2-Family Repressor HypR in Staphylococcus aureus.* Antioxid Redox Signal, 2018. **29**(7): p. 615-636.

265. Pompella, A. and A. Corti, *Editorial: the changing faces of glutathione, a cellular protagonist.* Front Pharmacol, 2015. **6**: p. 98.

266. Pompella, A., et al., *The changing faces of glutathione, a cellular protagonist.* Biochem Pharmacol, 2003. **66**(8): p. 1499-503.

267. Rogers, J.M. and E.S. Hunter, 3rd, *Redox redux: a closer look at conceptal low molecular weight thiols.* Toxicol Sci, 2001. **62**(1): p. 1-3.

268. Van Laer, K., C.J. Hamilton, and J. Messens, *Low-molecular-weight thiols in thiol-disulfide exchange.* Antioxid Redox Signal, 2013. **18**(13): p. 1642-53.

269. delCardayre, S.B., et al., *Coenzyme A disulfide reductase, the primary low molecular weight disulfide reductase from Staphylococcus aureus. Purification and characterization of the native enzyme.* J Biol Chem, 1998. **273**(10): p. 5744-51.

270. Fahey, R.C., *Glutathione analogs in prokaryotes.* Biochim Biophys Acta, 2013. **1830**(5): p. 3182-98.

271. Newton, G.L., et al., *Low-molecular-weight thiols in streptomycetes and their potential role as antioxidants.* J Bacteriol, 1993. **175**(9): p. 2734-42.

272. Helmann, J.D., *Bacillithiol, a new player in bacterial redox homeostasis.* Antioxid Redox Signal, 2011. **15**(1): p. 123-33.

273. Perera, V.R., G.L. Newton, and K. Pogliano, *Bacillithiol: a key protective thiol in Staphylococcus aureus.* Expert Rev Anti Infect Ther, 2015. **13**(9): p. 1089-107.

274. Posada, A.C., et al., *Importance of bacillithiol in the oxidative stress response of Staphylococcus aureus.* Infect Immun, 2014. **82**(1): p. 316-32.

275. Reyes, A.M., et al., *Chemistry and Redox Biology of Mycothiol.* Antioxid Redox Signal, 2018. **28**(6): p. 487-504.

276. Imber, M., A.J. Pietrzyk-Brzezinska, and H. Antelmann, *Redox regulation by reversible protein S-thiolation in Gram-positive bacteria.* Redox Biol, 2018. **20**: p. 130-145.

277. Wang, M., Q. Zhao, and W. Liu, *The versatile low-molecular-weight thiols: Beyond cell protection.* Bioessays, 2015. **37**(12): p. 1262-7.

278. delCardayre, S.B. and J.E. Davies, *Staphylococcus aureus coenzyme A disulfide reductase, a new subfamily of pyridine nucleotide-disulfide oxidoreductase. Sequence, expression, and analysis of cdr.* J Biol Chem, 1998. **273**(10): p. 5752-7.

279. Newton, G.L., et al., *Distribution of thiols in microorganisms: mycothiol is a major thiol in most actinomycetes.* J Bacteriol, 1996. **178**(7): p. 1990-5.

280. Tsuchiya, Y., et al., *Protein CoAlation and antioxidant function of coenzyme A in prokaryotic cells.* Biochem J, 2018. **475**(11): p. 1909-1937.

281. Newton, G.L., et al., *Bacillithiol is an antioxidant thiol produced in Bacilli.* Nat Chem Biol, 2009. **5**(9): p. 625-7.

282. Newton, G.L., N. Buchmeier, and R.C. Fahey, *Biosynthesis and functions of mycothiol, the unique protective thiol of Actinobacteria.* Microbiol Mol Biol Rev, 2008. **72**(3): p. 471-94.

283. Rajkarnikar, A., et al., *Analysis of mutants disrupted in bacillithiol metabolism in Staphylococcus aureus.* Biochem Biophys Res Commun, 2013. **436**(2): p. 128-33.

284. Pother, D.C., et al., *Distribution and infection-related functions of bacillithiol in Staphylococcus aureus.* Int J Med Microbiol, 2013. **303**(3): p. 114-23.

285. Park, S. and J.A. Imlay, *High levels of intracellular cysteine promote oxidative DNA damage by driving the fenton reaction.* J Bacteriol, 2003. **185**(6): p. 1942-50.

286. Carlsson, J., et al., *Bactericidal effect of cysteine exposed to atmospheric oxygen.* Appl Environ Microbiol, 1979. **37**(3): p. 383-90.

287. Klopper, S.L., *Cloning and functional characterization of thiol sidulfide interchange system proteins from Staphylococcus aureus*, in *Department of Biochemistry*. 2013, Stellenbosch University: Stellenbosch. p. 90.

288. Ojha, S., E.C. Meng, and P.C. Babbitt, *Evolution of function in the "two dinucleotide binding domains" flavoproteins.* PLoS Comput Biol, 2007. **3**(7): p. e121.

289. Mallett, T.C., et al., *Structure of coenzyme A-disulfide reductase from Staphylococcus aureus at 1.54 A resolution.* Biochemistry, 2006. **45**(38): p. 11278-89.

290. Hille, R., S. Miller, and B. Palfey, *Handbook of Flavoproteins: Complex flavoproteins, dehydrogenases and physical methods*, R. Hille, Editor. 2013, DE GRUYTER. p. 1-429.

291. Luba, J., V. Charrier, and A. Claiborne, *Coenzyme A-disulfide reductase from Staphylococcus aureus: evidence for asymmetric behavior on interaction with pyridine nucleotides.* Biochemistry, 1999. **38**(9): p. 2725-37.

292. van der Westhuyzen, R. and E. Strauss, *Michael acceptor-containing coenzyme A analogues as inhibitors of the atypical coenzyme A disulfide reductase from Staphylococcus aureus.* J Am Chem Soc, 2010. **132**(37): p. 12853-5.

293. van der Westhuyzen, R., et al., *The antibiotic CJ-15,801 is an antimetabolite that hijacks and then inhibits CoA biosynthesis.* Chem Biol, 2012. **19**(5): p. 559-71.

294. Thorpe, C. and C.H. Williams, Jr., *Lipoamide dehydrogenase from pig heart. Pyridine nucleotide induced changes in monoalkylated two-electron reduced enzyme.* Biochemistry, 1981. **20**(6): p. 1507-13.

295. Hemila, H., *Lipoamide dehydrogenase of Staphylococcus aureus: nucleotide sequence and sequence analysis.* Biochim Biophys Acta, 1991. **1129**(1): p. 119-23.

296. Williams, C.H., Jr., et al., *Lipoamide dehydrogenase, glutathione reductase, thioredoxin reductase, and thioredoxin.* J Biol Chem, 1967. **242**(22): p. 5226-31.

297. Westphal, A.H. and A. de Kok, *Lipoamide dehydrogenase from Azotobacter vinelandii. Molecular cloning, organization and sequence analysis of the gene.* Eur J Biochem, 1988. **172**(2): p. 299-305.

298. Sahlman, L. and C.H. Williams, Jr., *Lipoamide dehydrogenase from Escherichia coli. Steady-state kinetics of the physiological reaction.* J Biol Chem, 1989. **264**(14): p. 8039-45.

299. Ravindran, S., et al., *Lipoyl domain-based mechanism for the integrated feedback control of the pyruvate dehydrogenase complex by enhancement of pyruvate dehydrogenase kinase activity.* J Biol Chem, 1996. **271**(2): p. 653-62.

300. Grayczyk, J.P., et al., *A Lipoylated Metabolic Protein Released by Staphylococcus aureus Suppresses Macrophage Activation.* Cell Host Microbe, 2017. **22**(5): p. 678-687 e9.

301. Voyich, J.M., et al., *Insights into Mechanisms Used by Staphylococcus aureus to Avoid Destruction by Human Neutrophils.* J Immunol, 2005. **174**(6): p. 3907-3919.

302. Gustafsson, T.N., et al., *Bacillus anthracis thioredoxin systems, characterization and role as electron donors for ribonucleotide reductase.* J Biol Chem, 2012. **287**(47): p. 39686-97.

303. Gaballa, A., et al., *Redox regulation in Bacillus subtilis: The bacilliredoxins BrxA(YphP) and BrxB(YqiW) function in de-bacillithiolation of S-bacillithiolated OhrR and MetE.* Antioxid Redox Signal, 2014. **21**(3): p. 357-67.

304. Mikheyeva, I.V., et al., *YpdA, a putative bacillithiol disulfide reductase, contributes to cellular redox homeostasis and virulence in Staphylococcus aureus.* Mol Microbiol, 2019.

Chapter 2

# CHARACTERIZATION OF *S. AUREUS* "MERA"

## 2.1 Introduction

As described in Chapter 1, *S. aureus* produces a tDBDF of unknown molecular function in response to oxidative stress, currently named "MerA" (designated as *Sa*MerA here on forth).

*Sa*MerA derives its name from its putative annotation as a mercuric reductase homologue (UniprotA0A224B076). This annotation is based on it showing sequence homology to known mercuric ion reductase (true "MerA") proteins. There are a few studies published to date that make mention of *Sa*MerA, yet the exact function of this protein remains unknown.

The first study that highlighted the physiological relevance of *Sa*MerA was done by Voyich *et al*, which showed that *Sa*MerA is upregulated more than 80 fold in *S. aureus* strains MW2, MnCop, LAC, MRSA252 and COL following phagocytosis by neutrophils [2]. In a separate study, it was found that *hypR-merA*, which encodes for the Rrf2-family regulator HypR and *Sa*MerA, were upregulated more than 180 fold under hypochlorite stress [3]. Finally, it was found that the *hypR merA* double mutant is also more sensitive to hypochlorite stress than the wild type [3].

Interestingly, the *E. coli* homologue of *Sa*MerA (referred to as YkgC or RclA) has also been studied. Jakob and coworkers identified a new *E. coli* reactive chlorine-specific transcription factor, RclR. They found, amongst other important results, that RclR is responsible for the control of the expression of three genes (one of which is YkgC/RclA) which are essential for bacterial survival when confronted with chlorine stress [4]. In the same study *E. coli* mutants lacking RclA/YkgC are found to show increased sensitivity towards hypochlorite [4]. In a different study, Wang *et al* reported that the gene *ykgC* was significantly upregulated in *E. coli O157:H7* human pathogen strains when exposed to hypochlorite [5].

Taken together, the results published to date all appear to point to the *Sa*MerA enzyme and its homologues playing a very important role in oxidative stress resistance in bacteria; however the exact function or substrate/s upon which this enzyme acts remains elusive. The fact that oxidants such as $H_2O_2$ and HOCl also produce a large variety of secondary oxidants—any of which could be the target of *Sa*MerA's enzymatic action—further complicates analysis of the system.

The current chapter describes the results of a study focused on the characterization of *Sa*MerA and identification of its most plausible physiological substrate, and as such the potential role it plays in *S. aureus'* oxidative stress resistance.

## 2.2 Results and discussion

### 2.2.1 Sequence analysis of *Sa*MerA compared to other tDBDFs

The tDBDF enzymes represent a diverse superfamily, with more than 1600 members [6]. Phylogenetic trees generated from structure-based alignments show that tDBDFs can be divided into two major groups consisting of nine subgroups in total (Table 2). Despite low pairwise sequence identity all members contain highly conserved domains including (from N- to C-terminal) an FAD binding domain, an ATG motif, a pyridine nucleotide binding domain, and GxxP and GD motifs. The active sites of the tDBDFs are found between the FAD binding domain and the ATG motif [6]. Despite the conservation amongst subgroups of tDBDFs, they have evolved to act on an extremely diverse range of substrates, including small molecules but also extending to larger protein partners [6-9]. The tDBDFs all share a common catalytic cycle, i.e. a reductive and oxidative half reaction. The reductive half reaction involves a hydride transfer from the pyridine nucleotide to FAD producing $FADH_2$. The oxidative half reaction involves the passing of two electrons—one at a time or both simultaneously— to additional redoc centers in the same enzyme before being transferred to the final substrate acceptors. In the case of sequential single electron transfer, this usually involves a protein partner or intermediate small molecule acceptor (such as Fe-S clusters or heme) [6].

**Table 2. Groups and subgroups of tDBDF superfamily [6].**

| Group | Subgroup | Family name |
|---|---|---|
| 1 | Monooxygenase (**MOX**) | Flavin containing monooxygenase |
| | | *N*-hydroxylating monooxygenase |
| | | Baeyer-Villiger monooxygenase |
| | 2,4-dienoyl-CoA reductase (**DCR**) | 2,4-dienoyl-CoA reductase |
| | Adrenodoxin reductase (**ADR**) | Adrenodoxin reductase |
| | Glutamate synthase (**GMS**) | Glutamate synthase |
| | Alkylhydroperoxide reductase (**AHR**) | Alkylhydroperoxide reductase |
| 2 | Disulfide reductase (**DSR**) | Low molecular weight thioredoxin reductase |
| | | Glutathione reductase |
| | | Dihydrolipoamide dehydrogenase |
| | | Mercuric ion reductase |
| | NADH ferredoxin reductase (**NFR**) | NADH ferredoxin reductase |
| | | NADH ferredoxin |
| | | Nitrite Reductase |
| | NADH peroxidase/oxidase and disulfide CoA reductase (**POR**) | NADH peroxidase/oxidase |
| | NADH dehydrogenase (**NDH**) | NADH dehydrogenase |
| | | Sulfide dehydrogenase |

*S. aureus* MerA is annotated as a hypothetical mercuric ion reductase homologue and is classified as a member of the DSR subgroup, which includes glutathione reductase (Gor), dihydrolipoamide dehydrogenase (LipDH) and true mercuric ion reductases (MerA). The DSR subfamily contains additional highly conserved motifs, most important of which are the active site disulfide CxxxxC motif and a lysine residue that is shown to stabilize the reduced FAD intermediate. The sequence of *Sa*MerA was therefore aligned to members of the DSR subgroup as well as its *E.coli* homologue RclA, for comparison purposes (Figure 2.1).

Overall the sequences show strong similarities as expected from their assignment to the same subgroup in the tDBDF enzyme family. Considering *Sa*MerA is annotated as a mercuric ion reductase homologue it was also compared to a known mercuric ion reductase from *Pseudomonas aeruginosa*, *Pa*MerA Tn501, which is by far the best studied mercuric ion reductase [10-25]. In addition to the active site motif CxxxxC, true mercuric ion reductases have a distinct pair of auxiliary Cys residues at their N-terminus (in the so-called NMerA domain) as well as an extended C-terminal region that also contains a Cys pair. The C-terminal Cys residues are critical for mercuric ion reductase activity [17]. Comparing the sequences of *Sa*MerA to *Pa*MerA Tn501, it becomes clear that both the N-terminal and C-terminal Cys residues are absent in *Sa*MerA. Consequently, *Sa*MerA is not expected to have activity for $Hg^{2+}$ reduction due to the absence of the critical auxiliary C-terminal Cys pair.

*Sa*MerA was also compared to other well-known members of the DSR subgroup, namely *Ec*Gor and *Ec*LipDH; which reduce disulfide substrates GSSG and Lipoamide respectively. They both contain the CxxxxC motif which is involved in reducing their respective disulfide substrates. Based on alignment alone, *Sa*MerA looks more like a Gor or LipDH than a true MerA. However, it is important to recall that in most cases LipDH, does not function in isolation, but rather forms part of a multi-enzyme complex. In addition, LipDH's substrate, namely the lipoamide cofactor, is bound as an adduct to a Lys on the E2 domain of the multi-enzyme complex [26]. It is therefore not likely that *Sa*MerA has lipDH activity. It is also unlikely that *it* should show activity towards GSSG (i.e. act as a Gor) since *S. aureus* lacks the LMW thiol GSH [27, 28].


**Figure 2.1 T-coffee multiple sequence alignment of *S. aureus* MerA (*Sa*MerA), *P. aeruginosa* MerA Tn501 (*Pa*Tn501MerA), *E. coli* Glutathione disulfide reductase (*Ec*Gor), *E. coli* Lipoamide dehydrogenase (*Ec*LipDH) and the *E.coli* MerA homologue (*Ec*RclA). Pink/Salmon highlighted regions show good sequence conservation. Section enclosed in the black box (*Sa*MerA a.a 162-229) is the pyridine nucleotide binding domain. The box outlined in the thick grey line shows the conserved active site CxxxxC motif. All Cys residues are highlighted as blue dots.**

### 2.2.2 Cloning and plasmid constructs used

This *Sa*MerA wild-type (WT) plasmid was prepared by a previous member of the Strauss lab [1]. Briefly, the *Sa*MerA gene (SAOUHSC_00581) was cloned from genomic DNA from the *S. aureus* RN4220 strain. The gene was inserted into a pET28a(+) expression vector for expression of a protein with a C-terminal 6×His-tag. The predicted active site of *Sa*MerA contains the conserved CxxxxC motif; therefore, both single Cys→Ala mutants as well as the double mutant were produced to aid in studying the enzyme's catalytic mechanism. The *Sa*MerA C48A mutant was generated by site-directed mutagenesis PCR using the pET28a-MerA WT plasmid as template DNA, while the *Sa*MerA pET28a-C43A and C43A C48A expression plasmids were kindly provided by Prof. Haike Antelmann (Institute of Biology - Microbiology. Freie Universität Berlin). The gene sequences contained in all plasmids were confirmed by sequencing prior to use.

### 2.2.3 Protein expression

All plasmids were each separately transformed into *E. coli* BL21* (DE3) cells to be used in heterologous expression of the proteins. Optimum protein expression was obtained for *Sa*MerA WT as well as the Cys→Ala mutants by growing cultures in LB broth at 37°C overnight after induction with 0.5 mM IPTG at $OD_{600nm}$ = 0.5-0.6.

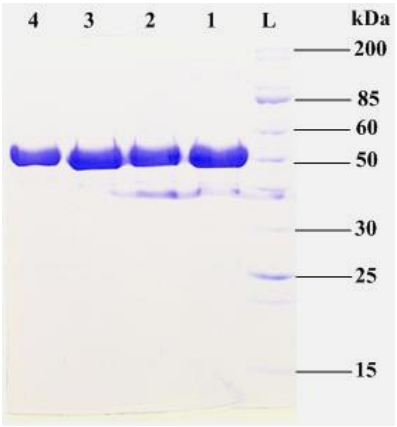


**Figure 2.2 10% SDS-PAGE analysis of *Sa*MerA WT (1), *Sa*MerA C43A (2), *Sa*MerA C48A (3) and *Sa*MerA C43A C48A (4). Molecular weight marker (L) shown with respective kDa increments.**

## 2.2.4 Protein purification

After growth and expression each pellet was lysed and proteins purified from the cell lysate using immobilized metal affinity chromatography (IMAC) on an ÄKTAPrime system. The purified fraction of each protein was then analysed by SDS-PAGE (Figure 2.2). The protein concentration was determined using the Bradford method as well as by measuring enzyme concentration using the FAD molar extinction coefficient. All of the proteins expressed well and yielded yellow/orange purified fractions characteristic of flavin-containing proteins. From an 500 mL LB broth culture an average of 21 mg of protein was obtained. The *Sa*MerA C43AC48A mutant gave slightly lower yields, but overall the proteins expressed and purified very well.

## 2.2.5 Enzyme characterization

### 2.2.5.1 General flavin spectral analysis

In order to determine the cofactor requirement, *Sa*MerA was anaerobically titrated with increasing amounts of either NADPH or NADH (Figure 2.3). This data was collected by a previous Strauss lab member [1].

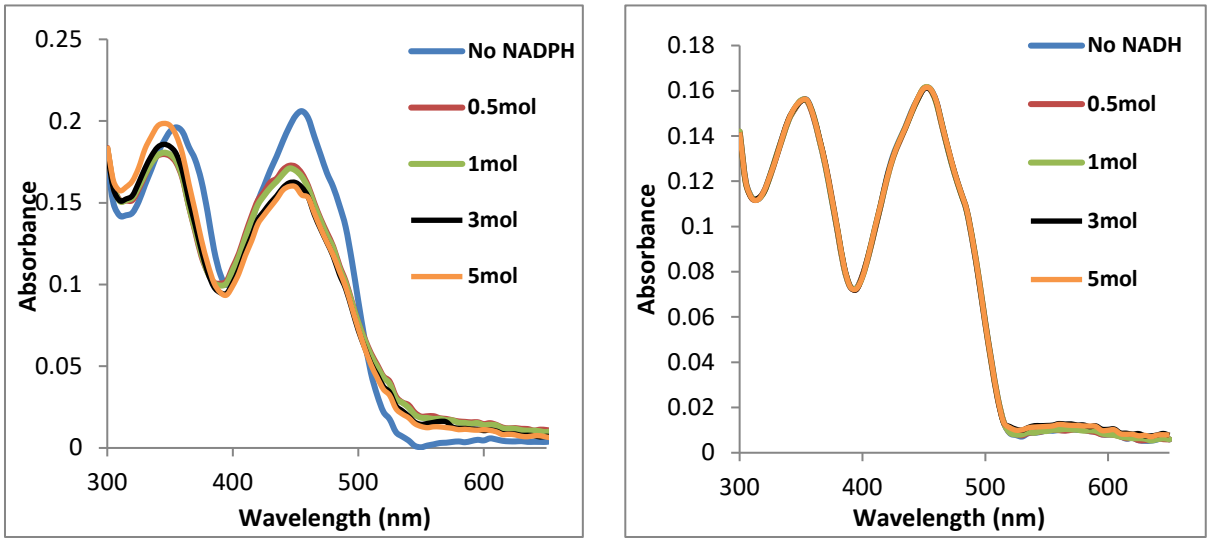


**Figure 2.3 Anaerobic titrations of *Sa*MerA WT against NADPH (left spectrum) and NADH (right spectrum). The protein was titrated via sequential addition of NADPH/NADH (0.5mol) per flavin (1mol) up to an excess of 5mol. This data was previously collected [1].**

Like many of the DSRs, *Sa*MerA showed a preference for NADPH over NADH in which the flavin was readily reduced by NADPH (as evidenced by a decrease of the 450 nm absorption

band), although it resisted full reduction despite the addition of excess NADPH. No reduction of the flavin cofactor was observed following the addition of NADH.

### 2.2.5.2 Circular dichroism (CD) spectroscopy

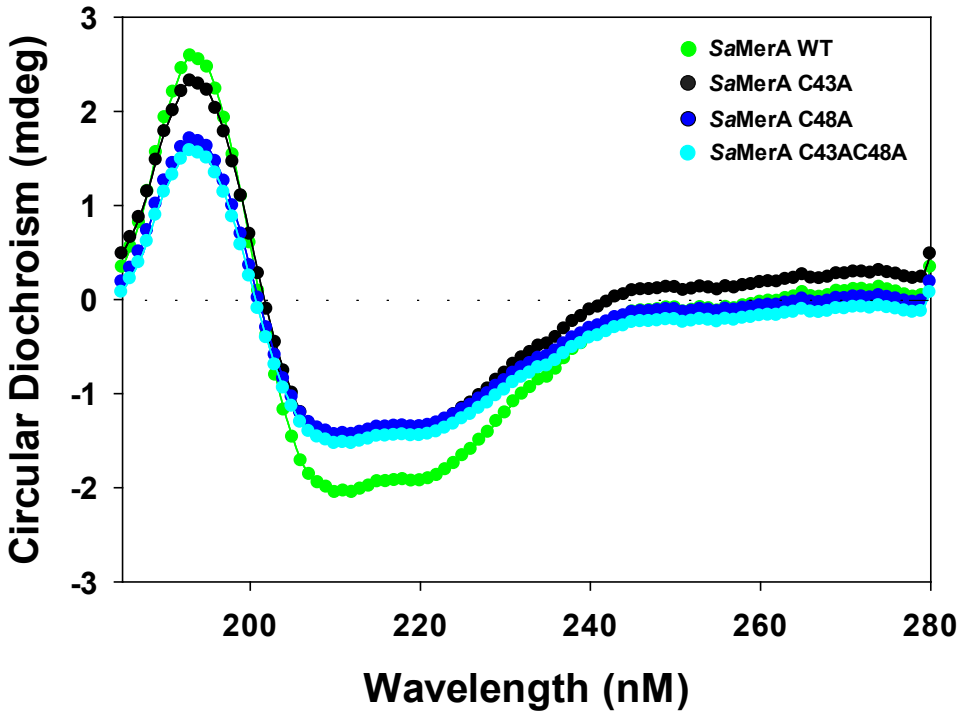


**Figure 2.4. CD spectroscopic analysis of *Sa*MerA WT, *Sa*MerA C43A, *Sa*MerA C48A and *Sa*MerA C43A C48A.**

The point mutations of the Cys residues of the CxxxxC motif in the *Sa*MerA active site were done in order to aid in determining the catalytic mechanism of the enzyme with its potential substrate. CD spectroscopy was used to assess the effect these mutations may have on the overall folding of the enzyme. The CD spectra showed well folded proteins composed mainly of a mix of α-helixes and β-sheets as expected for tDBDF enzymes. Many of the tDBDFs are composed of approximately 50% α-helix and β-sheet. The *Sa*MerA WT spectrum looked similar to the CD spectra of glutathione reductase and thioredoxin reductase [29, 30]. The mutants appear to have overall similar spectra to the wild type with positive increase in rotation values from 210 nm to 230nm and from 250 nm to 280 nm possibly due to a slight decrease in α-helix content or slightly lower concentration of stock protein used in analysis.

### 2.2.5.3 X-ray crystal structure comparison

The crystal structure of SaMerA WT was obtained at 1.9 Å resolution in conjunction with collaborators under direction of Professor Matthew Redinbo at the University of North Carolina at Chapel Hill, USA. The structure contained the bound FAD cofactor, but not NADPH or other molecules apart from solvent.

The homodimeric structure of *Sa*MerA (Figure 2.5) was solved with the FAD cofactor bound within the active site. As expected, the overall structure of *Sa*MerA resembled that of other tDBDFs.

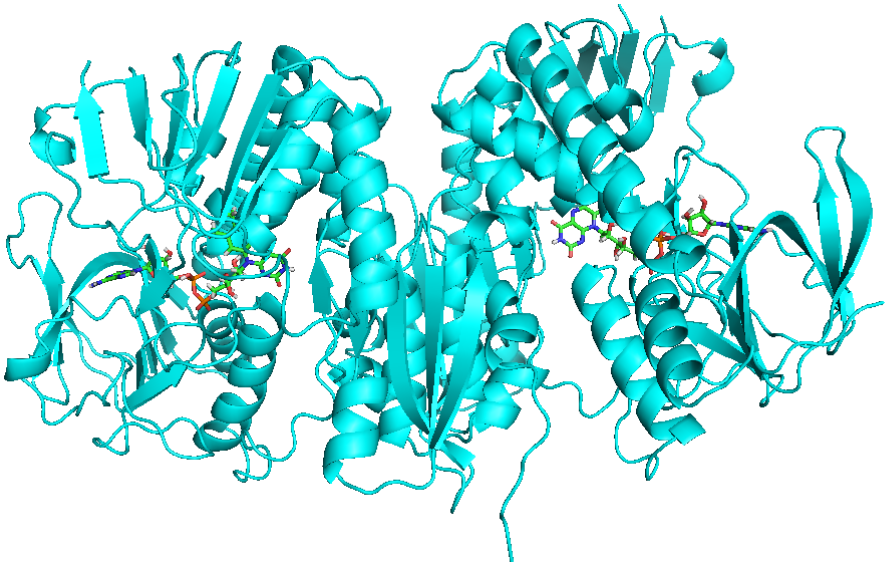

**Figure 2.5. X-ray crystal structure of homodimeric *Sa*MerA WT at 1.9 Å resolution showing one FAD molecule per monomer.**

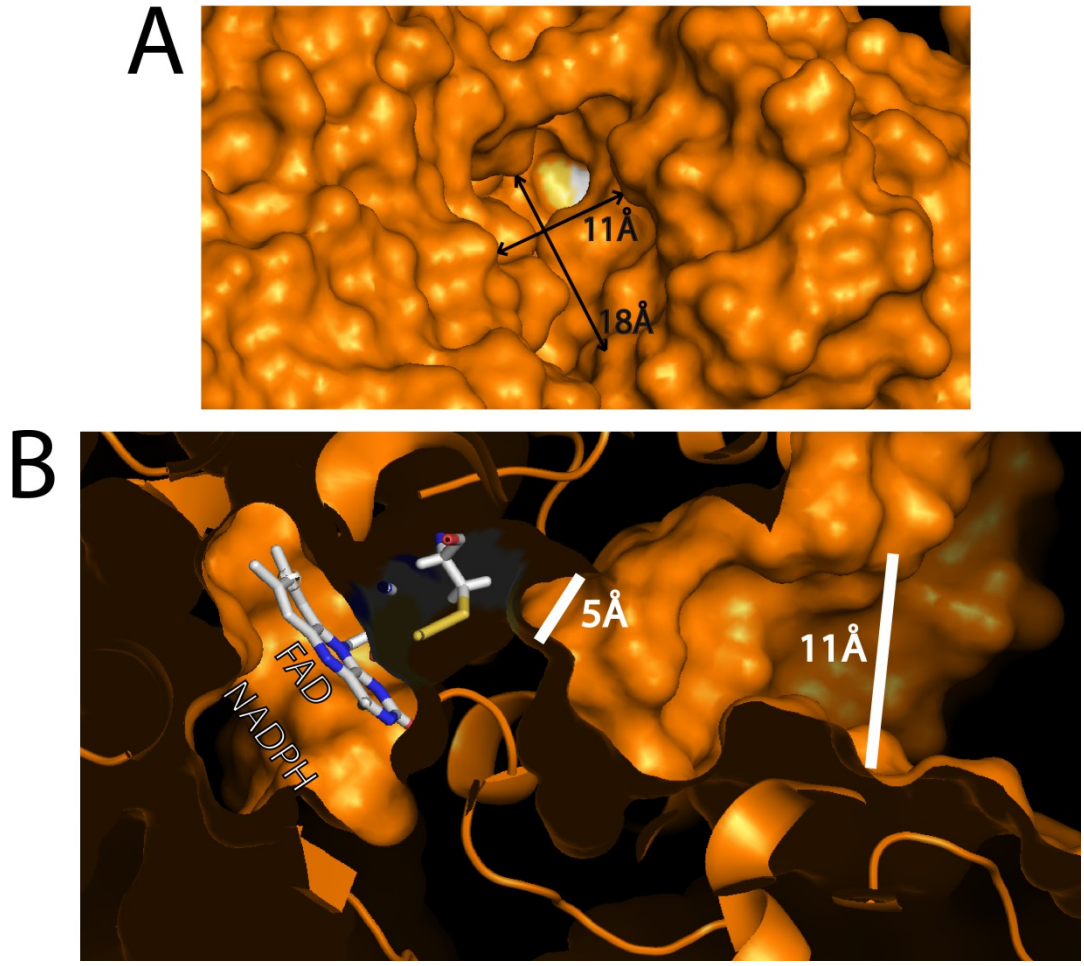


**Figure 2.6 Model showing the surface of *Sa*MerA, indicating the active site's location and its size on one of the monomers. (A) Top view of the active site entrance of *Sa*MerA with Cys43 of the active site motif highlighted in yellow. (B) Side view of the active site showing the disulfide formed between Cys43 and Cys48 (yellow stick structure), the FAD cofactor and the NAPDH binding site (labelled as NADPH). The active site is small and compact (~5Å) closest to the cysteine residues, but opens to a larger entrance (~11Å × 18Å).**

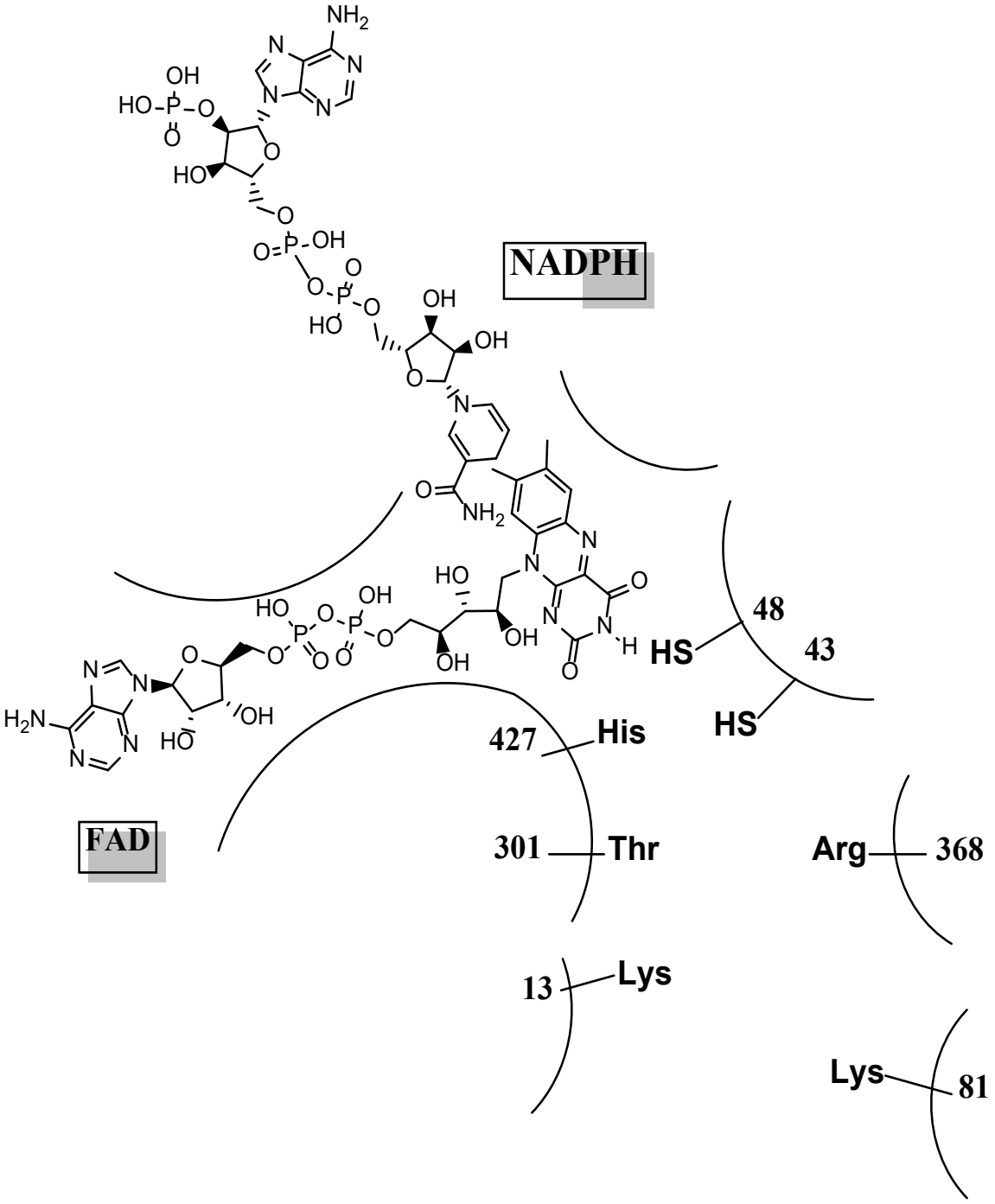


**Figure 2.7 Schematic 2-dimensional diagram of the relative positions of the residues in the active site of *Sa*MerA, as derived from the X-ray crystal structure. The active site's entrance is at the bottom of the schematic. The position of the NADPH molecule is predicted based on comparison to similar tDBDF enzyme structures.**

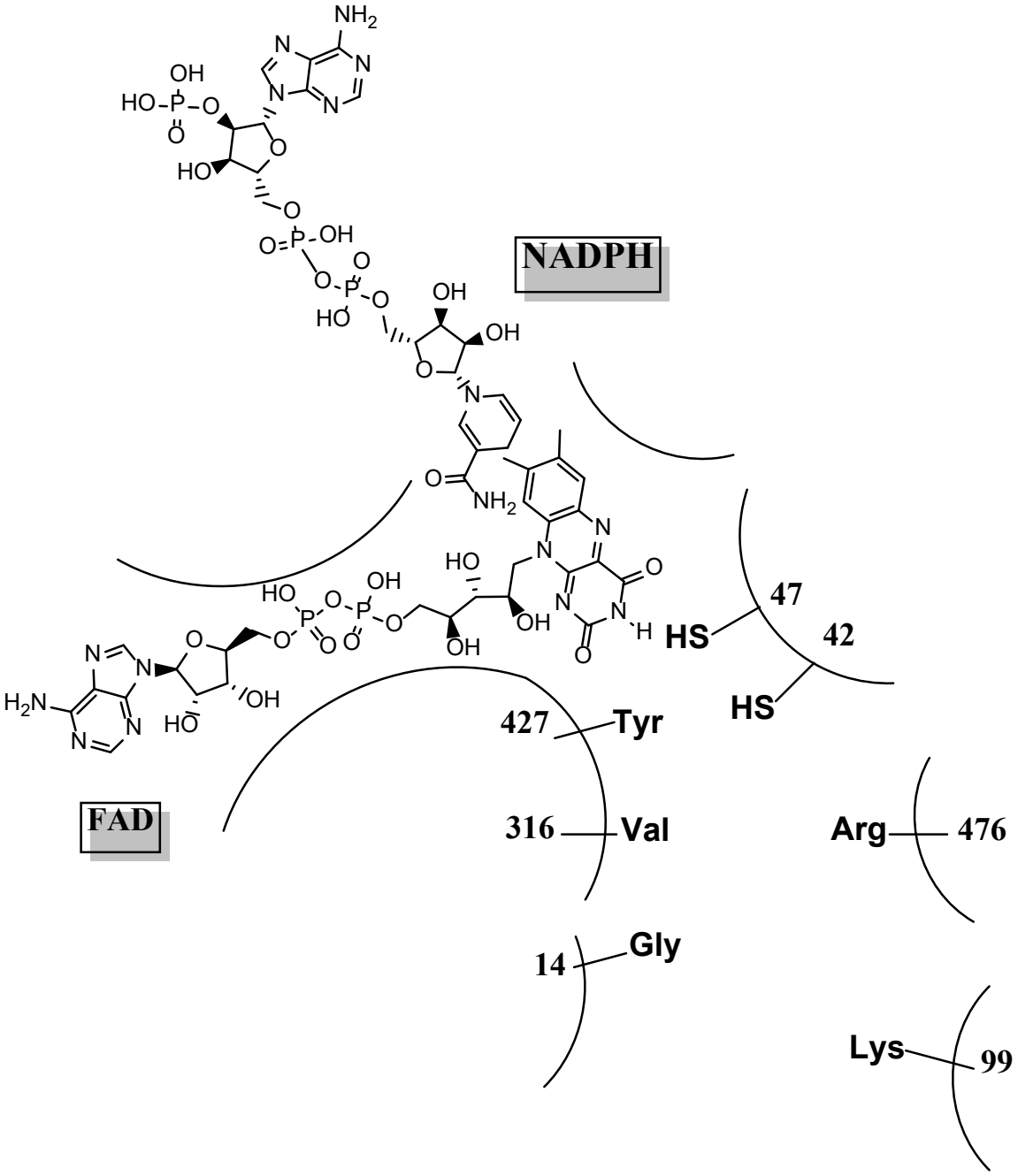


**Figure 2.8 Schematic 2-dimensional diagram of the relative positions of the residues in the active site of *Pa*MerA Tn501 as derived from its X-ray crystal structure (PDB:1ZK7). The active site's entrance is at the bottom of the schematic. The amino acid residue numbering relates to the corresponding residues in *Sa*MerA to facilitate comparison.**

In terms of the active site CxxxxC motif there is very little difference compared to other tDBDFs, as expected. The active site opening around the disulfides of *Sa*MerA is small and compact, forming a 5Å wide channel closest to the disulfides but opening up to a larger entrance (Figure 2.6). Considering that tDBDFs act on their substrates that range from small molecules like peroxide and disulfides to fairly larger substrates such as small proteins (thioredoxins), the size and shape of the *Sa*MerA active site suggests that it acts on a small molecule. The schematic diagram of *Sa*MerA active site is shown in Figure 2.7. Compared to *Pa*MerA Tn501 (shown in Figure 2.8) there are notable differences in the amino acids lining the active site. Specifically, the His427 residue in *Sa*MerA is replaced by a Tyr in Tn501, and the polar and charged Thr301 and Lys13 is exchanged for Val and Gly. In addition, Miller and coworkers have shown that binding and transfer of $Hg^{2+}$ in *Pa*MerA Tn501 takes place by using an exogenous thiol and with the help of the critical N-terminal Cys pair. *Sa*MerA lacks both auxiliary Cys pairs and is therefore unlikely to be able to bind $Hg^{2+}$. However, the amino acids that line the active site (Lys13, Thr301, His427, Lys81, Arg368) are most likely involved in the binding of substrate. Considering the polar and positively charged nature of these residues, this suggests that the substrate likely contains groups that are negatively charged at physiological pH.

### 2.2.6 Assessing *Sa*MerA's activity as a mercuric ion reductase

Considering *Sa*MerA is annotated as a hypothetical mercuric ion ($Hg^{2+}$) reductase homologue, it was therefore investigated if *Sa*MerA shows any activity towards mercuric ions. True mercuric ion reductases such as *Pa*MerA Tn501 make use of extra Cys pairs that play an important role in the catalytic mechanism of mercuric ion reductase as shown in Figure 2.9.The overall mechanism is essentially a ligand exchange or "passing on" of the $Hg^{2+}$ between the Cys pairs. In Step 1 the enzyme encounters the exogenous thiol (Trx or GSH) which brings in the $Hg^{2+}$ and passes this onto the first N-terminal Cys pair (C11/14) of MerA (Step 2). This results in the release of reduced Trx and the $Hg^{2+}$ is subsequently passed onto the second C-terminal Cys residues (C558/559) (Step 4-5). Finally it is passed into the active site (Step 6-7) CxxxxC (Cys136/141 pair) where the mercuric ion is reduced (2 electron transfer from NADPH) to $Hg^0$ and subsequently released, together with $NADP^+$. The enzyme cycle restarts with the binding of a new NADPH and an incoming Trx/GSH-$Hg^{2+}$. It has also been shown in extensive work by Miller and co-workers that the N-terminal Cys (Cys 11/14) residues are dispensable and the catalytic cycle can still continue via the truncated pathway (Step 1 to 5 via step 8). The crystal structure and quantum mechanics

shows the energetically favorable transfer of the $Hg^{2+}$ as well as the interplay between the competition of the Cys thiols/thiolates for $Hg^{2+}$ versus protons [20, 21]. Miller and co-workers have also shown that the C-terminal Cys pair (Cys558/559) is critical for the full catalytic cycle [17, 23]. Single mutations of Cys558/559 drastically reduce catalytic activity, whilst a double Cys→Ala mutant abolishes all activity. An additional feature of the mercuric ion reductase, like other enzymes associated with heavy metal binding, is that they have a heavy metal associated domain (HMA) in the extended N-terminal domain. It is hypothesized that the HMA is involved in heavy metal sensing [31].

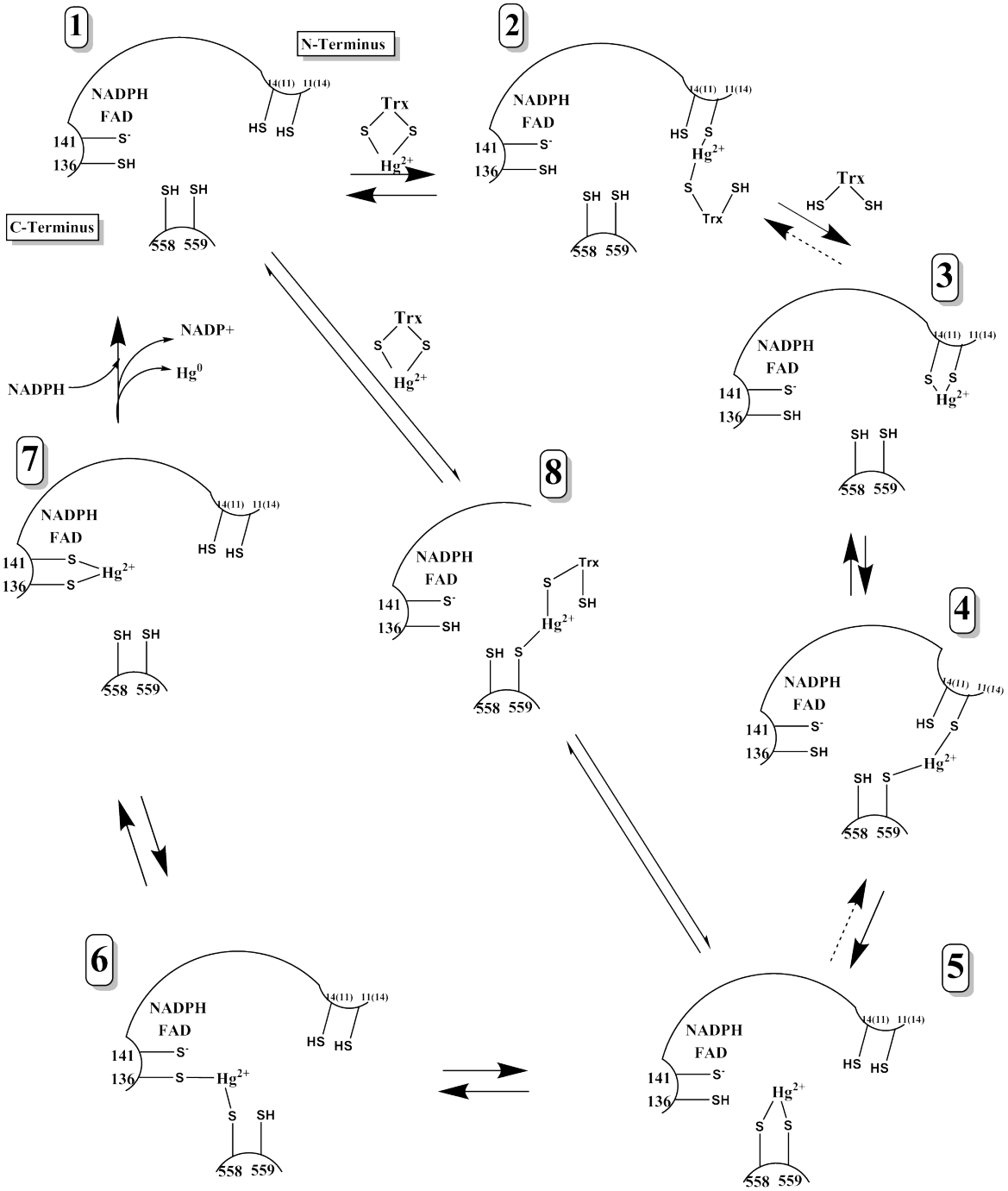


**Figure 2.9 Substrate exchange pathway of *Pa*MerA Tn501. The outer reactions 1-7 show the full catalytic cycle of *Pa*MerA Tn501 reducing $Hg^{2+}$ to form $Hg^0$. An exogenous thiol is required for substrate transfer to the auxiliary and active site disulfides. Exogenous thiol TrxA-$Hg^{2+}$ is shown in the catalytic cycle. Truncated *Pa*MerA Tn501, in which the auxiliary disulfides are proteolytically removed, can also reduce $Hg^{2+}$ - albeit at a reduced efficiency - which enters in the cycle at reaction 5. Redrawn from [17].**

Assay conditions for the putative mercuric ion reductase activity were based upon those reported by Miller and co-workers, using $Hg(GSH)_2$ as the exogenous $Hg^{2+}$-thiol [17]. In Figure 2.10, it can be seen that under aerobic conditions *Sa*MerA appears to have a low level activity in the presence of GSH (2.10.d), but then clearly increases when mercuric ion is included (2.10.f). This assessment is based on reactions lacking substrate (*Sa*MerA WT + NADPH reactions Figure 2.10(b)). This was surprising considering *Sa*MerA lacks the features of a true mercuric ion reductase. However, the $V_{max}$ rates reported for true mercuric ion reductases under similar enzyme concentrations are approximately 8-16 µM/Min (depending on the source of the enzyme). In comparison to these values, *Sa*MerA average reaction rate of 1.0 µM/Min does not constitute meaningful activity towards mercury. In addition to using GSH as an exogenous thiol, β-mercaptoethanol was also tried in test reactions; however, this did not make a difference in activity. Furthermore under anaerobic conditions (Figure 2.10. c, e and g) *Sa*MerA appears to have a low level activity in the presence of GSH (e) and does not appear to increase when mercuric ion is included (g).

In light of the low mercuric ion reductase activity observed for *Sa*MerA in our hands, we decided to express and purify *Pa*MerA Tn501 to perform a direct comparison in their activities to exclude any potential error in the execution of the assay.

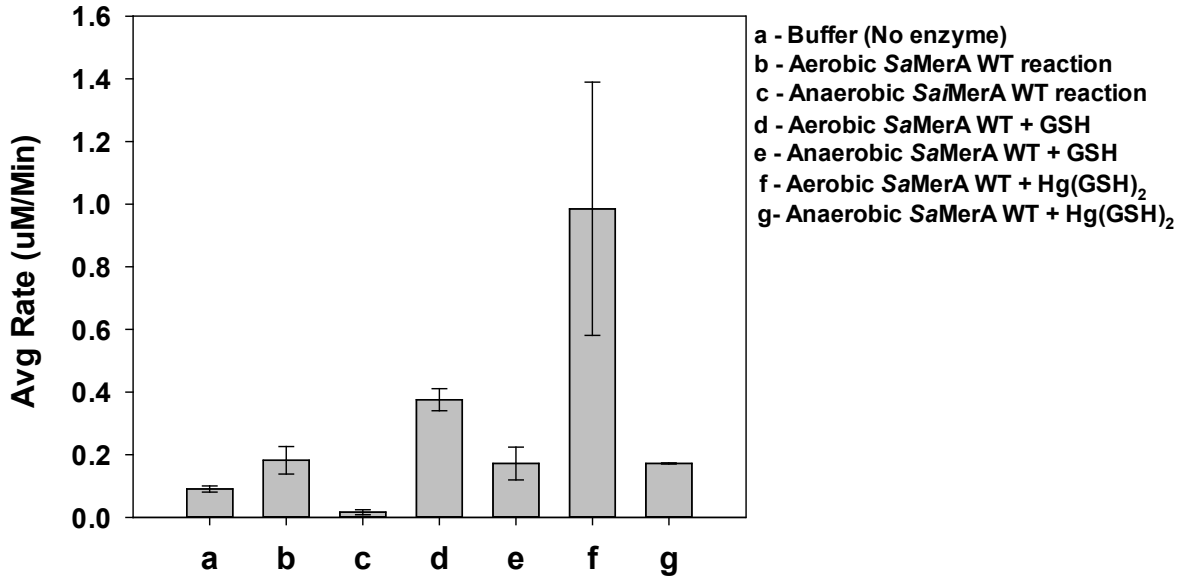


**Figure 2.10 Assessment of *Sa*MerA's mercuric ion reductase activity by following the rate of oxidation of NADPH at 340 nm. (a) Reaction buffer (No enzyme), (b)Aerobic *Sa*MerA WT, (c) Anaerobic *Sa*MerA WT, (d) Aerobic *Sa*MerA WT + GSH, (e) Anaerobic *Sa*MerA WT + GSH, (f) Aerobic *Sa*MerA WT + $Hg(GSH)_2$, (g) Anaerobic *Sa*MerA WT + $Hg(GSH)_2$. All reactions contained NADPH. Concentrations used: 100 µM NADPH, 100 µM $Hg(GSH)_2$, 1 mM GSH, 25 nM enzyme. Data shown is the average rate obtained in four biological repeats SEM (n=4).**

Figure 2.11 shows the activity of *Sa*MerA WT (a-d) compared to that of *Pa*MerA Tn501 (e-f). The data showed that *Pa*MerA Tn501 indeed did require the exogenous thiol as previously described. In addition, the pretreatment step of the enzyme with DTT and refolding (described in literature and section 2.4.3) to ensure disulfides are reduced was indispensable when testing mercuric ion reductase activity. This data confirmed that *Sa*MerA WT had no appreciable mercuric ion reductase activity. The *Sa*MerA C43AC48A mutant also showed no activity (g-i) confirming that the low level activity observed for the wild-type does involve the active cysteine residues (d).

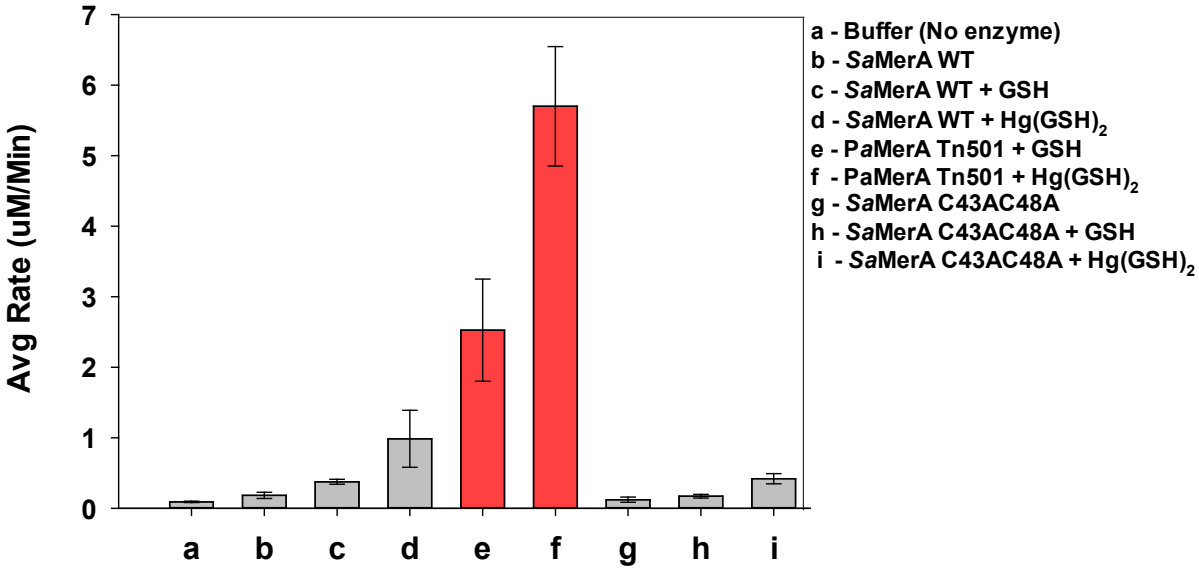


**Figure 2.11 Assessment of *Sa*MerA's mercuric ion reductase activity against *Pa*MerA Tn501 activity based on oxidation of the NADPH cofactor. (a) Reaction buffer (No enzyme), (b) *Sa*MerA WT, (c) *Sa*MerA WT + GSH, (d) *Sa*MerA WT + $Hg(GSH)_2$, (e) *Pa*MerA Tn501 + GSH, (f) *Pa*MerA Tn501 + Hg(GSH)2, (g) *Sa*MerA C43AC48A, (h) *Sa*MerA C43AC48A + GSH, (i) *Sa*MerA C43AC48A + $Hg(GSH)_2$. Concentrations used: 100 µM NADPH, 100µM $Hg(GSH)_2$, 1mM GSH, 25nM Enzyme. All reactions contained NADPH. Data shown is the average rate obtained in four biological repeats SEM (n=4).**

We were also interested as to why there appeared to be some activity observed for *Sa*MerA WT towards mercuric ion. We therefore investigated whether instead of direct reduction of the metal ion, the heavy metal might be potentiating the oxygen reducing activity of the flavoprotein [32, 33]. This was determined by assessing the *Sa*MerA WT mercuric ion reductase activity in the presence of horse radish peroxidase (HRP) and substrate ABTS [34, 35]. ABTS is a chromogenic compound used as an indicator in a number of applications. ABTS is also used in the determination of $H_2O_2$ in the presence of an appropriate peroxidase (Figure 2.12). ABTS is colorless in solution but upon oxidation by HRP and $H_2O_2$ forms the

green ABTS radical which has an intense broad spectrum at 415 nm - 820 nm [35]. It can therefore be used to establish if $H_2O_2$ is being formed from $O_2$.

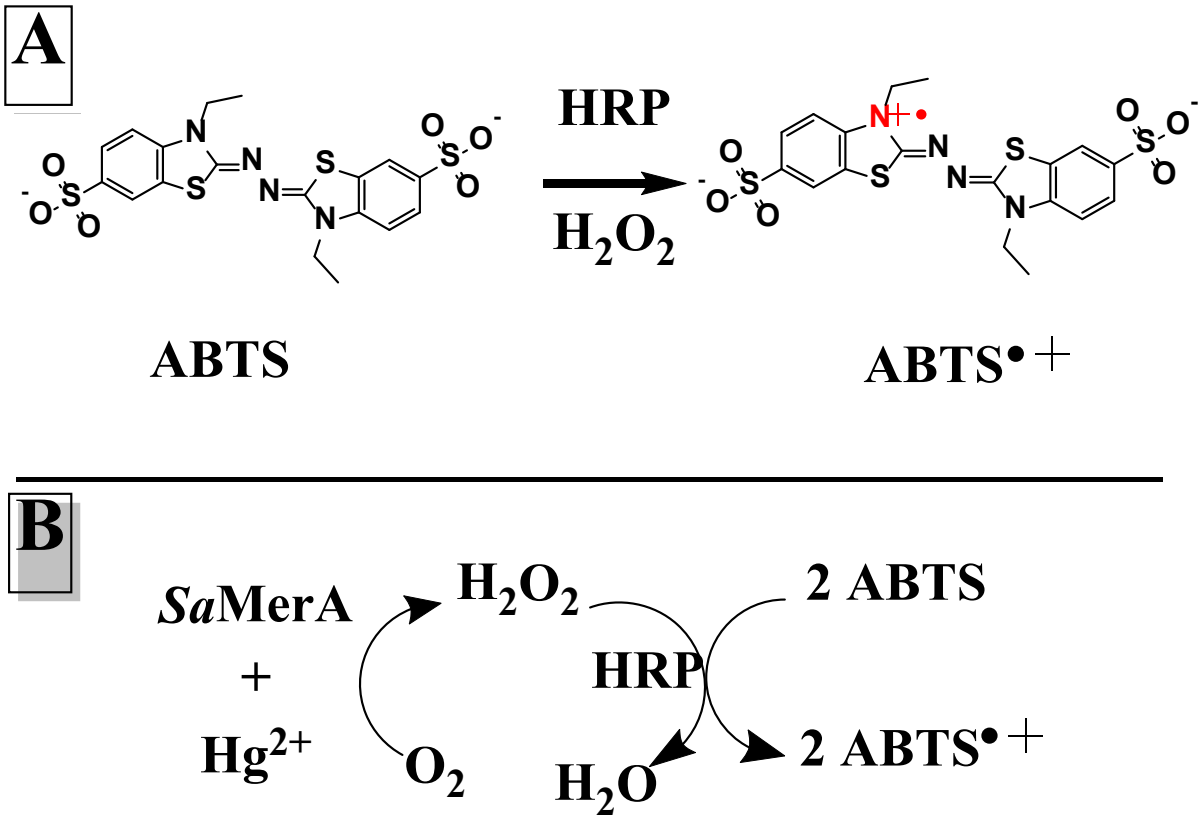


**Figure 2.12 Determination of $H_2O_2$ formation using ABTS and HRP. (A) ABTS is oxidized in the presence of $H_2O_2$ and HRP to form an ABTS radical which can be measured spectrophotometrically at 415-420 nm. (B) $Hg^{2+}$ attenuates SaMerA's formation of $H_2O_2$ from $O_2$, as measured by coupling its production to formation of the ABTS radical as catalyzed by HRP.**

The results (Figure 2.13) show that *Sa*MerA WT did indeed produce hydrogen peroxide in the presence of mercuric ion under aerobic conditions (Figure 2.13. column d), while very little formed under anaerobic conditions (Figure 2.13. column e). *Sa*MerA C43A48A showed very little $H_2O_2$ - producing activity in the presence of mercuric ion under both aerobic and anaerobic conditions (Figure 2.13. column f and g).

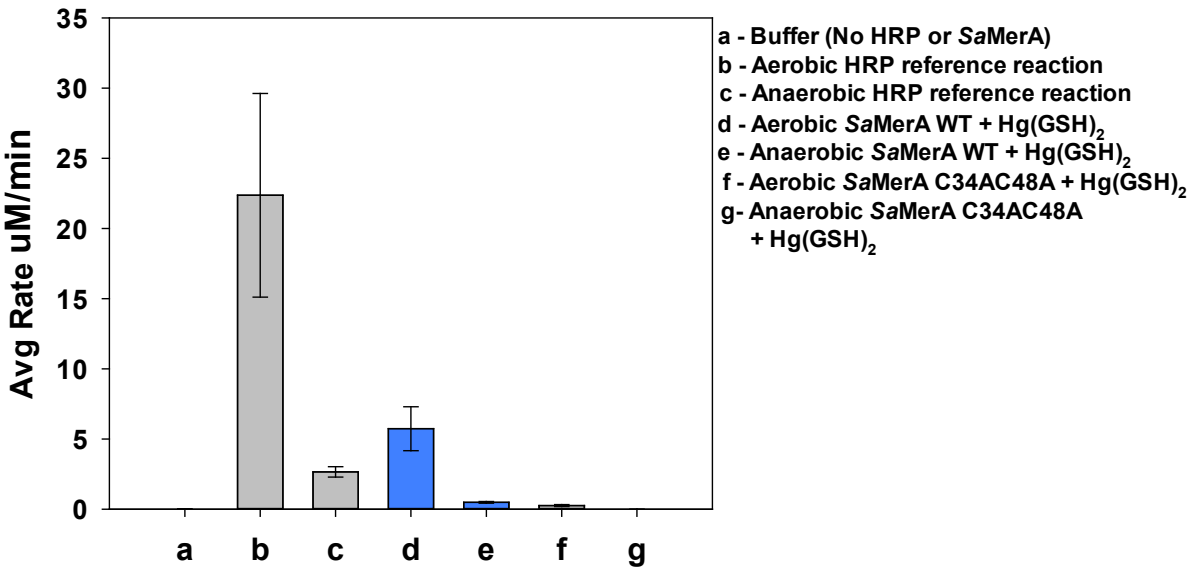


**Figure 2.13 Assessing the formation of $H_2O_2$ by *Sa*MerA WT. The formation of $H_2O_2$ by *Sa*MerA in the presence of $Hg^{2+}$ was coupled to the formation of chromophore ABTS radical as catalyzed by horse radish peroxidase (HRP). Both aerobic and anaerobic conditions were evaluated. (a) Buffer (No HRP or *Sa*MerA), (b) Aerobic reference reaction: HRP + ABTS + 100 µM $H_2O_2$, (c) Anaerobic reference reaction: HRP + ABTS + 100 µM $H_2O_2$, (d) Aerobic *Sa*MerA WT + $Hg(GSH)_2$, (e) Anaerobic *Sa*MerA WT + $Hg(GSH)_2$, (f) Aerobic *Sa*MerA C43AC48A + $Hg(GSH)_2$, (g) Anaerobic *Sa*MerA C43C48A + $Hg(GSH)_2$. Concentrations used: 100 µM NADPH, 100 µM ABTS, 100 µM $Hg(GSH)_2$, 25 nM enzyme. All reactions contained NADPH, HRP and ABTS. Only reference reactions contained exogenous $H_2O_2$. Data shown is the average rate obtained in one biological repeat performed in triplicate, with the errors showing the standard deviation.**

Taken together, this data suggests that the NAPDH oxidizing activity observed for *Sa*MerA WT in the presence of mercuric ion is rather due to the low level of oxygen reduction being potentiated by the presence of the metal ion, rather than due to reduction of the metal ion itself. Moreover, the disulfide is clearly required for this oxygen reducing activity, further supporting the role of mercuric ion in potentiating this activity upon binding of the active site cysteine residues. It can be concluded that despite *Sa*MerA WT having some apparent (albeit very little) activity towards mercuric ion, when compared to a true mercuric ion reductase like *Pa*MerA Tn501 and when taking into account the results obtained in the absence of oxygen, this low level of activity does not constitute the enzyme's native activity.

## 2.2.7 Assessing *Sa*MerA's activity towards other metals

After concluding that *Sa*MerA has no appreciable activity as a mercuric ion reductase, we considered whether it acts on a different biological metal that is also relevant to oxidative stress such as iron ($Fe^{3+}$), zinc ($Zn^{2+}$) or copper ($Cu^{2+}$) [36-42]. The metals iron, zinc and copper are important metal cofactors that are found in a number of redox active enzymes. The most well-known are Fe-S clusters that are particularly sensitive towards oxidation by ROS and RCS, forming toxic $Fe^{3+}$. *Sa*MerA was thus assessed for its ability to reduce $Fe^{3+}$ thus repairing the effects of $Fe^{2+}$ oxidation. For comparison, *Sa*MerA was also assessed for its ability to reduce $Zn^{2+}$ and $Cu^{2+}$.

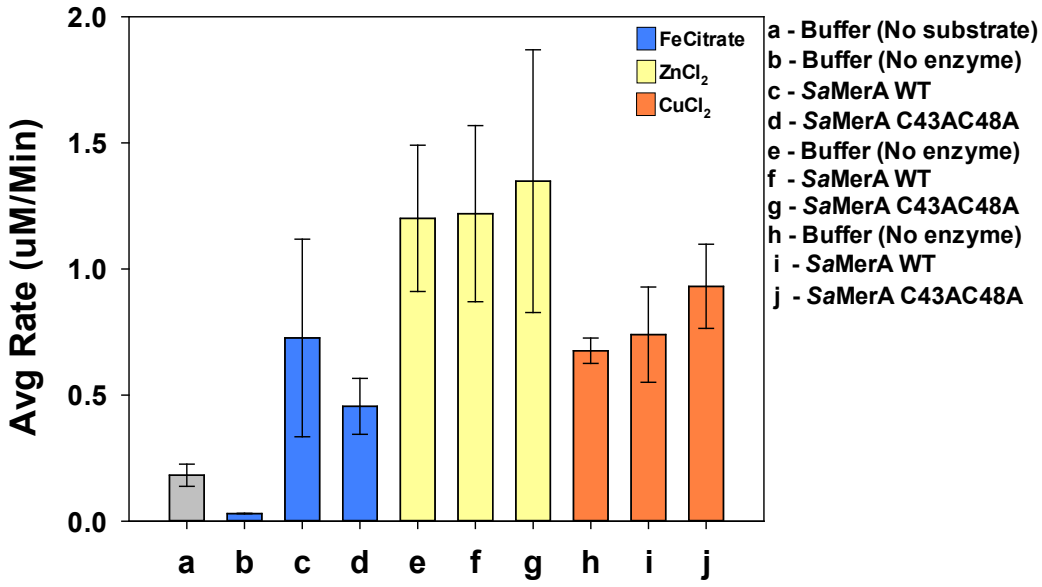


**Figure 2.14 *Sa*MerA WT and *Sa*MerA C43C48A activity for the reduction of iron, zinc and copper ions. (a) *Sa*MerA WT (No metal substrate), (b) Buffer + FeCitrate, (c) *Sa*MerA WT + FeCitrate, (d) *Sa*MerA C43C48A + FeCitrate, (e) Buffer + $ZnCl_2$, (f) *Sa*MerA WT + $ZnCl_2$, (g) *Sa*MerA C43AC48A + $ZnCl_2$, (h) Buffer + $CuCl_2$, (i) *Sa*MerA WT + $CuCl_2$, (j) *Sa*MerA C43AC48A + $CuCl_2$. Concentrations used: 100 µM NADPH, 100 µM metal substrate, 25 nM enzyme. All reactions contained NADPH. Data shown is the average rate obtained for one biological repeat (n=1) performed in triplicate; the error bars show standard deviation.**

The figure above (Figure 2.14) shows *Sa*MerA activity towards reducing $Fe^{3+}$ (FeCitrate) and other metals $Zn^{2+}$ ($ZnCl_2$) and $Cu^{2+}$ ($CuCl_2$). For *Sa*MerA's activity towards FeCitrate no difference is observed between the WT and the C43A C48A mutant (blue bars). Similarly, there is no difference between the WT and C43A C48 mutant against either $Zn^{2+}$ or $Cu^{2}$. In summary *Sa*MerA does not appear to reduce $Fe^{3+}$, $Zn^{2+}$ or $Cu^{2+}$.

## 2.2.8 Assessing potential substrates for *Sa*MerA

With no appreciable activity towards mercury, iron, zinc or copper ions other potential substrates were explored. Considering *Sa*MerA is classified in the DSR group, which includes glutathione reductase and thioredoxin reductase perhaps *Sa*MerA WT is able to reduce the disulfides of a low molecular weight thiol or of a protein such as thioredoxin? Or does it act on such substrates only in context of the oxidants $H_2O_2$ or HOCl? We therefore set out to answer these questions by a conducting a variety of activity assays.

### 2.2.8.1 Assessing potential protein partner/s

Identifying suspected partners of a protein is an important aspect in an attempt to understand protein function or physiochemical properties of an unknown protein. Pull-down or "protein fishing" experiments using affinity tags have been widely used in determining potential protein binding partners [43-45]. A number of studies, including ones on thioredoxin and thioredoxin reductase, have been conducted using GST-fusion tagged proteins in identifying protein partners [46-48]. The same principle was used in evaluating the possibility that *Sa*MerA might require a protein partner for its activity. Briefly the GST-fusion of *Sa*MerA WT was expressed and purified (described in section 2.2.8) and used in a pull-down assay to identify any potential protein partners present in *S. aureus* JE2 lysates. *S. aureus* JE2 was cultured until exponential phase and thereafter oxidative stress was elicited by exposure to 10 mM $H_2O_2$ during growth (see experimental section for details). This was done taking into consideration that *Sa*MerA is overexpressed under conditions of oxidative stress. The lysate obtained from cells treated in this manner was subsequently used in a pull-down experiment with the GST-tagged *Sa*MerA. The results, as determined by SDS-PAGE analysis, are shown in Figure 2.15.

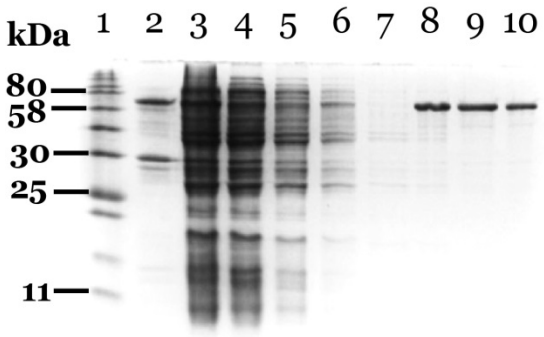


**Figure 2.15 Pull-down assay for *Sa*MerA WT against *S. aureus* JE2 lysate. Lanes (1) molecular weight ladder, (2) purified GST-tagged *Sa*MerA WT, (3) *S. aureus* JE2 lysate wash 1, (4) *S. aureus* JE2 lysate wash 2, (5) *S. aureus* JE2 lysate wash 3, (6) *S. aureus* JE2 lysate wash 4, (7) *S. aureus* JE2 lysate wash 5, (8-10) GST-*Sa*MerA WT elution fractions.**

It can be seen that the only protein that eluted during the elution step was the GST-*Sa*MerA. There are a few faint bands below the *Sa*MerA bands (lane 8-10) but these faint bands were also present in the wash steps (lane 3-7). This confirms that GST-*Sa*MerAWT was bound to the GSH resin, although no other protein appeared to bind to *Sa*MerA. This result suggests that *Sa*MerA WT does not require a protein partner.

#### 2.2.8.2 Assessing potential disulfide substrates

Reactive oxygen species (ROS) as well as reactive chlorine species (RCS) are known to oxidize thiol groups. Cysteine thiols can undergo oxidation to sulfenic acids (via sulfenyl chlorides in the case of HOCl oxidation) which can react with another cysteine within close proximity forming disulfides [49-51]. The thioredoxin system (TrxA/TrB) is in place to reduce protein disulfides formed through ROS/RCS [52]. On the other hand, *S. aureus* also produces a number of LMW thiols (Cys, CoA, BSH, LipA) which can also form disulfides due to oxidative stress such as neutrophil derived $H_2O_2$ or HOCl. In order to recycle the disulfide form of the LMW thiol there are specific reductases (depending on the species) in place. Indeed, with the formation of LMW thiol disulfides *S. aureus* produces dedicated enzymes that are able to reduce the disulfide substrates. For $(CoAS)_2$, *S.* aureus has a dedicated CoA disulfide reductase that recycles the CoA disulfide back to the free CoA-SH [53-55]. In regards to lipoamide/dihydrolipoamide, *S. aureus* produces a dedicated lipoamide dehydrogenase [8, 56, 57]. Currently there is no direct evidence of a BSSB reductase being present in *S. aureus*, or any other organism. Another potential disulfide substrate is pantethine, the disulfide form of pantetheine, which is also a metabolic degradation product of CoA.

In continuation for the search of potential substrates for *Sa*MerA, selected disulfides were as assessed. In context to the neutrophil, LMW thiol disulfides were prepared via $H_2O_2$ oxidation of LMW thiols (details described in 2.4.6). Known disulfide reductases Gor, LipDH and CoADR were used as positive control reactions towards disulfides $(GSH)_2$, dihydrolipoamide $(DHLA)_2$ and $(CoAS)_2$ respectively. The same reaction conditions were used in assessing *Sa*MerA's activity towards the disulfide substrates. The results of these activity tests are shown in Figure 2.16 and Figure 2.17.

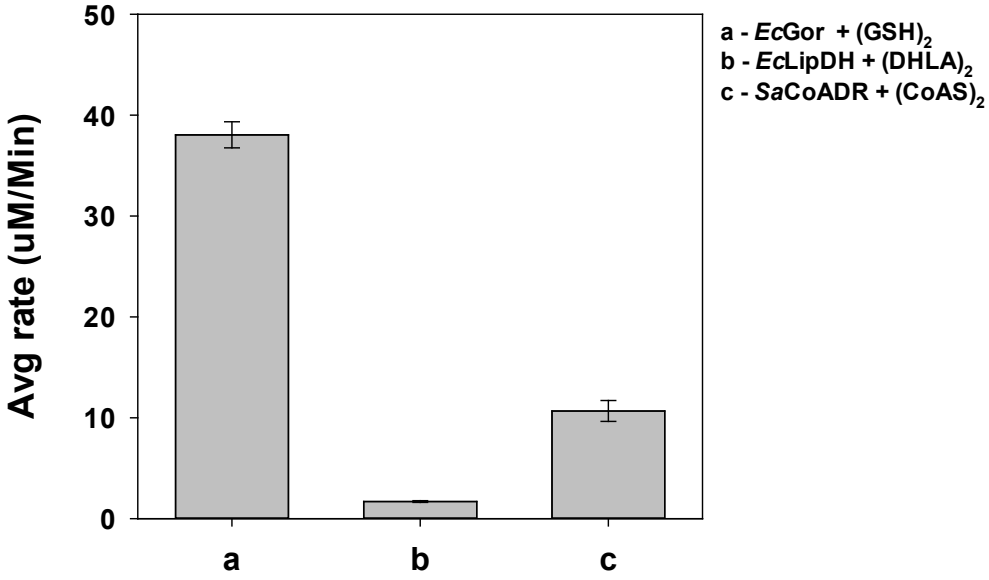


**Figure 2.16 *Ec*Gor, *Ec*LipDH and *Sa*CoADR activity towards disulfides respectively. (a) *Ec*Gor + $(GSH)_2$, (b) *Ec*LpDH + dihydrolipoamide, (c) *Sa*CoADR + $(CoAS)_2$. Concentrations used: 100 µM NADPH, 100 µM disulfide substrate, 25 nM enzyme. All reactions contained NADPH except LipDH which contains NADH. Data shown is the average rate obtained for one biological repeat performed in triplicate; the error bars show standard deviation.**

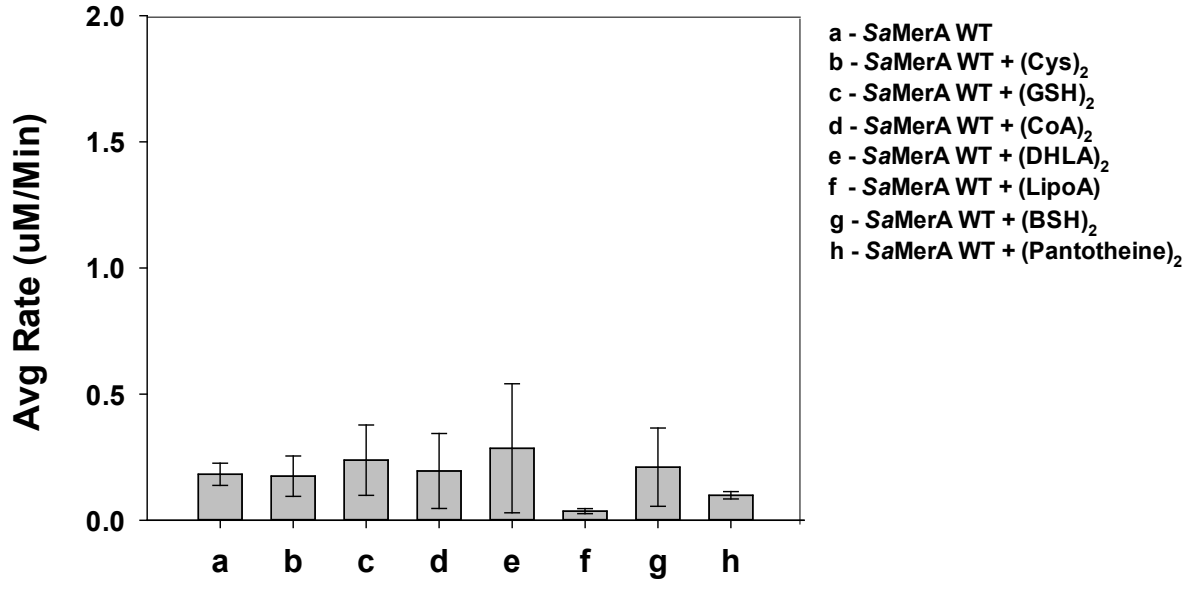


**Figure 2.17 Assessing *Sa*MerA's activity towards selected disulfides. (a) *Sa*MerA, (b) *Sa*MerA + $(Cys)_2$, (c) *Sa*MerA + $(GSH)_2$, (d) *Sa*MerA + $(CoAS)_2$, (e) *Sa*MerA + $(DHLA)_2$, (f) *Sa*MerA + lipoamide, (g) *Sa*MerA + $(BSH)_2$, (h) *Sa*MerA + Pantethine. Concentrations used: 100 µM NADPH, 100 µM disulfide substrate, 25 nM enzyme. All reactions contained NADPH. Data shown is the average rate obtained for one biological repeat performed in triplicate; the error bars show standard deviation.**

These results demonstrate that *Sa*MerA did not show any substantial activity towards any of the selected disulfides tested.

#### 2.2.8.3 Hypochlorous acid and thiols

Hypochlorous acid (HOCl) is an abundant myeloperoxidase-derived RCS found within the neutrophil environment [58-61]. Considering *Sa*MerA did not show any appreciable activity towards $H_2O_2$- or $H_2O_2$ - derived disulfides it was therefore assessed if any activity would be shown towards HOCl or HOCl-derived thiol compounds.

*Sa*MerA's activity towards HOCl was first attempted to be tested directly, but addition of NADPH to reaction mixtures containing HOCl caused immediate oxidation of the NADPH (as evidenced by disappearance of the absorbance at 340 nm). At higher HOCl concentrations, the NADPH was shown to be chlorinated (presumably on the amine of the adenine moiety) [62]. In the context of the neutrophil that produces HOCl, this suggests that it would most likely also react with molecules in the immediate vicinity of the neutrophil as soon as it is formed. Likely major primary and secondary targets for HOCl would be thiols and amines respectively. Consequently, the bulk of HOCl is expected to rather result in the formation of reactive or nonreactive chlorinated species within the neutrophil and engulfed pathogen, and that it is one or more of these compounds that would act as the substrate of *Sa*MerA [58, 63-66]. With this in mind, it was further investigated if *Sa*MerA shows activity towards LMW disulfides derived from HOCl oxidation. Towards this end, each thiol was reacted with an equimolar amount of HOCl. The absence of residual HOCl was confirmed using the absorbance maximum for HOCl at 291 nm ($\varepsilon$=142 $M^{-1}.cm^{-1}$). Figure 2.18 shows *Sa*MerA's activity towards these HOCl-derived thiols. *Sa*MerA showed very little activity towards any of the tested HOCl-derived compounds.

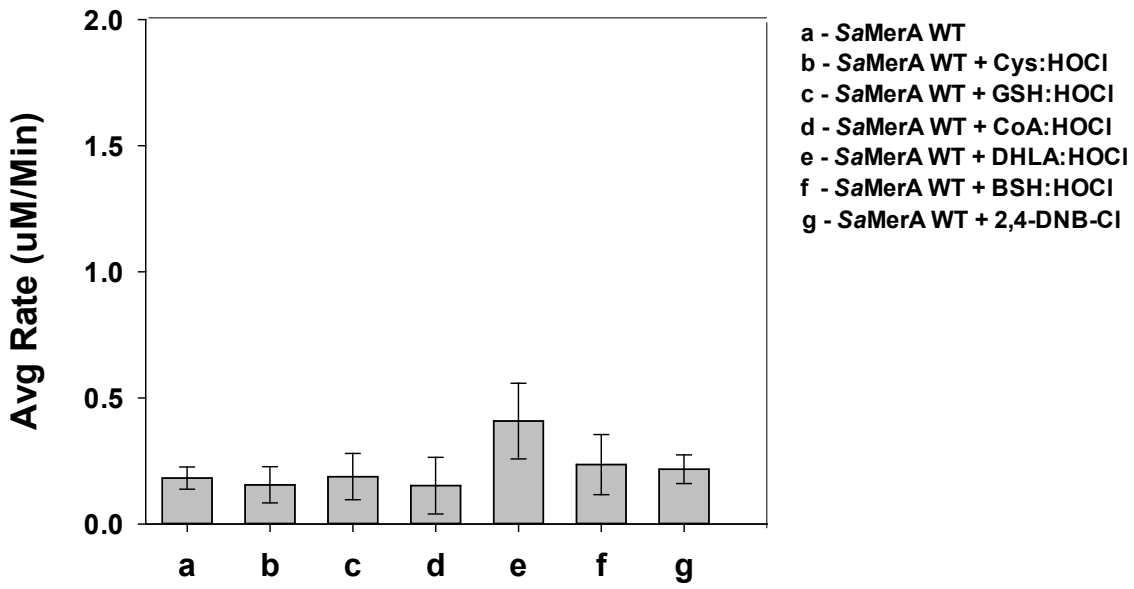


**Figure 2.18 *Sa*MerA's activity towards HOCl-derived disulfides. (a) *Sa*MerA WT, (b) *Sa*MerA WT + Cys:HOCl, (c) *Sa*MerA WT + GSH:HOCl, (d) *Sa*MerA WT + CoA:HOCl, (e) *Sa*MerA WT + DHLA:HOCl, (f) *Sa*MerA WT + BSH:HOCl, (g) *Sa*MerA WT + 2,4-dinitrobenzenesulfenyl chloride. Concentrations used: 100µM NADPH, 100µM sulfenyl chloride substrate, 25nM enzyme. All reactions contained NADPH. Data shown is the average rate obtained in three biological repeats (n=3), each performed in triplicate. The error bars show the SEM.**

### 2.2.8.4 Hypochlorous acid and amino acids

In the context of the neutrophil environment the secondary target of HOCl (after thiols) are amines. Considering that HOCl-treated LMW thiols showed no activity towards *Sa*MerA, it was investigated whether HOCl-derived chloramine compounds would act as substrates of *Sa*MerA as a means to rendering them harmless. A number of chloramines were tested as shown in Figure 2.19. The various amino acid chloramines were prepared using HOCl and amino acid mixed in a 1:1 ratio, following which their concentrations were confirmed using the chloramine absorbance maximum at 252 nm ($\varepsilon$ = 429 $M^{-1}.cm^{-1}$) [66].

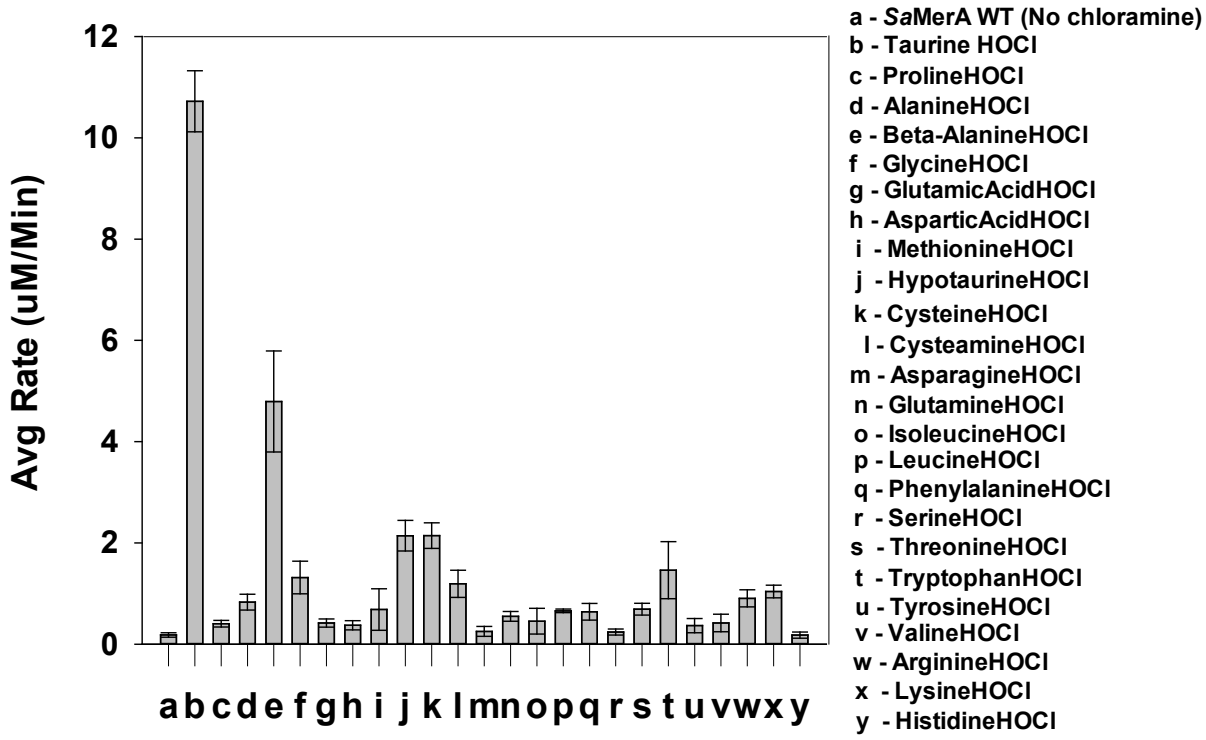


**Figure 2.19 *Sa*MerA's activity towards various chloramines. All reactions contain NADPH and enzyme. Concentrations used: 100 µM NADPH, 100 µM chloramine substrate, 25 nM enzyme. Data shown is the average rate obtained in two biological repeats (n=2), each performed in triplicate. The error bars show the range/2.**

*Sa*MerA showed varied activity towards the range of chloramines tested, with greatest activity towards *N*-chlorotaurine and *N*-chloro-β-alanine. In addition to the amino acid chloramines, the chloramine of the taurine variant hypotaurine was also tested (j). Hypotaurine is involved in the biosynthesis of taurine, but also shows structural similarities to both taurine and β-alanine. We were interested if the enzyme can distinguish between these compounds. The chloramine of hypotaurine showed much lower activity than *N*-chlorotaurine which can be in part due to the binding of the sulfinic acid (hypotaurine) compared to the sulfonic acid (taurine) in *Sa*MerA's active site. The reaction product of HOCl with cysteamine was also assessed (l), although in its case it is unclear if the HOCl reacts with thiol first, following transfer to form the more stable chloroamine. Regardless, there have been some reports of the role cysteamine plays in antimicrobial mechanisms of a number of pathogens [67-72]. *Sa*MerA showed low activity towards the cysteamine/HOCl mixture.

Taurine is probably the most prominent amino acid in the neutrophil environment [73]. It is an abundant non-proteogenic sulfonated β-amino acid that is found in all cell types, with

particularly high concentrations (up to 50 mM) found in neutrophils [58, 60, 61, 66, 73-81]. It is well established that most of the HOCl that is formed by myeloperoxidases reacts with taurine to form *N*-chlorotaurine (NCT) [82-89]. NCT is a proven antimicrobial with activity in the micromolar range as demonstrated in a number of studies [82, 83, 90-135]. The activity of *Sa*MerA for *N*-chloro-β-alanine was not surprising, considering β-alanine is structurally similar to taurine. The high activity of *Sa*MerA towards NCT was an exciting finding that potentially links the enzyme directly to a key neutrophil-derived compound.

Considering that *Sa*MerA showed activity towards chloramines, the activity of the *E. coli* homologue YkgC/RclA was also assessed under similar conditions.

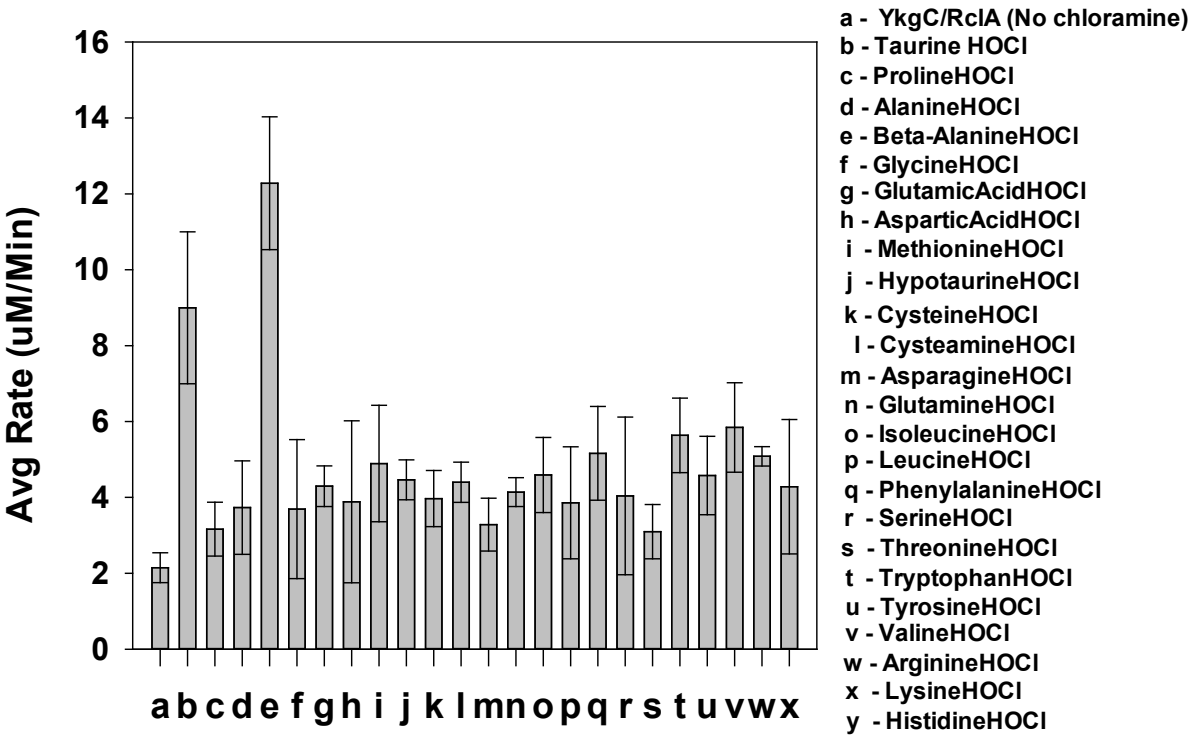


**Figure 2.20 YkgC's activity towards various chloramines. All reactions contain NADPH and enzyme. Concentrations used: 100 µM NADPH, 100 µM chloramine substrate, 25 nM enzyme. Data shown is the average rate obtained for one biological repeat (n=1) performed in triplicate. The error bars show the standard deviation.**

YkgC/RclA indeed showed activity towards the various chloramines. Gratifyingly, the highest activity was also seen for NCT and chloro-β-alanine, although YkgC seemed to show a preference for the latter substrate, in contrast to *Sa*MerA that clearly prefers to act on NCT. The chloramines of other physiologically relevant amino acids such as γ-aminobutyric acid (GABA), ε-caproic acid, 1-aminopropanoic acid and 2-aminoethylphosphonic acid were also tested as substrates of *Sa*MerA and YkgC; however, their activity (data not shown) was not

found to be considerably different to the activity seen for chloramines of the amino acids (excluding NCT and chloro-β-alanine) as shown in Figure 2.19 and Figure 2.20.

### 2.2.9 *N*-chlorotaurine (NCT)

Both *Sa*MerA and YkgC/RclA showed good activity towards NCT when prepared by mixing HOCl and taurine in a 1:1 ratio, followed by confirmation of its concentration using its absorbance maximum at 252 nm (ε =429 $M^{-1}.cm^{-1}$) [66]. NCT can also be prepared in a pure form by using an ethanolic mixture of taurine sodium salt and chloramine T (see experimental methods for details) [97, 136]. The NCT produced via both these methods was analysed by proton NMR to confirm the formation of the chloramine. Since the synthetic NCT can be prepared directly at a specific concentration, all further experiments enzyme activity assays were performed using this form of the compound.

Initially the enzyme concentration was set to 25 nM and the concentration of NCT incrementally increased to establish if the enzyme adhered to the Michaelis-Menten model of kinetic behavior. However, this proved to be problematic as various studies have shown that NCT reacts with nucleotides [66, 85, 137-144], thus giving a basal background oxidation rate in reactions that contain NADPH/NADH. To address this problem all activity results are therefore reported as the catalysed vs uncatalysed (cat/uncat) ratio, i.e. the ratio of the rate of NADPH oxidation seen in the presence of enzyme compared to the rate when enzyme is absent. In the first set of experiments two concentrations of NCT were used to assess the activity of *Sa*MerA WT and its mutants.

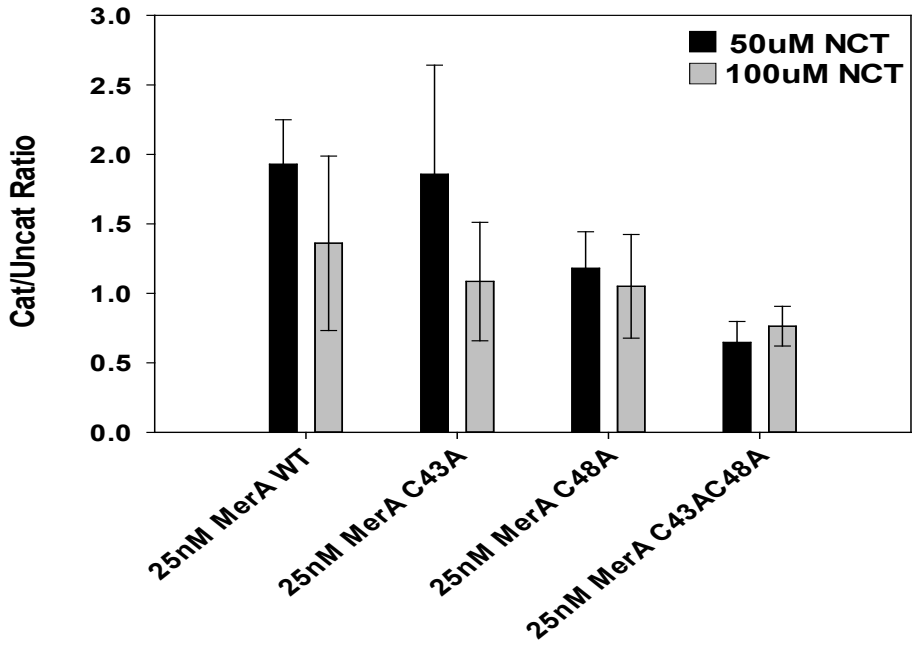


**Figure 2.21 Cat/uncat ratio of NADPH oxidation by 50 µM or 100 µM NCT as mediated by *Sa*MerA. NADPH was 100 µM in all reactions. Data represents the result of one biological repeat (n=1) performed in triplicate. The error bars show the standard deviation.**

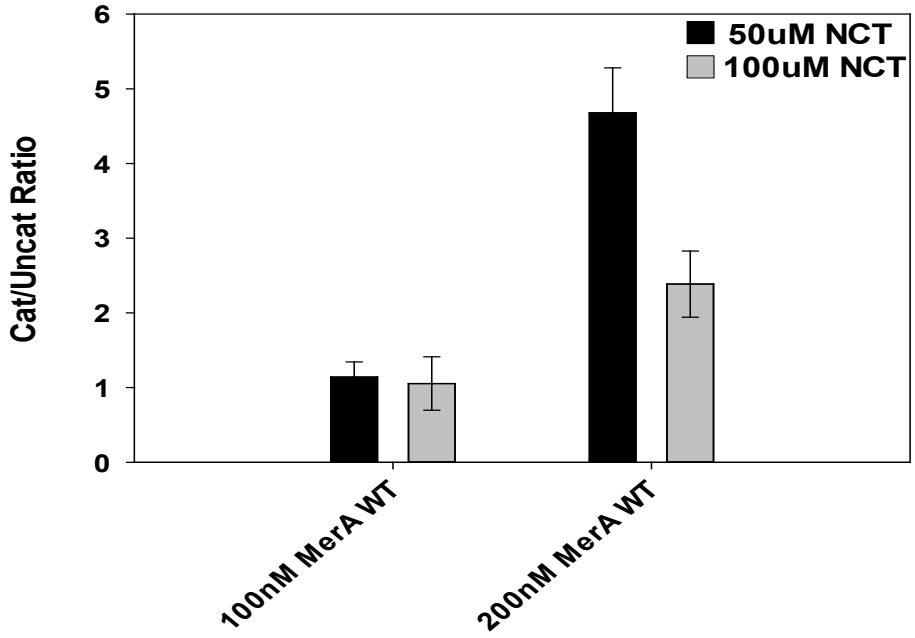


**Figure 2.22 Cat/uncat ratio of NADPH oxidation by 50 µM or 100 µM NCT as mediated by 100 nM or 200 nM *Sa*MerA. NADPH was 100 µM in all reactions. Data represents the result of one biological repeat (n=1) performed in triplicate. The error bars show the standard deviation.**

The cat/uncat ratio at 50 µM NCT using 25 nM *Sa*MerA WT was more than 2.0 the cat/uncat ratio for that seen using *Sa*MerA C43AC48A (Figure 2.21). In regards to the single mutants *Sa*MerA C43A showed some residual activity, which could be due to the fact that the Cys48, which is in close proximity to the FAD (Figure 2.7), may perform a modified monothiol-based reaction. In the case of the C48A mutant, the remaining Cys43 is still intact but since it is further away from the FAD it may not able to be regenerated after one round of catalysis. Increasing the NCT concentration showed a decrease in the cat/uncat ratio which is due to a higher background rate of the chlorination of nucleotide. Importantly, increasing the enzyme concentration showed an increase in cat/uncat ratio, confirming the involvement of the enzyme in catalysis (Figure 2.22). Considering the background rate due chlorination of nucleotide, as well as the cat/uncat data at 50 µM NCT (Figure 2.21), the approach to confirm enzyme activity towards NCT was then altered such that the substrates NCT and NADPH were kept constant at 50 µM and 100 µM respectively while the enzyme concentration was increased incrementally.

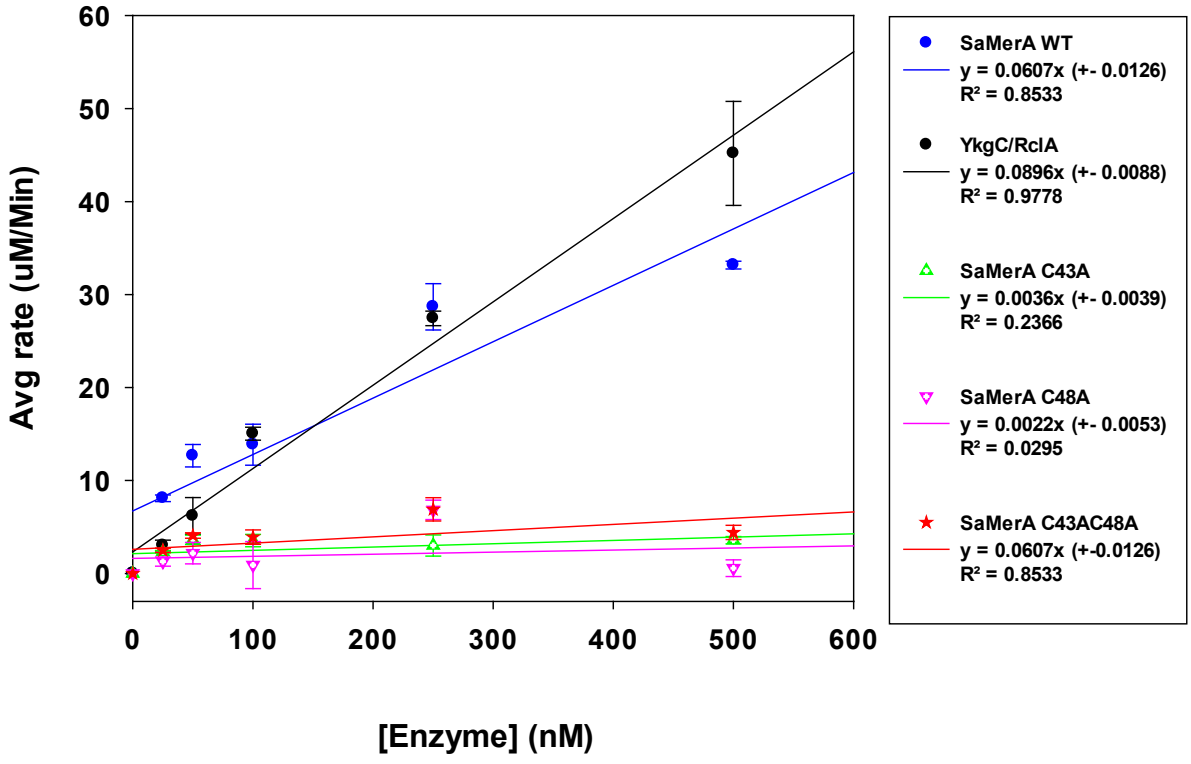


**Figure 2.23 Activity (as determined from initial rates) of *Sa*MerA WT, its single and double mutants and YkgC/RclA acting on 50 µM NCT (prepared synthetically). Data represents the result of one biological repeat (n=1) performed in triplicate. The error bars show the standard deviation. The solid lines represent the best fit straight line through the data points. The slopes of the fitted lines (the specific activity in µM/min/nM enzyme) are given in the legend.**

The result in Figure 2.23 gratifyingly showed a linear relationship of *Sa*MerA and YkgC/RclA's activity towards NCT as the enzymes' concentration increased. This result further confirmed the enzymatic activity of *Sa*MerA and YkgC/RclA towards NCT. All three the *Sa*MerA mutants showed very low specific activities for NCT under these conditions, indicating the requirement of the active site CxxxxC motif for catalysis.

With these positive results obtained using NCT synthesized directly, we decided to repeat the experiment using NCT made by mixing HOCl and taurine. This was based on the consideration that the HOCl produced by MPO in the neutrophil would most likely form NCT in a similar manner by reaction with taurine. Using the same reaction conditions used to obtain the data in Figure 2.23, we tested NCT and *N*-chloro-β-alanine made by mixing HOCl and the amino acid in a 1:1 ratio.

The first attempt at this experiment using *Sa*MerA acting on either 50 μM NCT or *N*-chloro-β-alanine worked well (Figure 2.24). The specific activities obtained in this manner agreed closely with the values obtained in the previous experiment.

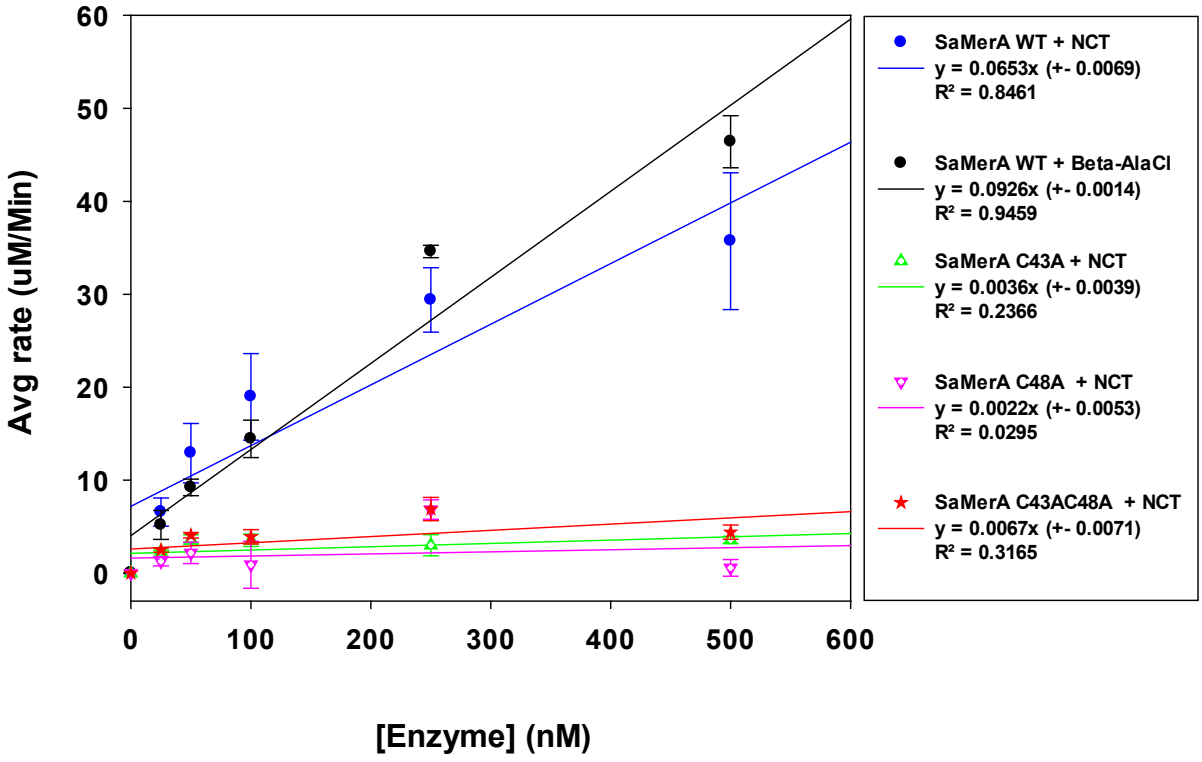


**Figure 2.24 Activity (as determined from initial rates) of *Sa*MerA WT and its mutants acting on 50 µM NCT (prepared by mixing HOCl and taurine) and 50 µM *N*-chloro-β-alanine (prepared by mixing HOCl and β-Ala). Activity of *Sa*MerA WT against NCT shown as black data points whilst *Sa*MerA WT against *N*-chloro-β-alanine shown in bue. Data represents the result of one biological repeat (n=1) performed in triplicate. The error bars show the standard deviation. The solid lines represent the best fit straight line through the data points. The slopes of the fitted lines (the specific activity in µM/min/nM enzyme) are given in the legend.**

Experiments conducted with YkgC/RclA under similar reaction conditions showed that the reaction had already reached completion before analysis commenced (data not shown). That is, all the NADPH substrate had been consumed before the first reading could be taken on the spectrophotometer. To address this, the YkgC/RclA concentration was decreased below 25 nM while maintaining the substrate concentrations as in the previous experiment (Figure 2.25). The resulting specific activities towards NCT and *N*-chloro-β-alanine were very similar, and ~4-fold higher than the values obtained with *Sa*MerA.

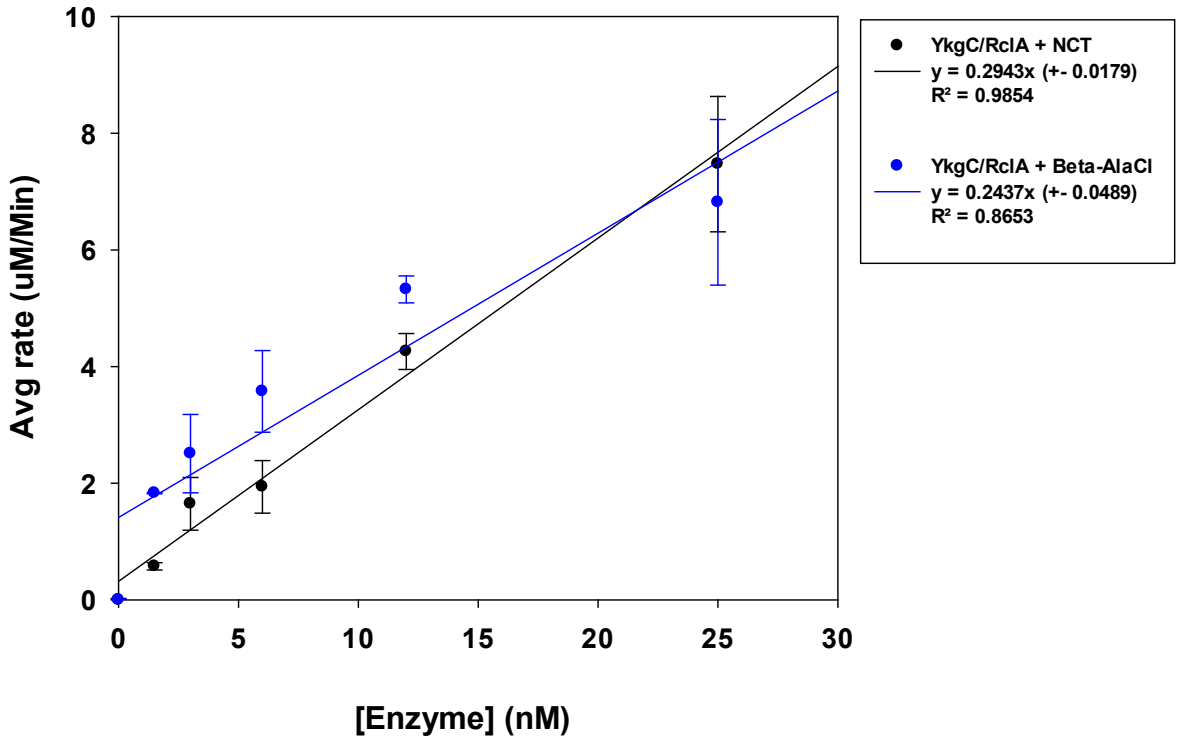


**Figure 2.25 Activity (as determined from initial rates) of YkgC/RclA towards 50 µM NCT (prepared by mixing HOCl and taurine) and 50 µM N-chloro-β-alanine (prepared by mixing HOCl and β-Ala). Data represents the result of one biological repeat (n=1) performed in triplicate. The error bars show the standard deviation. The solid lines represent the best fit straight line through the data points. The slopes of the fitted lines (the specific activity in µM/min/nM enzyme) are given in the legend.**

Taken together, these results indicate that both *Sa*MerA and YkgC/RclA show a linear enzyme concentration-dependent increase in activity towards HOCl-derived NCT and *N*-chloro-β-alanine. This data further supports the hypothesis that *Sa*MerA and YkgC/RclA detoxifies chloramines that form from neutrophil-produced HOCl that reacts with abundant amino acids, such as taurine and β-alanine.

#### 2.2.9.1 Proposed catalytic mechanism of SaMerA

A search of the protein database (PDB) shows a number of X-ray crystal structures with the ligand taurine bound. These include the taurine/alpha-ketoglutarate dioxygenase from *E. coli* (1GQW, 1GY9), iron-free TauD from *E. coli* (1OTJ, 1OS7), bile acid hydrolase from *Clostridium perfringens* (2BJF), *E. coli* GTP cyclohydrolase II (2BZ1), peptidoglycan endopeptidase from *Bdellovibrio bacteriovorus* (3V39), NanB sialidase from *Streptococcus pneumoniae* (4FOQ), Ternary complex of DNA polymerase epsilon (4M8O) and the ligand binding domain *Vibrio cholerae* chemoreceptor Mlp37 (5AVF). These enzymes are unrelated to *Sa*MerA or YkgC/RclA; however, some are involved in the biosynthesis of hypotaurine and finally taurine (1GQW, 1GY9, 1OTJ). Mapping the ligand interactions of the active site residues of these enzymes with taurine shows hydrogen bonding and ionic interactions with the sulfonic acid moiety mediated by arginine, valine, lysine or histidine. The amino portion of taurine is usually bound to aspartic acid, asparagine or tyrosine. Examples of ligand binding plots with taurine in various proteins are shown in Figure 2.26.

*Sa*MerA has similar amino acids arranged around the entrance of the active site, and therefore the schematic diagram of its active site layout was drawn showing the potential interactions with NCT (Figure 2.27). The 3-dimensional model of the active site shown in Figure 2.28 gives one a sense of the relative size of the active site, and how taurine/NCT could potentially be accommodated.

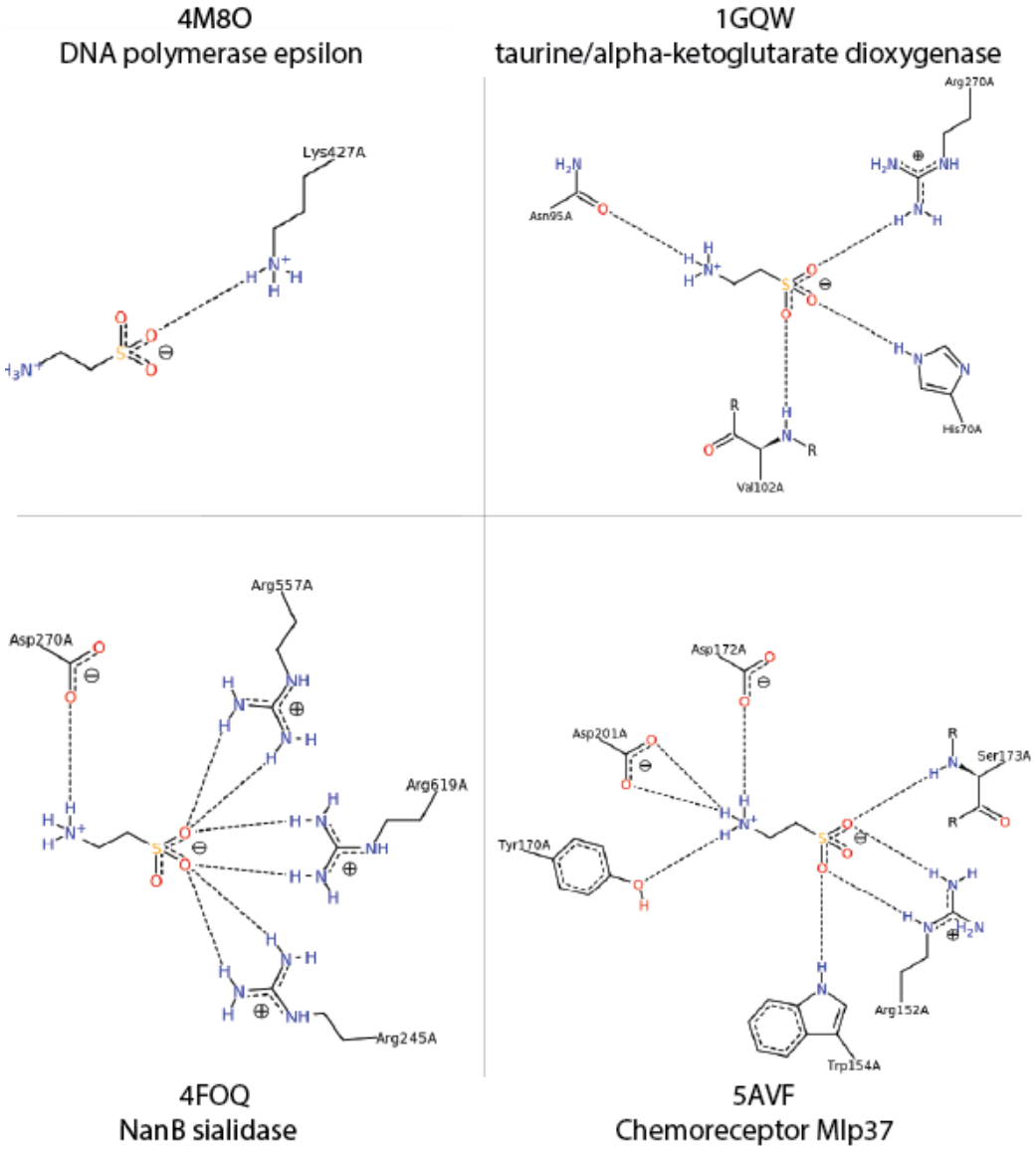


**Figure 2.26 Examples of ligand binding plots of taurine bound in the active sites of a variety of enzymes, as indicated.**

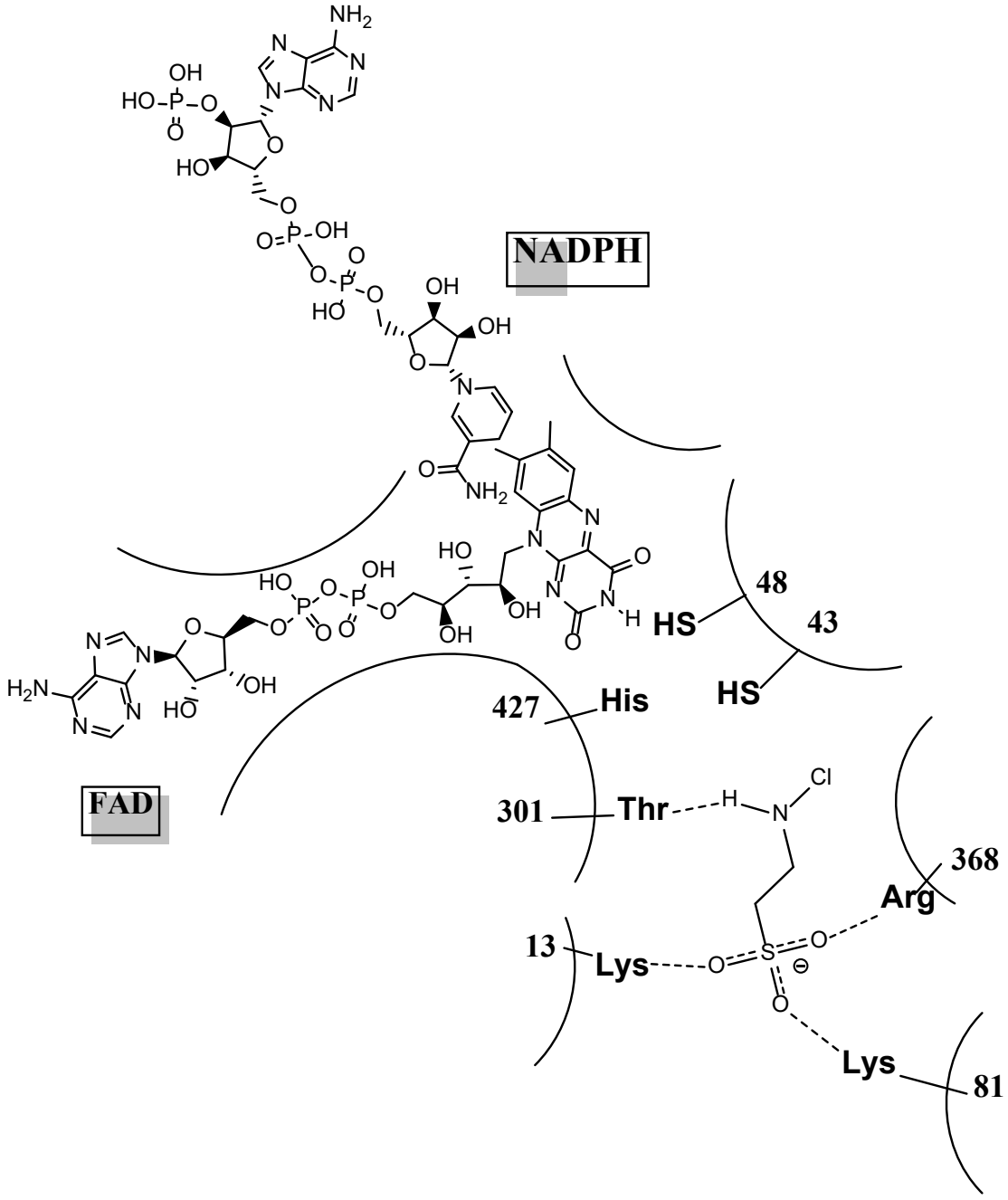


**Figure 2.27 Schematic diagram showing potential binding interactions between residues in *Sa*MerA's active site and NCT, based on the ligand plots showed in the previous figure.**

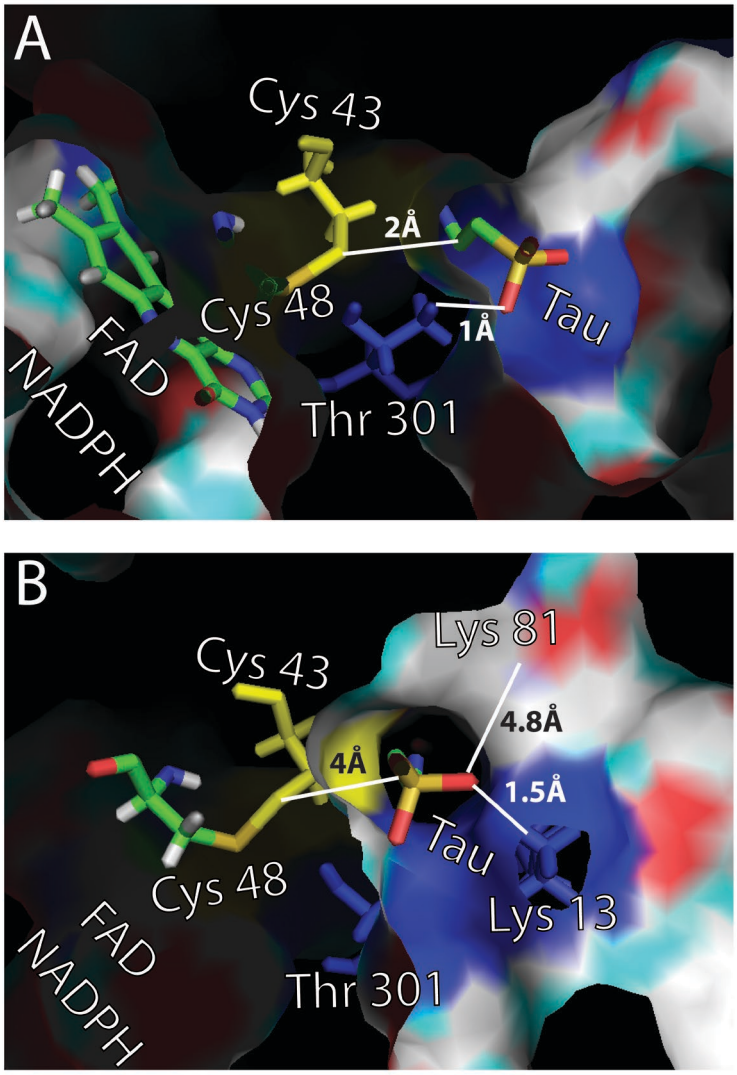


**Figure 2.28 Vacuum electrostatics (protein contact potential) of the *Sa*MerA active site showing the potential binding mode of taurine from two different views (A) and (B). Taurine was manually placed into *Sa*MerA's active site using the manual mode in Pymol. The taurine molecule was obtained from the PDB. Amino acids potentially involved in taurine binding Thr301, Lys13 and Lys81 are colored in blue and labelled accordingly. Arg368 (above the plane of view and not showed) can also form a hydrogen bond to taurine.**

The proposed mechanism of *Sa*MerA ($E_{ox}$) with NCT is shown in Figure 2.29 A and B. The proposed mechanism follows that of other DSRs involving a reductive and oxidative half reaction, and the known mechanism of thiols reacting with chloramines. The reductive half reaction involves the transfer of electrons from the incoming NADPH to the FAD, which subsequently reduces the resting disulfide of $E_{ox}$. Cys48 would be able to form a charge transfer complex with the FAD at this stage ($EH_2.NADP^+$). The oxidative half reaction

involves the deprotonation of Cys43 (most likely by His427) to give a thiolate that can attack the chloramine of the incoming NCT. This would result in formation of a sulfenyl chloride enzyme intermediate, and release of taurine following the protonation of its amine (most likely by His427). Thereafter the thiolate of Cys48 attacks the Cys43-Cl, releasing $Cl^-$ and followed by $NADP^+$. This completes the cycle regenerating $E_{ox}$ for another round of catalysis.

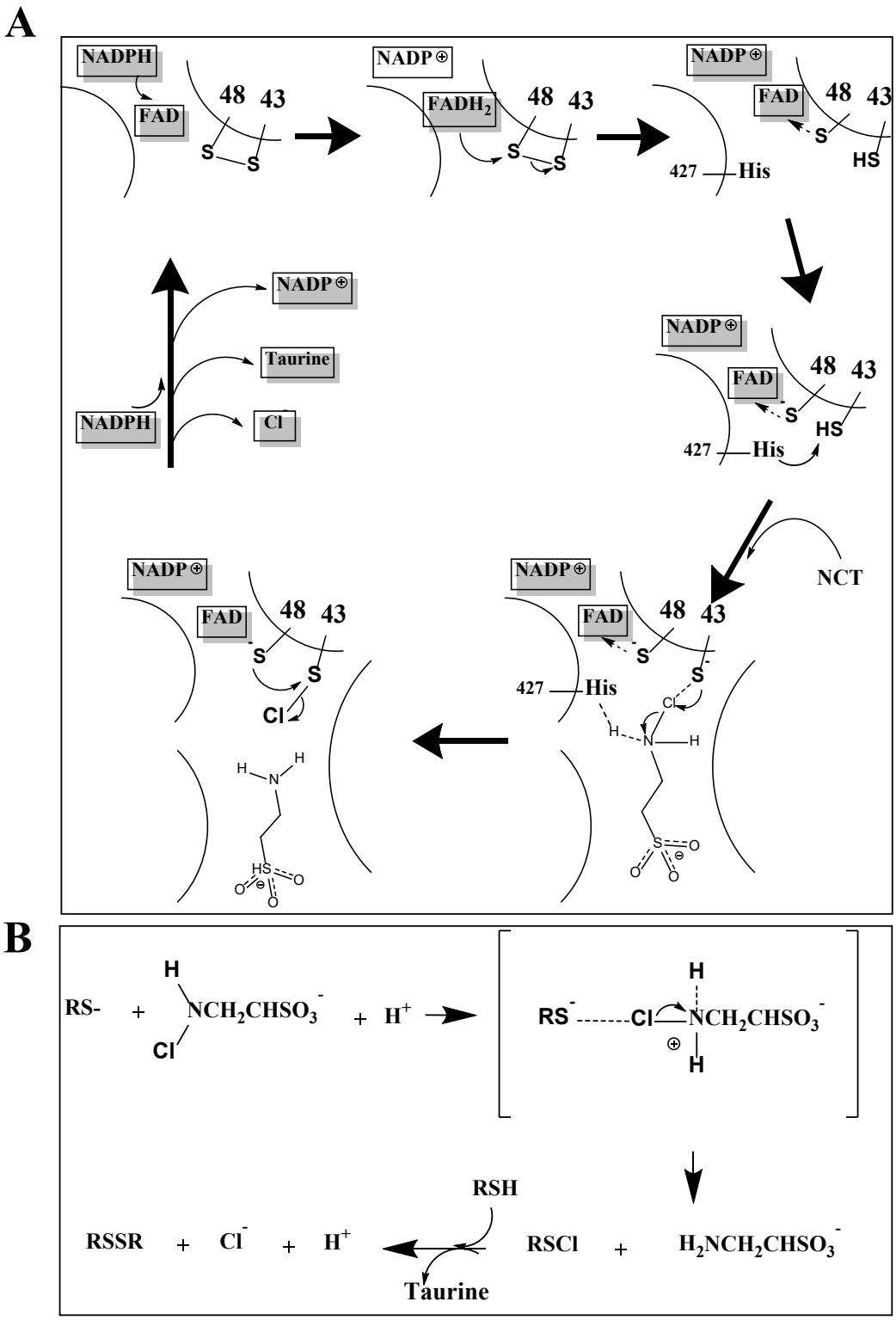


**Figure 2.29 Proposed mechanism of *Sa*MerA with NCT. (A) Briefly *Sa*MerA (Eox) with resting disulfide (top right-hand side) is reduced by the incoming NADPH via FAD. Cys48 forms a charge transfer complex with FAD and a proton is abstracted by His427 from Cys43 which attacks the chloramine of NCT, forming a sulfenyl chloride intermediate and releasing taurine. The Cys48 thiolate attacks the Cys43-Cl, resulting in the release of $Cl^-$ and $NADP^+$ to regenerate $E_{ox}$ for another round of catalysis. (B) shows a short-hand scheme of NCT reacting with thiol. Redrawn from [66].**

## 2.2.10 Synthesis of potential inhibitors of *Sa*MerA

To further strengthen our mechanistic hypothesis for *Sa*MerA, we set out to synthesize small molecule mechanism-based inhibitors of the enzyme. As a proof of principle, we investigated the use of small molecule "warhead" type inhibitors, namely the acivicin derivatives (isoxazolines) [145-148]. These inhibitors form irreversible covalent modifications (via addition-elimination) with the nucleophilic cysteine residue/s in enzyme active sites (Scheme 1). Isoxazoline inhibitors have been used to inhibit plasmodium glyceraldehyde-3-phopshate dehydrogenase *in vitro* [149] as well as bacterial murein/peptidoglycan biosynthesis (MurE inhibition) [150].

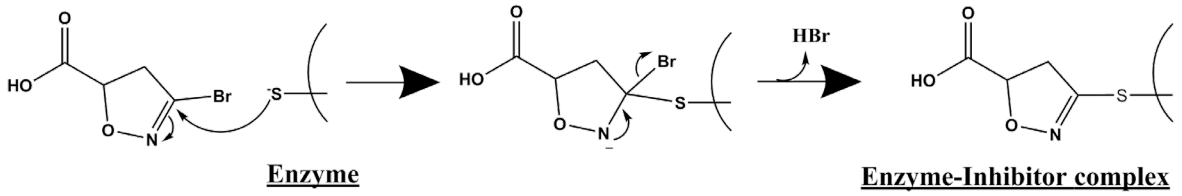


**Scheme 1. Bromoisoxazole reacting with active site Cys to form irreversible enzyme-inhibitor complex.**

The following section is based upon the synthesis and in *vitro* testing of 3-bromo-4,5-dihydro-isoxazole-5-carboxylic acid (compound **6k**), 3-bromo-5-tert-butyl-4,5-dihydro-isoxazole (compound **6l**), 3-bromo-5-cyclohexyl-4,5-dihydro-isoxazole (compound **6b**), 3-bromo-4,5-dihydro-isoxazole-5-sulfonic acid (compound **6s**) (Figure 2.30).

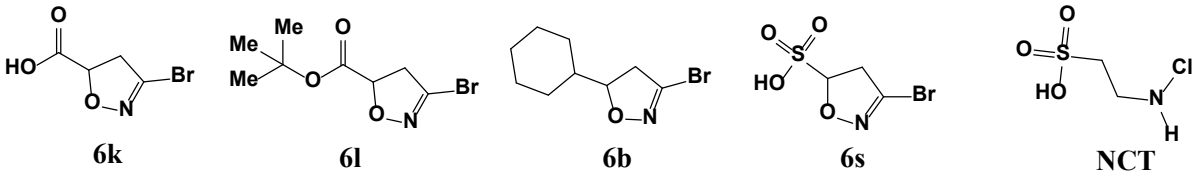


**Figure 2.30 Putative *Sa*MerA inhibitors 3-bromo-4,5-dihydro-isoxazole-5-carboxylic acid (compound 6k), 3-bromo-5-tert-butyl-4,5-dihydro-isoxazole (compound 6l), 3-bromo-5-cyclohexyl-4,5-dihydro-isoxazole (compound 6b), 3-bromo-4,5-dihydro-isoxazole-5-sulfonic acid (compound 6s), *N*-chlorotaurine (NCT) is shown for comparison.**

The only differences to the four compounds are the entities attached to the bromoisoxazole group. *Sa*MerA and YkgC/RclA showed considerable activity towards *N*-chloro-β-alanine and NCT, therefore the four compounds were chosen to mimic the structures of these substrates. Compound **6k** contains the free carboxylic group which shares close similarity to β-alanine, whereas compound **6s** has a sulfonic group which resembles taurine.

Compounds **6l** and **6b** contain large and more hydrophobic groups, which we predicted may affect them gaining access to the active site Cys residue/s, and could therefore be used to demonstrate selectivity. However, compounds **6l** and **6b** are more likely to be able to cross the bacterial cell membrane compared to **6s** or **6k**. With these considerations in mind, we set out to synthesise and test these compounds.

### 2.2.10.1 Synthesis of compounds 6k, 6l, 6b, 6s

The synthesis of compound **6k**, **6a** and **6b** was based upon an established method by Girardin *et al* [151]. Although compound **6s** was not part of the small library published by Girardin *et al*, the same procedure was used in its synthesis. The reactions proceed via cycloaddition of dibromoformaldoxime and the appropriate acrylates (Figure 2. 31).

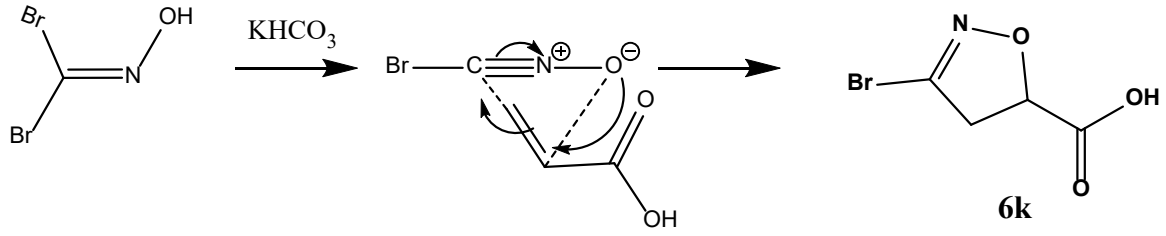


**Figure 2. 31 Cycloaddition reaction of dibromoformaldoxime and acrylic acid forming compound 6k.**

All compounds were UV active and hence product formation could easily be tracked via TLC analysis. For details of the reaction conditions, see the experimental section.

### 2.2.10.2 $^{1}$H NMR analysis of purified compounds

The structures of compounds **6k**, **6l** and **6b** were successfully confirmed by $^{1}$H NMR. Difficulties were encountered with the synthesis of the sulphonate-containing compound **6s**. NMR analysis of potential products revealed that it was mainly unreacted vinysulfonic acid/acrylate species. Synthesis of compound **6s** was thus abandoned and the study was continued with compounds **6k**, **6l** and **6b**.

## 2.2.11 Assessment of enzyme inhibition of *Sa*MerA and YkgC/RclA

Compounds **6k**, **6l** and **6b** were made up in DMSO to a stock concentration of 100 mM, and were used as such in subsequent experiments. Each compound was separately incubated on ice for 30 mins with either *Sa*MerA or YkgC/RclA respectively (that had previously been

treated with DTT) at a 1:10 ratio of enzyme:inhibitor. Thereafter, excess compound was removed using a membrane spin concentrator with MW cutoff of 3,000 Da. The treated enzymes were then assayed for activity on 50 µM NCT using the same experimental approach as described previous for the data obtained and shown in Figure 2.23. In addition to enzymes treated with inhibitor, enzymes were also treated with DMSO (i.e. without inhibitor) as control. In addition, iodoacetamide and *N*-methylmaleimide, which are known cysteine-alkylating agents, were used as positive controls [152].

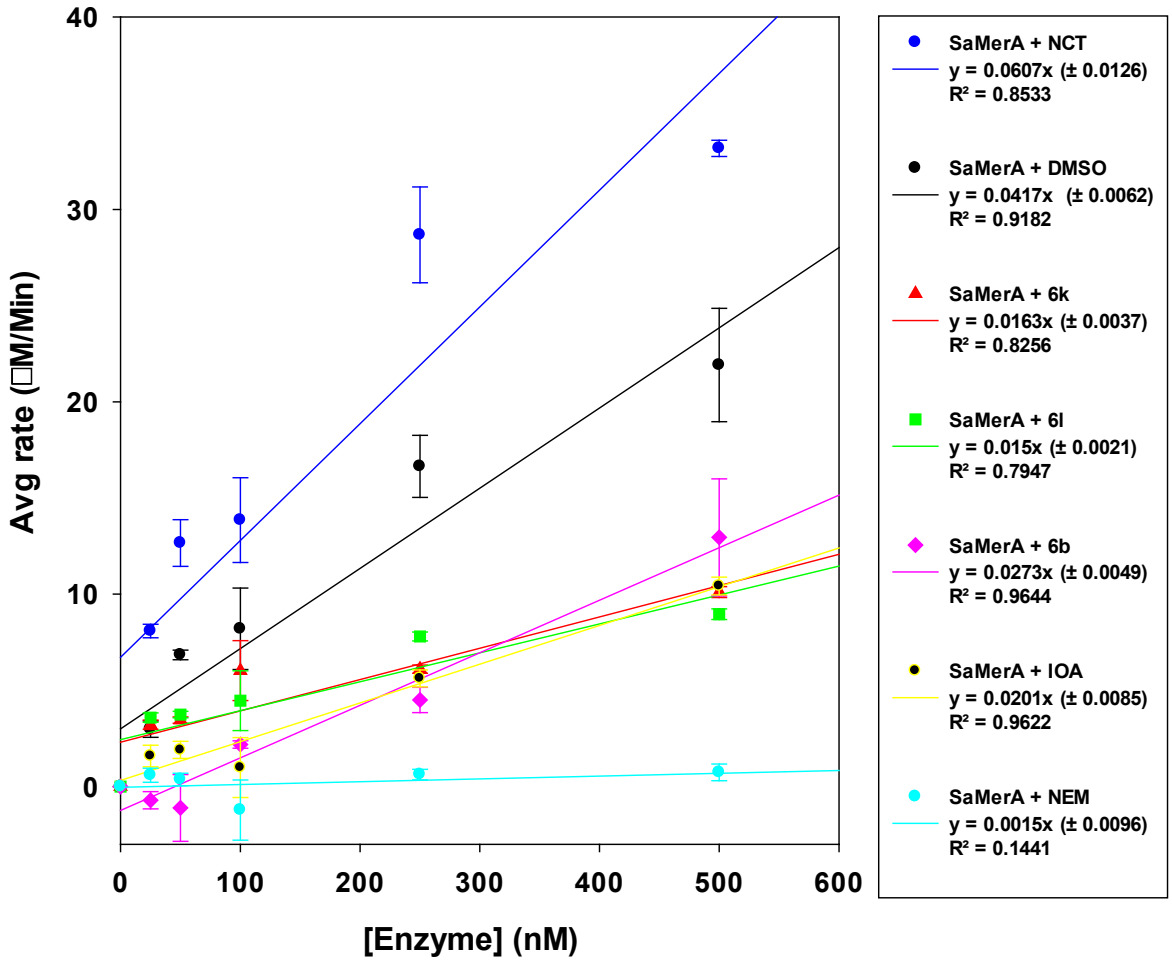


**Figure 2.32 Activity of inhibitor treated *Sa*MerA WT (1:10 Enz: Inhibitor) acting on 50 µM NCT. Control reactions with DMSO, iodacetamide (IOM) and *N*-methylmaleimide (NEM)-treated *Sa*MerA WT are also shown for comparison. Data represents the result of one biological repeat (n=1) performed in triplicate. The error bars show the standard deviation. The solid lines represent the best fit straight line through the data points. The slopes of the fitted lines (the specific activity in µM/min/nM enzyme) are given in the legend.**

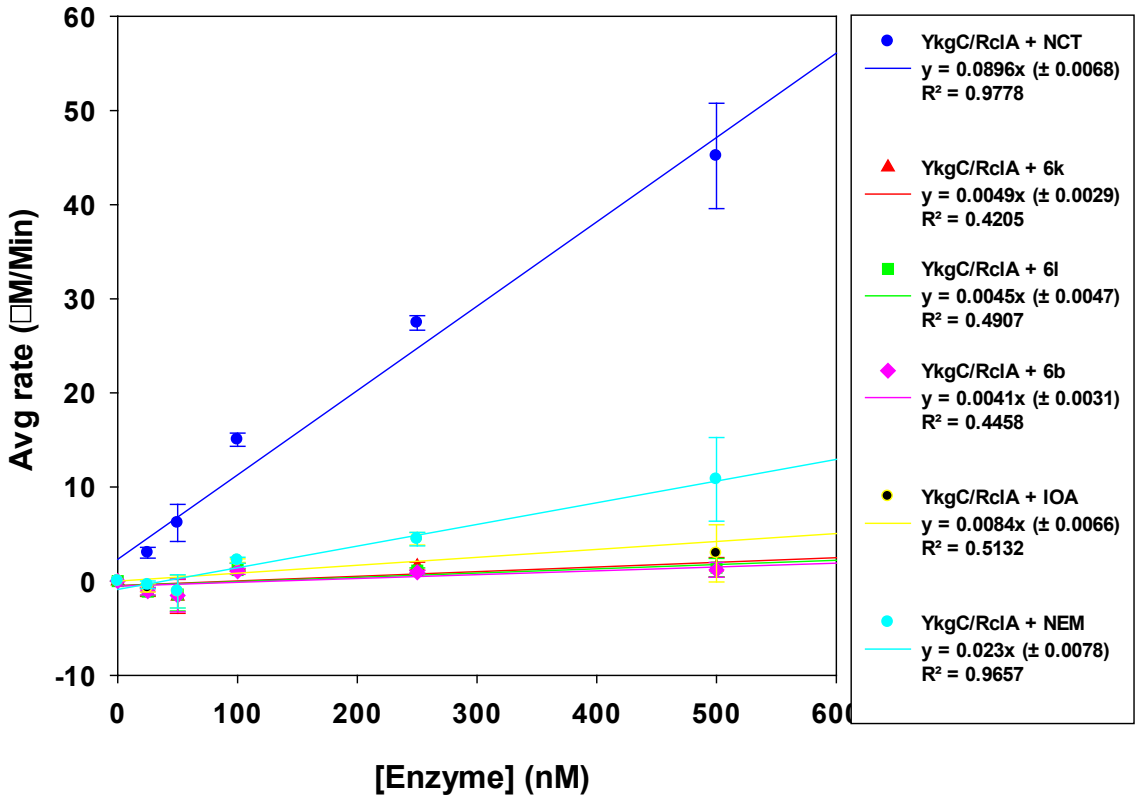


**Figure 2.33 Activity of inhibitor treated YkgC/RclA (1:10 Enz: Inhibitor) acting in 50 µM NCT. Shown for comparisons are YkgC/RclA untreated (DMSO control) as well as control reactions using iodacetamide- and *N*-methylmaleimide-treated YkgC/RclA. Data represents the result of one biological repeat (n=1) performed in triplicate. The error bars show the standard deviation. The solid lines represent the best fit straight line through the data points. The slopes of the fitted lines (the specific activity in µM/min/nM enzyme) are given in the legend.**

All the tested compounds were able to inhibit *Sa*MerA (Figure 2.32). The compounds inhibited the activity of *Sa*MerA by reducing its specific activity approximately 4-fold compared to the untreated *Sa*MerA. Likewise, the tested compounds were also able to inhibit YkgC/RclA (Figure 2.33). When comparing the specific activities of *Sa*MerA treated with **6k**, **6l** and **6b** (Figure 2.32) to those of YkgC/RclA treated with the same compounds, YkgC/RclA showed a greater inhibition. The positive controls, *Sa*MerA and YkgC/RclA treated with iodacetamide and *N*-methylmaleimide, also showed substantial inhibition compared to the untreated enzymes. Overall, the compounds and controls showed a greater inhibition of YkgC/RclA.

To rule out the possibility that the compounds are denaturing or unfolding upon treatment (i.e. that observed inhibition is unrelated to the mechanism), the treated enzymes' structures

were analysed by CD spectroscopy (see Additonal Experimetal data section for data). The CD spectra showed that the compounds did not cause any severe unfolding or change to the overall structure of the enzymes. On the contrary, there was some notable difference in the β-sheet turns (24-260 nm) and an increase (at 210 nm) of the dichroism for the enzyme treated with **6k**, **6l** and **6b**. These differences suggest a tighter folding (rigidification) of the enzyme. The more compact/tighter folding relates to the β-sheet turns which are found between the interface of the two monomers. Directly behind these β-sheet turns are four helixes in which the active site is located. Thus it does appear that the active site forms a more compact or stabilized state upon binding the inhibitor compounds, and hence the observed differences in the CD spectra.

#### 2.2.11.1 Time-dependent enzyme inhibition

After determining that the compounds do not unfold the enzyme, it was investigated whether the compounds inhibit the enzymes in a time-dependent manner. One of the characteristics of mechanism-based inhibition is the time-dependent loss of enzyme activity [153]. To assess time-dependent inhibition *Sa*MerA and YkgC/RclA were separately incubated with 10-fold excess compound. Aliquots were then taken out at time 0, 5, 10, 20 and 30 minutes and the sample tested for activity using 50 μM NCT as substrate. Initial rates were then plotted against time. Control reactions of untreated enzyme as well as enzyme without NCT were also analysed. Data for the time-dependent inhibition of *Sa*MerA is shown in Figure 2.34.

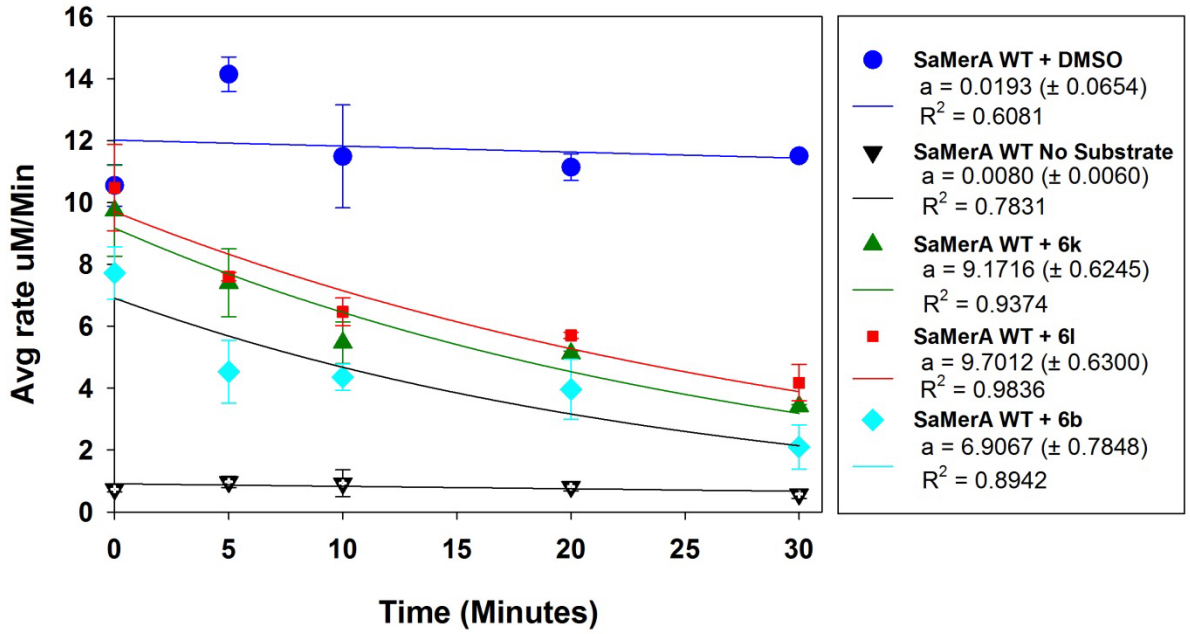


**Figure 2.34 Time-dependent inhibition of *Sa*MerA activity towards 50 µM NCT by compounds 6k, 6l and 6b. 25 nM *Sa*MerA : 250 nM inhibitor compound was used in each experiment. Data represents the result of one biological repeat (n=1) performed in triplicate. The error bars show the standard deviation. The solid lines represent the best fit straight line through the data points. Linear regression used for *Sa*MerA WT DMSO, No Substrate. Exponential decay used for *Sa*MerA WT + inhibitors 6k,6l, and 6b.**

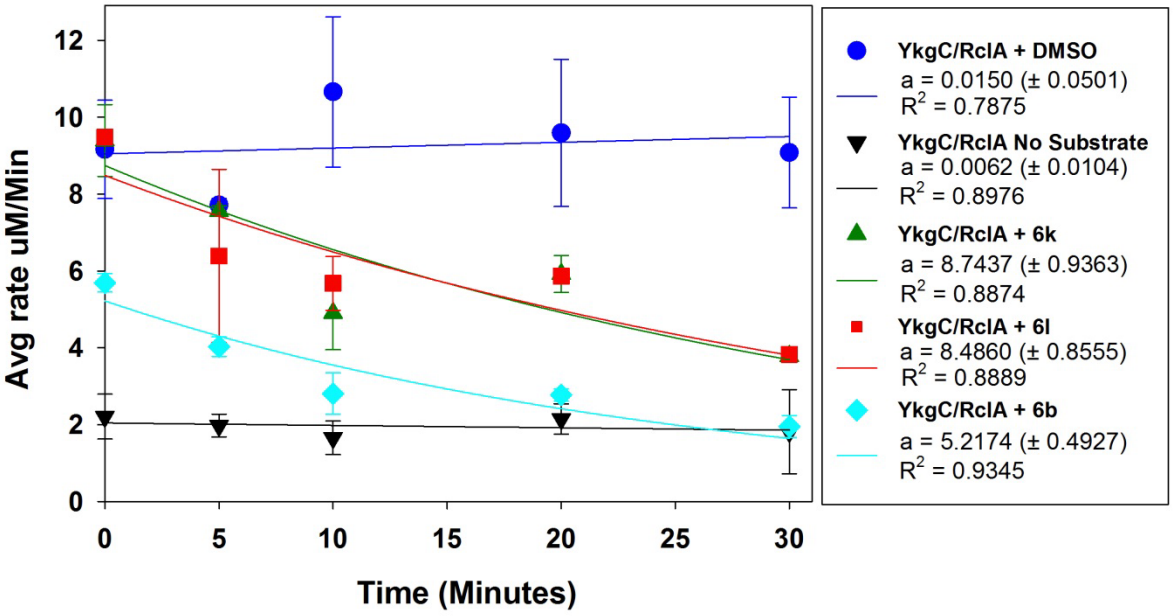


**Figure 2.35 Time-dependent inhibition of YkgC/RclA activity towards 50 µM NCT by compounds 6k, 6l and 6b. 25 nM YkgC : 250 nM inhibitor compound was used in each experiment. Data represents the result of one biological repeat (n=1) performed in triplicate. The error bars show the standard deviation. The solid lines represent the best fit straight line through the data points. Linear regression used for YkgC/RclA DMSO, No Substrate. Exponential decay used for *Sa*MerA WT + inhibitors 6k,6l, and 6b.**

All the tested compounds show time-dependent inhibition of *Sa*MerA (Figure 2.34) and YkgC/RclA (Figure 2.35) respectively, supporting the analysis that the compounds are indeed mechanism-based inhibitors. Interestingly compounds **6k** and **6l** showed similar trends in the rate of inactivation of the enzymes, while compound **6b** showed an increased rate of inhibition.

The three inhibitors were chosen to mimic the structures of the substrates *N*-chloro-β-alanine and NCT. Compound **6k** contains the free carboxylic group whereas compounds **6l** and **6b** contain more hydrophobic groups. Based on the amino acids around the active site as well as the reactivity of *Sa*MerA and YkgC/RclA towards *N*-chloro-β-alanine and NCT, it was expected that the carboxylate-containing compound **6k** would show inhibition. However, we did not expect compounds **6l** and **6b** to show inhibition comparable to **6k** considering the presence of the hydrophobic and sterically bulky tert-butyl (**6l**) and cyclohexane (**6b**) groups that we predicted would affect binding to *Sa*MerA or YkgC/RclA. Nonetheless, the data shows that the active site of *Sa*MerA and YkgC/RclA is sensitive to covalent modification by compounds acting as nucleophile traps.

#### 2.2.11.2 Mass spectrometry

Variants of compound **6k** and **6l** have both been used in inhibition studies targeting the enzyme MurE, which is involved in murein biosynthesis [154]. These studies showed that the compounds inhibited the MurE enzyme by forming a covalent adduct to a lysine residue (Lys391) in the enzyme, preventing catalysis [154]. For the present study we assumed that compounds **6k**, **6l** and **6b** would attach to *Sa*MerA's active site Cys residue/s based upon the proposed reaction mechanism and the reactivity of bromoisoxazoles towards thiols. However, there is also a lysine residue (Lys13) within the active site of *Sa*MerA, thus it was also possible that the compound might attach to this lysine. To determine which amino acid residue was modified by the bromoisoxazolines, the treated enzymes were digested with trypsin, followed by mass spectrometry analysis of the resulting fragments. The MS analysis was performed by Dr M Vlok (Stellenbosch Central Analytical Facility). For these experiments compound **6k** was used for demonstration of the proof of principle. The result is shown in Figure 2.36.

**Table 3. Mass spectrometry results for *Sa*MerA treated with 6k.**

| **Protein identified**: Mercuric reductase homologue OS=Staphylococcus aureus OX=1280 GN=JP02758_0526 PE=3 SV=1 - [A0A224B076_STAAU] | |
|---|---|
| **Sequence:** | **Modification:** |
| AASTGQHVAVIEQSSKMYGGTCINIGCIPSK | C22(6k) |

```
  1 M K T Y D L I V I G F G K A G K T L A K 20
 21 Y A A S T G Q H V A V I E Q S S K M Y G 40
 41 G T C I N I G C I P S K T L V H D G L E 60
 61 G K S F E A S Y N R K N D V V N A L N N 80
 81 K N Y H L L A D D N N I D V L D F K A Q 100
101 F K S N T E V N L L D Q H G D I V D S I 120
121 T A P H I I I N T G A T S V I P N I K G 140
141 L D Q A K H V F D S T G L L N I S Y Q P 160
161 K H L V I V G G G Y I A L E F A S M F A 180
181 N L G S K V T V L E C G E S F M P R E D 200
201 Q D V V A H A I T D L E N K G I A L H I 220
221 N V E T T E L S S D D H H T T V H T N V 240
241 G N F E A D A V L L A I G R K P N T D L 260
261 A L E N T D I E L G D R G E I K V N A Q 280
281 L Q T T V P H I Y A A G D V K G G L Q F 300
301 T Y I S L D D Y R I I K S A L Y G N Q S 320
321 R T T D N R G S V P Y T V F I D P P L S 340
341 R V G L T S K E A V A Q H Y D Y T E H Q 360
361 L L V S A I P R H K I N N D P R G L F K 380
381 V V I N N E N N M I L G A T L Y G K Q S 400
401 E E L I N I I K L A I D Q N I P Y T V L 420
421 R D N I Y T H P T M A E S F N D L F N F 440
```

**Figure 2.36 *Sa*MerA protein sequence showing fragment identifying modified cys43 residue.**

The mass spectrometry data (Table 3) showed that indeed compound **6k** was attached to an active site cysteine. The modification (i.e. following reaction with **6k**) was identified on several peptide fragments, including that shown in Table 3. The specific modification was localized to Cys43 by subsequent fragmentation in the MS. Interestingly, the peptide fragments obtained from the treated enzyme were much larger and fewer in number than those obtained from a SaMerA DMSO-treated sample. This finding could also further support the analysis that binding of the compound leads to the establishment of a tighter, more stable protein complex. This is in agreement with the CD spectroscopy data for enzymes treated with the inhibitor compounds.

In regards to the bromoisoxazole warhead, there are a few structures in the PDB of unrelated enzymes that have isoxozale-derived inhibitors (e.g. glutamate receptor 1M5D, 1M5C, T-cell PTPase 1XBO, farnesoid X receptor (FXR) agonist 3P88) that share a number of common interacting amino acids, namely Pro, Thr, Tyr, Phe and His. These amino acids

are also found around the active site of *Sa*MerA (Phe10, Thr17, Thr301, Pro367, Phe434, Phe438, Phe440). In addition to crystal structures containing isoxazole derivatives, there are a few structures that contain acivicin (2Z8K, 3WHS) and they also share similar amino acid coordination to the inhibitor. It is therefore plausible that all compounds would be able to coordinate to any of the above mentioned amino acids lining the entrance of the active site of *Sa*MerA. However, in the SaMerA structure many of these amino acids are far apart (3-6Å) or point towards the inside of the entrance leading towards the active site. Thus presumably upon binding to inhibitor these amino acids would coordinate closer together. This proposed ligand binding interactions would have to be confirmed by a co-crystal structure of *Sa*MerA bound to the inhibitor.

### 2.2.12 *In vitro* assessment of NCT against *S. aureus* and *E. coli* wild type and *Sa*MerA mutant

Voyich *et al* have shown that the expression of *Sa*MerA is upregulated more than 80-fold in *S. aureus* strains MW2, MnCop, LAC, MRSA252, COL following phagocytosis by neutrophils [2]. In addition, a separate study showed that both *hypR* and the *merA* gene were upregulated 180-fold under hypochlorite stress in *S. aureus* [3]. The *hypR-merA* mutant was more sensitive to hypochlorite than the wild type [3]. In a study by Jakob and co-workers, YkgC/RclA-lacking mutants had increased sensitivity towards 2.5 mM hypochlorite [4]. Thus these studies indicate that *Sa*MerA (and YkgC/RclA) responds to the HOCl produced in the neutrophil environment, which we previously suggested likely forms NCT that itself has known antimicrobial properties.

In the present study, we demonstrated that *Sa*MerA (and its *E. coli* homologue) have substantial activity towards NCT. We therefore used genetic knockout strains of *S. aureus* and *E. coli* that do not express *Sa*MerA or YkgC/RclA to investigate if these strains show an increased sensitivity specifically towards NCT when compared to the wild type strains.

The antimicrobial activity of NCT against *S. aureus* JE2 and *S. aureus* NE785 (Δ*merA*) was assessed every hour for 8 hours. Several studies have shown that NCT has antimicrobial activity against various bacterial species [83, 90, 92, 93, 95, 99, 105, 106, 111, 112, 120, 121, 123, 125]. In addition, these studies have shown that the concentration of NCT required to kill bacteria are strain-dependent. In the present study concentrations ranging from 25-100 µM NCT were initially used, based on similar ranges used by Nagl *et al* against *S. aureus* ATCC 25923 [83]. These concentration ranges did not result in a decrease in cell viability for either the wild-type (*S. aureus* JE2) or mutant (*S. aureus* NE785) strains after 6 hours exposure (data not shown). The concentration of NCT was thus increased to 1 mM and 2 mM. At 2 mM, *S. aureus* JE2 was killed within 1 hour (data not shown), and at 1 mM killing occurred gradually over a 6 hour-period (Figure 2.37).

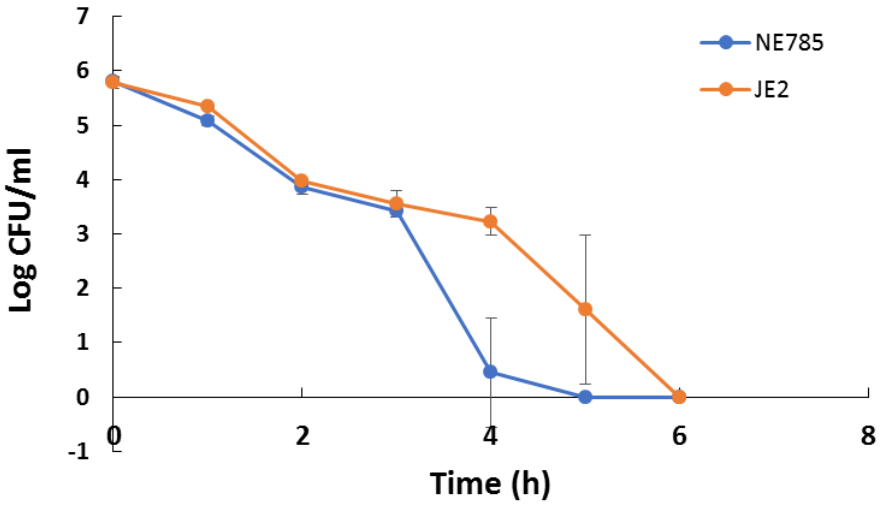


**Figure 2.37 *S. aureus* JE2 and NE785 (Δ*merA*) susceptibility to 1 mM NCT. The data represents the average of one biological experiment performed in triplicate. Error bars indicate standard deviation.**

The results of Figure 2.37 confirm that the *S. aureus* Δ*merA* mutant (NE785) is more sensitive to NCT than the wild-type (JE2). The NE785 strain starts decreasing in number more than 2 fold log CFU/ml after 3 hours. At 4 hours the NE785 strain has decreased more than 3 fold log CFU/ml compared to the wild-type strain.

With this positive result, we then assessed whether the same effect is observed with *E.coli* K12 and JW5040 *(Δykg*C) (Figure 2.38).

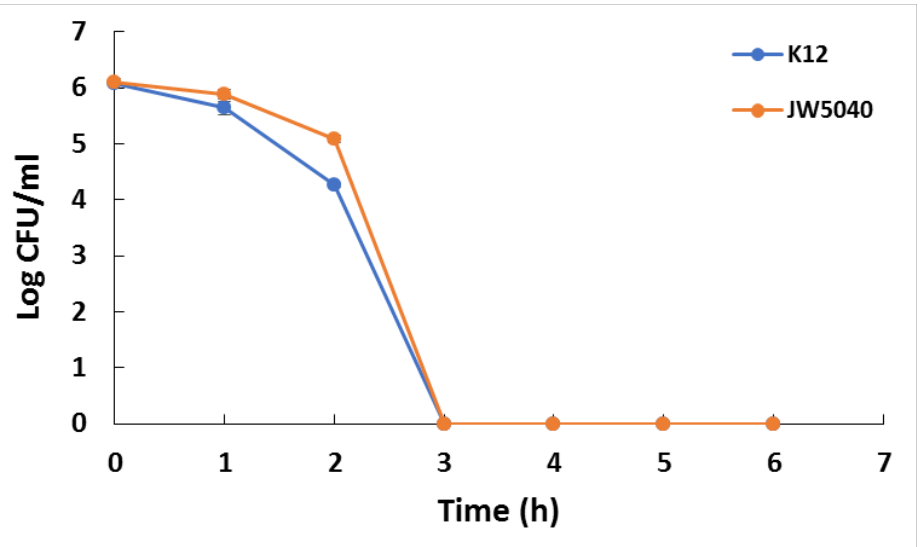


**Figure 2.38 *E. coli* K12 and JW5040 (Δ*ykgC*) susceptibility to 1 mM NCT. The data represents the average of one biological experiment performed in triplicate. Error bars indicate standard deviation.**

Both *E.coli* strains were sensitive to NCT with complete cell death after 3 hours exposure. There was no significant difference between the wild type (K12) and the YkgC/RclA-lacking mutant (JW5040). The *E. coli* cells appear to be more sensitive to NCT under these conditions when compared to *S. aureus*, which only showed complete cell death after 5.5-6 hours exposure. We were unsure as to the reason why the *E.coli* wild type and mutant showed very little difference in NCT sensitivity. Other conditions, such as using shorter time periods as well as increasing the NCT concentration to 2 mM, were also explored for *E.coli* strains however there still appeared to be no differences between the wild type and JW5040 strain. Nonetheless, Jakob and co-workers have shown that the *E. coli* YkgC/RclA-lacking mutant is more sensitive to 2 mM HOCl compared to the wild type [4]. The present study made use of a different growth media, a different wild-type strain and the use of NCT (not HOCl) which could account for different outcomes observed.

#### 2.2.12.1 *In vitro* assessment of compound 6k against *S. aureus* JE2.

To complement the result obtained with the genetic knockout of *S. aureus* (NE785), the wild type *S. aureus* JE2 was also treated with compound **6k** in an attempt to chemically knockout *Sa*MerA. As a proof of principle, the chemical knockout of *Sa*MerA in wild-type JE2, should also show sensitivity to NCT compared to the untreated wild-type.

Initially an excess of compound **6k** (1 mM) was incubated with *S. aureus* JE2 for 2 hours, and thereafter assayed for susceptibility to NCT (Figure 2.39). A high concentration of **6k** was used in hopes of abolishing *Sa*MerA, making it more susceptible to NCT. However, there were no noteworthy differences observed in comparing the controls and treated samples. The approach was then altered to pretreatment of *S. aureus* JE2 with low doses of NCT (50 µM) in order to allow *S. aureus* to overexpress MerA due to the oxidative stress conditions induced by NCT. Thereafter, the cells were incubated with 1 mM compound **6k** followed by testing the susceptibility to NCT (Figure 2.40).

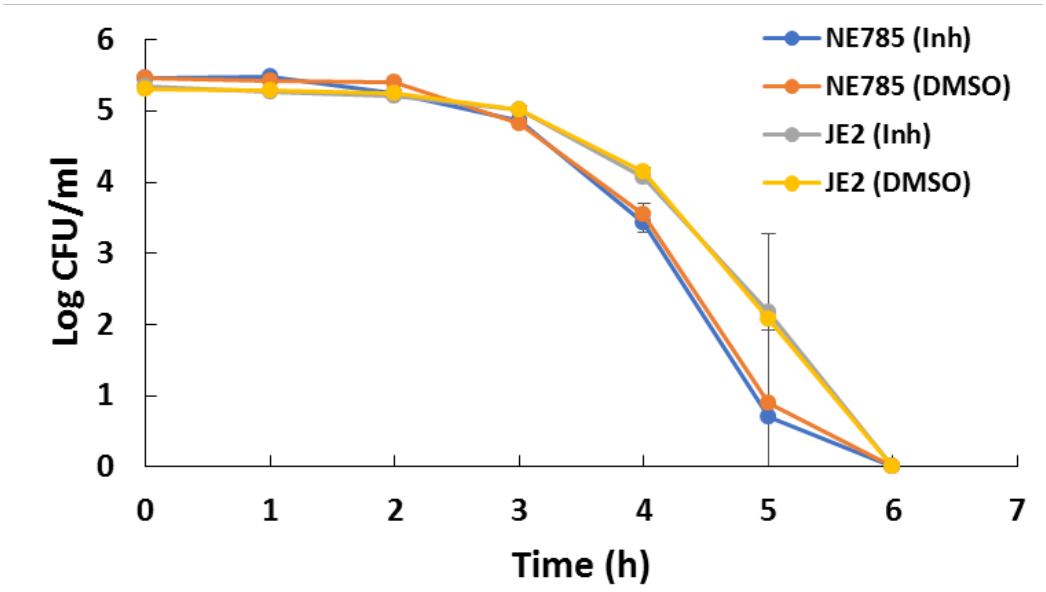


**Figure 2.39 *S. aureus* JE2 and NE785 pre-incubated with compound 6k for 2 hours before performing the susceptibility test using 1 mM NCT. The data represents the average of one biological experiment performed in triplicate. Error bars indicate standard deviation.**

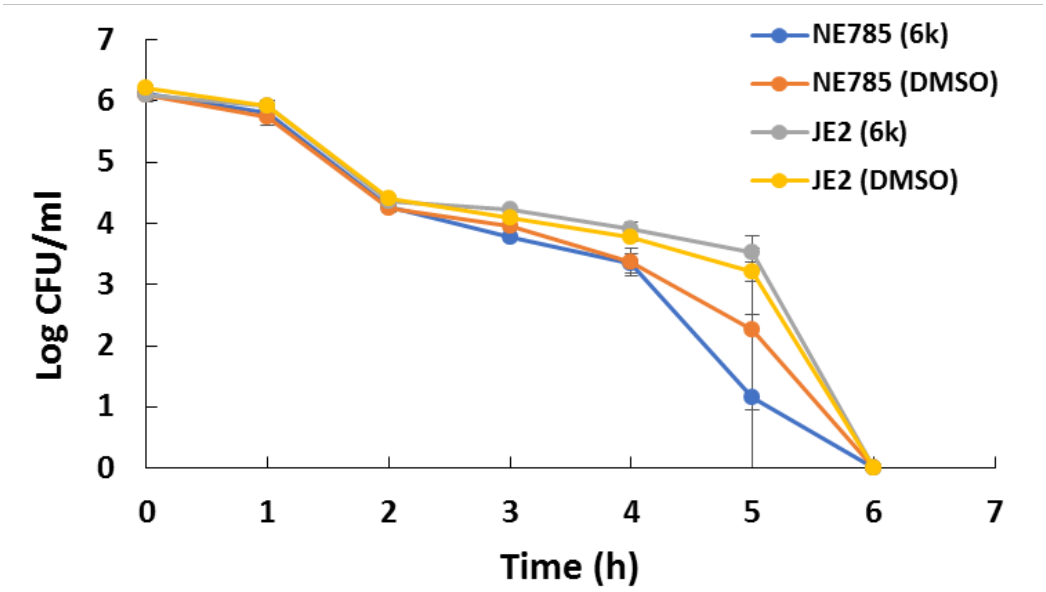


**Figure 2.40 *S. aureus* JE2 and NE785 pre-incubated with 50 µM NCT for 18 hours, following by treatment with 1 mM compound 6k for 3 hours before performing the susceptibility test using 1 mM NCT. The data represents the average of one biological experiment performed in triplicate. Error bars indicate standard deviation.**

The data shows that neither strategy was successful in demonstrating an effect following treatment with **6k**. Nonetheless, the positive outcome from these experiments is the confirmation that the NE785 strain (*Sa*MerA-lacking knockout) is more sensitive to NCT than the wildtype JE2. It is unknown as to why compound **6k** is not affecting JE2. The most likely reasons are that compound **6k** is not entering the cell, it is being effluxed out of the cell or that it binds to another target (such as the cell wall synthesizing proteins).

## 2.3 Conclusion

When *S. aureus* is challenged by neutrophils or HOCl, the expression of *Sa*MerA is significantly upregulated [2, 3]. Furthermore, *Sa*MerA-lacking mutants have been shown to be more sensitive to HOCl than the wild-type *S. aureus* [3]. *Sa*MerA has previously putatively been assigned as a mercuric ion reductase homologue. The question arose as to the physiological relevance a mercuric ion reductase-like enzyme would have under oxidative stress conditions.

This study set out to characterize and identify *Sa*MerA's potential substrate and its role in oxidative stress resistance. The first crystal structure obtained of *Sa*MerA, shows that it indeed it looks very similar to many tDBDFs. *Sa*MerA is classified in the DSR subgroup of the tDBDF superfamily. This subgroup includes glutathione reductase, dihydrolipoamide dehydrogenase, mercuric ion reductase and high molecular weight thioredoxin reductase. Considering that *Sa*MerA has been annotated as a mercuric ion reductase it was initially investigated if *Sa*MerA was able to reduce $Hg^{2+}$. Based on a sequence analysis alone, *Sa*MerA was already shown to lack the critical Cys residues that are required for true mercuric ion reductase catalysis as previously described for *Pa*MerA Tn501. *Sa*MerA was unable to show any mercuric ion reductase activity but did show potentiated hydrogen peroxide formation in the presence of NADPH and $Hg^{2+}$ (i.e. the ability of the NADPH-treated flavoprotein to reduce oxygen was augmented in the presence of $Hg^{2+}$). *Sa*MerA was also found to be unable to reduce other biologically relevant metals.

Other members of the DSR subgroup such as thioredoxin reductase require a cognate protein partner, which is involved in the catalytic cycle (Trx/TrR). Thus it was assessed if *Sa*MerA required a protein partner through pull-down experiments. *Sa*MerA did not show any protein partners in the pull-down experiments.

Glutathione reductase is well characterized in its' involvement reducing GSSG. Since *S. aureus* does not produce the LMW thiol GSH, other disulfides of LMW thiols were tested for

activity against *Sa*MerA. *Sa*MerA showed little to no activity for low molecular weight disulfides.

In context to other biological relevant reactive species produced by the neutrophil, HOCl and HOCl-derived reactive species were tested. HOCl alone was shown to abolish all activity, presumably through oxidation as well as chlorination of NADPH. *Sa*MerA showed particularly high activity towards chlorinated amino acids with highest activity for found for *N*-chlorotaurine, followed by *N*-chloro-β-alanine.

This finding was particularly interesting considering the high concentrations of taurine (up to 50 mM) produced by the neutrophil [58, 60, 61, 66, 73-81]. In addition, it is known that HOCl is heterogeneously produced in the phagolysosomes [88]. The product of the reaction of HOCl and taurine is *N*-chlorotaurine (NCT), which is a key component of the human defense system with proven antimicrobial properties [82, 83, 90-92, 94, 95, 99, 102, 106, 120-122]. In addition to *Sa*MerA showing activity towards NCT, its *E. coli* homologue YkgC/RclA also showed highest activity towards NCT and *N*-chloro-β-alanine. YkgC/RclA has previously been implicated in the defense against reactive chlorine species [4]. YkgC mutants are also much more sensitive to HOCl stress when compared to the *E. coli* wild-type [4, 5]. In addition, the YkgC/RclA-encoding gene was significantly up regulated in the human pathogenic bacterial *E. coli* strain O157:H7 when exposed to HOCl [5].

Having established that *Sa*MerA and YkgC/RclA have considerable activity towards NCT, three inhibitors containing bromoisoxazole-type "warheads" that also mimic the structure of the substrate NCT were synthesized. The three compounds **6k**, **6l** and **6b** were chemically different from one another in hopes of seeing a selective inhibition of *Sa*MerA and YkgC/RclA. We were pleased to find that the compounds inhibited SaMerA and YkgC/RclA, although no clear selectivity was observed. To further support the hypothesis of mechanism-based inhibition the compounds were found to inhibit both *Sa*MerA and YkgC/RclA in a time-dependent manner. It was also shown that the compound **6k** formed a covalent adduct toward the active site Cys43 of *Sa*MerA. Using structures from the PDB that have bound ligands such as taurine and isoxazole derivatives, plausible binding modes for the substrate NCT as well as the inhibitor were proposed.

The antimicrobial activity of NCT against *S. aureus* JE2 and *S. aureus* NE785 (Δ*merA*) was also assessed. *S. aureus* NE785 showed an increased sensitivity towards NCT compared to the wild-type JE2. Under the conditions using in these tests, there was no significant difference observed between the *E. coli* wildtype and its YkgC-lacking mutant. However, a

study done by Jakob *et al* revealed that the YkgC/RclA mutant is more sensitive to HOCl than the wild-type [4].

To complement the genetic knock out data, compound **6k** was used against *S. aureus* wild type in attempts of creating a chemical knockout of *Sa*MerA. Under various approaches, there was no phenotypic change observed between the treated (with **6k**) or untreated *S. aureus* strains. This was proposed to be due to the compound **6k** not entering the cells, or it is in fact targeting an alternative target (murein/peptidoglycan synthesis (MurE)). Other possibilities could be that compound **6k** is effluxed out of the cell or rendered inactive by other bacterial defense mechanisms.

These results described in this chapter revealed for the first time a link between a key compound of the human immune system (NCT) and a microbial enzyme (*Sa*MerA and YkgC) that renders this compound inactive (Figure 2.41).

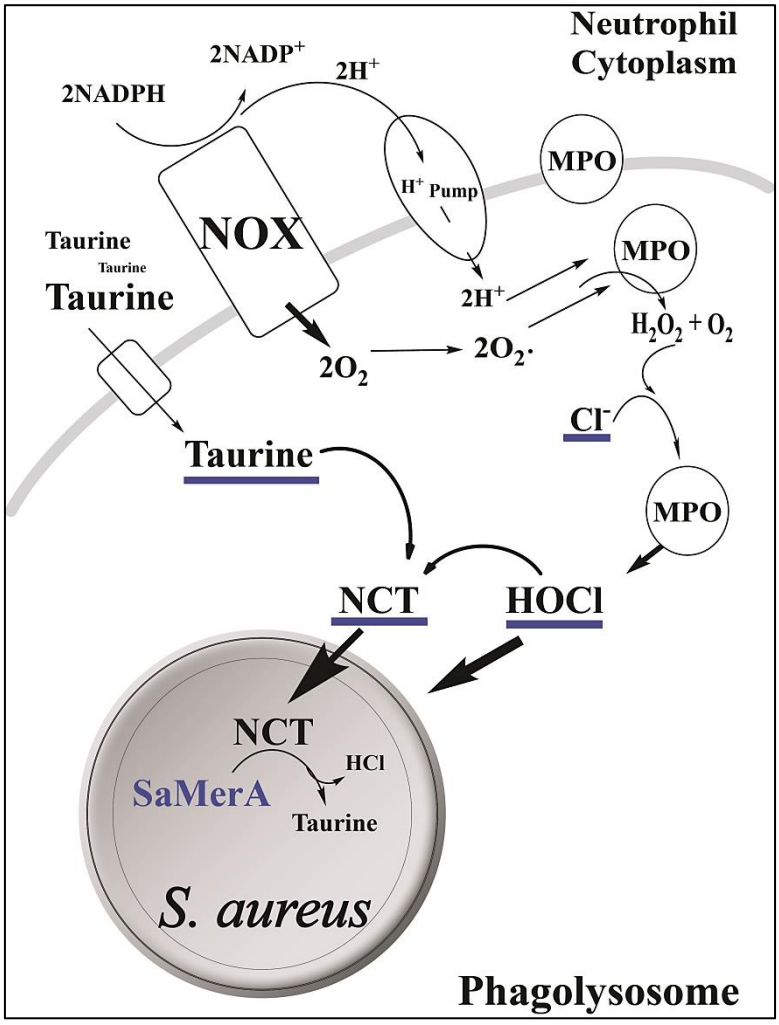


**Figure 2.41 A section of the neutrophil showing engulfed bacterium within phagolysosome. Shown in blue are the key compounds that lead to the formation of NCT, and the proposed role of *Sa*MerA.**

Overall, we were pleased to find that *Sa*MerA and YkgC/RclA show considerable activity towards NCT, a major component of the human immune system. We are therefore proposing that the enzyme should be more appropriately renamed as a taurine chloraminase. This enzyme is also conserved in a number of other pathogenic bacteria. These results provide insight into how *S.* aureus (and *E. coli*) responds to oxidative stress, specifically the reactive chlorine species NCT and how the bacteria protects itself against its antimicrobial effects.

This study also sets a basis upon which a larger/more diverse library of compounds can be tested against a novel bacterial target such as *Sa*MerA or YkgC/RclA, which play an important role in defense against the reactive chlorine species NCT. In this manner it sets the larger stage for the discovery of new therapeutics that are active at the host-microbe interface.

## 2.4 Materials and methods

Unless otherwise stated, the majority of all chemicals and compounds were purchased from Sigma-Aldrich. All reactions were done in triplicate unless otherwise stated or indicated in text or figures. All enzyme assays were done at 25°C, unless otherwise stated. All compounds or substrates were made up in reaction buffer as used in each section, unless otherwise stated.

### 2.4.1 Cloning and plasmids used

***Sa*MerA WT** - *merA* gene (SAOUHSC_00581/ JP02758_0526) was amplified from genomic *S. aureus* DNA strain RN4220 (isolated using a genomic DNA extraction kit from Novagen) using the primers, forward: 5'-GCA GTC ACT GTC ACC ATG GTC GTA ATA TTG -3' (NcoI site underlined) and reverse: 5'-CAC CAG GTT TTT ATG TTT CTC GAG GAA ATT AAATAA -3' (*XhoI* site underlined). The PCR reaction of *merA* involved 1 µL Pfu buffer, 0.4 mM dNTP mix, 1 mM forward primer, 1 mM reverse primer, 1 ng genomic DNA, 1.25 U Pfu DNA polymerase and the final volume made up to 25 µl with distilled, deionized water. The PCR program involved a 2 minute initial step at 94°C followed by 30 cycles of denaturation at 94°C for 15 seconds. Thereafter the annealing cycle was done at 55°C for 30 seconds and a final extension cycle for 1 min at 70°C. The reaction mixtures were subjected to gel electrophoresis on a 1% agarose gel and subsequently visualized through gel staining with SYBR™ gold (Invitrogen) and viewed on a UV gel reader. The band for *merA* gene (~1400bps) was excised and purified using a Novagen gel clean-up kit. The *merA* gene was then subsequently used to generate the pET28a-*Sa*MerA WT plasmid. Briefly the pET28a plasmid as well as the *merA* gene were digested separately with NcoI and XhoI (New England Biolabs) for 1 hour at 37°C without shaking. The restriction digestion of pET28a and merA gene were then subjected to gel electrophoresis on a 1% agarose gel and subsequently visualized through gel staining with SYBR™ gold (Invitrogen) and viewed on a UV gel reader. The NcoI/XhoI cut plasmid band and *merA* band were then excised and purified using a Novagen gel clean-up kit. Approximately 10 ng of NcoI/XhoI cut pET28a and *merA* were incubated with 10 U of T4 DNA ligase and ligase buffer for 1 Hour at 37°C without shaking. Thereafter 1 µL of the plasmid-insert construct was added to 80 µL of chemically-competent Mach 1 cells, and incubated on ice for 30 mins. The cell mixture was heat-shocked at $42^0$C for 45 seconds, and then cooled on ice for 5 mins. Approximately 900 µL or prewarmed LB broth was added to the transformation mixture and incubated at $37^0$C and shaking for 1 hour. The sample was then centrifuged at 4500 rpm for 10 mins. Half of

the supernatant was discarded, with the cell pellet being re-suspended in the remaining supernatant. The resuspended cells were then plated onto LB plates containing 30 mg/L kanamycin and incubated overnight at 37°C. Colonies were then selected and restriction digestion checks were done by loading the digestion mixture onto 1% agarose gels to assess which colony liberated the *merA* gene of correct size. The positive colonies were then sent for sequencing for confirmation. The correctly sequenced colonies were grown up overnight at 37°C in 5 ml LB containing 30 mg/L kanamycin. Thereafter the pET28a-*Sa*MerA plasmid was isolated and purified using a Zyppy Plasmid Miniprep I Kit (Zymo Research). The plasmid was then used for transformation into respective cloning/expression cells for further use.

***Sa*MerA C43A** – Using site directed mutagenesis, the pET28a-*Sa*MerA WT plasmid was used as a template and the following primers were used. Forward primer: 5'- GGA GGC ACT GCT ATA AAC ATA GGA TGT ATA CCT TCG -3', reverse primer: 5'-CGA AGG TAT ACA TCC TAT GTT TAT AGC AGT GCC TCC -3'. The PCR reaction involved 5 µL of KAPA hotstart buffer, 1 µL PolIII hotstart mixture, 1 ng of pET28a-*Sa*MerA template, 10 ng of forward primer, 10 ng of reverse primer and the final volume made up to 50 µl with distilled, deionized water. The PCR program involved an initial 1 minute step at 95°C. This was followed by 45 cycles of denaturation at 95°C for 30 seconds, annealing cycle at 52°C for 3 min 30 seconds and a final extension cycle for 3 min at 65°C. After the 45 cycles a final extension step of 1 minute was done at 65°C, thereafter the heating block was set to 4°C. The reaction mixtures were subjected to gel electrophoresis on a 1% agarose gel and subsequently visualized through gel staining with NANCY™-520 gel electrophoresis stain and viewed on a UV gel reader. The band for pET28a-*Sa*MerA C43A (~5500bps) was excised and purified using a Thermo Scientific DNA gel extraction kit. The purified plasmid was then subjected to digestion by 1 µL DpnI (New England Biolabs) for 1 hour at 37°C without shaking. The sample was then cooled on ice for 5 minutes and used directly for transformation into respective cloning/expression cells.

***Sa*MerA C48A and C43AC48A** – These pET28a-*Sa*MerA C48A and C43C48A plasmids were kindly provided by Prof. Haike Antelmann (Institute of Biology - Microbiology. Freie Universität Berlin). The *Sa*MerA mutants were produced by site-directed mutagenesis and inserted into the pET28a plasmid with *NheI* and *HindIII* restriction sites. The plasmids were sequenced and then used for transformation into respective cloning/expression cells.

**GST-*Sa*MerA-** *Sa*MerA was cloned into pGEX-6P-1 using *BamHI* and *XhoI* restriction sites by Dr A Schenkmayerova, a previous member in the Strauss Lab. The plasmid was then used directly for transformation into respective cloning/expression cells.

***Ec*Gor, *Ec*Lpd(LipDH) and *Ec*YkgC** – Over expressing clones were purchased from the ASKA collection (National BioResource Project) [155]. These clones were used directly in overexpression and enzyme purification.

***Sa*TrxA** – The *S. aureus* Thioredoxin pET28a plasmid was synthesized by GenScript®, USA. The gene was flanked by *NdeI* and *XhoI* restriction sites. The plasmid was codon optimized for overexpression in *E.coli*. The plasmid was then used directly for transformation into respective cloning/expression cells.

***Sa*CoADR** – The pET28a-CoADR plasmid was already available in the Strauss lab. The gene was flanked by *NdeI* and *XhoI* restriction sites. This plasmid was subsequently used directly for transformation into respective cloning/expression cells.

***Pa*MerA Tn501** –The *Pa*MerA Tn501 pET28a plasmid was synthesized by GenScript®, USA. The gene was flanked by *NdeI* and *XhoI* restriction sites. The plasmid was codon optimized for overexpression in *E.coli*. The plasmid was then used directly for transformation into respective cloning/expression cells.

### 2.4.2 Protein purification

All purified and sequenced plasmids were then transformed into *E. coli* BL21(Star)DE3 for protein overexpression. Overexpression was performed in LB broth supplemented with 30 mg/L kanamycin (except GST-*Sa*MerA, Ampicillin 100 mg/L) and grown at 37°C whilst shaking in non-baffled flasks. Once an $OD_{600nm}$ = 0.5-0.6 was reached the cultures were then induced with IPTG at a final concentration of 0.5 mM. Cultures were then continued overnight (except *Sa*CoADR: 3h growth) at 37 °C. Thereafter the cells were harvested by centrifugation at 8000 rpm. Each cell pellet (except GST-*Sa*MerA) was resuspended in approximately 10 mL of sonication buffer (5 mM imidazole, 500 mM NaCl and 20 mM Tris–HCl, pH 7.9; 10 mL/1 g cell paste) and subsequently sonicated to elicit cell lysis. After centrifugation at 15 000×g for 30 min, the crude extract (supernatant) was applied to a 0.45 µm syringe filter (AMICON) to remove any further debris. The clarified lysate was then applied to a previously prepared ($Ni^{2+}$) 1 mL HisTrapFF metal affinity purification column using an ÅKTAprime purification system. After an initial wash step of 5-10% elution buffer to

remove unbound protein, the protein of interest was then eluted by increasing the imidazole concentration to 500 mM. Protein elution was monitored by UV at 280 nm on the ÄKTAPrime. Residual imidazole was then removed from the purified protein fractions and buffer exchanged using a 5ml HiTrap Desalting columns (50 mM potassium phosphate, 5 mM $MgCl_2$, pH 8.0). Thereafter a 10% SDS-PAGE gel was run for each protein purified. Protein concentration of non-flavin proteins was determined using Bradford reagent (BIO-RAD). However for all flavoproteins the concentrations were determined using their FAD molar extinction coefficients at 450 nm. Molar extinction coefficients of each were determined using literature and EXPASY Protpram. Glycerol was added to the pure protein solution to a final concentration of 5%, after which the protein was aliquoted and stored at -80 °C.

In addition to the above mentioned general purification protocol, *Pa*MerA Tn501 was purified using adapted method from Ledwidge *et al* [17] and *S. aureus* coenzyme A disulfide reductase was purified using an established protocol [156]. Images of SDS-PAGE gels of purified proteins *Ec*Gor, *Ec*LipDH and *Ec*YkgC are shown in the Appendix. All proteins yielded yellow fractions and concentrations were measuring using their FAD molar extinction coefficients.

## 2.4.3 Enzyme characterization

### 2.4.3.1 General flavin spectra of SaMerA

*Sa*MerA was separately titrated with NADPH and NADH (0.5 – 5.0 mol NADPH per mol FAD) under anaerobic conditions at $25^0$C in 50 mM Tris-HCl (pH 7.5), and 150 mM NaCl. The titration was conducted in an anaerobic cuvette, sealed with a gas-tight rubber septum and repeatedly flushed with nitrogen gas. All reactants were flushed with nitrogen gas prior to titration. The reduction of the enzyme flavin by NADPH was monitored by collecting spectra from 800 nm to 240 nm on a Cary 60 UV-Vis Spectrometer (Agilent Technologies).

### 2.4.3.2 General flavin spectra of other enzymes used in this chapter.

All enzymes (*Ec*Gor, *Ec*RclA/YkgC, *Ec*LipDH, *Sa*CoADR) were separately made up in 50mM potassium phosphate pH 8 to a final concentration of 2.5 µM and placed in a 1 mL 1cm quartz cuvette. Absorbance scans were done on a Cary 60 UV-Vis Spectrometer (Agilent Technologies). The flavin spectra of *Ec*Gor, *Ec*RclA/YkgC, *Ec*LipDH, *Sa*CoADR can be found in the Additional Experimental Data section.

#### 2.4.3.3 Circular Dichroism (CD) spectroscopy

All measurements were done on a Chirascan plus (Applied Photophysics) and data processed with Pro-data Viewer 4.2.6 (Applied Photophysics). An air blank (cell holder only) as well as a buffer/solvent blank of 10 mM potassium phosphate pH 8 in cell was done. Each protein sample was made up in 10 mM potassium phosphate pH 8 to a final concentration of 1µM in a total volume of 180 µl and placed in a 0.5 mm quartz suprasil cell with demountable window and cell holder 013.000 (Hellma Analytics). The captured data represents an average of three independent spectra combined.

### 2.4.4 Assessing *Sa*MerA as a mercuric-ion reductase

All assays were based upon Miller et al using 25 nM *Pa*MerA Tn501, 50 mM potassium phosphate, pH 7.3, 100 µM NADPH and 100 µM Hg-substrate [17]. Prior to each reaction, *Pa*MerA Tn501 was purified and treated with DTT (5 mM for each 30 µM of enzyme) thereafter ammonium precipitated and refolded as described. Two exceptions were done in the present study, the first being that an IMAC column was used instead of an anion-exchange, and secondly a 5ml HiTrap Desalting column was used instead of a gel filtration column. The concentration of the enzyme was determined using the molar extinction coefficient of FAD [17]. Similarly, *Sa*MerA was also purified, pretreated with DTT, refolded and purified as described. $Hg(GSH)_2$ was prepared and used as a substrate for both *Pa*MerA Tn501 and *Sa*MerA [17]. Considering that the assays worked with $Hg(GSH)_2$, $Hg(Trx)_2$ was not tested as done in literature [17]. In all reactions the substrate ($Hg(GSH)_2$) was placed in the wells and the enzyme mixture (25 nM enzyme, 100 µM NADPH in buffer) added thereafter to initiate the reaction. Reactions were done at 25°C in clear flat-bottom 96 well plates (Griener Bio-one) and absorbance at 340 nm read using a Thermo Scientific Varioskan microplate spectrophotometer.

For *peroxidase assays*: initially a peroxidase kit was used (Pierce peroxidase detection kit), however after numerous attempts in optimizing, this kit was abandoned due to inconsistent results. The strategy was then changed to the use of horseradish peroxidase, HRP (Sigma#9003-99-0) and ABTS (2,2'-azino-bis(3-ethylbenzothiazoline-6-sulphonic acid)).

For *aerobic reactions*: Assay conditions used were 25 nM *Sa*MerA, 50 nM HRP, 50 mM potassium phosphate, pH 7.4, 100 µM NADPH, 100 µM Hg-substrate and 100 µM ABTS. The substrate ABTS was made up to a concentration of 10 mM in 50 mM potassium phosphate, pH 7.4. This was made fresh prior to use. Control reactions made use of 30%

w/v $H_2O_2$ solution as is. Each reaction contained 25 nM *Sa*MerA enzyme, 100 µM NADPH in buffer with 50 nM HRP incubated at room temperature for 2 minutes. This reaction mixture was then added to the wells of a clear flat-bottom 96 well plate (Griener Bio-one) already containing the substrates (100 µM $Hg(GSH)_2$ and 100 µM ABTS) and initial rates obtained from increase in absorbance at 420 nm. All absorbance readings were done using a Thermo Scientific Varioskan microplate spectrophotometer.

For *anaerobic reactions*: The same reactions conditions and buffer was used. However all reagents (except enzymes) were made anaerobic prior to use using a tonometer and anaerobic cuvette which were all repeatedly flushed with nitrogen. The substrates (100 µM $Hg(GSH)_2$ and 100 µM ABTS) were first placed into the cuvette and the reaction initiated upon addition of reaction mixture (SaMerA, HRP, 100 µM NADPH) and initial rates obtained from an increase in absorbance at 420 nm. All absorbance readings were done on a Cary 60 UV-Vis Spectrometer using the 1 cm anaerobic cuvette.

### 2.4.5 Assessing potential protein partners of *Sa*MerA

GST-*Sa*MerA was expressed and purified as described in protein expression and purification section.

*S. aureus* JE2 (USA300) was grown in a large batch culture (2 litres) in LB broth. After reaching an $OD_{600}$ = 0.5, the cells were challenged with 10 mM $H_2O_2$ every 20 minutes over an hour. After a further 2 hours growth the cells were then spun down and the pellet stored until use for pull down experiments.

The pellet of *S. aureus* JE2 culture was freeze thawed and sonicated immediately in 10ml of binding buffer (140 mM NaCl, 2.7 mM KCl, 10 mM $NaHPO_4$, 1.8 mM $KH_2PO_4$, pH 7.3). The lysates were used in pull down experiments. Batch purification was done using glutathione sepharose 4B (GE Healthcare) and supplied product instructions. Briefly, GST-*Sa*MerA was bound to the GSH resin using binding buffer, followed by incubation of resin bound *Sa*MerA-GST with *S. aureus* JE2 lysate. The resin was washed several times with binding buffer to remove unbound proteins and finally GST-*Sa*MerA was eluted with elution buffer (50 mM Tris-HCl, 10 mM reduced glutathione, pH 8). All eluted fractions were run on a 10% SDS-PAGE gel.

### 2.4.6 Assessing potential disulfide substrates

Enzymes used included *Sa*CoADR, *Ec*Gor, *Ec*LipDH, and *Sa*MerA. Prior to use, all purified enzymes were treated with 10-fold DTT to ensure reduction of disulfides. Excess DTT was removed using Amicon centrifugal concentrators with MW 3,000 Da cutoff. Reaction conditions involved 25 nM enzyme, 50 mM potassium phosphate, pH 7.4, 100 µM NADPH, 100 µM substrate.

Substrate $(CoAS)_2$ was prepared using an established method [157]. A solution of 10 mL of CoA (final concentration of 2 mM) in 50 mM Tris pH 7.6 was prepared followed by the addition of powdered diamide (final concentration of 1 mM). The solution was gently shaken for 30 mins at room temperature. Thereafter the diamide was removed using DCM extraction (4×4 ml). The absorbance maximum at 260 nm of the resulting $(CoAS)_2$ solution was then used to calculate the concentration of the stock solution. The formation of $(CoAS)_2$ was also assessed through incubating CoA with10 fold HOCl or $H_2O_2$ for 1 hour at room temperature. The disulfide $(CoAS)_2$ did not form with HOCl but did indeed form with $H_2O_2$ treatment.

Disulfides ($(Cys)_2$, $(GSH)_2$, $(BSH)_2$, $(DHLA)_2$) were formed by incubating thiols with 10-fold $H_2O_2$ at room temperature for 1 hour. The concentration of each was determined at an absorbance maximum of 261 nm. Interestingly the disulfides ($(Cys)_2$, $(GSH)_2$, $(BSH)_2$, $(DHLA)_2$) did not appear to form (lack of disulfide peak) when treated with HOCl.

Enzyme reactions were carried out as follows: a solution containing 25 nM *Sa*MerA,100 µM NADPH in reaction buffer was added to a clear flat-bottom 96well plate already containing the disulfide substrates (100 µM). Similarly control reactions were performed using 25 nM *Sa*CoADR + ($(CoAS)_2$), *Ec*Gor + ($(GSH)_2$), *Ec*LipDH + dihydrolipoamide respectively. Initial rates were determined following the decrease in absorbance at 340 nm. All absorbance readings were done using a Thermo Scientific Varioskan microplate spectrophotometer.

### 2.4.7 Assessing various reactive chlorine species

All assays involved the following reaction conditions, 25 nM enzyme, 50 mM potassium phosphate, pH 7.4, 100 µM NADPH, 100 µM "chlorinated" compound. Substrates were first added to wells of a clear flat-bottom 96well plate and the enzyme mixture (enzyme, NADPH, buffer) was then added to initiate the reaction. Initial rates were determined following the decrease in absorbance at 340 nm. All absorbance readings were done using a Thermo Scientific Varioskan microplate spectrophotometer.

For amino acid chloramines: Various ratios of HOCl:amino acid were tried. Ratios of 1:1 (HOCl:amino acid) gave the best results (i.e. no residual HOCl left unreacted as confirmed by UV spectroscopy 291 nm). All amino acids showed the typical chloramine UV maximum at 252 nm ($\varepsilon$ = 429 $M^{-1}$. $cm^{-1}$). However methionine, tyrosine, tryptophan did show broader peaks as well as additional peaks, owing to the possibility that chlorination can occur on other functional groups of these amino acids.

### 2.4.8 Enzyme assays involving NCT

All assays involved the following reaction conditions, 25 nM enzyme, 50 mM potassium phosphate, pH 7.4, 100 µM NADPH, 100 µM NCT. Substrates were first added to wells of a clear flat-bottom 96-well plate and the enzyme mixture (enzyme, NADPH, buffer) was then added to initiate the reaction. Initial rates were determined following the decrease in absorbance at 340 nm. All absorbance readings were done using a Thermo Scientific Varioskan microplate spectrophotometer.

NCT was prepared via two methods. HOCl mixing with taurine involving 1:2 (HOCl: taurine). The solution was allowed to stand for 10 minutes at room temperature before use. NCT was also prepared by mixing 5 g of powdered taurine (sodium salt) in 100 mL absolute ethanol. To this 12 g of chloramine-T was added and the solution stirred for 5 hours at room temperature. The resulting sodium salt of NCT was filtered off and washed with 2×20 mL of absolute ethanol. The NCT powder was further dried overnight by high vac. The NCT prepared from both methods were confirmed by UV spectroscopy and $^{1}$HNMR. Unless otherwise stated, the NCT prepared using chloramine-T was used in subsequent assays.

### 2.4.9 *In vitro* assessment of NCT against *S. aureus* and *E.coli* wildtype and *Sa*MerA mutant

*S. aureus* susceptibility to NCT

Bacterial strains *S. aureus* JE2 and *S. aureus* NE785 (obtained from the NARSA repository) were streaked out on LB agar and grown at 37°C for 24 hours. A single colony was selected and inoculated into LB broth and incubated aerobically at 37°C for 18 hours. *N*-Chlorotaurine (NCT) was dissolved to 1 mM in 0.01 M phosphate-buffer (pH 7.1). An overnight culture was inoculated into the 1 mM NCT solution to 6 log CFU/mL, and subsequently incubated at room temperature. The survivability of strains was followed every

hour for 6 hours by serially diluting cells and plating on agar. To inactivate the antimicrobial action of NCT, cells were initially diluted ($10^{-1}$) in 0.6 % (m/v) sodium thiosulphate in PBS (pH 7), and thereafter serially diluted in PBS ($10^{-2}$ and subsequent dilutions). Colony forming units were determined by plating the serially diluted cells on LB agar and incubating at 37°C for 24 hours. After incubation cells were counted and expressed as log CFU/mL.

*Escherichia coli* susceptibility to NCT

Bacterial strains *E. coli* K12 and *E. coli* JW5040 (obtained from the Keio collection) were streaked out on LB agar and grown at 37°C for 24 hours. A single colony was selected and inoculated into LB broth and incubated aerobically at 37°C for 18 hours. N-Chlorotaurine (NCT) was dissolved to 1 mM in 0.01 M phosphate-buffer (pH 7.1). An overnight culture was inoculated into the 2 mM NCT solution to 6 log CFU/mL, and subsequently incubated at room temperature. The survivability of strains was followed every hour for 6 hours by serially diluting cells and plating on agar. The survivability of strains was also followed over shorter time points (0, 5, 10, 20, 30, 45 and 60 min) by serially diluting cells and plating on agar. To inactivate the antimicrobial action of NCT, cells were initially diluted ($10^{-1}$) in 0.6 % (m/v) sodium thiosulphate in PBS (pH 7), and thereafter serially diluted in PBS ($10^{-2}$ and subsequent dilutions). Colony forming units were determined by plating the serially diluted cells on LB agar and incubating at 37 °C for 24 hours. After incubation cells were counted and expressed as log CFU/mL.

## 2.4.10 Potential inhibitors of *Sa*MerA

### 2.4.10.1 Synthesis and purification

The general procedure was followed: To a solution of 1,1,-dibromoformaldoxmine (1 eq.) in DMF (5 mL/g) at -10°C was added to the alkene (1.2 eq.) whilst stirring. Thereafter a solution of $KHCO_3$ (2.5 eq.) in water (6 mL/g) was added over a period of 1 hour. The reaction mixture was then warmed to room temperature over 1 hour. 1N HCl was added and the mixture extracted with MTBE (3×). The combined organic layers were washed with water and brine and dried over $MgSO_4$ and concentrated under reduced pressure using a rotary evaporator. The crude product was purified by column chromatography (Merck silica gel 60 (particle size 0.040-0.063 mm)) and progress visualized by TLC (aluminium-backed Merck silica gel 60 F254). The purified fractions were pooled and dried overnight under high vacuum.

#### 2.4.10.2 Purification and analysis

Column solvent conditions used for compounds: Compound 6k (Ethyl acetate: Methanol: $H_2O$ (7:2:1)). Compound 6l (Hexane: Ethyl Acetate (9.5:0.5)). Compound 6b (Hexane: Ethyl Acetate (9.5:0.5)). All $^1$H NMR spectra were collected using a 300 MHz Varian VNMRS instrument at the Central Analytical Facility (CAF) of the University of Stellenbosch. Chemical shifts (δ), reported in ppm were recorded using the residual solvent peak as reference. Proton spectral data are reported as: chemical shift, multiplicity (ovlp = overlapping, s = singlet, d = doublet, t = triplet, q = quartet, p =pentet, m = multiplet, br = broad), coupling constant (J) in Hz, and proton integration. TLC analysis and $^1$HNMR of compounds are shown in section 2.5 (Additional Experimental Data).

**Compound 6k** (980mg of a clear odorless oil was obtained, 61% yield) $^1$HNMR (300MHz, DMSO-$d_6$) δ 4.8 (dd, *J*=11.7, 6.9Hz, 1H), δ 2.9 (dd, *J*=17.6, 11.7Hz, 1H), δ 2.7 (dd, *J*=17.6, 7Hz, 1H). **Compound 6l** (1310mg of a white powder was obtained, 86% yield) $^1$HNMR (300MHz, DMSO-$d_6$) δ 5.08 (dd, *J*=10.7, 7Hz, 1H), δ 3.68 (d, *J*=11.7Hz, 1H), δ 3.62 (dd, *J*=11.7Hz, 1H), δ 1.43 (s, 9H). **Compound 6b** (1903mg of a clear oil with a pungent peppermint odor was obtained, 53% yield) $^1$HNMR (300MHz, chloroform-d) δ 4.52-4.27 (m, 1H), δ 3.16 (dd, *J*=17.3Hz, 1H), δ 2.93 (dd, *J*=17.3Hz, 1H), δ 1.9-1.4 (m, 6H), δ 1.39-1.1 (m, 3H), δ 0.97 (m, 2H).

#### 2.4.10.3 Enzyme inhibition studies

All assays involved the following buffer conditions, 50 mM potassium phosphate, pH 7.4. Each enzyme was pretreated with DTT as previously described, to ensure all disulfides were reduced. Excess DTT was removed using an Amicon centrifugal concentrator with 3,000 Da MW cutoff. Enzyme concentration was calculated using an FAD molar extinction coefficient of 11.3 $mM^{-1}cm^{-1}$ [17]. There after each enzyme was incubated on ice with 10 fold excess compound for 30 minutes. Excess compound was removed using an Amicon centrifugal concentrator with 3,000 Da MW cutoff. There after the pre-treated enzymes were then placed on ice for further use. Control reactions of enzyme with DMSO (no compound), iodoacetamide and N-methylmaleimide were treated in the same fashion. Using these pre-treated enzymes, reactions were setup and tested against 50 μM NCT as described in results section. Substrate (NCT) was first added to wells of a clear flat-bottom 96 well plate and the enzyme mixture (pre-treated enzyme, NADPH, buffer) was then added to initiate the reaction. Initial rates were determined following the decrease in absorbance at 340 nm. All

absorbance readings were done using a Thermo Scientific Varioskan microplate spectrophotometer.

#### 2.4.10.4 Circular Dichroism (CD) spectroscopy

All measurements were done at 25°C on a Chirascan plus (Applied Photophysics) and data processed with Pro-data Viewer 4.2.6 (Applied Photophysics). An air blank (cell holder only) as well as a buffer/solvent blank of 10 mM potassium phosphate pH 8 in cell was done. Each pre-treated protein sample (compound treated) was made up in 10 mM potassium phosphate pH 8 to a final concentration of 10 µM in a total volume of 180 µL and placed in a 0.5 mm quartz suprasil cell with demountable window and cell holder 013.000 (Hellma Analytics). The captured data represents an average of three independent spectra combined.

#### 2.4.10.5 Time-dependent enzyme inhibition studies

All assays involved the following buffer conditions, 50 mM potassium phosphate, pH 7.4. A clear flat-bottom 96 well plate was prepared with appropriate wells containing 50 µM NCT. Each enzyme was pre-treated with DTT and excess removed as previously described. However instead of leaving the compound to incubate for 30 minutes, appropriate aliquots were taken out at time zero (immediately after adding compound), 5 minutes, 10 minutes, 20 minutes and 30 minutes. Control reactions were done using enzyme and DMSO (No compound) as well as enzyme with no substrate NCT. Final reaction conditions were 25 nM pre-treated enzyme (250 nM compound), 50 mM potassium phosphate, pH 7.4, 100 µM NADPH and 50 µM NCT. Initial rates were determined following the decrease in absorbance at 340 nm. All absorbance readings were done using a Thermo Scientific Varioskan microplate spectrophotometer.

#### 2.4.10.6 Mass spectrometry analysis

*In-gel Digest*

All reagents are analytical grade or equivalent. Gel slices supplied were destained in an Eppendorf 1.5 mL tube with 200 mM $NH_4HCO_3$: Acetonitrile 50:50 (Sigma) until clear. Samples were dehydrated and desiccated before reduction with 2 mM triscarboxyethyl phosphine (TCEP; Fluka) in 25 mM $NH_4HCO_3$ for 15 minutes at room temperature with agitation. Excess TCEP were removed and the gel pieces again dehydrated. Cysteine residues were thiomethylated with 20 mM *S*-methyl methanethiosulfonate (Sigma) in 25 mM $NH_4HCO_3$ for 30 minutes at room temperature. After thiomethylation the gel pieces were dehydrated and washed with 25 mM $NH_4HCO_3$ followed by another dehydration step.

Proteins were digested by rehydrating the gel pieces in trypsin (Pierce) solution (20ng/µl) and incubating at 37°C overnight. Peptides were extracted from the gel pieces once with 50 µL water and once with 50% acetonitrile. The samples were dried down and resuspended in 30 µL 2% acetonitrile: water; 0.1% FA.

Residual digest reagents were removed using an in-house manufactured C18 stage tip (Empore Octadecyl C18 extraction discs; Supelco). The samples were loaded onto the stage tip after activating the C18 membrane with 30 µL methanol (Sigma) and equilibration with 30 µL 2% acetonitrile: water; 0.05% TFA. The bound sample was washed with 30 µL 2% acetonitrile: water; 0.1% TFA before elution with 30 µL 50% acetonitrile: water 0.05% TFA. The eluate was evaporated to dryness. The dried peptides were dissolved in 2% acetonitrile: water; 0.1% FA for LC-MS analysis.

*Liquid chromatography - Dionex nano-RSLC*

Liquid chromatography was performed on a Thermo Scientific Ultimate 3000 RSLC equipped with a 2 cm×100 µm C18 trap column and a 35cmx75µm in-house manufactured C18 column (Luna C18, 5 µm; Phenomenex) analytical column. The solvent system employed was loading: 2% acetonitrile: water; 0.1% Formic acid (FA); Solvent A: 2% acetonitrile: water; 0.1% FA and Solvent B: 100% acetonitrile: water. The samples were loaded onto the trap column using loading solvent at a flow rate of 15 µL/min from a temperature controlled autosampler set at 7°C. Loading was performed for 5 min before the sample was eluted onto the analytical column. Flow rate was set to 500 nL/minute and the gradient generated as follows: 2.0% -10%B over 5 min; 5% -25% B from 5 -50 minutes using Chromeleon non-linear gradient 6, 25%-45% from 50-65 minutes, using Chromeleon non-linear gradient 6. Chromatography was performed at 50°C and the outflow delivered to the mass spectrometer through a stainless steel nano-bore emitter.

*Mass spectrometry*

Mass spectrometry was performed using a Thermo Scientific Fusion mass spectrometer equipped with a Nanospray Flex ionization source. The sample was introduced through a stainless steel emitter. Data was collected in positive mode with spray voltage set to 2.2 kV and ion transfer capillary set to 280°C. Spectra were internally calibrated using polysiloxane ions at m/z = 445.12003 and 371.10024. MS1 scans were performed using the orbitrap detector set at 120 000 resolution over the scan range 350-1650 with AGC target at 3 E5 and maximum injection time of 40 ms. Data was acquired in profile mode.

MS2 acquisitions were performed using monoisotopic precursor selection for ion with charges +2±6 with error tolerance set to +/- 0.02 ppm. Precursor ions were excluded from fragmentation once for a period of 30s. Precursor ions were selected for fragmentation in HCD mode using the quadrupole mass analyzer with HCD energy set to 32.5%. Fragment ions were detected in the orbitrap mass analyzer set to 15 000 resolution. The AGC target was set to 1E4 and the maximum injection time to 45 milliseconds. The data was acquired in centroid mode.

*Data Analysis*

The raw files generated by the mass spectrometers were imported into Proteome Discoverer v1.4 (Thermo Scientific) and processed using both Sequest and Mascot algorithms. Database interrogation was performed against a concatenated database created by using the Uniprot Staphylococcucea and E. coli databases. Sequences of common contaminants were also added to the database. Semi-tryptic cleavage allowing for 2 missed cleavages was used and precursor mass tolerance was set to 10 ppm and fragment mass tolerance set to 0.5 Da. Protein deamidation (NQ) and oxidation (M) was allowed as dynamic modifications and thiomethyl of C as static modification. Peptide validation was performed using the peptide validator node set to search against a decoy database with strict FDR 1%.

#### 2.4.10.7 *In vitro* assessment of compound 6k against *S. aureus* JE2 wildtype and *Sa*MerA mutant

*Pretreatment of S. aureus with 1 mM compound 6k then exposure to 1 mM NCT*

Bacterial strains *S. aureus* JE2 and *S. aureus* NE785 (obtained from the NARSA repository) were streaked out on LB agar and grown at 37°C for 24 hours. A single colony was selected and inoculated into LB broth and incubated aerobically at 37 °C for 18 hours. After incubation, cultures were inoculated at 1 % (v/v) in LB broth supplemented with 1 mM **6k** and incubated aerobically at 37 °C for 2 hours. After exposure to **6k**, bacterial cells were inoculated in 1 mM NCT in 0.01 M phosphate-buffer (pH 7.1) solution to 6 log CFU/ml, and subsequently incubated at room temperature. The survivability of strains was followed every hour for 6 hours by serially diluting cells and plating on agar. To inactivate the antimicrobial action of NCT, cells were initially diluted ($10^{-1}$) in 0.6 % (m/v) sodium thiosulphate in PBS (pH 7), and thereafter serially diluted in PBS ($10^{-2}$ and subsequent dilutions). Colony forming units were determined by plating the serially diluted cells on LB agar and incubating at 37 °C for 24 hours. After incubation cells were counted and expressed as log CFU/mL.

*Pretreatment of S. aureus with 50 µM NCT overnight then exposure to compound 6k followed by 1 mM NCT*

Bacterial strains *S. aureus* JE2 and *S. aureus* NE785 (obtained from the NARSA repository) were streaked out on LB agar and grown at 37 °C for 24 hours. A single colony was selected and inoculated into LB broth and incubated aerobically at 37 °C for 18 hours. After incubation, cultures were inoculated at 1 % (v/v) in LB broth supplemented with 50 µM NCT and incubated aerobically at 37 °C for 18 hours. After incubation, bacterial cells (9 log CFU/ml) were exposed to 1 mM **6k** at room temperature for 3 hours. After exposure to **6k**, bacterial cells were inoculated in 1 mM NCT in 0.01 M phosphate-buffer (pH 7.1) solution to 6 log CFU/ml, and subsequently incubated at room temperature. The survivability of strains was followed every hour for 5 hours by serially diluting cells and plating on agar. To inactivate the antimicrobial action of NCT, cells were initially diluted ($10^{-1}$) in 0.6 % (m/v) sodium thiosulphate in PBS (pH 7), and thereafter serially diluted in PBS ($10^{-2}$ and subsequent dilutions). Colony forming units were determined by plating the serially diluted cells on LB agar and incubating at 37 °C for 24 hours. After incubation cells were counted and expressed as log CFU/ml.

## 2.5 Additional experimental data

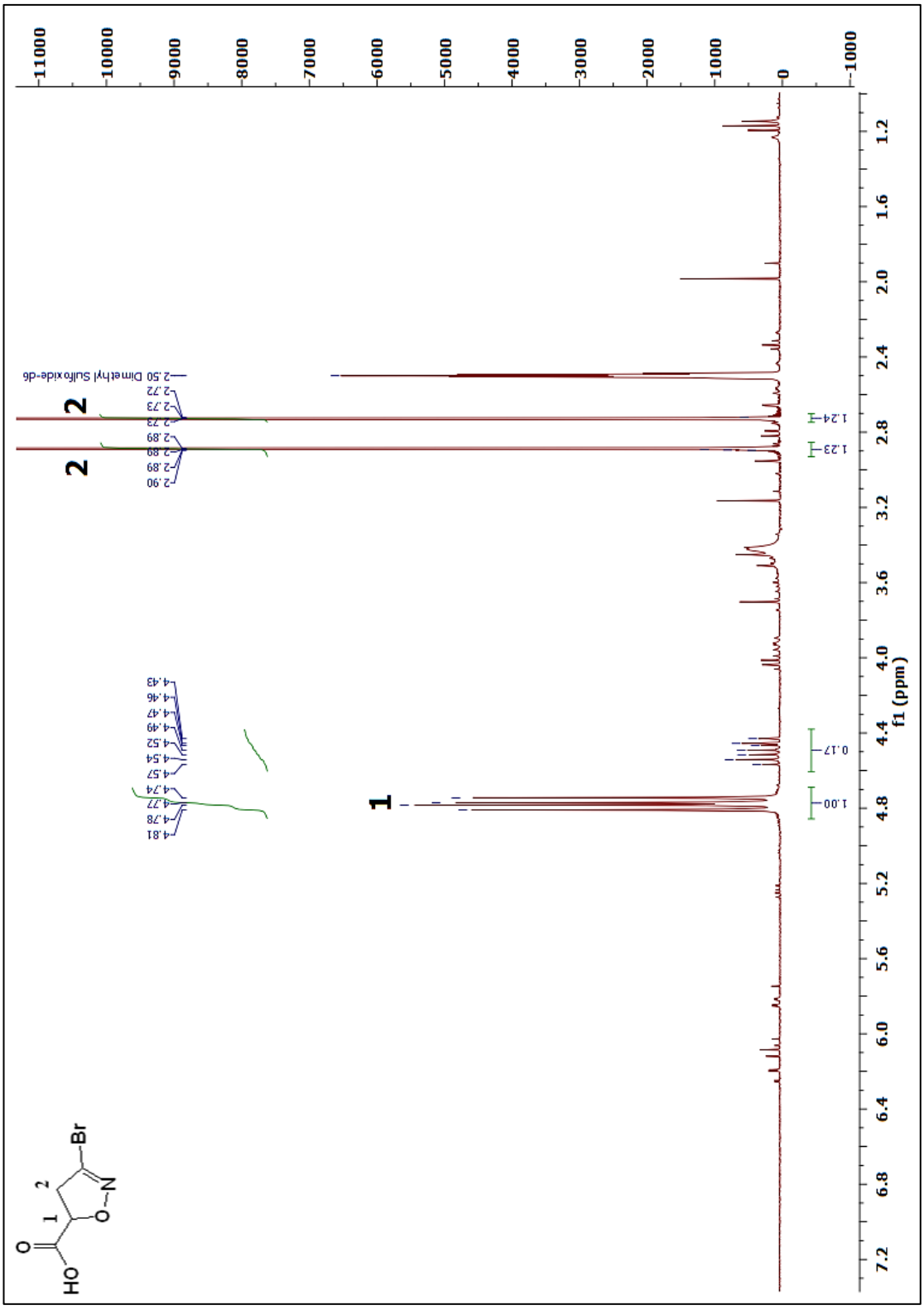


**Figure 2.42 $^{1}$HNMR of Compound 6k.**

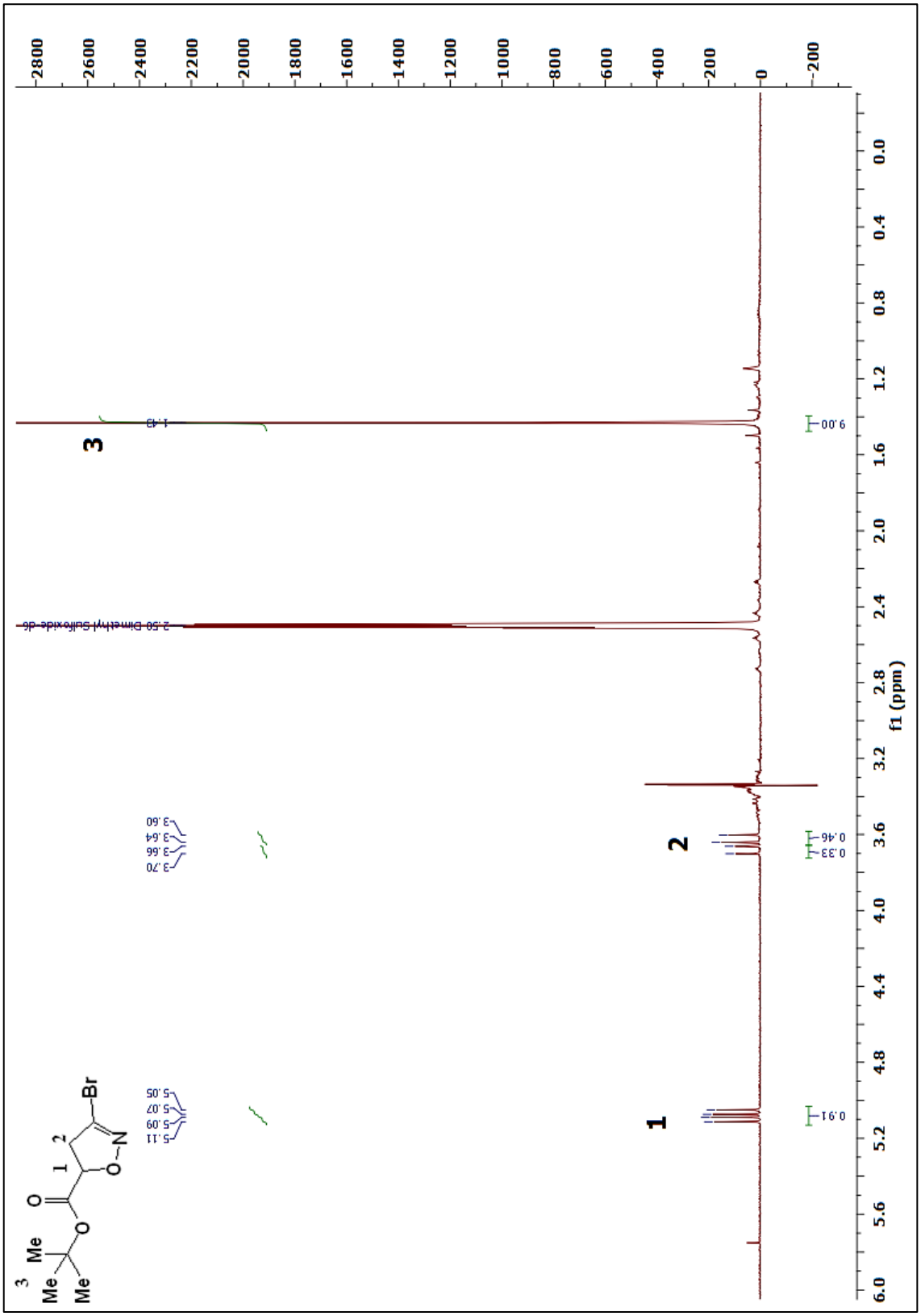


**Figure 2.43 $^{1}$HNMR of Compound 6l.**

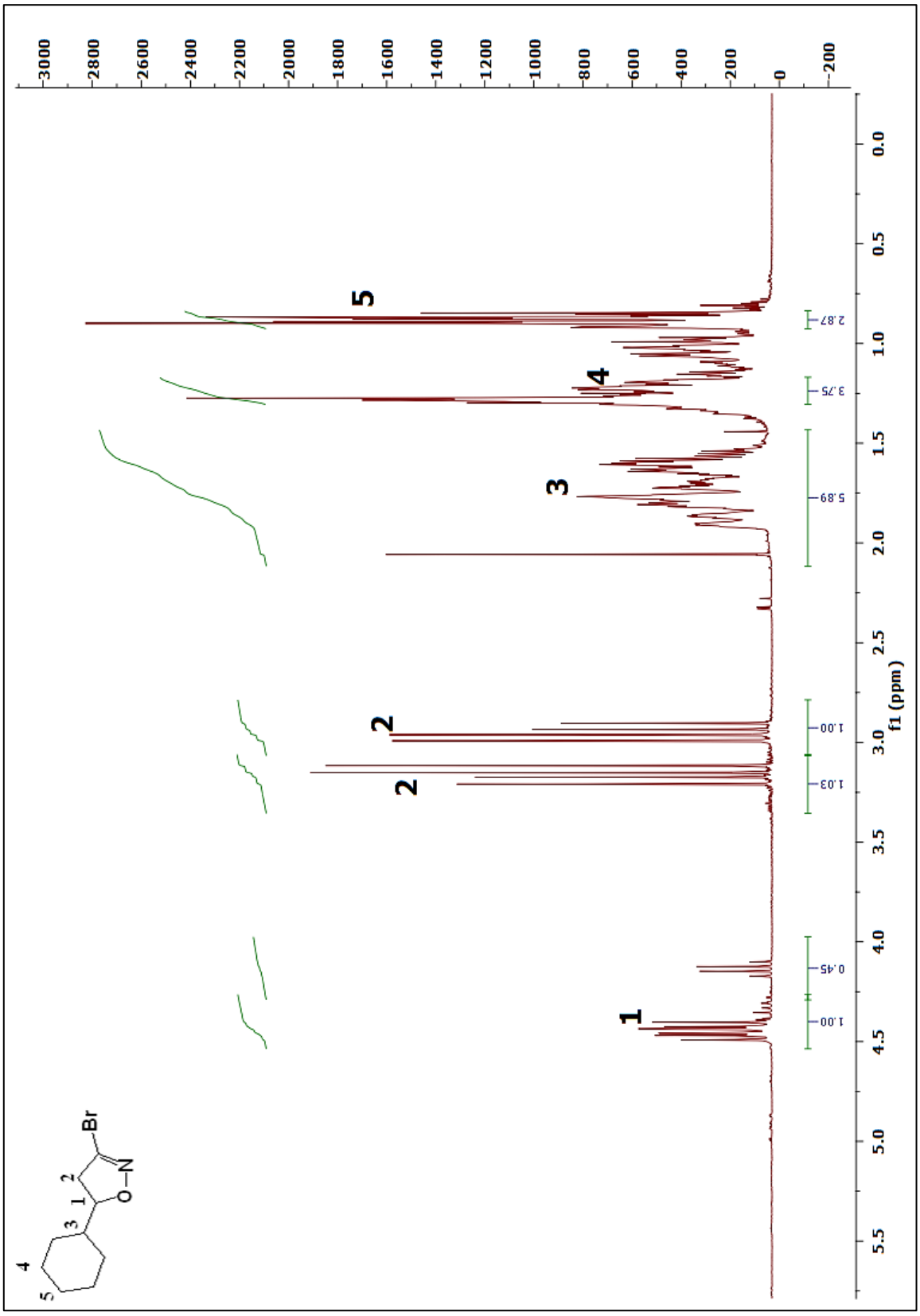


**Figure 2.44 $^{1}$HNMR of Compound 6b.**

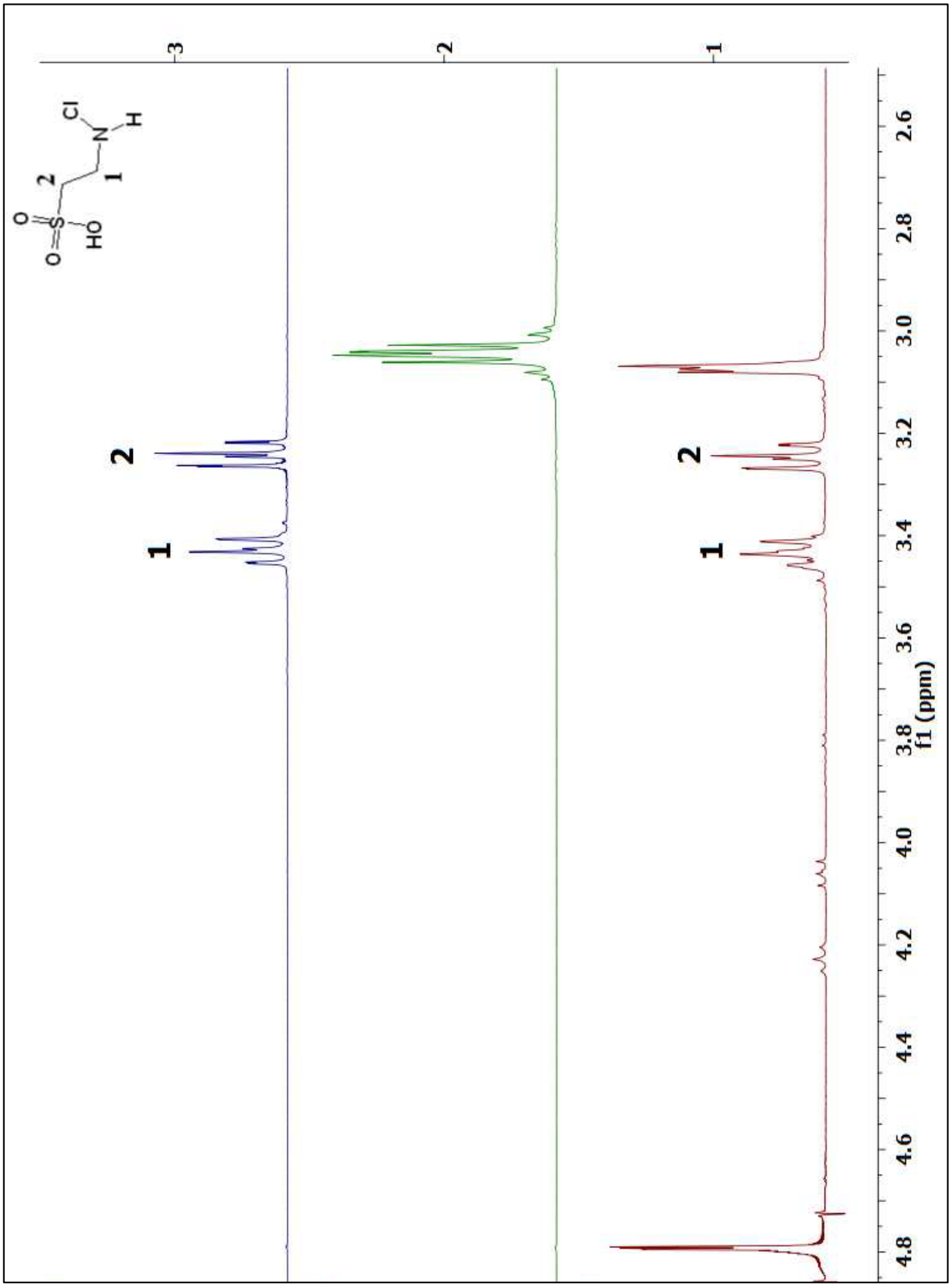


**Figure 2.45 [1]HNMR of Compound NCT. Spectrum (1) NCT made via mixing HOCl:Taurine 1:2, (2) Taurine sodium salt, (3) NCT made via ethanolic mixture of Chloramine-T and Taurine sodium salt.**

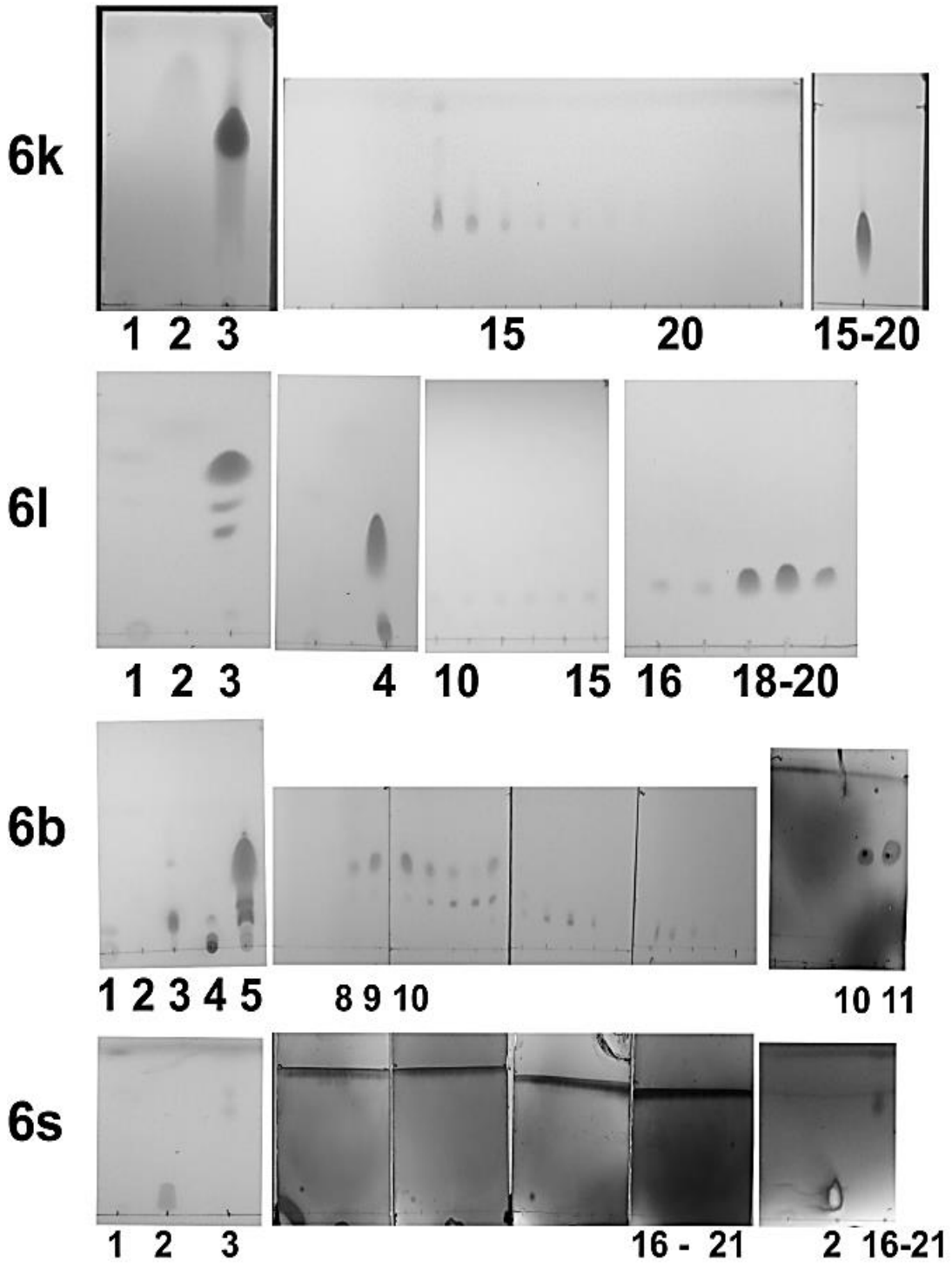


**Figure 2.46 TLC of compounds synthesized and silica column purified. Compound 6K crude product (3), 15- 20 pooled fractions from column and sent for NMR (15-20). Compound 6l crude product (3), change of solvents (4), fractions 18-20 combined from column and sent for NMR (18-20). Compound 6b crude product (5), fractions 8-10 combined from column and put on a second column, purified compound from second column fractions 10-11 combined and sent for NMR. Compound 6s crude product (3), very faint spots seen on fractions 16-21 combined and sent for NMR.**

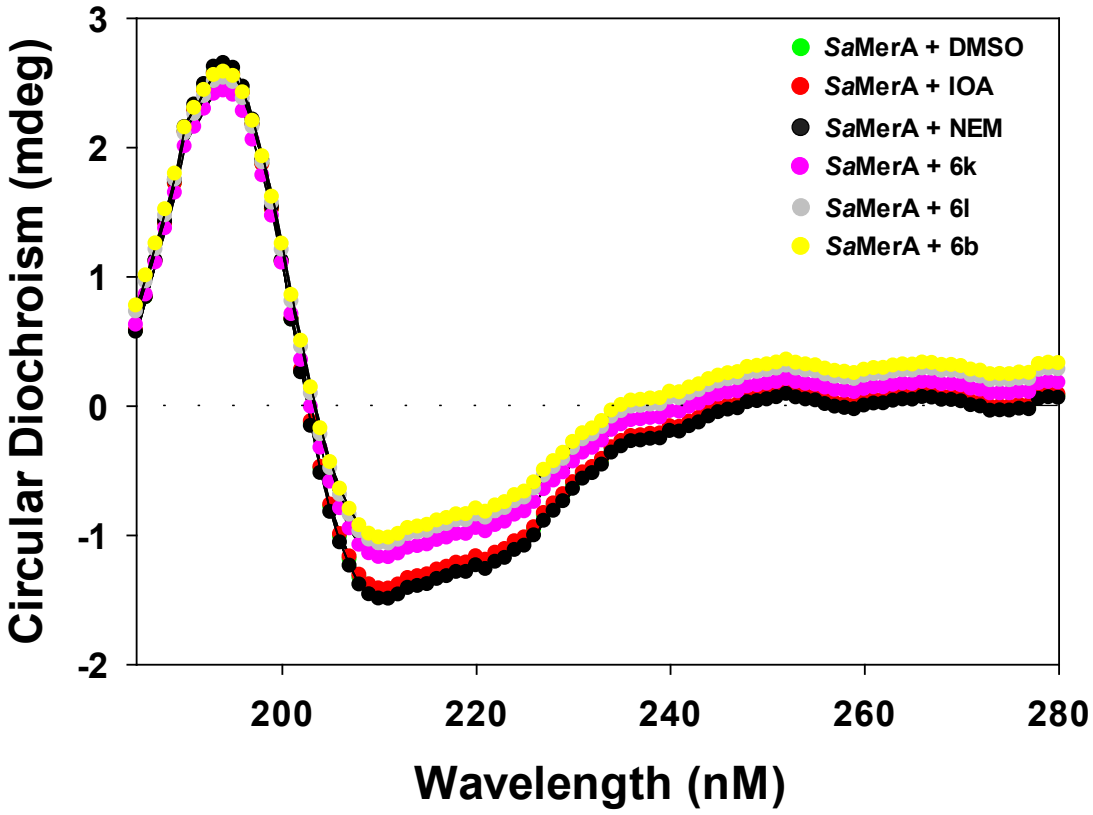


**Figure 2.47 CD spectroscopy of treated *Sa*MerA WT with DMSO, IOA (iodacetamide), NEM (n-methylmaleimide), compounds 6k, 6l and 6b.**

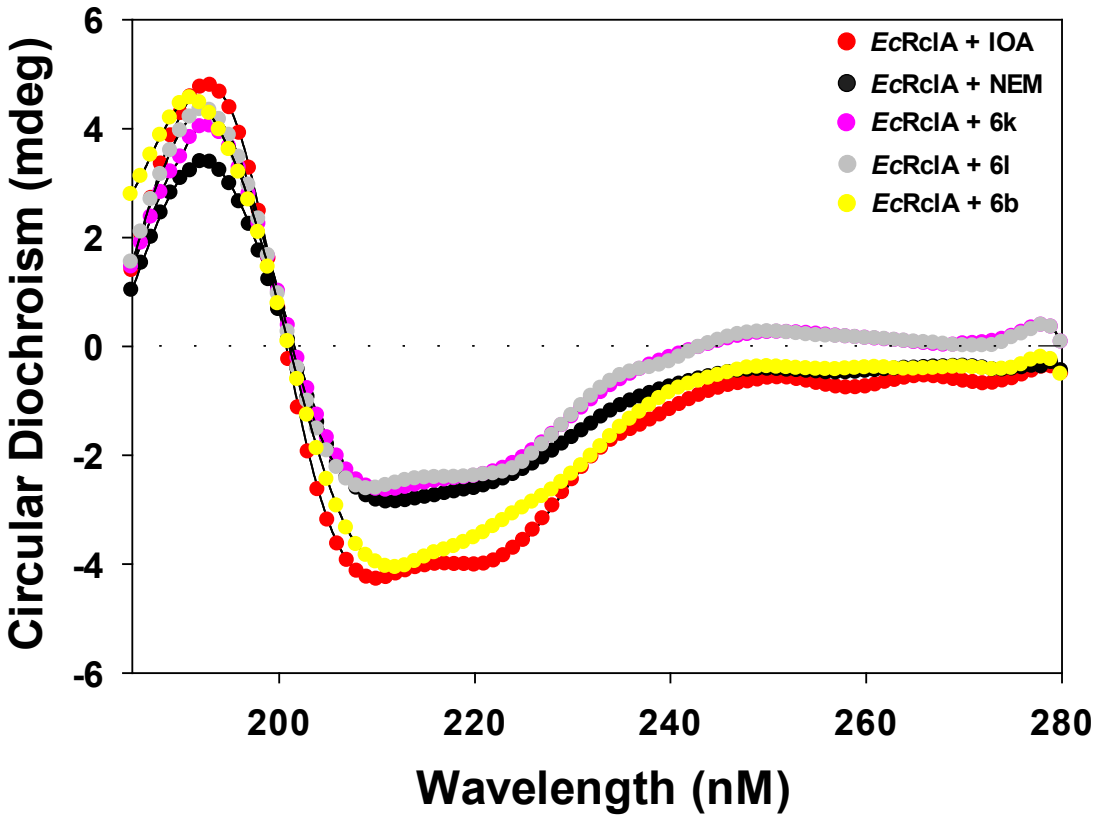


**Figure 2.48 CD spectroscopy of treated YkgC/RclA WT with IOA (iodacetamide), NEM (n-methylmaleimide) and compounds 6k, 6l and 6b.**

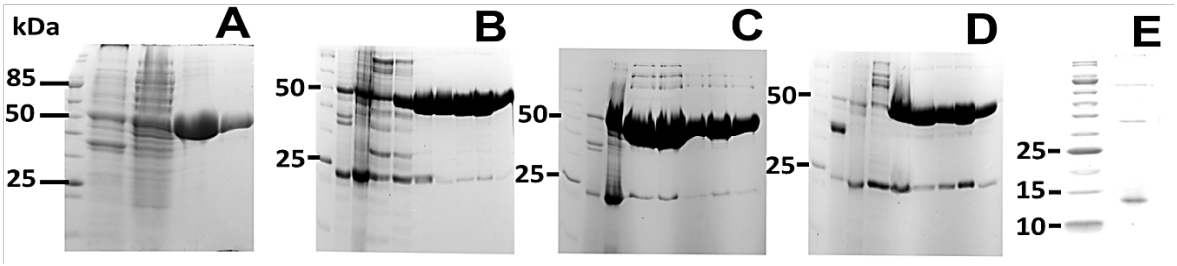


**Figure 2.49 10% SDS-PAGE of (A) *Pa*MerA Tn501, (B) *Ec*Gor, (C) *Ec*LipDH, (D) *Ec*YkgC/RclA, (E) *Sa*TrA. Far fight lanes of each gel were the final purified samples used for assays.**

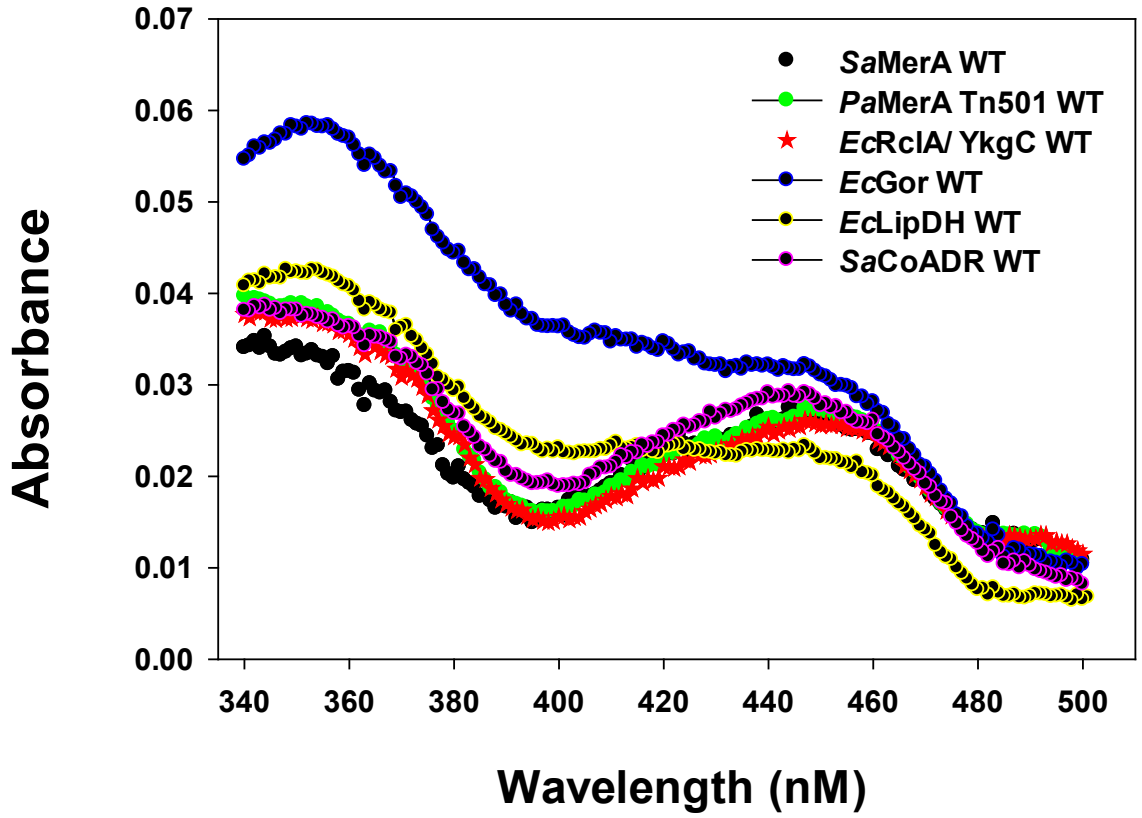


**Figure 2.50 Flavin Spectra of 2.5 µM *Sa*MerA WT, *Pa*MerA Tn501 WT, *Ec*RclA, *Ec*Gor, *Ec*LipDH and *Sa*CoADR.**

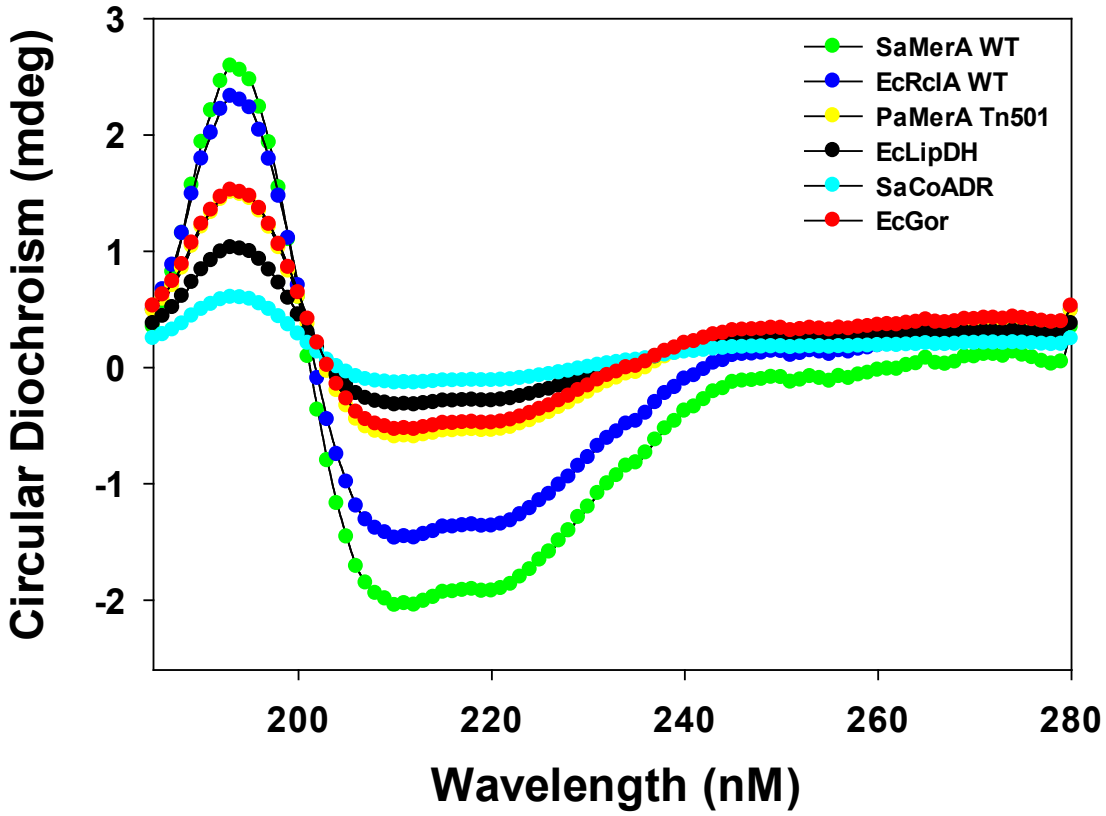


**Figure 2.51 CD Spectroscopy of SaMerA WT, EcRclA/YkgC, *Pa*MerA Tn501, *Ec*LipDH, *Sa*CoADR and *Ec*Gor,**

## 2.6 References

1. Klopper, S.L., *Cloning and functional characterization of thiol sidulfide interchange system proteins from Staphylococcus aureus*, in *Department of Biochemistry*. 2013, Stellenbosch University: Stellenbosch. p. 90.
2. Voyich, J.M., et al., *Insights into Mechanisms Used by Staphylococcus aureus to Avoid Destruction by Human Neutrophils.* J Immunol, 2005. **174**(6): p. 3907-3919.
3. Loi, V.V., et al., *Redox-Sensing Under Hypochlorite Stress and Infection Conditions by the Rrf2-Family Repressor HypR in Staphylococcus aureus.* Antioxid Redox Signal, 2018. **29**(7): p. 615-636.
4. Parker, B.W., et al., *The RclR protein is a reactive chlorine-specific transcription factor in Escherichia coli.* J Biol Chem, 2013. **288**(45): p. 32574-84.
5. Wang, S., et al., *Transcriptomic response of Escherichia coli O157:H7 to oxidative stress.* Appl Environ Microbiol, 2009. **75**(19): p. 6110-23.
6. Ojha, S., E.C. Meng, and P.C. Babbitt, *Evolution of function in the "two dinucleotide binding domains" flavoproteins.* PLoS Comput Biol, 2007. **3**(7): p. e121.
7. Hille, R., S. Miller, and B. Palfey, *Handbook of Flavoproteins: Complex flavoproteins, dehydrogenases and physical methods*, R. Hille, Editor. 2013, DE GRUYTER. p. 1-429.
8. Argyrou, A. and J.S. Blanchard, *Flavoprotein disulfide reductases: advances in chemistry and function.* Prog Nucleic Acid Res Mol Biol, 2004. **78**: p. 89-142.
9. Gerlt, J.A. and P.C. Babbitt, *Divergent evolution of enzymatic function: mechanistically diverse superfamilies and functionally distinct suprafamilies.* Annu Rev Biochem, 2001. **70**: p. 209-46.
10. Distefano, M.D., K.G. Au, and C.T. Walsh, *Mutagenesis of the redox-active disulfide in mercuric ion reductase: catalysis by mutant enzymes restricted to flavin redox chemistry.* Biochemistry, 1989. **28**(3): p. 1168-83.
11. Walsh, C., M. Distefano, and M. Moore, *Mutagenesis of paired cysteine residues in the disulphide-containing flavoprotein mercuric ion reductase from mercury-resistant bacteria.* Biochem Soc Trans, 1988. **16**(2): p. 90-1.
12. Miller, S.M., et al., *Communication between the active sites in dimeric mercuric ion reductase: an alternating sites hypothesis for catalysis.* Biochemistry, 1991. **30**(10): p. 2600-12.
13. Moore, M.J., S.M. Miller, and C.T. Walsh, *C-terminal cysteines of Tn501 mercuric ion reductase.* Biochemistry, 1992. **31**(6): p. 1677-85.
14. Miller, S.M., *2'-fluoro-2'-deoxy-D-arabinoflavin: characterization of a novel flavin and its effects on the formation and stability of two-electron-reduced mercuric ion reductase.* Biochemistry, 1995. **34**(40): p. 13066-73.
15. Engst, S. and S.M. Miller, *Rapid reduction of Hg(II) by mercuric ion reductase does not require the conserved C-terminal cysteine pair using HgBr2 as the substrate.* Biochemistry, 1999. **38**(2): p. 853-4.
16. Engst, S. and S.M. Miller, *Alternative routes for entry of HgX2 into the active site of mercuric ion reductase depend on the nature of the X ligands.* Biochemistry, 1999. **38**(12): p. 3519-29.

17. Ledwidge, R., et al., *NmerA, the metal binding domain of mercuric ion reductase, removes Hg2+ from proteins, delivers it to the catalytic core, and protects cells under glutathione-depleted conditions.* Biochemistry, 2005. **44**(34): p. 11402-16.

18. Hong, B., et al., *Direct measurement of mercury(II) removal from organomercurial lyase (MerB) by tryptophan fluorescence: NmerA domain of coevolved gamma-proteobacterial mercuric ion reductase (MerA) is more efficient than MerA catalytic core or glutathione.* Biochemistry, 2010. **49**(37): p. 8187-96.

19. Ledwidge, R., et al., *NmerA of Tn501 mercuric ion reductase: structural modulation of the pKa values of the metal binding cysteine thiols.* Biochemistry, 2010. **49**(41): p. 8988-98.

20. Johs, A., et al., *Structural characterization of intramolecular Hg(2+) transfer between flexibly linked domains of mercuric ion reductase.* J Mol Biol, 2011. **413**(3): p. 639-56.

21. Hong, L., et al., *Structure and dynamics of a compact state of a multidomain protein, the mercuric ion reductase.* Biophys J, 2014. **107**(2): p. 393-400.

22. Moore, M.J. and C.T. Walsh, *Mutagenesis of the N- and C-terminal cysteine pairs of Tn501 mercuric ion reductase: consequences for bacterial detoxification of mercurials.* Biochemistry, 1989. **28**(3): p. 1183-94.

23. Miller, S.M., et al., *Evidence for the participation of Cys558 and Cys559 at the active site of mercuric reductase.* Biochemistry, 1989. **28**(3): p. 1194-205.

24. Fox, B.S. and C.T. Walsh, *Mercuric reductase: homology to glutathione reductase and lipoamide dehydrogenase. Iodoacetamide alkylation and sequence of the active site peptide.* Biochemistry, 1983. **22**(17): p. 4082-8.

25. Fox, B. and C.T. Walsh, *Mercuric reductase. Purification and characterization of a transposon-encoded flavoprotein containing an oxidation-reduction-active disulfide.* J Biol Chem, 1982. **257**(5): p. 2498-503.

26. Williams, C.H., Jr., et al., *Lipoamide dehydrogenase, glutathione reductase, thioredoxin reductase, and thioredoxin.* J Biol Chem, 1967. **242**(22): p. 5226-31.

27. Helmann, J.D., *Bacillithiol, a new player in bacterial redox homeostasis.* Antioxid Redox Signal, 2011. **15**(1): p. 123-33.

28. Chandrangsu, P., et al., *The Role of Bacillithiol in Gram-Positive Firmicutes.* Antioxid Redox Signal, 2018. **28**(6): p. 445-462.

29. Reutimann, H., et al., *A conformational study of thioredoxin and its tryptic fragments.* J Biol Chem, 1981. **256**(13): p. 6796-803.

30. Carlberg, I., T. Sjodin, and B. Mannervik, *Circular dichroism studies of glutathione reductase.* Eur J Biochem, 1980. **112**(3): p. 487-91.

31. Rosenzweig, A.C., et al., *Crystal structure of the Atx1 metallochaperone protein at 1.02 A resolution.* Structure, 1999. **7**(6): p. 605-17.

32. Vasiliou, V., D. Ross, and D.W. Nebert, *Update of the NAD(P)H:quinone oxidoreductase (NQO) gene family.* Hum Genomics, 2006. **2**(5): p. 329-35.

33. Massey, V., *Activation of molecular oxygen by flavins and flavoproteins.* J Biol Chem, 1994. **269**(36): p. 22459-62.

34. ALDRICH, S., *Enzymatic assay of peroxidase (E.C 1.11.1.7) 2,2'-Azino-bis(3-Ethylbenzthiazoline-6-Sulfonic Acid) as substrate* 1996, SIGMA ALDRICH.

35. Cai, H., et al., *Multi-wavelength spectrophotometric determination of hydrogen peroxide in water with peroxidase-catalyzed oxidation of ABTS.* Chemosphere, 2018. **193**: p. 833-839.

36. Galaris, D. and K. Pantopoulos, *Oxidative stress and iron homeostasis: mechanistic and health aspects.* Crit Rev Clin Lab Sci, 2008. **45**(1): p. 1-23.

37. Puntarulo, S., *Iron, oxidative stress and human health.* Mol Aspects Med, 2005. **26**(4-5): p. 299-312.

38. McCord, M.C. and E. Aizenman, *The role of intracellular zinc release in aging, oxidative stress, and Alzheimer's disease.* Front Aging Neurosci, 2014. **6**: p. 77.

39. Marreiro, D.D., et al., *Zinc and Oxidative Stress: Current Mechanisms.* Antioxidants (Basel), 2017. **6**(2).

40. Lee, S.R., *Critical Role of Zinc as Either an Antioxidant or a Prooxidant in Cellular Systems.* Oxid Med Cell Longev, 2018. **2018**: p. 9156285.

41. Gaetke, L.M. and C.K. Chow, *Copper toxicity, oxidative stress, and antioxidant nutrients.* Toxicology, 2003. **189**(1-2): p. 147-63.

42. Uriu-Adams, J.Y. and C.L. Keen, *Copper, oxidative stress, and human health.* Mol Aspects Med, 2005. **26**(4-5): p. 268-98.

43. Louche, A., S.P. Salcedo, and S. Bigot, *Protein-Protein Interactions: Pull-Down Assays.* Methods Mol Biol, 2017. **1615**: p. 247-255.

44. Corthell, J.T., *Immunoprecipitation*. Basic Molecular Protocols in Neuroscience: Tips, Tricks, and Pitfalls. 2014, Elsevier Inc.: Academic Press. 1-124.

45. Protocol, N.M., *Detection of protein-protein interactions using the GST fusion protein pull-down technique.* Nature Methods, 2004. **1**: p. 275.

46. Jacob, C., et al., *Thioredoxin 2 from Escherichia coli is not involved in vivo in the recycling process of methionine sulfoxide reductase activities.* FEBS Lett, 2011. **585**(12): p. 1905-9.

47. Peng, H., et al., *Thioredoxin Profiling of Multiple Thioredoxin-Like Proteins in Staphylococcus aureus.* Front Microbiol, 2018. **9**: p. 2385.

48. Smith, D.B. and K.S. Johnson, *Single-step purification of polypeptides expressed in Escherichia coli as fusions with glutathione S-transferase.* Gene, 1988. **67**(1): p. 31-40.

49. Poole, L.B., *The basics of thiols and cysteines in redox biology and chemistry.* Free Radic Biol Med, 2015. **80**: p. 148-57.

50. Claiborne, A., et al., *Protein-sulfenic acids: diverse roles for an unlikely player in enzyme catalysis and redox regulation.* Biochemistry, 1999. **38**(47): p. 15407-16.

51. Gray, M.J., W.Y. Wholey, and U. Jakob, *Bacterial responses to reactive chlorine species.* Annu Rev Microbiol, 2013. **67**: p. 141-60.

52. Arner, E.S. and A. Holmgren, *Physiological functions of thioredoxin and thioredoxin reductase.* Eur J Biochem, 2000. **267**(20): p. 6102-9.

53. delCardayre, S.B., et al., *Coenzyme A disulfide reductase, the primary low molecular weight disulfide reductase from Staphylococcus aureus. Purification and characterization of the native enzyme.* J Biol Chem, 1998. **273**(10): p. 5744-51.

54. delCardayre, S.B. and J.E. Davies, *Staphylococcus aureus coenzyme A disulfide reductase, a new subfamily of pyridine nucleotide-disulfide oxidoreductase. Sequence, expression, and analysis of cdr.* J Biol Chem, 1998. **273**(10): p. 5752-7.

55. Mallett, T.C., et al., *Structure of coenzyme A-disulfide reductase from Staphylococcus aureus at 1.54 A resolution.* Biochemistry, 2006. **45**(38): p. 11278-89.

56. Hemila, H., *Lipoamide dehydrogenase of Staphylococcus aureus: nucleotide sequence and sequence analysis.* Biochim Biophys Acta, 1991. **1129**(1): p. 119-23.

57. Grayczyk, J.P., et al., *A Lipoylated Metabolic Protein Released by Staphylococcus aureus Suppresses Macrophage Activation.* Cell Host Microbe, 2017. **22**(5): p. 678-687 e9.

58. Winterbourn, C.C., A.J. Kettle, and M.B. Hampton, *Reactive Oxygen Species and Neutrophil Function.* Annu Rev Biochem, 2016. **85**: p. 765-92.

59. Hampton, M.B., A.J. Kettle, and C.C. Winterbourn, *Inside the neutrophil phagosome: Oxidants, myeloperoxidase, and bacterial killing.* Blood, 1998. **92**(9): p. 3007-3017.

60. Winterbourn, C.C., *Neutrophil Oxidants: Production and Reactions*, in *Oxygen Radicals: systematic events and disease processes*, D.K. Das and W.B. Essman, Editors. 1990, Karger: Basel, N.Y. p. 31-70.

61. Winterbourn, C.C. and A.J. Kettle, *Redox reactions and microbial killing in the neutrophil phagosome.* Antioxid Redox Signal, 2013. **18**(6): p. 642-60.

62. Prutz, W.A., *Interactions of hypochlorous acid with pyrimidine nucleotides, and secondary reactions of chlorinated pyrimidines with GSH, NADH, and other substrates.* Arch Biochem Biophys, 1998. **349**(1): p. 183-91.

63. Chapman, A.L., et al., *Chlorination of bacterial and neutrophil proteins during phagocytosis and killing of Staphylococcus aureus.* J Biol Chem, 2002. **277**(12): p. 9757-62.

64. Green, J.N., A.J. Kettle, and C.C. Winterbourn, *Protein chlorination in neutrophil phagosomes and correlation with bacterial killing.* Free Radic Biol Med, 2014. **77**: p. 49-56.

65. Peskin, A.V., et al., *Oxidation of methionine to dehydromethionine by reactive halogen species generated by neutrophils.* Biochemistry, 2009. **48**(42): p. 10175-82.

66. Peskin, A.V. and C.C. Winterbourn, *Kinetics of the reactions of hypochlorous acid and amino acid chloramines with thiols, methionine, and ascorbate.* Free Radic Biol Med, 2001. **30**(5): p. 572-9.

67. Dupre, S., M.T. Graziani, and M.A. Rosei, *A new method for the determination of enzymatic pantethine--splitting activity.* Ital J Biochem, 1970. **19**(2): p. 132-8.

68. Dupre, S., et al., *The enzymatic breakdown of pantethine to pantothenic acid and cystamine.* Eur J Biochem, 1970. **16**(3): p. 571-8.

69. Shrestha, C.L., et al., *Cysteamine-mediated clearance of antibiotic-resistant pathogens in human cystic fibrosis macrophages.* PLoS One, 2017. **12**(10): p. e0186169.

70. Fraser-Pitt, D.J., et al., *Cysteamine, an Endogenous Aminothiol, and Cystamine, the Disulfide Product of Oxidation, Increase Pseudomonas aeruginosa Sensitivity to Reactive Oxygen and Nitrogen Species and Potentiate Therapeutic Antibiotics against Bacterial Infection.* Infect Immun, 2018. **86**(6).

71. Devereux, G., et al., *Cysteamine as a Future Intervention in Cystic Fibrosis Against Current and Emerging Pathogens: A Patient-based ex vivo Study Confirming its Antimicrobial and Mucoactive Potential in Sputum.* EBioMedicine, 2015. **2**(10): p. 1507-12.

72. Charrier, C., et al., *Cysteamine (Lynovex(R)), a novel mucoactive antimicrobial & antibiofilm agent for the treatment of cystic fibrosis.* Orphanet J Rare Dis, 2014. **9**: p. 189.

73. Fukuda, K., et al., *Free amino acid content of lymphocytes and granulocytes compared.* Clin Chem, 1982. **28**(8): p. 1758-61.

74. Chesney, R.W., *Taurine: its biological role and clinical implications.* Adv Pediatr, 1985. **32**: p. 1-42.

75. Folkes, L.K., L.P. Candeias, and P. Wardman, *Kinetics and mechanisms of hypochlorous acid reactions.* Arch Biochem Biophys, 1995. **323**(1): p. 120-6.

76. Huxtable, R.J., *Physiological actions of taurine.* Physiol Rev, 1992. **72**(1): p. 101-63.

77. Izumi, K., et al., *Effects of taurine on tolerance to [D-Ala2, Met5]enkephalinamide in rats.* Eur J Pharmacol, 1982. **82**(1-2): p. 55-63.

78. Learn, D.B., V.A. Fried, and E.L. Thomas, *Taurine and hypotaurine content of human leukocytes.* J Leukoc Biol, 1990. **48**(2): p. 174-82.

79. Niu, X., et al., *Protective effects of taurine against inflammation, apoptosis, and oxidative stress in brain injury.* Mol Med Rep, 2018. **18**(5): p. 4516-4522.

80. Schuller-Levis, G.B. and E. Park, *Taurine and its chloramine: modulators of immunity.* Neurochem Res, 2004. **29**(1): p. 117-26.

81. Schuller-Levis, G.B. and E. Park, *Taurine: new implications for an old amino acid.* FEMS Microbiol Lett, 2003. **226**(2): p. 195-202.

82. Gottardi, W. and M. Nagl, *Chemical properties of N-chlorotaurine sodium, a key compound in the human defence system.* Arch Pharm (Weinheim), 2002. **335**(9): p. 411-21.

83. Nagl, M., et al., *Bactericidal activity of micromolar N-chlorotaurine: evidence for its antimicrobial function in the human defense system.* Antimicrob Agents Chemother, 2000. **44**(9): p. 2507-13.

84. Klamt, F. and E. Shacter, *Taurine chloramine, an oxidant derived from neutrophils, induces apoptosis in human B lymphoma cells through mitochondrial damage.* J Biol Chem, 2005. **280**(22): p. 21346-52.

85. Zgliczynski, J.M. and T. Stelmaszynska, *Chlorinating ability of human phagocytosing leucocytes.* Eur J Biochem, 1975. **56**(1): p. 157-62.

86. Weiss, S.J., et al., *Chlorination of taurine by human neutrophils. Evidence for hypochlorous acid generation.* J Clin Invest, 1982. **70**(3): p. 598-607.

87. Marcinkiewicz, J., et al., *Taurine chloramine, a product of activated neutrophils, inhibits in vitro the generation of nitric oxide and other macrophage inflammatory mediators.* J Leukoc Biol, 1995. **58**(6): p. 667-74.

88. Albrett, A.M., et al., *Heterogeneity of hypochlorous acid production in individual neutrophil phagosomes revealed by a rhodamine-based probe.* J Biol Chem, 2018. **293**(40): p. 15715-15724.

89. Pullar, J.M., M.C. Vissers, and C.C. Winterbourn, *Living with a killer: the effects of hypochlorous acid on mammalian cells.* IUBMB Life, 2000. **50**(4-5): p. 259-66.

90. Nagl, M. and W. Gottardi, *Rapid killing of Mycobacterium terrae by N-chlorotaurine in the presence of ammonium is caused by the reaction product monochloramine.* J Pharm Pharmacol, 1998. **50**(11): p. 1317-20.

91. Nagl, M., et al., *Tolerance and bactericidal action of N-chlorotaurine in a urinary tract infection by an omniresistant Pseudomonas aeruginosa.* Zentralbl Bakteriol, 1998. **288**(2): p. 217-23.

92. Nagl, M., et al., *Tolerance of N-chlorotaurine, an endogenous antimicrobial agent, in the rabbit and human eye--a phase I clinical study.* J Ocul Pharmacol Ther, 1998. **14**(3): p. 283-90.

93. Nagl, M., et al., *Tolerance of N-chlorotaurine, a new antimicrobial agent, in infectious conjunctivitis - a phase II pilot study.* Ophthalmologica, 2000. **214**(2): p. 111-4.

94. Nagl, M., C. Larcher, and W. Gottardi, *Activity of N-chlorotaurine against herpes simplex- and adenoviruses.* Antiviral Res, 1998. **38**(1): p. 25-30.

95. Nagl, M., et al., *The postantibiotic effect of N-chlorotaurine on Staphylococcus aureus. Application in the mouse peritonitis model.* J Antimicrob Chemother, 1999. **43**(6): p. 805-9.

96. Gruber, M., et al., *Bactericidal and Fungicidal Activity of N-Chlorotaurine Is Enhanced in Cystic Fibrosis Sputum Medium.* Antimicrob Agents Chemother, 2017. **61**(5).

97. Nagl, M., et al., *Enhanced fungicidal activity of N-chlorotaurine in nasal secretion.* J Antimicrob Chemother, 2001. **47**(6): p. 871-4.

98. Gottardi, W., M. Hagleitner, and M. Nagl, *The influence of plasma on the disinfecting activity of the new antimicrobial agent N-chlorotaurine-sodium in comparison with chloramine T.* J Pharm Pharmacol, 2001. **53**(5): p. 689-97.

99. Neher, A., et al., *N-chlorotaurine, a novel endogenous antimicrobial agent: tolerability testing in a mouse model.* Arch Otolaryngol Head Neck Surg, 2001. **127**(5): p. 530-3.

100. Ammann, C.G., et al., *Influence of poly-N-acetylglucosamine in the extracellular matrix on N-chlorotaurine mediated killing of Staphylococcus epidermidis.* New Microbiol, 2014. **37**(3): p. 383-6.

101. Arnitz, R., et al., *A novel N-chlorotaurine-corticosteroid combination as a preservative-free local disinfectant: influence on the ciliary beat frequency in vitro.* Acta Otolaryngol, 2006. **126**(3): p. 291-4.

102. Arnitz, R., et al., *Protein sites of attack of N-chlorotaurine in Escherichia coli.* Proteomics, 2006. **6**(3): p. 865-9.

103. Arnitz, R., et al., *Tolerability of inhaled N-chlorotaurine in humans: a double-blind randomized phase I clinical study.* Ther Adv Respir Dis, 2018. **12**: p. 1753466618778955.

104. Bellmann-Weiler, R., et al., *The endogenous antiseptic N-chlorotaurine irreversibly inactivates Chlamydia pneumoniae and Chlamydia trachomatis.* J Med Microbiol, 2018. **67**(9): p. 1410-1415.

105. Coraca-Huber, D.C., et al., *Bactericidal activity of N-chlorotaurine against biofilm-forming bacteria grown on metal disks.* Antimicrob Agents Chemother, 2014. **58**(4): p. 2235-9.

106. Eitzinger, C., et al., *N-chlorotaurine, a long-lived oxidant produced by human leukocytes, inactivates Shiga toxin of enterohemorrhagic Escherichia coli.* PLoS One, 2012. **7**(11): p. e47105.

107. Furnkranz, U., et al., *In vitro activity of N-chlorotaurine (NCT) in combination with NH4Cl against Trichomonas vaginalis.* Int J Antimicrob Agents, 2011. **37**(2): p. 171-3.

108. Furnkranz, U., et al., *Cytotoxic activity of N-chlorotaurine on Acanthamoeba spp.* Antimicrob Agents Chemother, 2008. **52**(2): p. 470-6.

109. Furnkranz, U., et al., *N-Chlorotaurine shows high in vitro activity against promastigotes and amastigotes of Leishmania species.* J Med Microbiol, 2009. **58**(Pt 10): p. 1298-302.

110. Geiger, R., et al., *Tolerability of inhaled N-chlorotaurine in the pig model.* BMC Pulm Med, 2009. **9**: p. 33.

111. Gottardi, W., R. Arnitz, and M. Nagl, *N-Chlorotaurine and ammonium chloride: an antiseptic preparation with strong bactericidal activity.* Int J Pharm, 2007. **335**(1-2): p. 32-40.

112. Gottardi, W. and M. Nagl, *N-chlorotaurine, a natural antiseptic with outstanding tolerability.* J Antimicrob Chemother, 2010. **65**(3): p. 399-409.

113. Gstottner, M., et al., *Refractory rhinosinusitis complicating immunosuppression: application of N-chlorotaurine, a novel endogenous antiseptic agent.* ORL J Otorhinolaryngol Relat Spec, 2003. **65**(5): p. 303-5.

114. Hofer, E., et al., *In vitro study on the influence of N-chlorotaurine on the ciliary beat frequency of nasal mucosa.* Am J Rhinol, 2003. **17**(3): p. 149-52.

115. Huber, J., et al., *Tolerability of N-chlorotaurine in the bovine mammary gland.* J Dairy Res, 2008. **75**(2): p. 248-56.

116. Huemer, H.P., M. Nagl, and E.U. Irschick, *In vitro prevention of vaccinia and herpesvirus infection spread in explanted human corneas by N-chlorotaurine.* Ophthalmic Res, 2010. **43**(3): p. 145-52.

117. Lackner, M., et al., *N-Chlorotaurine Exhibits Fungicidal Activity against Therapy-Refractory Scedosporium Species and Lomentospora prolificans.* Antimicrob Agents Chemother, 2015. **59**(10): p. 6454-62.

118. Lorenz, K., et al., *Effect of N-chlorotaurine mouth rinses on plaque regrowth and plaque vitality.* Clin Oral Investig, 2009. **13**(1): p. 9-14.

119. Lumassegger, M., et al., *[Therapy-resistant otitis externa with additional tympanic membrane perforation: local therapy using N-chlorotaurine and dexamethasone].* HNO, 2010. **58**(9): p. 927-30.

120. Martini, C., et al., *Antimicrobial and anticoagulant activities of N-chlorotaurine, N,N-dichloro-2,2-dimethyltaurine, and N-monochloro-2,2-dimethyltaurine in human blood.* Antimicrob Agents Chemother, 2012. **56**(4): p. 1979-84.

121. Mustedanagic, J., V.F. Ximenes, and M. Nagl, *Microbicidal activity of N-chlorotaurine in combination with hydrogen peroxide.* AMB Express, 2017. **7**(1): p. 102.

122. Nagl, M., R. Arnitz, and M. Lackner, *N-Chlorotaurine, a Promising Future Candidate for Topical Therapy of Fungal Infections.* Mycopathologia, 2018. **183**(1): p. 161-170.

123. Nagl, M., et al., *Impact of N-chlorotaurine on viability and production of secreted aspartyl proteinases of Candida spp.* Antimicrob Agents Chemother, 2002. **46**(6): p. 1996-9.

124. Nagl, M., et al., *Tolerability and efficacy of N-chlorotaurine in comparison with chloramine T for the treatment of chronic leg ulcers with a purulent coating: a randomized phase II study.* Br J Dermatol, 2003. **149**(3): p. 590-7.

125. Neher, A., et al., *Antimicrobial activity of dexamethasone and its combination with N-chlorotaurine.* Arch Otolaryngol Head Neck Surg, 2008. **134**(6): p. 615-20.

126. Neher, A., et al., *Tolerability of N-chlorotaurine in chronic rhinosinusitis applied via yamik catheter.* Auris Nasus Larynx, 2005. **32**(4): p. 359-64.

127. Neher, A., et al., *N-chlorotaurine--a new safe substance for postoperative ear care.* Auris Nasus Larynx, 2007. **34**(1): p. 19-22.

128. Neher, A., et al., *Acute otitis externa: efficacy and tolerability of N-chlorotaurine, a novel endogenous antiseptic agent.* Laryngoscope, 2004. **114**(5): p. 850-4.

129. Neher, A., et al., *Tolerability of N-chlorotaurine in the guinea pig middle ear: a pilot study using an improved application system.* Ann Otol Rhinol Laryngol, 2004. **113**(1): p. 76-81.

130. Reeves, E.P., et al., *Effect of N-chlorotaurine on Aspergillus, with particular reference to destruction of secreted gliotoxin.* J Med Microbiol, 2006. **55**(Pt 7): p. 913-8.

131. Romanowski, E.G., et al., *N-chlorotaurine is an effective antiviral agent against adenovirus in vitro and in the Ad5/NZW rabbit ocular model.* Invest Ophthalmol Vis Sci, 2006. **47**(5): p. 2021-6.

132. Schwienbacher, M., et al., *Tolerability of inhaled N-chlorotaurine in an acute pig streptococcal lower airway inflammation model.* BMC Infect Dis, 2011. **11**: p. 231.

133. Teuchner, B., et al., *N-chlorotaurine and its analogues N,N-dichloro-2,2-dimethyltaurine and N-monochloro-2,2-dimethyltaurine are safe and effective bactericidal agents in ex vivo corneal infection models.* Acta Ophthalmol, 2012. **90**(8): p. e632-7.

134. Teuchner, B., et al., *Tolerability and efficacy of N-chlorotaurine in epidemic keratoconjunctivitis--a double-blind, randomized, phase-2 clinical trial.* J Ocul Pharmacol Ther, 2005. **21**(2): p. 157-65.

135. Teuchner, B., et al., *Tolerability of N-chlorotaurine plus ammonium chloride in the rabbit and human eye--a phase 1 clinical study.* Graefes Arch Clin Exp Ophthalmol, 2008. **246**(12): p. 1723-30.

136. Kim, W., et al., *Role of heme oxygenase-1 in potentiation of phagocytic activity of macrophages by taurine chloramine: Implications for the resolution of zymosan A-induced murine peritonitis.* Cell Immunol, 2018. **327**: p. 36-46.

137. Zgliczynski, J.M., et al., *Chlorination by the myeloperoxidase-H2O2-Cl- antimicrobial system at acid and neutral pH.* Proc Soc Exp Biol Med, 1977. **154**(3): p. 418-22.

138. Albrich, J.M., C.A. McCarthy, and J.K. Hurst, *Biological reactivity of hypochlorous acid: implications for microbicidal mechanisms of leukocyte myeloperoxidase.* Proc Natl Acad Sci U S A, 1981. **78**(1): p. 210-4.

139. Bernofsky, C., *Nucleotide chloramines and neutrophil-mediated cytotoxicity.* FASEB J, 1991. **5**(3): p. 295-300.

140. Dukan, S. and D. Touati, *Hypochlorous acid stress in Escherichia coli: resistance, DNA damage, and comparison with hydrogen peroxide stress.* J Bacteriol, 1996. **178**(21): p. 6145-50.

141. Prutz, W.A., *Hypochlorous acid interactions with thiols, nucleotides, DNA, and other biological substrates.* Arch Biochem Biophys, 1996. **332**(1): p. 110-20.

142. Hawkins, C.L. and M.J. Davies, *Hypochlorite-induced damage to proteins: formation of nitrogen-centred radicals from lysine residues and their role in protein fragmentation.* Biochem J, 1998. **332 ( Pt 3)**: p. 617-25.

143. Stanley, N.R., D.I. Pattison, and C.L. Hawkins, *Ability of hypochlorous acid and N-chloramines to chlorinate DNA and its constituents.* Chem Res Toxicol, 2010. **23**(7): p. 1293-302.

144. Hawkins, C.L., D.I. Pattison, and M.J. Davies, *Reaction of protein chloramines with DNA and nucleosides: evidence for the formation of radicals, protein-DNA cross-links and DNA fragmentation.* Biochem J, 2002. **365**(Pt 3): p. 605-15.

145. Kelly, R.C., et al., *Total synthesis of alpha-amino-3-chloro-4,5-dihydro-5-isoxazoleacetic acid (AT-125), an antitumor antibiotic.* Journal of American Chemistry Society, 1979. **101**: p. 1054-1056.

146. Miles, B.W., et al., *Inactivation of the amidotransferase activity of carbamoyl phosphate synthetase by the antibiotic acivicin.* J Biol Chem, 2002. **277**(6): p. 4368-73.

147. Orth, R., T. Bottcher, and S.A. Sieber, *The biological targets of acivicin inspired 3-chloro- and 3-bromodihydroisoxazole scaffolds.* Chem Commun (Camb), 2010. **46**(44): p. 8475-7.

148. Powers, J.C., et al., *Irreversible inhibitors of serine, cysteine, and threonine proteases.* Chem Rev, 2002. **102**(12): p. 4639-750.

149. Bruno, S., et al., *Discovery of covalent inhibitors of glyceraldehyde-3-phosphate dehydrogenase, a target for the treatment of malaria.* J Med Chem, 2014. **57**(17): p. 7465-71.

150. Jost, C., et al., *Promiscuity and selectivity in covalent enzyme inhibition: a systematic study of electrophilic fragments.* J Med Chem, 2014. **57**(18): p. 7590-9.

151. Girardin, M., et al., *Synthesis of 3-aminoisoxazoles via the addition-elimination of amines on 3-bromoisoxazolines.* Org Lett, 2009. **11**(5): p. 1159-62.

152. Hill, B.G., et al., *Methods for the determination and quantification of the reactive thiol proteome.* Free Radic Biol Med, 2009. **47**(6): p. 675-83.

153. Silverman, R.B., *Mechanism-based Inactivation Enzyme Inactivation: Chemistry and Enzymology*. 1988: CRC.

154. El Zoeiby, A., F. Sanschagrin, and R.C. Levesque, *Structure and function of the Mur enzymes: development of novel inhibitors.* Mol Microbiol, 2003. **47**(1): p. 1-12.

155. Kitagawa, M., et al., *Complete set of ORF clones of Escherichia coli ASKA library (a complete set of E. coli K-12 ORF archive): unique resources for biological research.* DNA Res, 2005. **12**(5): p. 291-9.

156. van der Westhuyzen, R. and E. Strauss, *Michael acceptor-containing coenzyme A analogues as inhibitors of the atypical coenzyme A disulfide reductase from Staphylococcus aureus.* J Am Chem Soc, 2010. **132**(37): p. 12853-5.

157. Kosower, N.S. and E.M. Kosower, *Diamide: an oxidant probe for thiols.* Methods Enzymol, 1995. **251**: p. 123-33.

*Chapter 3*

# INVESTIGATION OF THE LMW THIOL-BASED REDOX SYSTEMS OF *S. AUREUS*

## 3.1 Introduction

For many organisms, living in an oxygen-rich environment can be a challenge. Over time, organisms have developed mechanisms for surviving in the presence of a range of oxygen levels, giving rise to obligate anaerobes, microaerophiles, and aerobes. However, the main challenge remains: overexposure to oxygen can result in stress and even death in any organism. The first hypothesis that proposed some form/entity of oxygen reactive species as the cause of stress in and the death of organisms was postulated in 1954 [1, 2]. It is now well known that oxygen can pass through cell membranes very easily and cause a wide range of damaging effects. Many studies have been conducted on understanding the mechanisms relating to the generation of the reactive species that cause oxidative stress in organisms. A number of studies have also shown that oxidative stress causes redox imbalance within cells which is one of the key underlying mechanisms to cell proliferation, signaling, aging and even cell death [3].

There are a number of ways in which organisms respond to oxidative stress. By far the best studied system is that of the bacterium *E. coli* [4]. This bacterium's defense mechanisms include oxidant scavenging enzymes (superoxide dismutase, catalase, alkyl hydroperoxidase or dedicated peroxidases), reactive oxygen sensors (regulators such as OxyR, SoxRS) and dedicated repair mechanisms for the damage caused by oxidative species. These include reactive oxygen species (ROS), reactive nitrogen species (RNS) and reactive chlorine species (RCS), which together target bacterial membranes, proteins that rely on metal cofactors, DNA and lipids.

Of these, proteins are by far the most abundantly targeted biomolecule and therefore account for the bulk of the damage caused by oxidative stress [5]. The most common consequence is the oxidation of protein cofactors (especially metals) and amino acid residue side chains. Sulfur-containing amino acids are particularly vulnerable and reactive towards ROS, RNS and RCS. Despite such amino acids having a low abundance within proteins, their location/s in protein sequences is often conserved due to their important roles in catalysis and/or the maintenance of structure [6]

In response to oxidative stress many organisms significantly increase the concentration of cysteine-based metabolites [7]. These compounds, collectively referred to as low molecular weight (LMW) thiols, are found in all living systems and primarily play a role in redox balance/homeostasis [7-9]. A number of LMW thiols have been discovered and are shown in Figure 3.2. The best studied of these is the tripeptide L-γ-glutamyl-L-cysteinylglycine, otherwise known as glutathione (GSH). GSH plays many roles in eukaryotes and Gram-negative bacteria, including acting as a redox buffer (by being sacrificially oxidized to its disulfide, GSSG), in the detoxification of reactive species, in the reduction of ribonucleotides and *S*-thiolation to name a few (Figure 3.1) [7, 10-23]. Glutathione peroxidase (Gpx) is oxidized by peroxide and reduced by GSH also forming GSSG. In turn GSSG is reduced by glutathione disulfide reductase (Gor). Harmful xenobiotics are removed by the action of glutathione-*S*-transferases (GSTs) through GSH conjugation. Ribonucleotide reductase (RNR) relies on a reducing system such as Grx/GSSG that recycles the RNR active site disulfides back to their free form to further continue the reduction of an incoming ribonucleotide substrate.

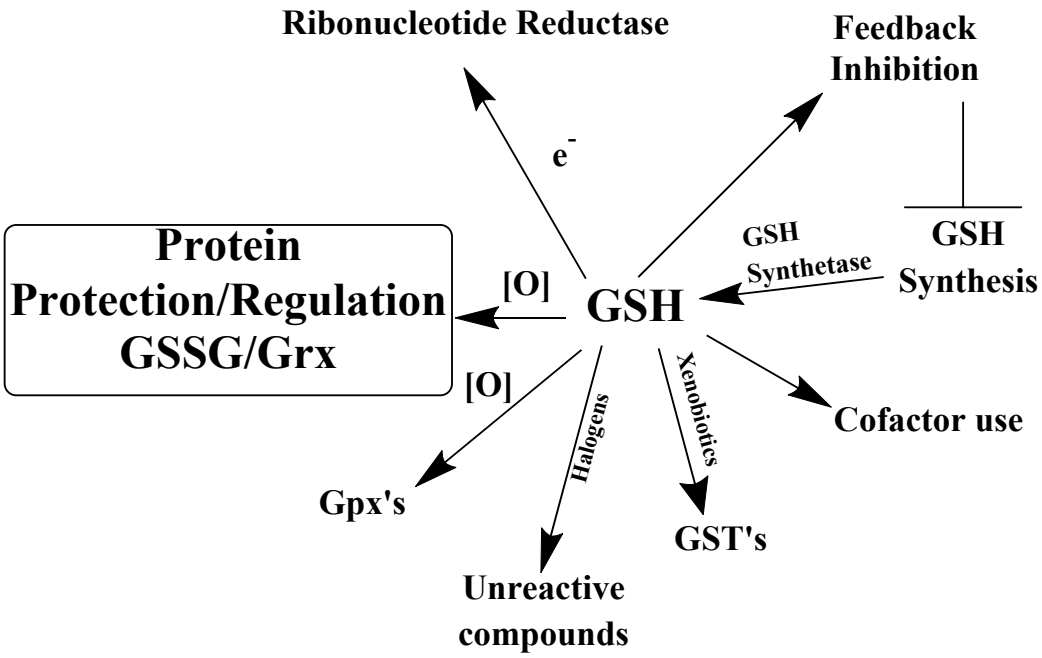


**Figure 3.1 Roles of GSH in redox-related functions in *E. coli*. The many roles of GSH include the maintenance of redox homeostasis, removal of toxic compounds, maintaining the ribonucleotide reductase catalytic cycle and acting as a cofactor. Grx (Glutaredoxin), Gpx (Glutathione peroxidase), GST (Glutahtione-S-Transferase). Redrawn and adapted from [20].**

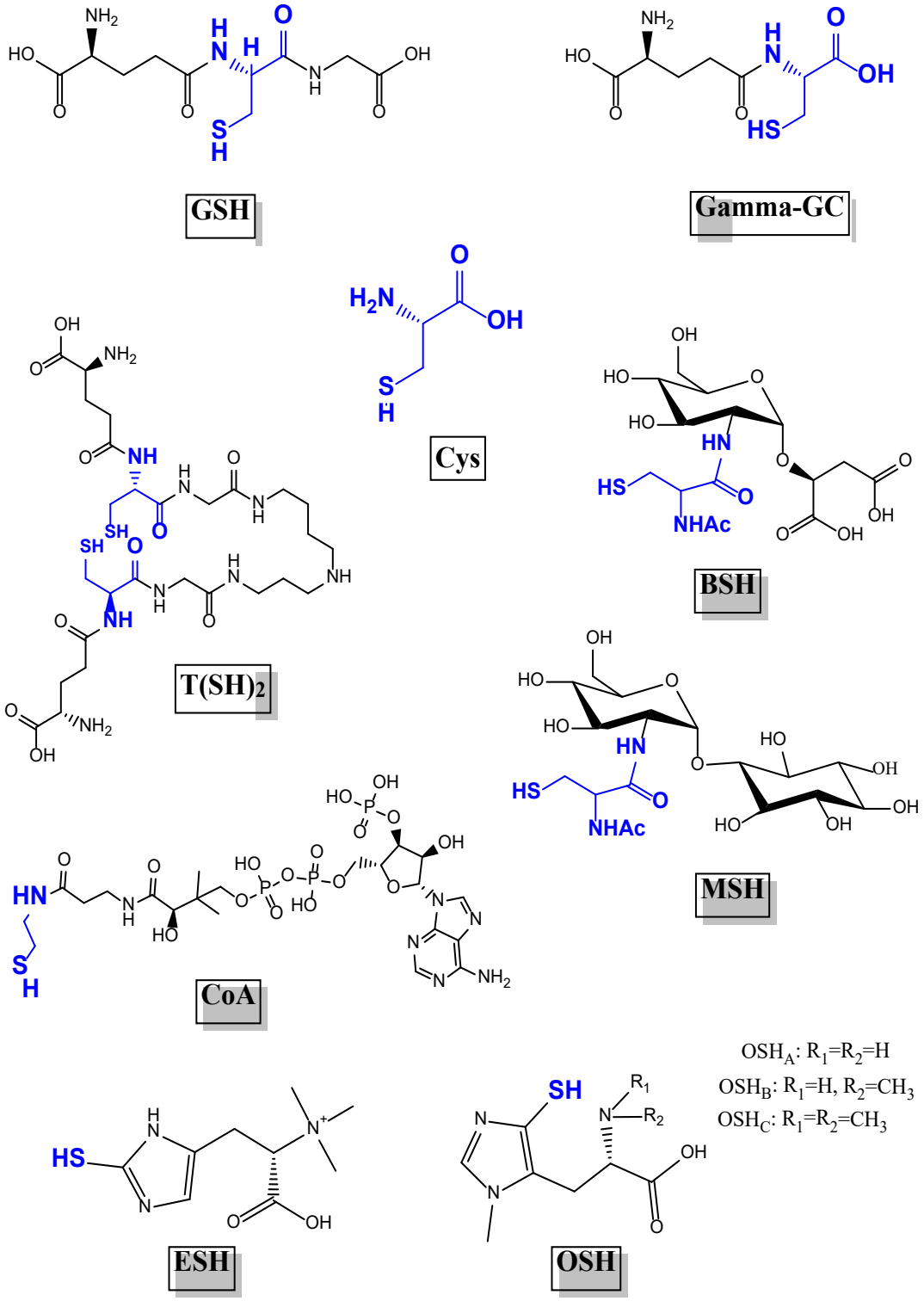


**Figure 3.2 Various LMW thiols implicated in oxidative stress responses. Glutathione (GSH, found in eukaryotes and Gram-negative bacteria), gamma-GlutamylCys (GGC, found in *halobacteria*, lactic acid bacteria), cysteine (Cys, found in all organisms), bacillithiol (BSH, found in *Firmicutes*), trypanothione (T(SH)2, found in *Trypanosomes*), mycothiol (MSH, found in *Actinomycetes*), coenzyme A (CoA, found in all organisms), ergothioneine (ESH, found in fungi and *Mycobacteria*), and ovothiol (OSH, found in *Leishmania* and marine invertebrates) Redrawn from [7].**

Another major function of GSH is in protein protection and regulation. Many important enzymes contain redox sensitive active site thiols and exposure to oxidants would result in a number of thiol species. As a protective mechanism, sulfenic acids and other labile thiol species are able to react with LMW thiols via *S*-thiolation. In the absence of such a protective mechanism, the cysteine residues would be susceptible to irreversible over-oxidation. The process of *S*-thiolation is a reversible process that returns the proteins to their native form. The best studied example of such a process is the GSSG/glutaredoxin-based system that is schematically shown in Figure 3.3 [6, 7, 24-40]. In this model system, glutaredoxin (Grx) enzymes harness the reducing power of GSH to maintain the cellular redox state as well as GSH-dependent reactions. Grxs belong to the Thioredoxin-fold protein (TFP) family and are classified into two groups based on the mechanism used to reduce protein disulfides (Figure 3.3) [37]. In the dithiol mechanism, Grx reduces a protein disulfide to form a mixed disulfide with the target protein (Figure 3.3; Step 1). The second thiol of Grx then reduces the mixed disulfide to release the target protein in a reduced state (Step 2). The Grx monothiol mechanism is primarily involved in the process of de-glutathionylation. In this mechanism one of the Cys residues of Grx attacks a *S*-glutathionylated protein complex to release the free protein while forming Grx-SSG by disulfide exchange (Figure 3.3; Step 6). This mixed disulfide, in turn, is exchanged with free GSH to recycle the Grx back to its reduced form, while producing glutathione disulfide (GSSG) (Figure 3.3; Step 4). The GSSG is recycled by Glutathione reductase (Gor), which reduces GSSG back to free GSH (Figure 3.3; Step 5) [11, 40-46].

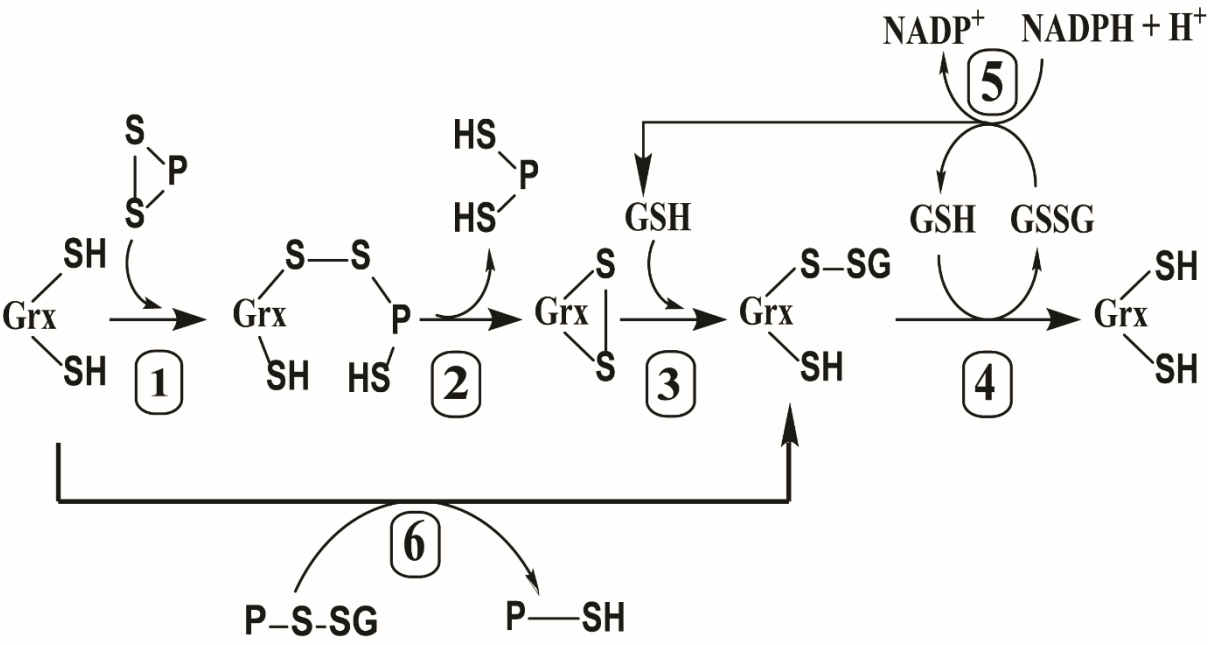


**Figure 3.3 The Glutaredoxin/GSSG redox system. The most well studied system of *S*-thiolation is *S*-Glutathionylation. The process of *S*-glutathionylation is a reversible process involving small proteins called glutaredoxins (Grxs). Glutaredoxins function via two mechanisms namely a mono- and – dithiol mechanism. In the dithiol mechanism, Grxs reduce protein disulfides using both of their active site thiols (Step 1-4). The monothiol mechanism is utilized in reversing *S*-glutathionylation. Both mechanisms of Grx utilize GSH and subsequently form glutathione disulfide (GSSG). GSSG is recycled by NADPH dependent glutathione disulfide reductase (Gor). Adapted from [37]**

*S. aureus* lacks GSH and therefore has to use alternative LMW thiol(s) to establish a redox system capable of resisting oxidative damage. Possible candidates include cysteine (Cys), lipoic acid/lipoamide, coenzyme A (CoA) and bacillithiol (BSH) [7, 30, 31, 47-49]. However, since high concentrations of Cys are particularly toxic to cells, it is therefore not usually directly involved in the maintenance of redox homeostasis [7, 49]. Similarly, lipoamide is also an unlikely candidate as it has not been directly implicated in maintaining redox homeostasis in any organism. Instead, it is usually found covalently attached to a Lys residue of lipoamide dehydrogenase, which itself forms part of multienzyme complexes such as those of keto acid dehydrogenase, pyruvate dehydrogenase (PDH) and ketoglutarate dehydrogenase (KDH) [50-52]. Consequently, BSH and CoA have been considered to be the major LMW thiols implicated in maintaining redox homeostasis in *S. aureus* and protecting it against oxidative stress [7, 30, 31, 47-49].

BSH is a LMW thiol that is found in members of the *Firmicutes* phylum. The structure and distribution of BSH was confirmed in 2009 through a large collaborative effort which has ultimately allowed for further studies on the biosynthetic pathway of BSH [32, 53-55]. Using

similarities to the MSH biosynthetic pathway and EMBL STRING, candidate genes for the first steps of BSH biosynthesis were identified in *Bacilli [32]*. Along with these candidate genes other genes were identified involving pantothenate biosynthesis (*panE* and *coaX*) as well as genes of unassigned function (Figure 3.4). The finding of CoA-associated genes linked to BSH biosynthesis might suggest that the biosynthesis of these two LMW thiols are linked in some manner [24, 56].

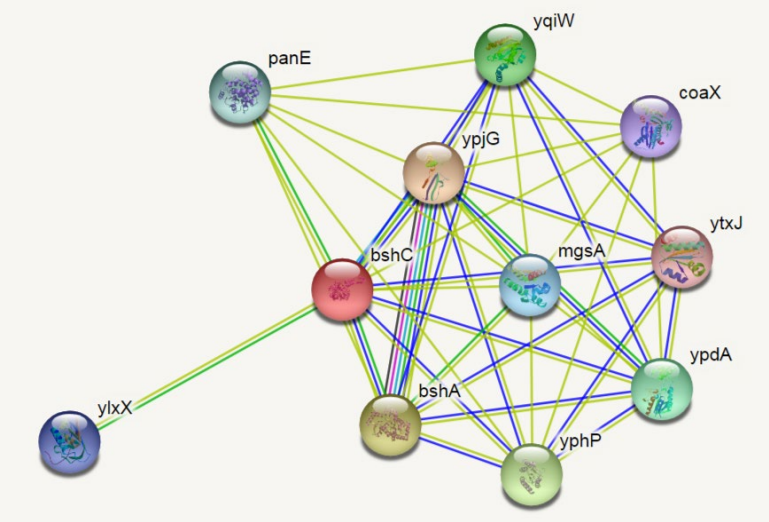


**Figure 3.4 EMBL STRING analysis of known BSH- and CoA-related genes and their association with genes of unknown function in *B. subtilis*. Some of the genes identified interacting with BSH biosynthesis include *panE* (encoding 2-dehydropantoate 2-reductase), *coaX* (encoding Type III pantothenate kinase), *mgsA* (encoding methylglyoxal synthase), *yphP* (encoding bacilliredoxin BrxA) and *yqiW* (encoding bacilliredoxin BrxB) as well as a number of uncharacterized genes.**

In addition to the known biosynthetic genes, others that are likely associated with BSH-dependent enzymology have also been identified. Two TFP-like proteins, YqiW and YphP, resemble Grx and have been shown to play a role in de-thiolation of bacillithiolated OhrR and MetE in *B. subtilis [57]*. YpjG is predicted to function as an ABC transporter protein although no experimental data shows this. Conserved DUF881-domain containing protein YlxX is yet to be characterized. Another protein of unknown function is YpdA, which shares close sequence identity to thioredoxin reductase and has been hypothesized as a protein with potential BSSB reductase activity. A similar analysis in *S. aureus* shows that it contains many of the homologues of the *Bacillus* spp. BSH biosynthetic genes, as well as homologues of YpdA, YphP, YqiW and YtxJ.

Since the identification of the BSH biosynthetic genes, BSH has been shown to have many diverse roles, including the reduction of thionitrosylated (-SNO) compounds, detoxification of

xenobiotics, maintaining metal homeostasis and also in virulence [24, 54, 56, 58, 59]. The many known functions of BSH are summarized in Figure 3.5. BSH is shown to regulate the peroxide sensor OhrR via *S*-thiolation under oxidative stress conditions [60]. BSH is also involved in the detoxification of RNS and electrophiles via aldehyde dehydrogenase and bacillithiol-S-conjugate amidase respectively [54]. It has also been shown that fosfomycin, methylglyoxal (MG) and formaldehyde (FA) are rendered harmless via BSH dependent-*S*-transferase [32]. Analogous to GSH, BSH has also been proposed to be involved in the chelation of zinc and copper as well as detoxification of selenite and thus potentially playing a role in metal homeostasis [32, 53, 54]. BSH has been shown to play a role in infection and virulence of clinical isolates of *S. aureus* with BSH-deficient strains showing decreased survival in infection assays [56, 61, 62].

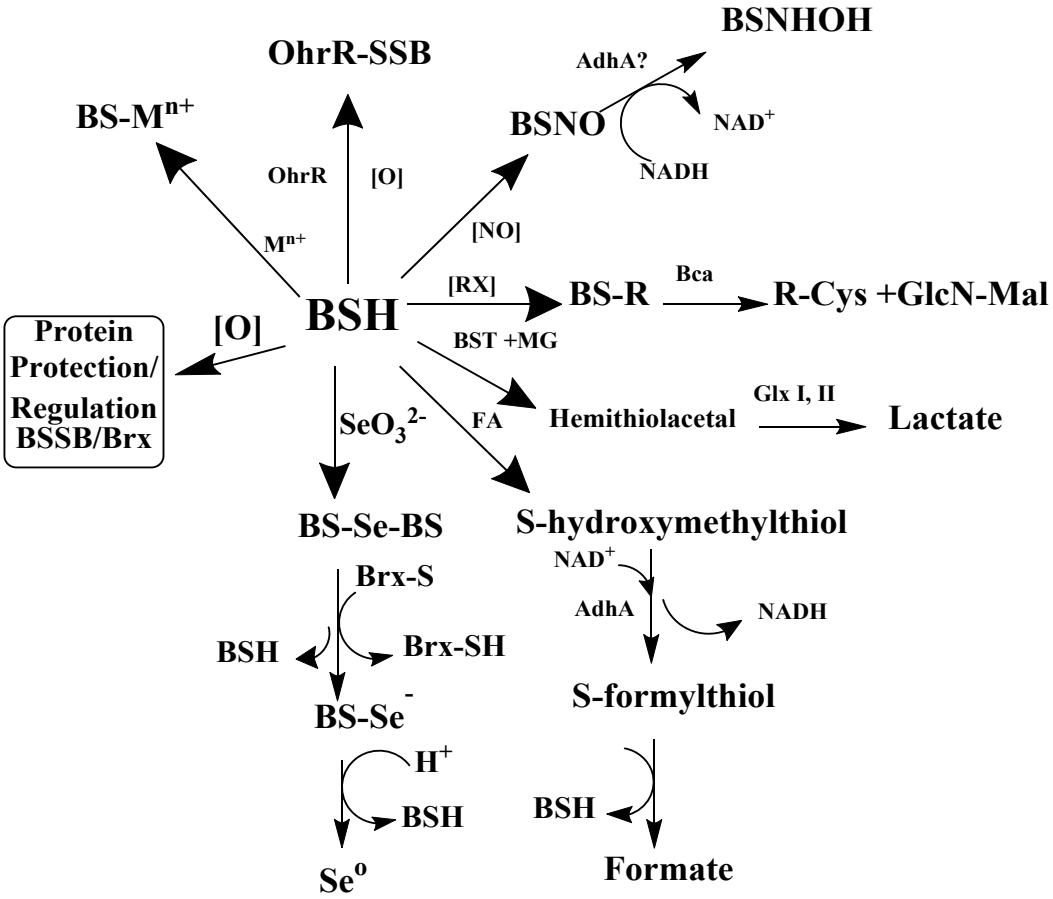


**Figure 3.5 Roles of BSH in redox-related and detoxification functions in Firmicutes. Clockwise from the top: Under oxidative stress BSH regulates the peroxide sensor OhrR through S-thiolation. BSH is also involved in the detoxification of reactive nitrogen species via BSH conjugation (BSNO). The removal of reactive electrophiles (RX) is also carried out via BSH conjugation (BS-R) using bacillithiol-S-conjugate amidase (Bca). Other harmful compounds such as fosfomycin, methylglyoxal (MG) and formaldehyde (FA) are rendered harmless by BSH dependent-S-transferase (BST). BSH has also been shown to play a role in zinc and copper chelation potentially affecting metal homeostasis. BSH reacts avidly with thiophilic metals and metalloids such as selenite which is removed by BSH conjugation. Adapted and redrawn from [32, 54].**

There is also evidence that many *Firmicutes*—including *S. aureus*—utilize BSH in *S*-thiolation of key enzymes as both a protection and regulatory mechanism [7, 24, 27, 29-31, 54, 56, 58, 59]. The manner in which bacillithiolation and debacillithiolation occurs is well established and shows similarities to that of the monothiol mechanism of *S*-glutathionylation/de-glutathionylation model system. Briefly, BSH-protected enzymes are de-bacillithiolated by bacilliredoxin proteins BrxA (YphP) or BrxB (YqiW) to form Brx-SSB mixed disulfides which are proposed to subsequently be reduced by BSH resulting in the formation of BSSB (Figure 3.6) [7, 24, 29, 54, 56, 57, 63]. However, this step remains to be experimentally confirmed. The Brx proteins are members of the TFP superfamily, although they have a shorter disulfide motif (CxC) rather than the CxxC motif seen in Grxs. Evidence shows that BrxA is able to reduce protein disulfides, albeit inefficiently with low $k_{cat}/K_M$ values (2.6–4.7 ± 0.2×$10^3$ $M^{-1}.s^{-1}$) when compared to thioredoxin or protein disulfide isomerase (11.2 ± 0.8 and 170 ± 50×$10^3$ $M^{-1}.s^{-1}$ respectively) [64]. There is no evidence that BrxB is able to directly reduce protein disulfides [57].

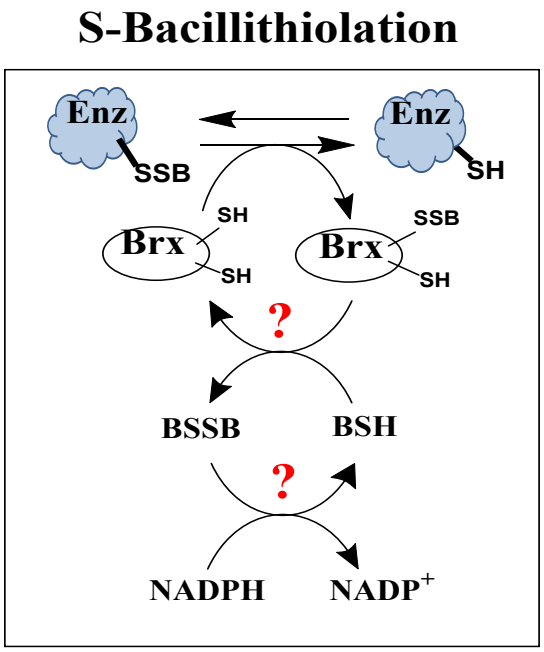


**Figure 3.6 Reversal of *S*-bacillithiolation by bacilliredoxin (Brx). The bacillithiolated protein is de-bacillithiolated by Brx, resulting in a Brx-SSB. This mixed disulfide is proposed to be reduced by BSH leading to the formation of BSSB, but this remains to be experimentally proven. It is unknown how BSSB is recycled back to BSH. All unconfirmed reactions are indicated in red. Adapted and redrawn from [29].**

As stated above, the mechanism whereby Brx-SSB is recycled back to its reduced form remains to be confirmed. Considering BSH is predominantly found in the free thiol (reduced) form, with a high BSH/BSSB ratio, suggests the presence of a BSSB reductase [53, 65]. The

current consensus candidate protein for having BSSB (bacillithiol disulfide) reductase activity is YpdA. A recent paper by Cheung and co-workers discussed the potential role of YpdA in maintaining intracellular redox homeostasis [66]. This study showed that the *ypdA* mutant caused an increase in levels of BSSB and a lower bacillithiol redox ratio compared to the isogenic parent. In addition, the YpdA over-expressing strain showed increased levels of BSH and decreasing amounts of BSSB. The YpdA protein was also purified and it was found that YpdA was able to consume NADPH and NADH in the absence of BSSB—presumably due to oxidation by $O_2$. Importantly, the authors were unable to direct demonstrate any BSSB reductase activity [66]. The potential role of YpdA in the mechanism of *S*-bacillithiolation/de-bacillithiolation therefore remains unclear, and its elucidation forms a central focus of the studies described in this chapter.

The other LMW thiol that is proposed to be involved in redox homeostasis in *S. aureus*, CoA, already plays an important role in central metabolism. However, the identification of a designated CoA disulfide reductase (CoADR) enzyme in a number of bacteria supports the analysis that CoA has role in redox homeostasis [7, 48, 49, 67-74]. Interestingly, CoA has been shown to *S*-thiolate proteins under conditions of oxidative stress to form mixed disulfide conjugated proteins [74-77]. However, it is unknown how proteins that are thiolated by CoA in this manner are returned to the free thiol form, as no CoA-specific redoxins have been identified to date (Figure 3.7 Panel A). While it may be possible that such “CoAlated” proteins (the term was coined by Gout and co-workers) could be de-thiolated by CoA itself to from CoA disulfide and the reduced protein (Figure 3.7 Panel B), this has not been demonstrated to occur experimentally. It therefore remains unclear to what extent CoA plays a role in the protection of proteins against oxidative stress.

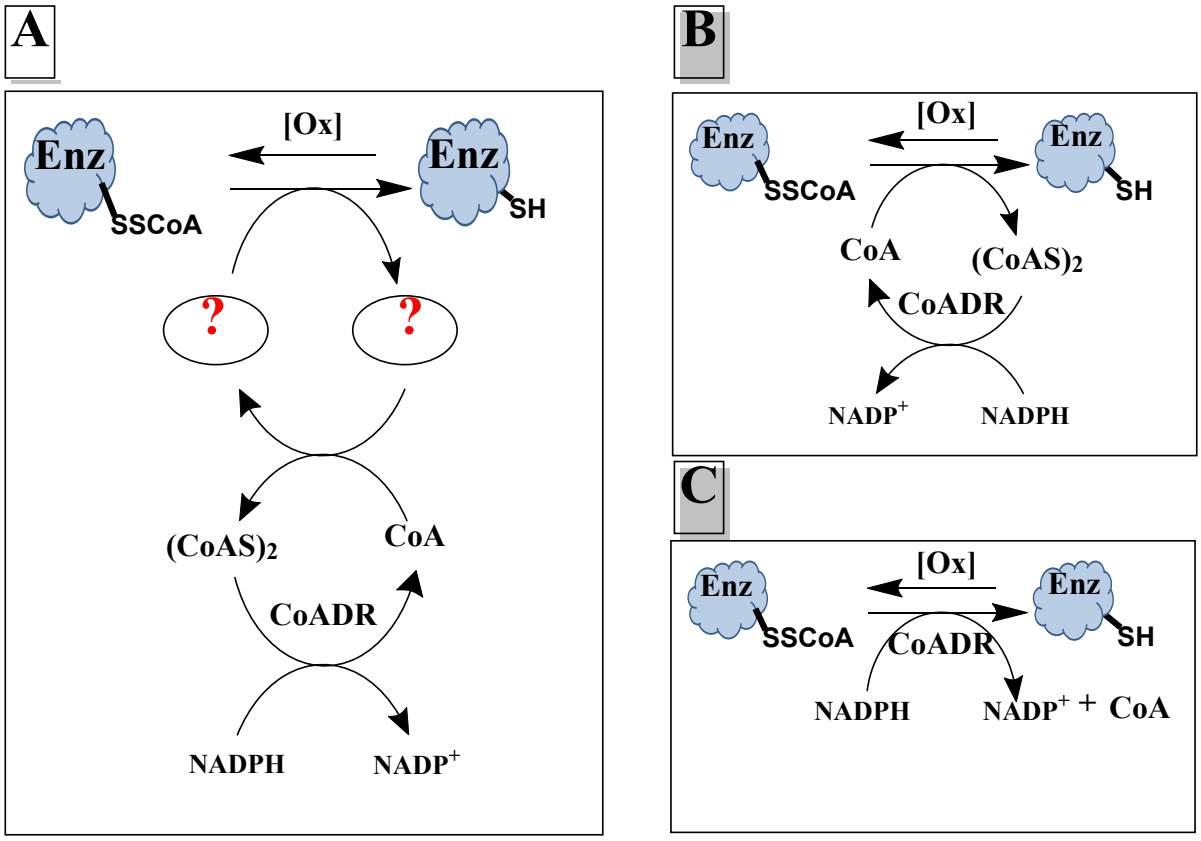


**Figure 3.7 The process of *S*-CoAlation/de-CoAlation. While the evidence of S-thiolated enzymes by CoA is clear, the mechanism of de-CoAlation is unknown (A). Since there are no CoA specific redoxins, it is possible that CoA itself is able to rescue CoAlated enzymes with the formation of $(CoAS)_2$ which would then be reduced by CoADR (B). An alternative hypothesis might be that CoADR is able to react directly with CoAlated proteins to form CoA and the free protein(C).**

In this chapter, we describe our studies that investigated the potential role of YpdA as the putative BSSB reductase in the bacillithiol/Brx pathway. We also report on a comparative analysis of the relative roles of BSH and CoA in the protection and regulation of a key metabolic enzyme in *S. aureus*. Together, these studies improve our understanding of the mechanisms that *S. aureus* uses to protect its proteins against the damage of oxidative stress, and the relative importance of BSH compared to CoA in the maintenance of redox homeostasis.

## 3.2 Results and discussion

### 3.2.1 Sequence analysis of *Sa*YpdA to other tDBDFs

YpdA was first identified by Helmann and co-workers. It is conserved among BSH-producing bacteria, including *S. aureus*, and has been proposed to function as a BSSB disulfide reductase [7, 24, 27, 31, 32, 53, 54, 56, 58, 62, 78-81]. *S. aureus* YpdA (*Sa*YpdA) shares highest sequence identity (~25-29%) to bacterial thioredoxin reductases (TrxR's) which form part of the alkylhydroperoxide reductase (AHR) subgroup of the tDBDFs [32, 54]. Two members of the AHR subgroup were previously described in chapter 1 namely, TrxR and AhpF. Members of this subgroup contain a characteristic CxxC motif that contains the two redox active cysteine residues that are critical for the catalytic mechanism in reducing the disulfide of their cognate thioredoxin-fold protein (TFP) partners via disulfide exchange. This results in oxidation of its own Cys residues, forming a disulfide which is reduced by NADPH via the flavin cofactor [13, 82-86].

A BLAST sequence homology search of *Sa*YpdA against the PDB database indeed reveals closest homology to TrxRs from a number of bacterial species, as well as to some ferredoxin $NADP^+$ oxidoreductase. Using the top hits a sequence alignment was generated using MUSCLE and ESPript with secondary elements shown based on the structure of the TrxR-like protein from *T. acidophilum* (PDB: 3CTY) (Figure 3.8). While a number of the regions are conserved for two dinucleotide binding, *Sa*YpdA lacks the conserved CxxC motif that has been shown to be essential for catalysis by AHR subgroup enzymes [13, 83, 86-88]. While *Sa*YpdA does have three Cys residues (Cys14, Cys118 and Cys287), none of these are in the location of the expected CxxC motif. Instead, a seemingly arbitrary HYFK sequence is found in its place. This indicates that *Sa*YpdA should not show any typical disulfide reductase activity. Moreover, the top hit in the PDB based on sequence homology to *Sa*YpdA is the TrxR-like enzyme from *T. acidophilum*. This protein has proven thioredoxin reductase activity, yet it is unable to use NAD(P)H as a reductant [89]. The amino acids important for NAD(P)H binding in TrxRs are found in a HRRxxxR/K motif, indicated in a green box in Figure 3.8. The TrxR-like enzyme from *T. acidophilum* lacks all the important residues of this motif, confirming that it does not use a nucleotide as reductant. However, the other TrxRs and one of the two ferredoxin $NADP^+$ oxidoreductase to which YpdA shows homology (PDB: 5YGQ) does contain the full motif, with the second ferredoxin $NADP^+$ oxidoreductase containing two of the key residues of the motif. In contrast, *Sa*YpdA has a Y**R**GGDYS sequence where the motif is expected to be found, suggesting that like the *T. acidophilum* TrxR-like protein it too has a unique reductant.

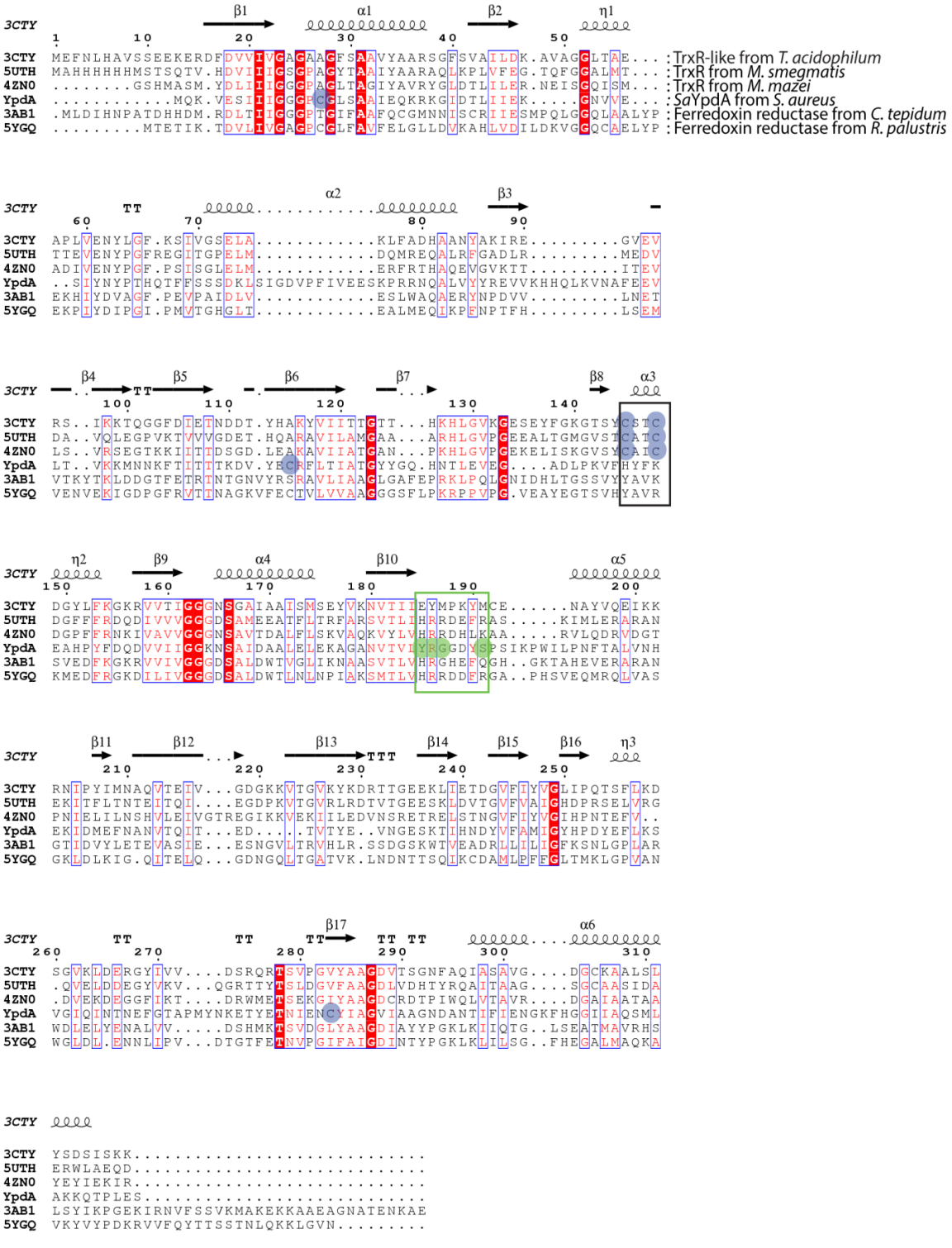


**Figure 3.8 ESPript sequence alignment of *S. aureus* YpdA (SAOUHSC_01499) against the top hits of sequence homology search against proteins in the PDB. These are TrxR proteins (3CTY, 5UTH, 4ZN0) and two ferredoxin reductases (3AB1, 5YGQ). Numbering and secondary elements shown are based on the 3CTY structure (the TrxR-like protein from *T. acidophilum*). Important structural elements are the FAD binding region that spans from residues ~20-150, the NAD(P)H binding region that spans from residues ~160-240 (residues 184-191 that are critical for NADPH binding is shown in a green box) and the CxxC motif found in many members of the AHR subgroup (residues 145-148 shown in the black box. Cys residues of the CxxC motif as well as Cys residues of *Sa*YpdA are highlighted as blue dots.**

Mechanistically, it is possible that *Sa*YpdA could bind a TFP-like protein partner like other members of the AHR subgroup, and that its flavin cofactor could reduce the TFP-based disulfide directly (i.e. without involving the usual CxxC motif as intermediary). Alternatively, one of the other Cys residues could act as an intermediary. To assess the likelihood that any of the Cys residues of *Sa*YpdA could come in close contact or are otherwise catalytically relevant, a structural model was built based on the TrxR from *S. aureus* (PDB id 4GCM). The resulting model is shown in Figure 3.9. It shows the typical Rossman folds where the FAD and NADPH (shown in blue) are expected to be bound. In the active site, the catalytic disulfides of TrxR (shown in red) are situated at the top of a helix in close proximity to the FAD cofactor (Figure 3.10). However, the corresponding sequence of *Sa*YpdA is not structurally defined. In addition, all three of its Cys resides are very far apart from one another, as well as from the FAD cofactor. Therefore, based on this model a considerable conformational change would need to occur in order for any of the Cys residues to be catalytically relevant.

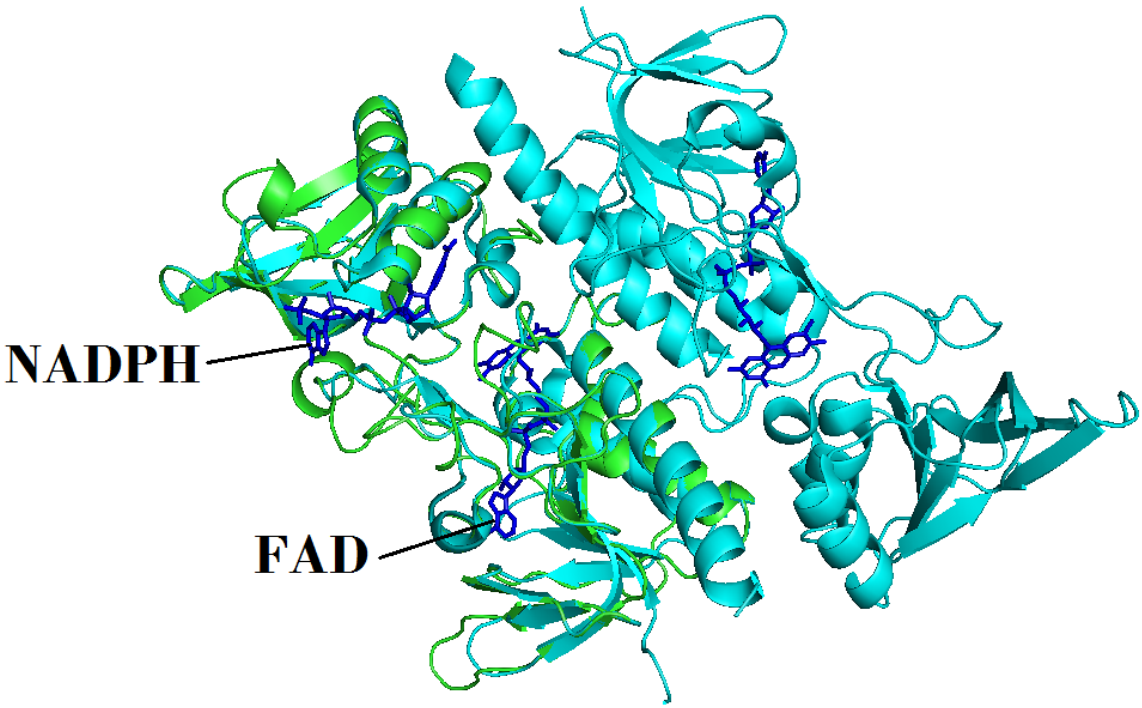


**Figure 3.9 Model_YpdA_SaTrxR (Cyan) using *Sa*TrxR (4GCM) as template (overlayed in Green). Model_YpdA_SaTrxR was built using Expasy SWISS-MODEL using *Sa*TrxR (4GCM) as template. Root-mean-square-deviation of model compared to template mean 2.11Å. Both NADPH and FAD shown in both monomers as dark blue stick structures.**

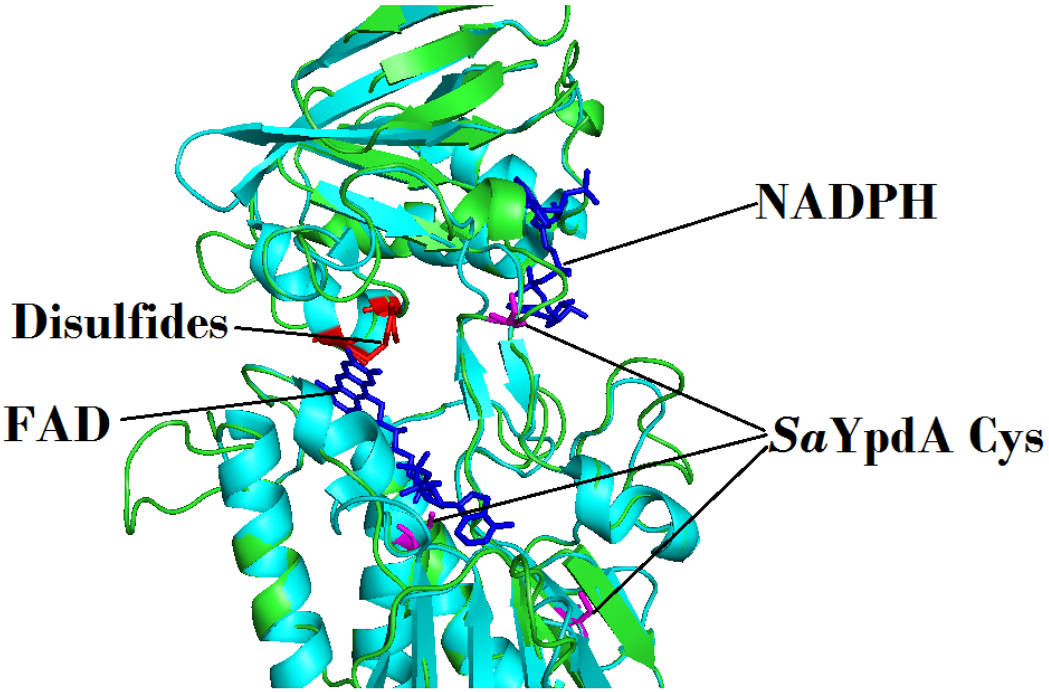


**Figure 3.10 Active site view of the one monomer of Model_YpdA_SaTrxR (Cyan) using *Sa*TrxR (4GCM) as template (Green). Both NADPH and FAD are shown in navy blue to highlight relative distance of each cofactor. The active site disulfide of *Sa*TrxR (4GCM) is shown in red. The Cys residues of *Sa*YpdA are shown in magenta.**

Importantly, it has been shown that a large conformational change does occur in bacterial TrxR protein upon Trx binding, involving a rotation of more than 67 degrees [90]. This rotation brings the NADPH within 1.4Å of the FAD cofactor. The large conformational change can be seen by comparing the structures shown Figure 3.11 and Figure 3.12. Before Trx binds NADPH is positioned approximately 16Å from the FAD, with the disulfides also buried within the protein (Figure 3.11). Upon binding of Trx, a large conformational change occurs via a rotation of the NADPH binding domain, including α-helixes 1, 2, 3) and β-sheet 1 (Figure 3.12). The α-helix 3 and β-sheet 1 twist while the disulfide swings out to interact with Trx. α-helix 1 and 2 rotate further behind the NADPH. The disordered region does not appear to undergo any significant conformational changes before and after binding of Trx.

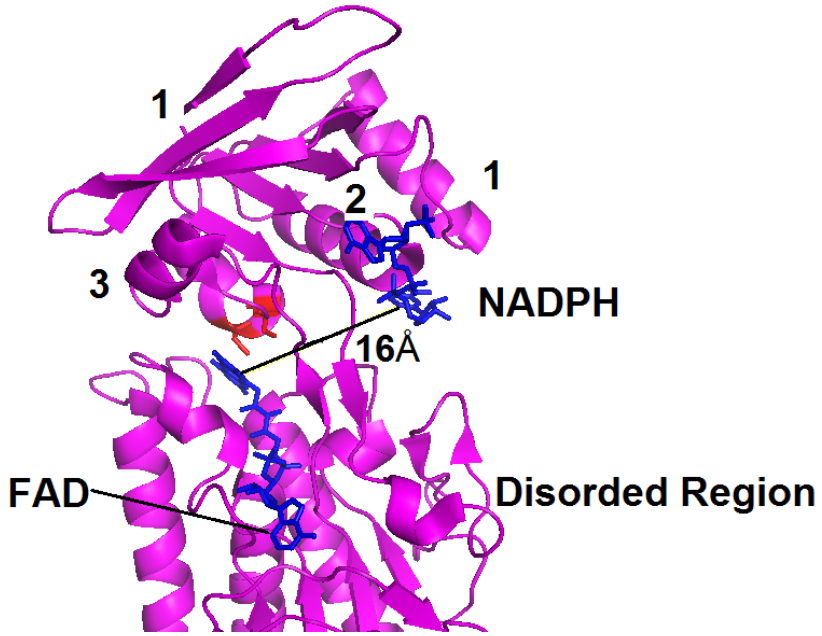


**Figure 3.11 X-ray crystal structure of *E. coli* TrxR (PDB id 1C10) showing the active site before substrate (Trx) binding. FAD and NADPH are shown in blue to highlight the large distance between the two cofactors. The disulfide CxxC motif is shown in red. α-helixes (1,2,3), β-sheet (1) and disordered region are labelled accordingly for comparison to the *Ec*TrxR after binding to substrate.**

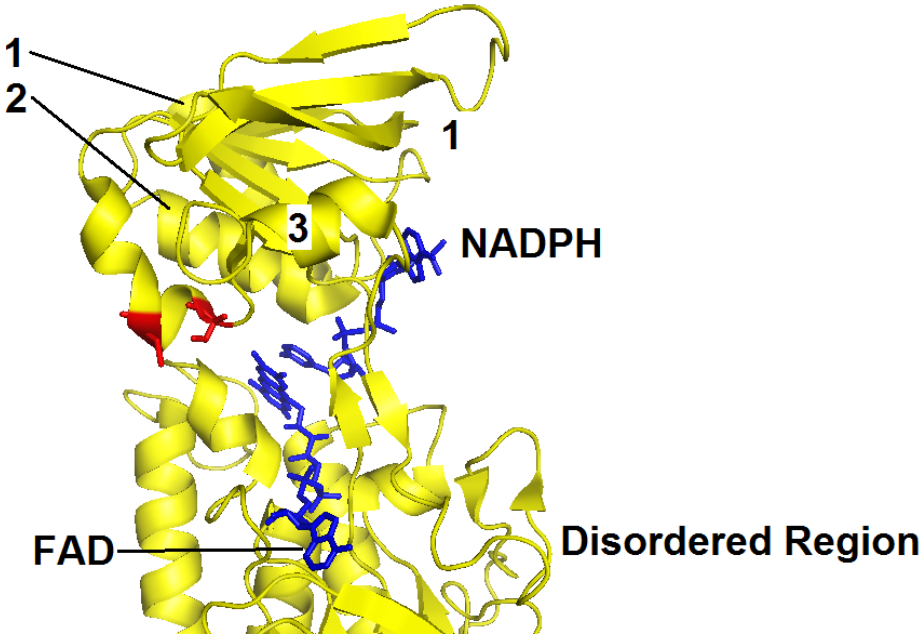


**Figure 3.12 X-ray crystal structure of *E. coli* TrxR (1F6M) showing the active site after substrate (Trx) binding. FAD and NADPH are shown in blue to highlight the distance between the two cofactors. The disulfide CxxC motif is shown in red. α-helixes (1,2,3), β-sheet (1) and disordered region are labelled accordingly for comparison to the *Ec*TrxR before binding to substrate. Trx, which would be bound to the disulfide CxxC, is omitted from this figure for clarity.**

In the *Sa*YpdA model (Figure 3.10), two of the Cys residues are found in the disordered region which does not undergo any significant changes in the *Ec*TrxR. Therefore, based on our current knowledge, and taking all the structural evidence together, it remains difficult to propose any reasonable mechanism whereby *Sa*YpdA could act as a protein or small molecule disulfide reductase. To investigate the protein biochemically, we set out to express and purify the enzyme, as well as other proteins pertinent to the study.

### 3.2.2 Protein expression and purification

Expression plasmids for *Sa*YpdA, *Sa*CoADR, *Sa*BrxB and *Sa*GAPDH were available in our laboratory or were obtained from collaborators. All plasmids were each separately transformed into *E. coli* BL21* (DE3) cells for heterologous expression of the target proteins. All proteins expressed well and were purified on an ÄKTAPrime using immobilized metal affinity chromatography (IMAC). The purified proteins were subsequently analysed by SDS-PAGE (Figure 3.13). The protein concentration was determined using the Bradford assay for GAPDH and BrxB. The enzyme concentration for *Sa*CoADR and *Sa*YpdA was determined using the FAD molar extinction coefficient (11.3 $mM^{-1}.cm^{-1}$).

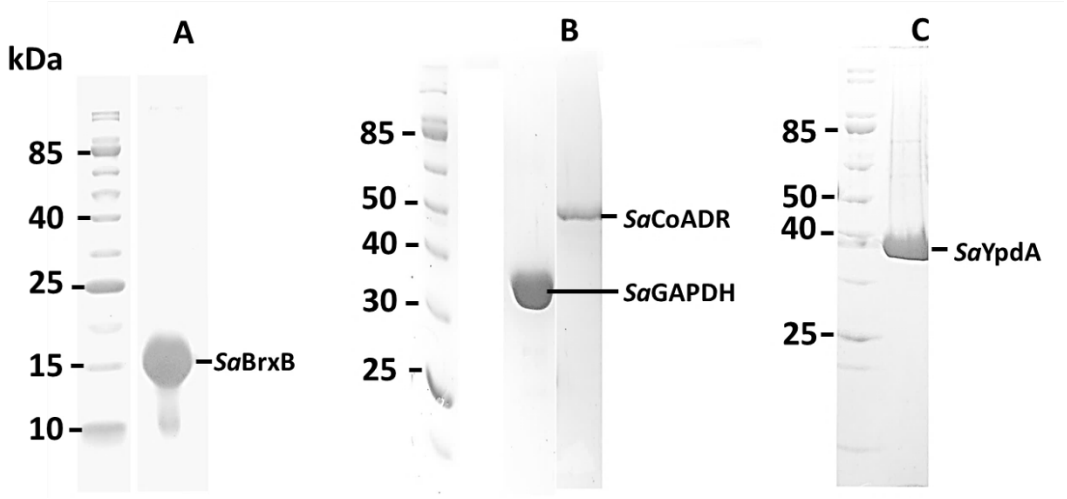


**Figure 3.13 10% SDS-PAGE gel analysis of proteins purified in this study. Gel (A) *Sa*BrxB, (B) *Sa*GAPDH and *Sa*CoADR, (C) *Sa*YpdA. Molecular weight marker shown with respective kDa increments. Lanes pertaining to other proteins not relevant to this section were omitted from each gel.**

### 3.2.3 Enzyme characterization

In light of *Sa*YpdA lacking the NADPH binding motif, an investigation into the cofactor requirement was carried out. *Sa*YpdA was titrated with either NADPH or NADH under

anaerobic conditions to exclude background effects due to reoxidation of the flavin by oxygen (Figure 3.14). This data was collected by a previous Strauss lab member [91].

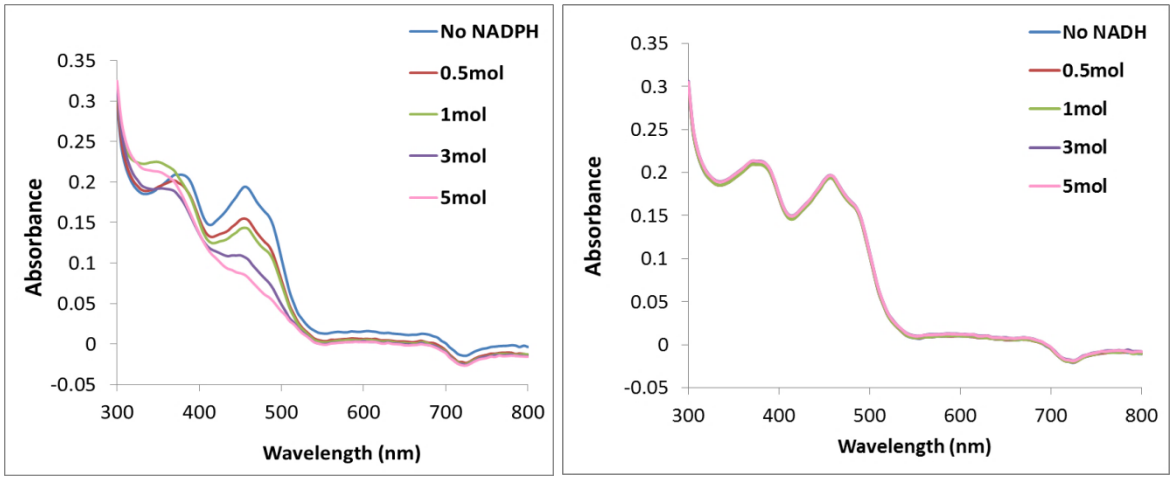


**Figure 3.14 Anaerobic titrations of *Sa*YpdA against NADPH (left spectrum) and NADH (right spectrum). The protein was titrated via sequential addition of NADPH/NADH (0.5mol) per flavin (1mol) up to an excess of 5mol. This data was previously collected [91].**

*Sa*YpdA showed a preference for NADPH over NADH with the flavin being readily reduced by NADPH (decrease of 450 nm). The recent report by Cheung and co-workers also showed that *Sa*YpdA consumed NADPH in the absence of any other substrates; however, considering that these experiments were done aerobically it is cannot be excluded that this was due to oxidation by oxygen. This is supported by their finding that *Sa*YpdA was also able to consume NADH, in contrast to our findings. These results indicate that in spite of conataining only part (GGGxxA) of the NADPH binding motif, *Sa*YpdA is still able to bind the nucleotide in a manner that leads to reduction of the flavin cofactor.

### 3.2.4 Evaluating potential protein partner/s of *Sa*YpdA

*Sa*YpdA shares highest level of sequence identity to the TrxRs from the AHR subgroup. It has been well documented that this subgroup of enzymes mainly act in conjunction with TFP partners to reduce oxidized protein disulfides. In light of this, it was evaluated whether *Sa*YpdA might require a protein partner for catalysis. Many biophysical studies, including that of TrxR and Trx, have been carried out using Glutathione-*S*-Transferase- (GST-) fusion tagged proteins in identifying potential protein partners via pull-down assays [92-94]. In these assays, the protein of interest is immobilized to a GSH affinity column via a GST-fusion tag and any potential protein partners will bind to the protein of interest. This assay is also referred to as “protein-fishing” in which potential protein partners are thus “fished” out of a complex lysate solution by passing it over the “bait” of immobilized target protein.

Pull-down experiments involved the use of purified *Sa*YpdA-GST that was used as the protein of interest or "bait" to be immobilized to GSH affinity column. Lysate was prepared by culturing *S. aureus* JE2 to exponential phase ($OD_{600}$ of 0.5), at which point the cultures were challenged with 1 mM $H_2O_2$ to elicit oxidative stress response. When bacteria are exposed to hydrogen peroxide the OxyR peroxide regulator is known to induce expression of a number of defense systems involved in counteracting oxidative stress, including AhpF, AhpC and TrxR/Trx [16, 95-97]. The lysate obtained after such treatment should therefore be enriched in proteins involved in oxidative stress resistance. After immobilizing GST-*Sa*YpdA to a GSH column, the *S. aureus* JE2 lysate was allowed to incubate with the immobilized GST-*Sa*YpdA. Thereafter any unbound protein and lysate was washed off the column, followed by elution of GST-*Sa*YpdA (and any proteins bound to it) by increasing the GSH concentration in the elution buffer. The resulting eluate was subsequently analysed by SDS-PAGE. The results of the pull-down experiments are shown in Figure 3.15. There were two other prominent bands below the GST-*Sa*YpdA (61 kDa). The lower band (26 kDa) in lane 6 and 7 is known to be GST cleaved from the tagged protein (GST-*Sa*YpdA) as cautioned in the manufacturer's guidelines. An extra band (indicated by the arrow) was observed between the GST-*Sa*YpdA and GST cleaved band in lane 6 and 7 with approximate size of 30 kDa. This band was isolated and sent for mass spectrometry (MS) identification. The MS results showed a positive identification for a fragment of *Sa*YpdA. Thus it appears that *Sa*YpdA underwent some degradation during the experiment. Nonetheless, the results provide no evidence for *Sa*YpdA having any possible protein partners (such as TFPs) other than itself under the test conditions. Furthermore, unpublished data obtained from a previous Strauss lab member showed that *Sa*YpdA was unable to reduce the *S. aureus* TFP thioredoxin A (TrxA, the cognate partner of *S. aureus* TrxR) [91]. This further indicates that *Sa*YpdA does not appear to require a protein partner for catalysis.

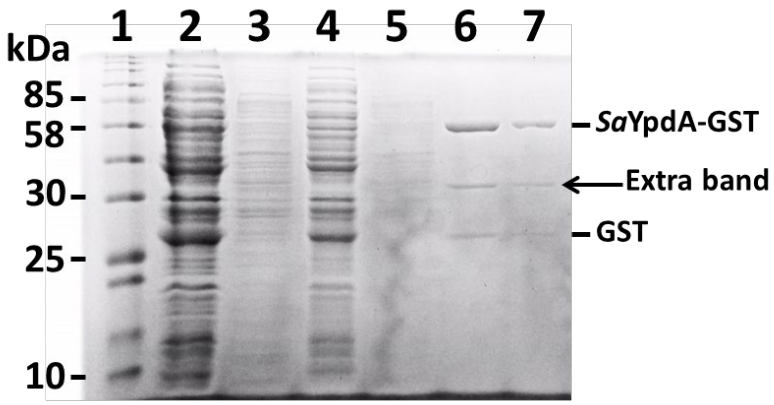


**Figure 3.15 Pull-down assay for *Sa*YpdA-GST using *S. aureus* JE2 lysate following exposure to $H_2O_2$. Lanes (1) molecular weight marker, (2) *S. aureus* JE2 lysate, (3) *S. aureus* JE2 lysate wash step 2 to remove any unbound proteins on column, (4) *S. aureus* JE2 lysate wash step 1 to remove any unbound protein, (5) *S. aureus* JE2 lysate wash step 3 to remove any unbound protein, (6-7) *Sa*YpdA-GST and any potentially bound protein partners were eluted using GSH elution buffer.**

### 3.2.5 Assessing the activity of *Sa*YpdA as BSSB reductase

As explained above, *Sa*YpdA has been hypothesized to function as a BSSB reductase by several groups [32, 54]. We therefore set out to directly determine if *Sa*YpdA could reduce BSSB. A number of different concentrations of enzyme and BSSB were used in the activity tests, which used the rate of reduction of NADPH as proxy for BBSB reductase activity. Some low levels of initial activity was observed but only at high BSSB concentrations (at 400 µM and above). Lower concentrations of BSSB showed no differences compared to the blank reaction without BSSB (Figure 3.16). However, the progress shown in panel A shows that there is in fact very little absorbance decrease (~0.06 AU, corresponding to ~ 10-15 µM NADPH) considering 400 µM BSSB was used. The initial rates of the first 15 seconds of the reaction of *Sa*YpdA acting on 400 µM BSSB, compared to several controls, are shown in panel B in triplicate. Based on these results the activity of *Sa*YpdA seems to be too low to be physiologically significant.

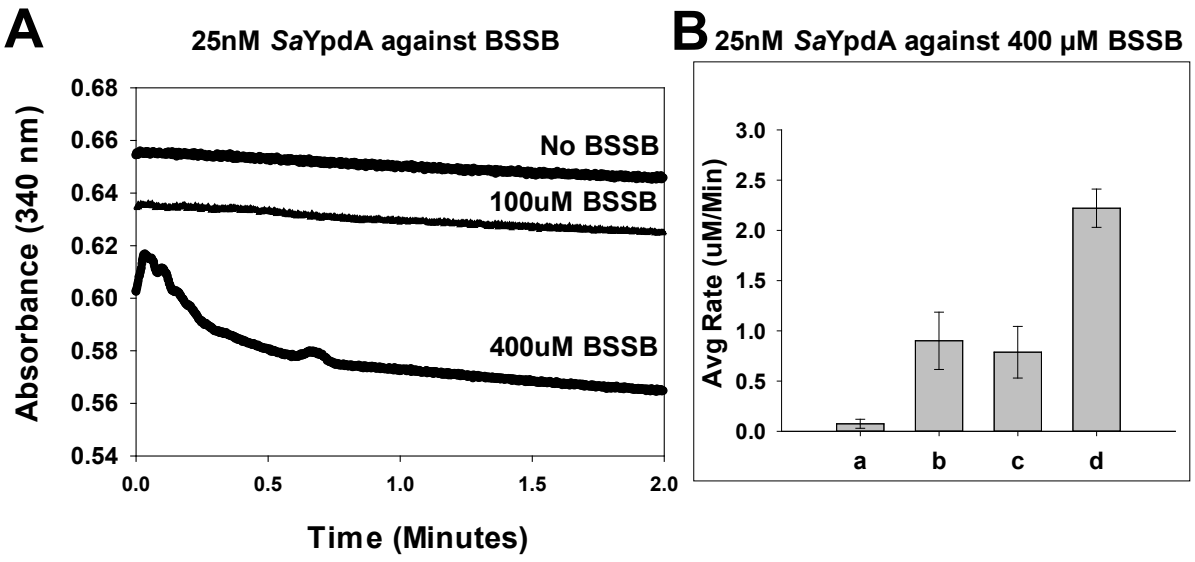


**Figure 3.16 Assessing 25 nM *Sa*YpdA's activity with BSSB as substrate. Panel A: *Sa*YpdA progress curves using BSSB at the indicated concentrations. Panel B: Average rate of *Sa*YpdA against 400 µM BSSB. (a) control reaction with 100 µM NADPH only, (b) control 25nM *Sa*YpdA+100 µM NADPH, (c) control 25nM *Sa*YpdA + 100 µM NADPH + 1mM $H_2O_2$ , (d) Reaction 25nM SaYpdA + 100 µM NADPH + 400uM BSSB. Each bar graph represents one experiment performed in triplicate. The error bars show the standard deviation.**

As mentioned in a previous section, Cheung and co-workers reported *Sa*YpdA's role as a potential BSSB reductase using a combination of genetic and biochemical experiments. [66]. While the study shows some interesting results relating to cellular/global changes in BSH/BSSB levels upon oxidative stress, the authors note that they were unable to show direct BSSB reductase activity from purified enzyme. In light of this finding, as well as the results of the current study, any evidence that *Sa*YpdA is a BSSB disulfide reductase remains elusive. We therefore set out determine if the protein could have another role within the context of BSH-based redox biology.

### 3.2.6 Establishing a model protein system for studying protein *S*-thiolation: GAPDH and BSH

A number of proteins have been shown to undergo *S*-thiolation in the cell in response to oxidative stress [24, 27, 29, 34, 35, 57, 77, 81, 98-136]. To date, a number of *S*-thiolated proteins have been identified in *Firmicutes* – these include OhrR, MetE, GuaB, Brx, GAPDH and AldA [24, 27].

Glyceraldehyde-3-phosphate (G3P) dehydrogenase (GAPDH) is a key glycolytic enzyme that catalyzes the reversible phosphorylation of G3P to 1,3-bisphosphoglycerate (1,3-BPG) in the presence of inorganic phosphate and $NAD^+$ [63]. GADPH contains a conserved redox-sensitive Cys within its active site. In *in vivo* studies GAPDH has been shown to be the most prominent target of *S*-thiolation by a number of low molecular weight thiols [34, 63, 108, 121, 122, 137-140]. Furthermore, *S*-thiolation of GAPDH by LMW thiols causes inactivation of the protein, which is only reversed upon de-thiolation. In this context, *S*-thiolation not only regulates enzyme activity, but also protects the vulnerable active site Cys from over-oxidation. GAPDH has also been found to be *S*-bacillithiolated in *S. aureus* [27, 29, 56, 63]. Antelmann and co-workers have established an *in vitro* method to study *S*-thiolation that occurs in response to oxidative stress by using GAPDH and bacilliredoxin (BrxB) as a model system [63]. Figure 3.17 shows the overall approach and experimental setup. GAPDH is first treated with excess DTT to ensure that the active site thiol is in a reduced state (1). Thereafter excess DTT is removed using a centrifugal concentrator with a membrane with MW cutoff of 3,000 Da (2). This desalted GAPDH sample is then *S*-bacillithiolated with 10-fold BSH in the presence of excess oxidant ($H_2O_2$ or HOCl). Subsequently, residual oxidant and unreacted LMW thiol is removed by again using a centrifugal concentrator as described above. *S*-bacillithiolated GAPDH is then assayed for residual GAPDH activity, or further treated with Brx prior to activity analysis to assess the reversibility of *S*-bacillithiolation (5).

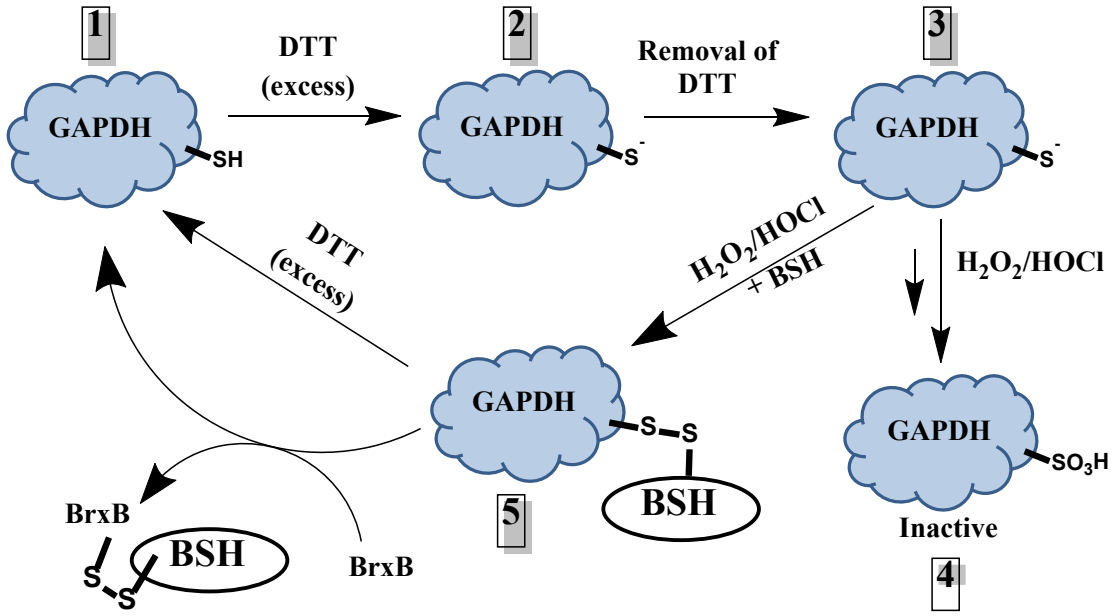


**Figure 3.17 Model system for studying *S*-thiolation based on GAPDH's thiolation by BSH. Active GAPDH is reduced with excess DTT (1), whereafter excess DTT is removed (2-3). Oxidation of GAPDH in absence of any LMW thiol results in inactive sulfonic acids (4). In the presence of BSH GAPDH is protected from over oxidation by S-thiolation, forming GAPDH-SSB (5). GAPDH-SSB has been shown to be de-bacillithiolated by the Brx system to regenerate active GAPDH (1).**

Using the above described method and approach (Figure 3.17), each reaction was assessed for GAPDH activity in the forward direction using excess G3P and $NAD^+$ in the presence sodium arsenate ($Na_3AsO_4$). Sodium arsenate was used as a co-substrate to form unstable 1-arseno-3-phosphoglycerate, which subsequently degrades forcing the GAPDH reaction in the forward direction [63].

The results of the experiment are shown in Figure 3.18. The reference reaction containing GAPDH pretreated with DTT showed full activity; as in the studies by Antelmann and co-workers was set as 100% activity [63]. DTT-pretreated GAPDH was then *S*-bacillithiolated in the presence of the two major types of biologically relevant oxidants, i.e. $H_2O_2$ and HOCl. *S*-bacillithiolated GAPDH (GAPDH-SSB, No DTT) showed no activity following treatment with either oxidant, confirming that *S*-bacillithiolation, like *S*-thiolation by many other LMW thiols, causes enzyme inactivation. The reversibility of the *S*-bacillithiolation of GAPDH was assessed using excess DTT (10 mM) as well as a previously demonstrated enzymatic mechanism that relies on bacilliredoxin (BrxB) [63]. *S*-bacillithiolated GAPDH was de-bacillithiolated by DTT (GAPDH-SSB + DTT) with GAPDH activity being restored to approximately 65%. Likewise, *S*-bacillithiolated GAPDH was de-bacillithiolated by BrxB (GAPDH-SSB + BrxB) and GAPDH activity was restored to levels similar as those following treatment with DTT. The lack of full restoration of activity (i.e. the failure to obtain 100% activity following de-bacillithiolation) after treatment with DTT and BrxB was also observed in studies by Antelmann and co-workers [63]. This suggests that under these experimental conditions some of the GAPDH enzyme is irreversibly inactivated via over-oxidation of the active site Cys to sulfonic acid.

The de-bacillithiolation of GAPDH-SSB was also evaluated using excess BSH (10 mM). BSH alone was only about half as efficient in restoring the activity of bacillithiolated GADPH (GAPDH-SSB + BSH). Finally, the ability of *Sa*YpdA to function as a bacilliredoxin was also evaluated (GAPDH-SSB + *Sa*YpdA). Interestingly, the results were similar to those obtained with BSH, with low but meaningful levels of activity restoration. This might suggest that *Sa*YpdA rather acts on mixed disulfides of BSH, rather than on BSSB.

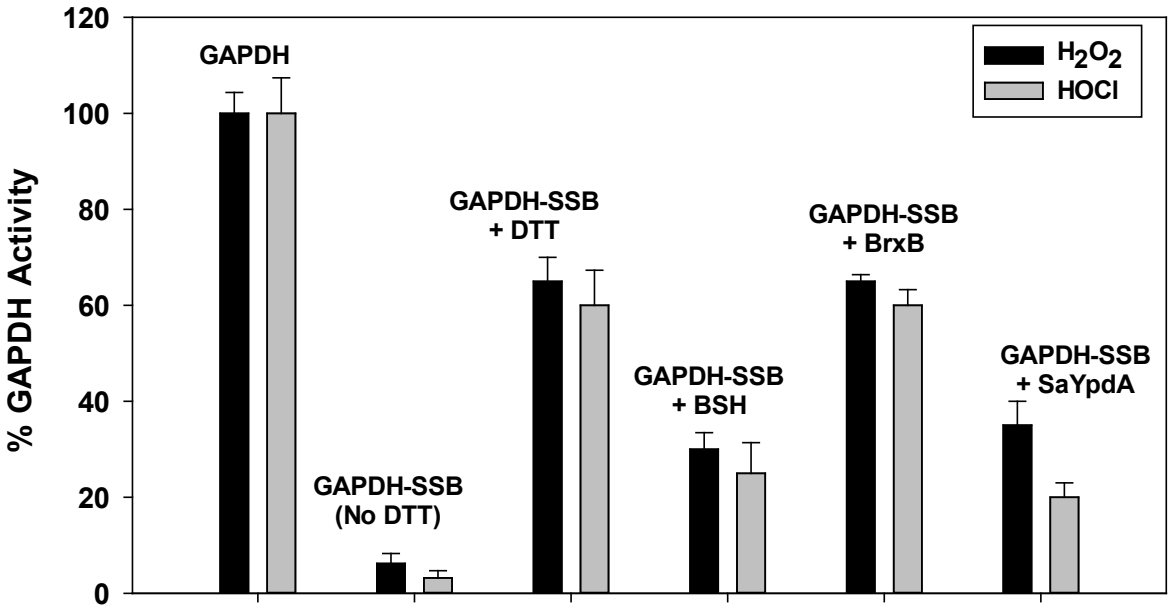


**Figure 3.18 The reversible *S*-bacilithiolation of GAPDH by BSH. GAPDH-SSB denotes *S*-bacillithiolated protein. All data is compared to the activity of untreated GAPDH as reference. GAPDH-SSB was generated *in vitro* by treatment of 40 µM GADPH with 2.5 mM $H_2O_2$ or HOCl in the presence of 400 µM BSH. For non-enzymatic de-bacillithiolation, 2.5 µM GAPDH-SSB was incubated with either 10 mM DTT or BSH for 30 min. For enzymatic de-bacillithiolation, 2.5 µM GAPDH-SSB was incubated with 12.5 µM Brx or SaYpdA proteins for 30 min. GAPDH activity was measured after addition of G3P and NAD+ by spectrophotometric monitoring of NADH generation at 340 nm [63]. Each bar graph represents one biological repeat (n=1) performed in triplicate, with the error bars denoting standard deviation.**

The results of these experiments support literature findings that *S*-bacillithiolation of GAPDH protects the enzyme from harmful over-oxidation, as well as regulating the enzyme's activity. BrxB was able to de-bacillithiolate GAPDH-SSB in line with previous literature reports [63]. The current experiments also show that excess BSH (10 mM) was able to de-bacillithiolate GADPH-SSB sufficiently to give low levels of GAPDH activity (~30%). Interestingly, *Sa*YpdA was also able to restore activity to levels similar to that seen following de-bacillithiolation by BSH. Both of these findings are new, and have not previously been reported. Importantly, the current studies still provide little insight in how Brx-SSB is recycled. Based on *Sa*YpdA's low level activity towards GAPDH-SSB, it is possible that it actually acts on Brx-SSB. Alternatively, Brx-SSB could be recycled to Brx by reaction with BSH to form BSSB, the more classically accepted route for redoxin reduction. Further studies will be needed to establish an experimental system in which these mechanistic models can be compared and evaluated.

### 3.2.7 *S*-thiolation by CoA: GAPDH and the recycling of CoA

CoA is an important cofactor that is found in all living systems and plays an important role in central metabolism [30, 47, 141-143]. There are a few documented studies that show *S*-thiolation of proteins by CoA; however the biological significance of this phenomenon still remains to be fully uncovered [74-77, 144]. Moreover, the mechanism by which proteins that are thiolated by CoA (so-called CoAlated proteins) is de-thiolated is also unclear.

To assess the role of CoA in protecting and regulating enzyme activity, the same GADPH-based model system described in the previous section was used. Briefly, GAPDH was first pretreated with DTT to ensure the active site thiol was in its reduced form. Thereafter, excess DTT was removed using a centrifugal concentrator with a membrane with a MW cutoff of 3,000 Da. *S*-CoAlation of GAPDH was achieved using 10-fold CoA in the presence of excess oxidant ($H_2O_2$ or HOCl). Thereafter, residual oxidant and unreacted LMW thiol was removed using a centrifugal concentrator as described above. Since there are no known CoA-redoxins, a number of strategies were evaluated for the de-thiolation of CoA from GAPDH-SCoA. These include the use of excess DTT, BSH and CoA. It was also investigated if BrxB could function in removing CoA from GADPH-SCoA. The results of this investigation are shown in Figure 3.19.

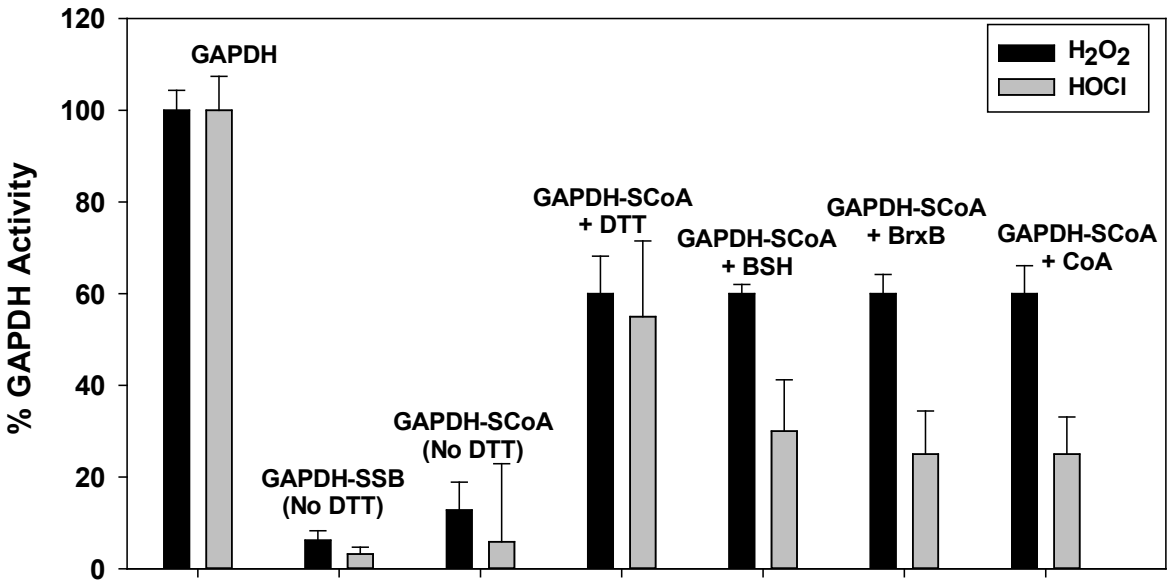


**Figure 3.19 The reversible *S*-CoAlation of GAPDH by CoA. GAPDH-SCoA denotes *S*-CoAlated protein. All activity results are compared to the activity of untreated GAPDH, which was set at 100%. GAPDH-SCoA was generated *in vitro* by treatment of 40 µM GAPDH with 2.5 mM $H_2O_2$ or HOCl in the presence of 400 µM CoA. Excess oxidant and CoA was removed using a centrifugal concentrator. For non-enzymatic de-thiolation, 2.5 µM GAPDH-SCoA was incubated with either 10 mM DTT, 10 mM BSH or 10 mM CoA for 30 min. For enzymatic de-thiolation, 2.5 µM GAPDH-SCoA was incubated with 12.5 µM Brx protein for 30 min. GAPDH activity was measured after addition of G3P and $NAD^+$ by spectrophotometric monitoring of NADH generation at 340 nm [63]. Each bar graph represents one biological repeat performed in triplicate, with the error bars denoting standard deviation.**

First and most importantly, GAPDH-SCoA was shown to be inactive, confirming the protective role that CoA may play under oxidative stress conditions. The activity of GAPDH-SCoA was restored upon non-enzymatic de-thiolation by DTT to approximately 60%, similar to what was previously seen in the BSH-based experiments. This failure to restore full activity (100%) again suggests that some GAPDH was irreversibly inactivated by the oxidants. We also examined whether the *S*-CoAlation of GAPDH can be reversed by excess CoA or BSH. Non-enzymatic de-thiolation of GAPDH-SCoA was found to be successful using both CoA and BSH, although twice as much so in the case of GAPDH-SCoA formed by pretreatment with $H_2O_2$ compared to the enzyme pretreated with HOCl. While this appears to indicate that less GAPDH-SCoA is de-thiolated when it was formed following HOCl treatment, the result could also be interpreted to show that more GAPDH is irreversibly inactivated by HOCl compared to $H_2O_2$. Indeed, it has been shown that thiol oxidation by HOCl occurs much faster than using other oxidants such as $H_2O_2$ [145, 146]. Nonetheless, the ability of CoA and BSH to act in de-thiolation reactions *in vivo* would depend on their free thiol-disulfide ratios within the cell. These findings also suggest that in the absence of an

enzymatic redoxin system, LMW thiols can provide a substitute reducing system for the de-thiolatation of protein mixed disulfides. Interestingly, the activity of GAPDH-SCoA was restored by BSH to much higher levels than observed in the previous experiment with GAPDH-SSB. This suggests that the formation of BS-SCoA mixed disulfides (the likely product of such a non-enzymatic de-thiolation reaction) is more likely than the formation of BSSB. Moreover, GAPDH-SCoA's activity was also restored using BrxB. These findings implicate a possible mechanism of de-thiolation of CoA from a protein as well as showing the non-specificity or multifaceted functions of BrxB in maintaining redox homeostasis.

Considering the lack of a specific CoA redoxin, further investigation was performed to identifying an alternative enzymatic mechanism of de-thiolation of CoA. In this regard, the CoADR enzyme has been implicated in fulfilling the role of reducing CoA disulfides [7, 48, 49, 67-72, 74, 147]. *Sa*CoADR forms part of the NADH peroxidase/oxidase and CoA-disulfide reductase (POR) subgroup of tDBDF's [48, 69, 82]. *Sa*CoADR has a unique mechanism that relies on a single Cys (Cys43) within a conserved SFXXXC motif for catalysis. This Cys thiolate attacks a single sulphur atom of the CoA-disulfide substrate, thereby displacing a molecule of CoA while forming a mixed disulfide (*Sa*CoADR-CoA). Subsequently, NADPH binds to the oxidized enzyme and reduces the mixed disulfide via the flavin cofactor, thereby regenerating the reduced enzyme as well as releasing the second CoA molecule. Interestingly, when *Sa*CoADR binds the CoA-disulfide substrate only one CoA molecule enters into the active site [48, 69, 82]. *Sa*CoADR could therefore play a role in removing CoA from CoA-thiolated proteins as the CoA portion of the *Sa*CoADR-SCoA mixed disulfide should be able to enter the enzyme's active site to form the enzyme-bound CoA mixed disulfide that is subsequently reduced by flavin. We set out to investigate such a proposal experimentally.

Using the same model system as described above, GAPDH-SCoA was generated *in vitro* using with 2.5 mM $H_2O_2$ in the presence of 400 µM CoA. Excess CoA and oxidant were removed using a centrifugal concentrator with a membrane with a 3,000 Da MW cutoff. GAPDH-SCoA was then used directly as a substrate for CoADR. The results, which indicate that GAPDH-SCoA can function as an alternate substrate of CoADR, are shown in Figure 3.20. This suggests a novel function for *Sa*CoADR in being able to reduce CoA that is attached to a protein, i.e. by acting on a CoAlated protein.

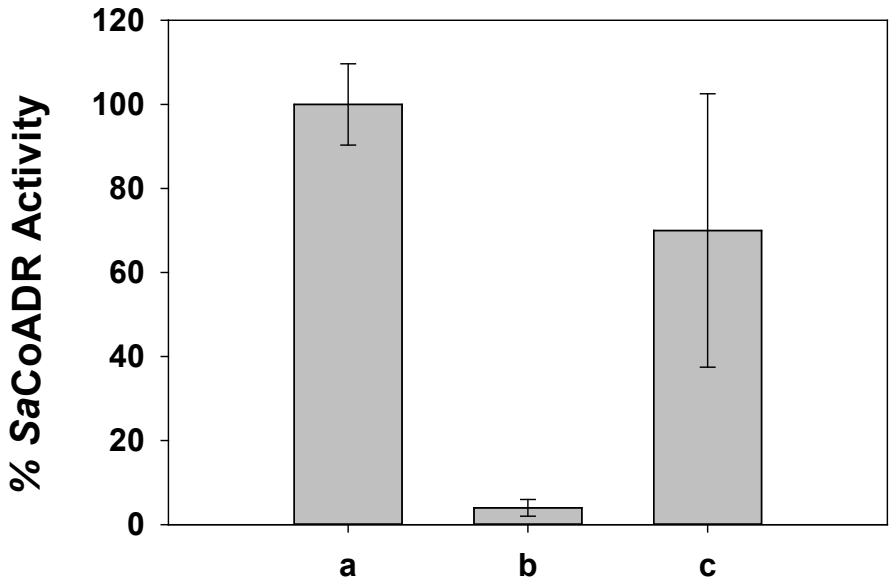


**Figure 3.20 Activity of *Sa*CoADR towards GAPDH-SCoA. (A) 25nM *Sa*CoADR + 100 µM $(CoAS)_2$ shown as 100% activity. (b) 25nM *Sa*CoADR + 100 µM GAPDH (c) 25nM *Sa*CoADR + 100 µM GAPDH-SCoA activity. Each bar graph represents one biological repeat performed in triplicate. The error bars denote standard deviation.**

## 3.3 Conclusion

*Sa*YpdA has been hypothesized to be a BSSB reductase [7, 24, 27, 31, 32, 53, 54, 56, 58, 62, 78-81]. Despite *Sa*YpdA sharing highest sequence identity to members of the AHR subgroup, it lacks the important CxxC motif critical for disulfide reductase activity. Pull-down experiments as well as direct enzymatic activity assays performed in this study did not support the hypothesis that *Sa*YpdA functions as a BSSB reductase. Recent published data on *Sa*YpdA showed interesting results relating to the change in levels of BSH/BSSB in *S. aureus* YpdA mutants; however, the authors of the study were unable to show direct biochemical evidence for BSSB reductase activity [66].

In light of these findings it was further investigated if *Sa*YpdA might play a role in the BSH system by mediating de-thiolation. This study revealed that *Sa*YpdA was able to directly act on *S*-bacillithiolated GAPDH at low activity levels. We speculate that *Sa*YpdA might also be involved in binding directly to Brx-SSB and de-thiolating Brx to recycle it in this manner. Further experiments are needed to investigate this hypothesis.

Protein *S*-thiolation by cellular LMW thiols is an important post-translational modification particularly in light of enzyme protection and regulation under oxidative stress. Using a model system based on *S. aureus* GAPDH—which is known to be regulated by *S*-thiolation— we assessed the relative importance of BSH and CoA in protecting proteins against oxidative damage by reversible *S*-thiolation. The results show that BSH indeed protects GAPDH from the adverse effects of oxidative stress in line with previous findings described in the literature [24, 32, 53, 56, 58, 62, 80, 81]. Furthermore, both DTT and *Sa*BrxB were able to reverse *S*-thiolation by BSH under conditions of oxidative stress.

CoA was also able to protect GAPDH from the effects of oxidative stress. There were clear differences in $H_2O_2$ and HOCl treatments. The *S*-thiolation of GAPDH by CoA showed similar reversibility with DTT, CoA, BSH and BrxB when it followed $H_2O_2$ treatment, but was lower following treatment with HOCl. These differences were not seen in the experiments using BSH, despite using the same experimental conditions and approach. Both BSH and CoA have similar redox potentials, i.e. -225 and -230mV respectively, while their $pK_a$s are 7.9 and 9.8 respectively. It could therefore be that under the experimental conditions CoA is less nucleophilic compared to BSH, showing less reactivity towards to thiol oxidation products formed under HOCl conditions compared to $H_2O_2$. This would lead to more GAPDH being irreversibly oxidized under the HOCl conditions when CoA is present. Literature reports also suggest that there are differences in *S*-thiolation/de-thiolation depending on the organism, enzyme isoforms and experimental conditions used [63].

Nevertheless, the *S*-thiolation of GAPDH, a key metabolic enzyme, further highlights the rationale of protein regulation and thiol protection against over oxidation. Without a protective thiol mechanism the cell would expend unnecessary energy to synthesize new protein. Furthermore, under oxidative stress, the cell would regulate GAPDH by *S*-thiolation therefore shuttling the energy requirements into the pentose phosphate pathway to supply the extra need for NADPH to reverse the imbalance in redox potential caused from such stress.

An exciting discovery of this study is the finding that *Sa*CoADR was able to de-thiolate GAPDH-SCoA. This suggests that *Sa*CoADR could act on any mixed disulfide of CoA. Further studies will need to be done in order to confirm this hypothesis. Taken together, the results of this study have provided several new and important insights regarding the LMW thiol-based redox systems of *S. aureus*.

## 3.4 Materials and methods

Unless otherwise stated, the majority of all chemicals and compounds were purchased from Sigma-Aldrich. A small amount of BSSB was kindly provided from Prof. Haike Antelmann (Institute of Biology - Microbiology. Freie Universität Berlin). Larger amounts of BSH were purchased from JEMA Biosciences, San Diego, USA. All reactions were done in triplicate unless otherwise stated or indicated in text or figures.

### 3.4.1 Cloning and plasmids used

***Sa*YpdA** - *S. aureus ypdA* gene (SAOUHSC_01499) was amplified from strain RN4220 using the following forward primer: 5'-GAG GCC GAA CAT ATG CAA AAA GTT GAA AGT-3 (NdeI site underlined) and reverse primer: 5'-GTA CAT AGA CCT CTCGAG TTA TGA TTC TAA GGG-3' (XhoI site underlined). The PCR reaction mixture included 1 µL Pfu buffer, 0.4 mM dNTP mix, 1 mM forward primer, 1 mM reverse primer, 1 ng genomic DNA, 1.25 U Pfu DNA polymerase and the final volume made up to 25 µL with distilled, deionized water. The PCR program involved a 2 minute initial step at 94°C followed by 30 cycles of denaturation at 94°C for 15 seconds. Thereafter the annealing cycle was done at 55°C for 30 seconds and a final extension cycle for 1 min at 70°C. The reaction mixtures were subjected to gel electrophoresis on a 1% agarose gel and subsequently visualized through gel staining with SYBR™ gold (Invitrogen) and viewed on a UV gel reader. The band corresponding to the expected size of the *ypdA* gene (~1200 bp) was excised and purified using a Novagen gel clean-up kit. The amplified *ypdA* gene was subsequently used to generate the pET28a-YpdA expression plasmid. Briefly, the pET28a plasmid as well as the amplified *ypdA* gene was digested separately with *NdeI* and *XhoI* (New England Biolabs) for 1 hour at 37°C without shaking. The restriction digestion mixtures of pET28a and *ypdA* gene were then subjected to gel electrophoresis on a 1% agarose gel and subsequently visualized through gel staining with SYBR™ gold (Invitrogen) and viewed on a UV gel reader. The NdeI/XhoI cut plasmid band and *ypdA* band were then excised and purified using a Novagen gel clean-up kit. Approximately 10 ng of *NdeI/XhoI* cut pET28a and *ypdA* were incubated with 10U of T4 DNA ligase and ligase buffer for 1 hour at 37°C without shaking. Thereafter 1 µL of the plasmid-insert construct was added to 80 µL of chemically-competent Mach 1 cells, and incubated on ice for 30 mins. The cell mixture was heat-shocked at 42°C for 45 seconds, and then cooled on ice for 5 mins. Approximately 900 µL of pre-warmed LB broth was added to the transformation mixture and incubated at 37°C and shaking for 1 hour. The sample was then centrifuged at 4500 RPM for 10 mins. Half of the supernatant was discarded, with the cell pellet being re-suspended in the remaining supernatant. The resuspended cells were then

plated onto LB plates containing 30 mg/L kanamycin and incubated overnight at 37°C. Colonies were then selected and restriction digestion checks were done by loading the digestion mixture onto 1% agarose gels to assess which colonies contained a plasmid that liberated a gene insert corresponding to the expected size of the *ypdA* gene. The colonies positively identified to contain inserts were then sent for sequencing to verify the identity of the insert. The correctly sequenced colonies were grown up overnight at 37°C in 5 ml LB containing 30 mg/L kanamycin. Thereafter the pET28a-*Sa*YpdA expression plasmid was isolated and purified using a Zyppy Plasmid Miniprep I Kit (Zymo Research). The plasmid was then used for transformation into respective cloning/expression cells for further use.

***Sa*YpdA-GST -** *S. aureus ypdA* was cloned into pGEX-6P-1 using BamHI and XhoI restriction sites by a previous member in the Strauss Lab. The plasmid was then used directly for transformation into respective cloning/expression cells.

***Sa*GAPDH** – The *Sa*GAPDH expression plasmid was kindly provided by Prof. Haike Antelmann (Institute of Biology - Microbiology. Freie Universität Berlin). Briefly, the *S. aureus gap* gene (SAUSA300_0756) was cloned from genomic DNA from the *S. aureus* USA300 strain into a pET11b plasmid vector with N-terminal *NdeI* and C-terminal *BamHI* sites.

***Sa*BrxB** – The *Sa*BrxB expression plasmid was kindly provided by Prof. Haike Antelmann (Institute of Biology - Microbiology. Freie Universität Berlin). The *S. aureus brxB* gene (SAUSA300_1321) was cloned from genomic DNA from *S. aureus* USA300 strain into a pET11b plasmid vector with N-terminal *NdeI* and C-terminal *BamHI* sites.

***Sa*CoADR -** A pET28a(+)-based *Sa*CoADR expression vector was available in our laboratory [147]. The *cdr* gene was cloned from genomic DNA from *S. aureus* ATCC 35556 strain and inserted into pET28a(+) flanked by N-terminal *NdeI* and C-terminal *XhoI* sites.

All plasmids were confirmed by sequencing and yielded His tag proteins.

### 3.4.1 Protein expression and purification

Each plasmid was separately transformed into *E. coli* BL21*(DE3) for protein overexpression. Overexpression was performed in LB broth supplemented with 100 mg/L ampicillin (except *Sa*CoADR and *Sa*YpdA, for which kanamycin at 30 mg/L was used instead) and grown at 37°C whilst shaking in non-baffled flasks. Once an $OD_{600nm}$ = 0.5-0.6 was reached the cultures were then induced with IPTG at a final concentration of 0.5 mM. Cultures were then continued at 37°C for 4 hours. Thereafter the cells were harvested by centrifugation at 8000 rpm.

Each cell pellet was resuspended in approximately 10 mL of sonication buffer (5 mM imidazole, 500 mM NaCl and 20 mM Tris–HCl, pH 7.9; 10 mL/1 g cell paste) and subsequently sonicated to elicit cell lysis. After centrifugation at 15 000 x g for 30 min, the crude extract (supernatant) was applied to a 0.45 µm syringe filter (AMICON) to remove any further debris. The clarified lysate was then applied to a previously prepared ($Ni^{2+}$) 1 mL HisTrapFF metal affinity purification column using an ÅKTAprime purification system. After an initial wash step of 5-10% elution buffer to remove unbound protein, the protein of interest was then eluted by increasing the imidazole concentration to 500 mM. Protein elution was monitored by UV at 280 nm on the ÄKTAPrime. Residual imidazole was then removed from the purified protein fractions and buffer exchanged using a 5 ml HiTrap Desalting column (50 mM potassium phosphate, 5 mM $MgCl_2$, pH 8.0). Thereafter a 10% SDS-PAGE gel was run for each protein purified. Protein concentration of *Sa*GAPDH and *Sa*BrxB was determined using Bradford reagent (BIO-RAD). However, for *Sa*YpdA and *Sa*CoADR the concentrations were determined using the FAD molar extinction coefficient at 450 nm (11.3 $mM^{-1}.cm^{-1}$). Molar extinction coefficients of each were determined using literature and EXPASY Protpram. Glycerol was added to the pure protein solution to a final concentration of 5%, after which the protein was aliquoted and stored at -80 °C.

### 3.4.2 Enzyme characterization – general flavin spectra of *Sa*YpdA

*Sa*YpdA was separately titrated with NADPH and NADH (0.5 – 5.0 mol NADPH per mol FAD) under anaerobic conditions at 25°C in 50 mM Tris-HCl (pH 7.5), and 150 mM NaCl. The titration was conducted in an anaerobic cuvette, sealed with a gas-tight rubber septum and repeatedly flushed with nitrogen gas. All reactants were flushed with nitrogen gas prior to titration. The reduction of the enzyme flavin by NADPH was monitored by collecting spectra from 800 nm to 240 nm on a Cary 60 UV-Vis Spectrometer (Agilent Technologies).

### 3.4.3 Assessing potential protein partner/s of *Sa*YpdA

*Sa*YpdA-GST was expressed and purified as described in protein expression and purification section.

*S. aureus* JE2 (USA300) was grown in a large batch culture (2 litres) in LB broth. After reaching an $OD_{600nm}$ = 0.5, the cells were challenged with 1 mM $H_2O_2$ every 20 minutes over an hour. After a further 2 hours growth the cells were then spun down and the pellet stored until use for pull down experiments.

Both pellets (*E. coli* expressing GST-*Sa*YpdA and *S. aureus* JE2) were freeze thawed and sonicated immediately in 10 ml of binding buffer (140 mM NaCl, 2.7 mM KCl, 10 mM

$NaHPO_4$, 1.8 mM $KH_2PO_4$, pH 7.3). The lysates were used in pull down experiments. Batch purification was done using glutathione sepharose 4B (GE Healthcare) and supplied product instructions. Briefly, GST-*Sa*YpdA was bound to the GSH resin using binding buffer, followed by incubation of resin bound GST-*Sa*YpdA with *S. aureus* JE2 lysate. The resin was washed several times with binding buffer to remove unbound proteins and finally GST-*Sa*YpdA was eluted with elution buffer (50 mM Tris-HCl, 10 mM reduced glutathione, pH 8). The eluate was collected and analysed by 10% SDS-PAGE analysis.

### 3.4.4 Assessing *Sa*YpdA as a BSSB reductase.

Each reaction consisted of 25 nM *Sa*YpdA 100 µM NADPH in 50 mM potassium phosphate buffer, pH 8. The substrate BSSB was prepared using 10 mM ammonium bicarbonate solution for each 1 mM BSH and incubated overnight at room temperature. The mixture was dried overnight using a Speedvac concentrator. The oily mixture was then made up in 50 mM potassium phosphate pH 8 to a stock concentration of 10 mM. The substrate BSSB was first placed into a quartz cuvette and the reaction initiated upon addition of reaction mixture (*Sa*YpdA pre-incubated with 100 µM NADPH) and initial rates obtained from a decrease in absorbance at 340 nm using a Cary 60 UV-Vis Spectrometer for raw data shown in Figure 3.16 A. Technical repeats using 400 µM BSSB were done using a 96-well plate setup. In all reactions the substrate (BSSB) was placed in the wells of a clear flat-bottom 96-well plate and the enzyme mixture (25 nM enzyme, 100 µM NADPH in buffer) added thereafter to initiate the reaction. Initial rates were determined following the decrease in absorbance at 340 nm using a Thermo Scientific Varioskan microplate spectrophotometer.

### 3.4.5 *Sa*GAPDH and BSH model system

Prior to each reaction 100 µM *Sa*GAPDH at a time was treated with 1 mM DTT on ice for 30 minutes. Thereafter excess DTT was removed using Amicon centrifugal concentrators with MW 3,000 Da cutoff.

All GAPDH activities were done using methods described in literature [63]. The activity was monitored spectrophotometrically in a 1 cm quartz cuvette at 340 nm and 25°C by the production of NADH. All readings were done on a Cary 60 UV-Vis Spectrometer.

**For GAPDH reaction** (DTT-treated, reduced GAPDH): The oxidation of G3P to 1,3-bisphosphoglycerate was measured in an assay mixture containing 1.25 mM $NAD^+$ and 0.25 µM GAPDH in argon-flushed 20 mM Tris-HCl, pH 8.7, with 1.25 mM ethylenediaminetetraacetic acid (EDTA) and 15 mM sodium arsenate. After pre-incubation, the reaction was initiated by the addition of 0.25 mM D,L-G3P. Sodium arsenate was used

as a co-substrate to form unstable 1-arseno-3-phosphoglycerate, which subsequently degrades forcing the reaction in the forward direction. Initial rates were determined using the linear slope of the first 30 seconds. The reaction was complete after 2 minutes. Percentage of residual GAPDH activity was calculated by comparison to the activity of the untreated enzyme [63, 148].

For **bacillithiolation reactions** - 40 µM reduced GAPDH was oxidized with 10 mM $H_2O_2$ or HOCl in the presence or absence of 10-fold excess BSH (400 µM) and incubated for 5 minutes on ice. The residual BSH, $H_2O_2$ or HOCl was removed by centrifugation through Amicon centrifugal concentrators with 3,000 Da cutoff. The resulting GAPDH-SSB, collected from the retentate, was then tested for GAPDH activity as described above.

For **de-bacillithiol reactions** (Brx reactions): 2.5 µM of GAPDH-SSB was incubated with 12.5 µM BrxB on ice for 30 minutes to allow for de-thiolation to occur. The same procedure was used to test the de-thiolation activity of 25 µM BSH, 25 µM CoA or 25 µM *Sa*YpdA by using these instead of BrxB in the same reaction setup. After completion of the 30 minute incubation, the residual GAPDH activity was measured in the presence of BrxB, BSH, CoA or YpdA measuring the forward reaction of GAPDH.

### 3.4.6 *Sa*GAPDH and CoA system

The preparation of GAPDH-SCoA *S*-thiolation as well as de-thiolation experiments involved the same procedures used with GAPDH and BSH described above.

### 3.4.7 *Sa*CoADR activity towards GAPDH-SCoA

GAPDH-SCoA was prepared as described previously. $(CoAS)_2$ was prepared according to literature [147]. All reaction buffers used for *Sa*CoADR reactions consisted of 100 µM NADPH and 100 µM substrate in 50 mM potassium phosphate at pH 7.4. Enzyme reactions were carried out at 25°C as follows: a solution containing 25 nM *Sa*CoADR, 100 µM NADPH in reaction buffer was added to a clear flat-bottom 96-well plate already containing either $(CoAS)_2$ or GAPDH-SCoA respectively. Initial rates were determined following the decrease in absorbance at 340 nm. All absorbance readings were done using a Thermo Scientific Varioskan microplate spectrophotometer.

## 3.5 References

1. Gerschman, R., et al., *Oxygen poisoning and x-irradiation: a mechanism in common.* Science, 1954. **119**(3097): p. 623-6.
2. Carlioz, A. and D. Touati, *Isolation of superoxide dismutase mutants in Escherichia coli: is superoxide dismutase necessary for aerobic life?* EMBO J, 1986. **5**(3): p. 623-30.
3. Banerjee, R., *Redox outside the box: linking extracellular redox remodeling with intracellular redox metabolism.* J Biol Chem, 2012. **287**(7): p. 4397-402.
4. Imlay, J.A., *The molecular mechanisms and physiological consequences of oxidative stress: lessons from a model bacterium.* Nat Rev Microbiol, 2013. **11**(7): p. 443-54.
5. Dahl, J.U., M.J. Gray, and U. Jakob, *Protein quality control under oxidative stress conditions.* J Mol Biol, 2015. **427**(7): p. 1549-63.
6. Poole, L.B., *The basics of thiols and cysteines in redox biology and chemistry.* Free Radic Biol Med, 2015. **80**: p. 148-57.
7. Van Laer, K., C.J. Hamilton, and J. Messens, *Low-molecular-weight thiols in thiol-disulfide exchange.* Antioxid Redox Signal, 2013. **18**(13): p. 1642-53.
8. Roos, G. and J. Messens, *Protein sulfenic acid formation: from cellular damage to redox regulation.* Free Radic Biol Med, 2011. **51**(2): p. 314-26.
9. Barron, E.S., *Thiol groups of biological importance.* Adv Enzymol Relat Subj Biochem, 1951. **11**: p. 201-66.
10. Holmgren, A., *Antioxidant function of thioredoxin and glutaredoxin systems.* Antioxid Redox Signal, 2000. **2**(4): p. 811-20.
11. Grant, C.M., *Role of the glutathione/glutaredoxin and thioredoxin systems in yeast growth and response to stress conditions.* Mol Microbiol, 2001. **39**(3): p. 533-41.
12. Holmgren, A., et al., *Thiol redox control via thioredoxin and glutaredoxin systems.* Biochem Soc Trans, 2005. **33**(Pt 6): p. 1375-7.
13. Holmgren, A., *Thioredoxin and glutaredoxin systems.* J Biol Chem, 1989. **264**(24): p. 13963-6.
14. Lillig, C.H. and A. Holmgren, *Thioredoxin and related molecules--from biology to health and disease.* Antioxid Redox Signal, 2007. **9**(1): p. 25-47.
15. Gleason, F.K. and A. Holmgren, *Thioredoxin and related proteins in procaryotes.* FEMS Microbiol Rev, 1988. **4**(4): p. 271-97.
16. Lu, J. and A. Holmgren, *The thioredoxin antioxidant system.* Free Radic Biol Med, 2014. **66**: p. 75-87.
17. Aslund, F., K.D. Berndt, and A. Holmgren, *Redox potentials of glutaredoxins and other thiol-disulfide oxidoreductases of the thioredoxin superfamily determined by direct protein-protein redox equilibria.* J Biol Chem, 1997. **272**(49): p. 30780-6.
18. Forman, H.J., H. Zhang, and A. Rinna, *Glutathione: overview of its protective roles, measurement, and biosynthesis.* Mol Aspects Med, 2009. **30**(1-2): p. 1-12.
19. Lushchak, V.I., *Glutathione homeostasis and functions: potential targets for medical interventions.* J Amino Acids, 2012. **2012**: p. 736837.

20. Masip, L., K. Veeravalli, and G. Georgiou, *The many faces of glutathione in bacteria.* Antioxid Redox Signal, 2006. **8**(5-6): p. 753-62.

21. Aquilano, K., S. Baldelli, and M.R. Ciriolo, *Glutathione: new roles in redox signaling for an old antioxidant.* Front Pharmacol, 2014. **5**: p. 196.

22. Deponte, M., *Glutathione catalysis and the reaction mechanisms of glutathione-dependent enzymes.* Biochim Biophys Acta, 2013. **1830**(5): p. 3217-66.

23. Kalinina, E.V., N.N. Chernov, and A.N. Saprin, *Involvement of thio-, peroxi-, and glutaredoxins in cellular redox-dependent processes.* Biochemistry (Mosc), 2008. **73**(13): p. 1493-510.

24. Imber, M., A.J. Pietrzyk-Brzezinska, and H. Antelmann, *Redox regulation by reversible protein S-thiolation in Gram-positive bacteria.* Redox Biol, 2019. **20**: p. 130-145.

25. Sao Emani, C., et al., *The functional interplay of low molecular weight thiols in Mycobacterium tuberculosis.* J Biomed Sci, 2018. **25**(1): p. 55.

26. Reyes, A.M., et al., *Chemistry and Redox Biology of Mycothiol.* Antioxid Redox Signal, 2018. **28**(6): p. 487-504.

27. Imber, M., A.J. Pietrzyk-Brzezinska, and H. Antelmann, *Redox regulation by reversible protein S-thiolation in Gram-positive bacteria.* Redox Biol, 2018. **20**: p. 130-145.

28. Wang, M., Q. Zhao, and W. Liu, *The versatile low-molecular-weight thiols: Beyond cell protection.* Bioessays, 2015. **37**(12): p. 1262-7.

29. Loi, V.V., M. Rossius, and H. Antelmann, *Redox regulation by reversible protein S-thiolation in bacteria.* Front Microbiol, 2015. **6**: p. 187.

30. Fahey, R.C., *Glutathione analogs in prokaryotes.* Biochim Biophys Acta, 2013. **1830**(5): p. 3182-98.

31. Sharma, S.V., et al., *Biophysical features of bacillithiol, the glutathione surrogate of Bacillus subtilis and other firmicutes.* Chembiochem, 2013. **14**(16): p. 2160-8.

32. Gaballa, A., et al., *Biosynthesis and functions of bacillithiol, a major low-molecular-weight thiol in Bacilli.* Proc Natl Acad Sci U S A, 2010. **107**(14): p. 6482-6.

33. Rogers, J.M. and E.S. Hunter, 3rd, *Redox redux: a closer look at conceptal low molecular weight thiols.* Toxicol Sci, 2001. **62**(1): p. 1-3.

34. Grant, C.M., K.A. Quinn, and I.W. Dawes, *Differential protein S-thiolation of glyceraldehyde-3-phosphate dehydrogenase isoenzymes influences sensitivity to oxidative stress.* Mol Cell Biol, 1999. **19**(4): p. 2650-6.

35. Seres, T., et al., *Protein S-thiolation and dethiolation during the respiratory burst in human monocytes. A reversible post-translational modification with potential for buffering the effects of oxidant stress.* J Immunol, 1996. **156**(5): p. 1973-80.

36. Newton, G.L., et al., *Low-molecular-weight thiols in streptomycetes and their potential role as antioxidants.* J Bacteriol, 1993. **175**(9): p. 2734-42.

37. Lillig, C.H., C. Berndt, and A. Holmgren, *Glutaredoxin systems.* Biochim Biophys Acta, 2008. **1780**(11): p. 1304-17.

38. Xiong, Y., et al., *S-glutathionylation: from molecular mechanisms to health outcomes.* Antioxid Redox Signal, 2011. **15**(1): p. 233-70.

39. Zhang, J., et al., *An evolving understanding of the S-glutathionylation cycle in pathways of redox regulation.* Free Radic Biol Med, 2018. **120**: p. 204-216.

40. Cooper, A.J., J.T. Pinto, and P.S. Callery, *Reversible and irreversible protein glutathionylation: biological and clinical aspects.* Expert Opin Drug Metab Toxicol, 2011. **7**(7): p. 891-910.

41. Iversen, R., et al., *Thiol-disulfide exchange between glutaredoxin and glutathione.* Biochemistry, 2010. **49**(4): p. 810-20.

42. Xia, B., et al., *Solution structure of Escherichia coli glutaredoxin-2 shows similarity to mammalian glutathione-S-transferases.* J Mol Biol, 2001. **310**(4): p. 907-18.

43. Kalinina, E.V., N.N. Chernov, and M.D. Novichkova, *Role of glutathione, glutathione transferase, and glutaredoxin in regulation of redox-dependent processes.* Biochemistry (Mosc), 2014. **79**(13): p. 1562-83.

44. Nikkola, M., et al., *A putative glutathione-binding site in T4 glutaredoxin investigated by site-directed mutagenesis.* J Biol Chem, 1991. **266**(24): p. 16105-12.

45. Wang, Y., et al., *Molecular mechanism of glutathione-mediated protection from oxidized low-density lipoprotein-induced cell injury in human macrophages: role of glutathione reductase and glutaredoxin.* Free Radic Biol Med, 2006. **41**(5): p. 775-85.

46. D'Ambrosio, K., et al., *Crystallization and preliminary X-ray studies of the glutaredoxin from poplar in complex with glutathione.* Acta Crystallogr D Biol Crystallogr, 2003. **59**(Pt 6): p. 1043-5.

47. Fahey, R.C., *Novel thiols of prokaryotes.* Annu Rev Microbiol, 2001. **55**: p. 333-56.

48. delCardayre, S.B. and J.E. Davies, *Staphylococcus aureus coenzyme A disulfide reductase, a new subfamily of pyridine nucleotide-disulfide oxidoreductase. Sequence, expression, and analysis of cdr.* J Biol Chem, 1998. **273**(10): p. 5752-7.

49. delCardayre, S.B., et al., *Coenzyme A disulfide reductase, the primary low molecular weight disulfide reductase from Staphylococcus aureus. Purification and characterization of the native enzyme.* J Biol Chem, 1998. **273**(10): p. 5744-51.

50. Moini, H., L. Packer, and N.E. Saris, *Antioxidant and prooxidant activities of alpha-lipoic acid and dihydrolipoic acid.* Toxicol Appl Pharmacol, 2002. **182**(1): p. 84-90.

51. Porras, P., et al., *Glutaredoxins catalyze the reduction of glutathione by dihydrolipoamide with high efficiency.* Biochem Biophys Res Commun, 2002. **295**(5): p. 1046-51.

52. de Kok, A. and W.J.H. van Berkel, *Lipoamide dehydrogenase*, in *Alpha-Keto Acid Dehydrogenase Complexes*, M.S. Patel, T.E. Roche, and R.A. Harris, Editors. 1996, Birkhäuser Basel: Basel. p. 53-70.

53. Newton, G.L., et al., *Bacillithiol is an antioxidant thiol produced in Bacilli.* Nat Chem Biol, 2009. **5**(9): p. 625-7.

54. Helmann, J.D., *Bacillithiol, a new player in bacterial redox homeostasis.* Antioxid Redox Signal, 2011. **15**(1): p. 123-33.

55. Sharma, S.V., et al., *Chemical and Chemoenzymatic syntheses of bacillithiol: a unique low-molecular-weight thiol amongst low G + C Gram-positive bacteria.* Angew Chem Int Ed Engl, 2011. **50**(31): p. 7101-4.

56. Chandrangsu, P., et al., *The Role of Bacillithiol in Gram-Positive Firmicutes.* Antioxid Redox Signal, 2018. **28**(6): p. 445-462.

57. Gaballa, A., et al., *Redox regulation in Bacillus subtilis: The bacilliredoxins BrxA(YphP) and BrxB(YqiW) function in de-bacillithiolation of S-bacillithiolated OhrR and MetE.* Antioxid Redox Signal, 2014. **21**(3): p. 357-67.

58. Perera, V.R., G.L. Newton, and K. Pogliano, *Bacillithiol: a key protective thiol in Staphylococcus aureus.* Expert Rev Anti Infect Ther, 2015. **13**(9): p. 1089-107.

59. Chandrangsu, P., et al., *Methylglyoxal resistance in Bacillus subtilis: contributions of bacillithiol-dependent and independent pathways.* Mol Microbiol, 2014. **91**(4): p. 706-15.

60. Lee, C., et al., *Redox regulation of OxyR requires specific disulfide bond formation involving a rapid kinetic reaction path.* Nat Struct Mol Biol, 2004. **11**(12): p. 1179-85.

61. Pother, D.C., et al., *Distribution and infection-related functions of bacillithiol in Staphylococcus aureus.* Int J Med Microbiol, 2013. **303**(3): p. 114-23.

62. Posada, A.C., et al., *Importance of bacillithiol in the oxidative stress response of Staphylococcus aureus.* Infect Immun, 2014. **82**(1): p. 316-32.

63. Imber, M., et al., *Protein S-Bacillithiolation Functions in Thiol Protection and Redox Regulation of the Glyceraldehyde-3-Phosphate Dehydrogenase Gap in Staphylococcus aureus Under Hypochlorite Stress.* Antioxid Redox Signal, 2018. **28**(6): p. 410-430.

64. Derewenda, U., et al., *Structure and function of Bacillus subtilis YphP, a prokaryotic disulfide isomerase with a CXC catalytic motif.* Biochemistry, 2009. **48**(36): p. 8664-71.

65. Parsonage, D., et al., *Characterization of the N-acetyl-alpha-D-glucosaminyl l-malate synthase and deacetylase functions for bacillithiol biosynthesis in Bacillus anthracis.* Biochemistry, 2010. **49**(38): p. 8398-414.

66. Mikheyeva, I.V., et al., *YpdA, a putative bacillithiol disulfide reductase, contributes to cellular redox homeostasis and virulence in Staphylococcus aureus.* Mol Microbiol, 2019.

67. Wallace, B.D., et al., *Turnover-dependent covalent inactivation of Staphylococcus aureus coenzyme A-disulfide reductase by coenzyme A-mimetics: mechanistic and structural insights.* Biochemistry, 2012. **51**(39): p. 7699-711.

68. Wallen, J.R., et al., *Pyridine nucleotide complexes with Bacillus anthracis coenzyme A-disulfide reductase: a structural analysis of dual NAD(P)H specificity.* Biochemistry, 2008. **47**(18): p. 5182-93.

69. Mallett, T.C., et al., *Structure of coenzyme A-disulfide reductase from Staphylococcus aureus at 1.54 A resolution.* Biochemistry, 2006. **45**(38): p. 11278-89.

70. Harris, D.R., et al., *Discovery and characterization of a Coenzyme A disulfide reductase from Pyrococcus horikoshii. Implications for this disulfide metabolism of anaerobic hyperthermophiles.* FEBS J, 2005. **272**(5): p. 1189-200.

71. Argyrou, A. and J.S. Blanchard, *Flavoprotein disulfide reductases: advances in chemistry and function.* Prog Nucleic Acid Res Mol Biol, 2004. **78**: p. 89-142.

72. Luba, J., V. Charrier, and A. Claiborne, *Coenzyme A-disulfide reductase from Staphylococcus aureus: evidence for asymmetric behavior on interaction with pyridine nucleotides.* Biochemistry, 1999. **38**(9): p. 2725-37.

73. Loewen, P.C., *Identification of a coenzyme A--glutathione disulfide (DSI), a modified coenzyme A disulfide (DSII), and a NADPH-dependent coenzyme A--glutathione disulfide reductase in E. coli.* Can J Biochem, 1977. **55**(10): p. 1019-27.

74. Setlow, B. and P. Setlow, *Levels of acetyl coenzyme A, reduced and oxidized coenzyme A, and coenzyme A in disulfide linkage to protein in dormant and germinated spores and growing and sporulating cells of Bacillus megaterium.* J Bacteriol, 1977. **132**(2): p. 444-52.

75. Huth, W., C. Pauli, and U. Moller, *Immunochemical detection of CoA-modified mitochondrial matrix proteins.* Biochem J, 1996. **320 ( Pt 2)**: p. 451-7.

76. Schwerdt, G., U. Moller, and W. Huth, *Identification of the CoA-modified forms of mitochondrial acetyl-CoA acetyltransferase and of glutamate dehydrogenase as nearest-neighbour proteins.* Biochem J, 1991. **280 ( Pt 2)**: p. 353-7.

77. Lee, J.W., S. Soonsanga, and J.D. Helmann, *A complex thiolate switch regulates the Bacillus subtilis organic peroxide sensor OhrR.* Proc Natl Acad Sci U S A, 2007. **104**(21): p. 8743-8.

78. Imber, M., et al., *The aldehyde dehydrogenase AldA contributes to the hypochlorite defense and is redox-controlled by protein S-bacillithiolation in Staphylococcus aureus.* Redox Biol, 2018. **15**: p. 557-568.

79. Eide, D.J., *Bacillithiol, a new role in buffering intracellular zinc.* Mol Microbiol, 2014. **94**(4): p. 743-6.

80. Chi, B.K., et al., *S-bacillithiolation protects conserved and essential proteins against hypochlorite stress in firmicutes bacteria.* Antioxid Redox Signal, 2013. **18**(11): p. 1273-95.

81. Chi, B.K., et al., *S-bacillithiolation protects against hypochlorite stress in Bacillus subtilis as revealed by transcriptomics and redox proteomics.* Mol Cell Proteomics, 2011. **10**(11): p. M111 009506.

82. Ojha, S., E.C. Meng, and P.C. Babbitt, *Evolution of function in the "two dinucleotide binding domains" flavoproteins.* PLoS Comput Biol, 2007. **3**(7): p. e121.

83. Stryer, L., A. Holmgren, and P. Reichard, *Thioredoxin. A localized conformational change accompanying reduction of the protein to the sulfhydryl form.* Biochemistry, 1967. **6**(4): p. 1016-20.

84. Holmgren, A. and F.J. Morgan, *Enzyme reduction of disulfide bonds by thioredoxin. The reactivity of disulfide bonds in human choriogonadotropin and its subunits.* Eur J Biochem, 1976. **70**(2): p. 377-83.

85. Holmgren, A., *Enzymatic reduction-oxidation of protein disulfides by thioredoxin.* Methods Enzymol, 1984. **107**: p. 295-300.

86. Holmgren, A., *Thioredoxin.* Annu Rev Biochem, 1985. **54**: p. 237-71.

87. Holmgren, A., *Thioredoxin catalyzes the reduction of insulin disulfides by dithiothreitol and dihydrolipoamide.* J Biol Chem, 1979. **254**(19): p. 9627-32.

88. Holmgren, A., *The function of thioredoxin and glutathione in deoxyribonucleic acid synthesis.* Biochem Soc Trans, 1977. **5**(3): p. 611-2.

89. Hernandez, H.H., et al., *Thioredoxin reductase from Thermoplasma acidophilum: a new twist on redox regulation.* Biochemistry, 2008. **47**(37): p. 9728-37.

90. Lennon, B.W., C.H. Williams, Jr., and M.L. Ludwig, *Twists in catalysis: alternating conformations of Escherichia coli thioredoxin reductase.* Science, 2000. **289**(5482): p. 1190-4.

91. Klopper, S.L., *Cloning and functional characterization of thiol sidulfide interchange system proteins from Staphylococcus aureus*, in *Department of Biochemistry*. 2013, Stellenbosch University: Stellenbosch. p. 90.

92. Jacob, C., et al., *Thioredoxin 2 from Escherichia coli is not involved in vivo in the recycling process of methionine sulfoxide reductase activities.* FEBS Lett, 2011. **585**(12): p. 1905-9.

93. Peng, H., et al., *Thioredoxin Profiling of Multiple Thioredoxin-Like Proteins in Staphylococcus aureus.* Front Microbiol, 2018. **9**: p. 2385.

94. Smith, D.B. and K.S. Johnson, *Single-step purification of polypeptides expressed in Escherichia coli as fusions with glutathione S-transferase.* Gene, 1988. **67**(1): p. 31-40.

95. Dukan, S. and D. Touati, *Hypochlorous acid stress in Escherichia coli: resistance, DNA damage, and comparison with hydrogen peroxide stress.* J Bacteriol, 1996. **178**(21): p. 6145-50.

96. Holmgren, A. and M. Bjornstedt, *Thioredoxin and thioredoxin reductase.* Methods Enzymol, 1995. **252**: p. 199-208.

97. Lu, J. and A. Holmgren, *Thioredoxin system in cell death progression.* Antioxid Redox Signal, 2012. **17**(12): p. 1738-47.

98. Auclair, J.R., et al., *Artifacts to avoid while taking advantage of top-down mass spectrometry based detection of protein S-thiolation.* Proteomics, 2014. **14**(10): p. 1152-7.

99. Ansong, C., et al., *Top-down proteomics reveals a unique protein S-thiolation switch in Salmonella Typhimurium in response to infection-like conditions.* Proc Natl Acad Sci U S A, 2013. **110**(25): p. 10153-8.

100. Kuzniak, E., et al., *Involvement of salicylic acid, glutathione and protein S-thiolation in plant cell death-mediated defence response of Mesembryanthemum crystallinum against Botrytis cinerea.* Plant Physiol Biochem, 2013. **63**: p. 30-8.

101. Antelmann, H. and C.J. Hamilton, *Bacterial mechanisms of reversible protein S-thiolation: structural and mechanistic insights into mycoredoxins.* Mol Microbiol, 2012. **86**(4): p. 759-64.

102. Coppo, L. and P. Ghezzi, *Thiol regulation of pro-inflammatory cytokines and innate immunity: protein S-thiolation as a novel molecular mechanism.* Biochem Soc Trans, 2011. **39**(5): p. 1268-72.

103. Chiang, B.Y., et al., *Protein S-thiolation by Glutathionylspermidine (Gsp): the role of Escherichia coli Gsp synthetASE/amidase in redox regulation.* J Biol Chem, 2010. **285**(33): p. 25345-53.

104. Liu, P., et al., *Characterization of S-thiolation on secreted proteins from E. coli by mass spectrometry.* Rapid Commun Mass Spectrom, 2009. **23**(20): p. 3343-9.

105. Ashraf, S.S., S. Galadari, and M. Patel, *Protein S-thiolation and depletion of intracellular glutathione in skin fibroblasts exposed to various sources of oxidative stress.* Environ Toxicol Pharmacol, 2006. **22**(1): p. 75-9.

106. Niture, S.K., et al., *S-thiolation mimicry: quantitative and kinetic analysis of redox status of protein cysteines by glutathione-affinity chromatography.* Arch Biochem Biophys, 2005. **444**(2): p. 174-84.

107. Eaton, P., et al., *Ischemic preconditioning: a potential role for protein S-thiolation?* Antioxid Redox Signal, 2005. **7**(7-8): p. 882-8.

108. Shenton, D. and C.M. Grant, *Protein S-thiolation targets glycolysis and protein synthesis in response to oxidative stress in the yeast Saccharomyces cerevisiae.* Biochem J, 2003. **374**(Pt 2): p. 513-9.

109. Wlodek, L. and M. Iciek, *[Protein S-thiolation as an antioxidative and regulatory mechanism].* Postepy Biochem, 2003. **49**(2): p. 77-84.

110. Shenton, D., et al., *Regulation of protein S-thiolation by glutaredoxin 5 in the yeast Saccharomyces cerevisiae.* J Biol Chem, 2002. **277**(19): p. 16853-9.

111. Del Corso, A., et al., *Physiological thiols as promoters of glutathione oxidation and modifying agents in protein S-thiolation.* Arch Biochem Biophys, 2002. **397**(2): p. 392-8.

112. Latour, I., et al., *Protein S-thiolation can mediate the inhibition of protein synthesis induced by tert-butyl hydroperoxide in isolated rat hepatocytes.* Toxicol Appl Pharmacol, 1999. **160**(1): p. 1-9.

113. Dominici, S., et al., *Redox modulation of cell surface protein thiols in U937 lymphoma cells: the role of gamma-glutamyl transpeptidase-dependent H2O2 production and S-thiolation.* Free Radic Biol Med, 1999. **27**(5-6): p. 623-35.

114. Lou, M.F., et al., *Correlation of nuclear color and opalescence with protein S-thiolation in human lenses.* Exp Eye Res, 1999. **68**(5): p. 547-52.

115. Padgett, C.M. and A.R. Whorton, *Cellular responses to nitric oxide: role of protein S-thiolation/dethiolation.* Arch Biochem Biophys, 1998. **358**(2): p. 232-42.

116. Sies, H., et al., *Protein S-thiolation and redox regulation of membrane-bound glutathione transferase.* Chem Biol Interact, 1998. **111-112**: p. 177-85.

117. Benard, O. and K.A. Balasubramanian, *Purification and properties of thioltransferase from monkey small intestinal mucosa: its role in protein-S-thiolation.* Int J Biochem Cell Biol, 1996. **28**(9): p. 1051-9.

118. Dafre, A.L., H. Sies, and T. Akerboom, *Protein S-thiolation and regulation of microsomal glutathione transferase activity by the glutathione redox couple.* Arch Biochem Biophys, 1996. **332**(2): p. 288-94.

119. Ubuka, T., *Protein disulfide isomerase-catalyzed renaturation of ribonuclease A modified by S-thiolation with glutathione and cysteine.* Biochem Mol Biol Int, 1996. **38**(6): p. 1103-10.

120. Thomas, J.A., B. Poland, and R. Honzatko, *Protein sulfhydryls and their role in the antioxidant function of protein S-thiolation.* Arch Biochem Biophys, 1995. **319**(1): p. 1-9.

121. Ravichandran, V., et al., *S-thiolation of glyceraldehyde-3-phosphate dehydrogenase induced by the phagocytosis-associated respiratory burst in blood monocytes.* J Biol Chem, 1994. **269**(40): p. 25010-5.

122. Schuppe-Koistinen, I., et al., *S-thiolation of human endothelial cell glyceraldehyde-3-phosphate dehydrogenase after hydrogen peroxide treatment.* Eur J Biochem, 1994. **221**(3): p. 1033-7.

123. Schuppe-Koistinen, I., et al., *Studies on the reversibility of protein S-thiolation in human endothelial cells.* Arch Biochem Biophys, 1994. **315**(2): p. 226-34.

124. Chai, Y.C., S. Hendrich, and J.A. Thomas, *Protein S-thiolation in hepatocytes stimulated by t-butyl hydroperoxide, menadione, and neutrophils.* Arch Biochem Biophys, 1994. **310**(1): p. 264-72.

125. Lii, C.K., et al., *S-thiolation and irreversible oxidation of sulfhydryls on carbonic anhydrase III during oxidative stress: a method for studying protein modification in intact cells and tissues.* Arch Biochem Biophys, 1994. **308**(1): p. 231-9.

126. Thomas, J.A., Y.C. Chai, and C.H. Jung, *Protein S-thiolation and dethiolation.* Methods Enzymol, 1994. **233**: p. 385-95.

127. Schuppe, I., P. Moldeus, and I.A. Cotgreave, *Protein-specific S-thiolation in human endothelial cells during oxidative stress.* Biochem Pharmacol, 1992. **44**(9): p. 1757-64.

128. Nakagawa, Y., P. Moldeus, and I.A. Cotgreave, *The S-thiolation of hepatocellular protein thiols during diquat metabolism.* Biochem Pharmacol, 1992. **43**(12): p. 2519-25.

129. Chai, Y.C., et al., *Identification of an abundant S-thiolated rat liver protein as carbonic anhydrase III; characterization of S-thiolation and dethiolation reactions.* Arch Biochem Biophys, 1991. **284**(2): p. 270-8.

130. Thomas, J.A., et al., *S-thiolation of protein sulfhydryls.* Adv Exp Med Biol, 1991. **283**: p. 95-103.

131. Rokutan, K., J.A. Thomas, and H. Sies, *Specific S-thiolation of a 30-kDa cytosolic protein from rat liver under oxidative stress.* Eur J Biochem, 1989. **179**(1): p. 233-9.

132. Thomas, J.A. and E.M. Park, *Oxy radical-initiated protein S-thiolation and enzymic dethiolation.* Basic Life Sci, 1988. **49**: p. 365-8.

133. Sies, H., R. Brigelius, and P. Graf, *Hormones, glutathione status and protein S-thiolation.* Adv Enzyme Regul, 1987. **26**: p. 175-89.

134. Thomas, J.A. and D. Beidler, *A thin-gel isoelectric focusing method for quantitation of protein S-thiolation.* Anal Biochem, 1986. **157**(1): p. 32-8.

135. Collison, M.W., et al., *A comparison of protein S-thiolation (protein mixed-disulfide formation) in heart cells treated with t-butyl hydroperoxide or diamide.* Biochim Biophys Acta, 1986. **885**(1): p. 58-67.

136. Grimm, L.M., et al., *Protein mixed-disulfides in cardiac cells. S-thiolation of soluble proteins in response to diamide.* Biochim Biophys Acta, 1985. **844**(1): p. 50-4.

137. Groitl, B. and U. Jakob, *Thiol-based redox switches.* Biochim Biophys Acta, 2014. **1844**(8): p. 1335-43.

138. Brandes, N., S. Schmitt, and U. Jakob, *Thiol-based redox switches in eukaryotic proteins.* Antioxid Redox Signal, 2009. **11**(5): p. 997-1014.

139. Bedhomme, M., et al., *Glutathionylation of cytosolic glyceraldehyde-3-phosphate dehydrogenase from the model plant Arabidopsis thaliana is reversed by both glutaredoxins and thioredoxins in vitro.* Biochem J, 2012. **445**(3): p. 337-47.

140. Hildebrandt, T., et al., *Cytosolic thiol switches regulating basic cellular functions: GAPDH as an information hub?* Biol Chem, 2015. **396**(5): p. 523-37.

141. Leonardi, R., et al., *Coenzyme A: back in action.* Prog Lipid Res, 2005. **44**(2-3): p. 125-53.

142. Begley, T.P., C. Kinsland, and E. Strauss, *The biosynthesis of coenzyme A in bacteria.* Vitam Horm, 2001. **61**: p. 157-71.

143. Srinivasan, B. and O.C. Sibon, *Coenzyme A, more than 'just' a metabolic cofactor.* Biochem Soc Trans, 2014. **42**(4): p. 1075-9.

144. Tsuchiya, Y., et al., *Protein CoAlation and antioxidant function of coenzyme A in prokaryotic cells.* Biochem J, 2018. **475**(11): p. 1909-1937.

145. Peskin, A.V. and C.C. Winterbourn, *Kinetics of the reactions of hypochlorous acid and amino acid chloramines with thiols, methionine, and ascorbate.* Free Radic Biol Med, 2001. **30**(5): p. 572-9.

146. Barton, J.P., J.E. Packer, and R.J. Sims, *Kinetics of the reaction of hydrogen peroxide with cysteine and cysteamine.* Journal of Chemical Society, Perkin Transactions 2, 1973(11): p. 1547-1549

147. van der Westhuyzen, R. and E. Strauss, *Michael acceptor-containing coenzyme A analogues as inhibitors of the atypical coenzyme A disulfide reductase from Staphylococcus aureus.* J Am Chem Soc, 2010. **132**(37): p. 12853-5.

148. Peralta, D., et al., *A proton relay enhances H2O2 sensitivity of GAPDH to facilitate metabolic adaptation.* Nat Chem Biol, 2015. **11**(2): p. 156-63.

*Chapter 4*

# EFFORTS TOWARDS THE CHEMOENZYMATIC PRODUCTION OF BACILLITHIOL (BSH)

## 4.1 Introduction

Many organisms produce cysteine derived low-molecular weight (LMW) thiols which play a role as cofactors and as cysteine reservoirs, as well as in redox homeostasis and enzyme protection and regulation [1-3]. The most well-known LMW thiol is glutathione (GSH) which is the predominant thiol in eukaryotes; however, many organisms lack glutathione and therefore employ surrogate LMW thiols [1]. Gram-positive bacteria with GC rich genomes such as *Actinobacteria* lack GSH and make use of mycothiol (MSH) as their predominant LMW thiol [4-6]. Other Gram-positive bacteria with low GC content genomes such as *Firmicutes* make use of the LMW thiols coenzyme A (CoA) and bacillithiol (BSH) (Figure 4.1) [2, 7-9]. In other organisms, specialized LMW thiols such as ergothioneine, trypanothione, γ-GC or ovothiol are employed.

Initially the major LMW thiol in *Staphylococcus aureus*—which lacks GSH—was assumed to be either Cys or CoA. However, neither of these thiol species are present at levels similar to those seen for GSH in GSH-producing organisms [7, 10]. Instead, it is now accepted that the major LMW thiol produced by *Firmicutes* bacteria is BSH. BSH was discovered just over 10 years ago and has been implicated in a number of functions analogous to GSH [2, 7-9, 11]. The many roles of BSH include the reduction of SNO compounds, the removal of toxic compounds (e.g. fosfomycin, methylgloxal), acting as a potential virulence factor, and maintaining metal homeostasis and protecting and regulating proteins through *S*-bacilithiolation [1, 2, 7, 9, 12-24].

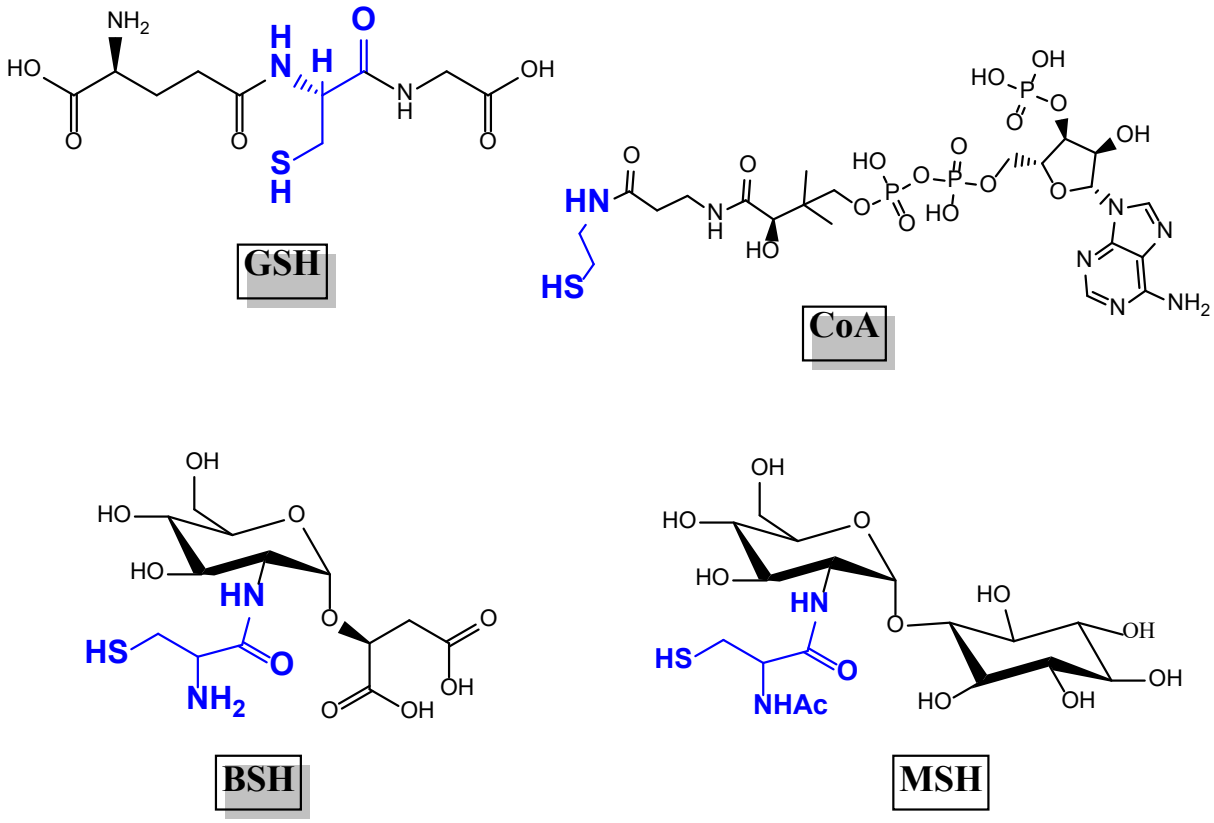


**Figure 4.1 Major LWW thiol compounds found in bacteria. Glutathione (GSH, also found in eukaryotes and Gram-negative bacteria), coenzyme A (CoA, found in all organisms), bacillithiol (BSH, found in *Firmicutes) and* mycothiol (MSH, found in *Actinomycetes*). Redrawn from [2].**

The genes involved in BSH biosynthesis have been identified in several *Bacilli* species by homology to the enzymes involved in MSH biosynthesis, and by using the EMBL String web-based tool [8, 25]. The String web-based tool identifies interacting partners of a protein query utilizing a number of criteria including co-localization in genomes via operon structural similarities, co-occurrence across genomes via phylogenomic profiling, correlated experimental data and published literature [25]. The network of BSH associated and interacting partners is shown in (Figure 4.2). A number of other genes were identified to have some association with BSH biosynthesis, including *panE* and *coaX* which are involved in pantothenate biosynthesis. Some genes associated with BSH biosynthesis do not have an assigned function [8].

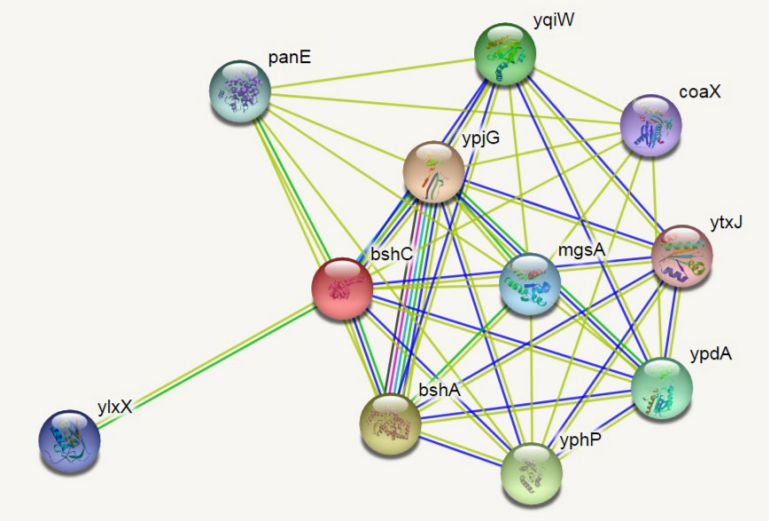


**Figure 4.2 EMBL STRING interaction network of proteins that have an associated function with BSH biosynthesis. Green lines indicate co-localization of operon structures, blue lines indicate statistically significant co-occurrence across multiple genomes, pink lines indicate experimentally determined, and aqua lines indicated published literature.**

Structurally, BSH shares some resemblance to the scaffold of MSH, with the most noticeable differences being the replacement of the inositol group by L-malate. Additionally, the amine of its cysteine moiety is not acetylated. The biosynthesis of BSH also follows similarities to MSH (Figure 4.3).The biosynthesis of BSH is carried out in three steps with the first reaction catalyzed by BshA involving the coupling of L-malate to glucosamine via the donor UDP-N-acetylglucosamine (UDP-GlcNAc) to form GlcNAc-Mal (Figure 4.3A). The second enzyme BshB hydrolyzes the GlcNAc acetyl group resulting in GlcN-Mal. The final step involves the coupling of cysteine via its carboxyl to the free amine of glucosamine to form BSH; this is catalyzed by BshC.

The biosynthesis of MSH (Figure 4.3 B) follows a similar sequence of reactions in which MshA couples 1-myo-inositol-1-phosphate to the glucosamine donor UDP-GlcNAc to form GlcNAc-Ins-P, which is subsequently dephosphorylated by MshA2 to form the first major intermediate of the pathway, GlcNAc-Ins. MshB then hydrolyzes the acetyl group of GlcNAc resulting in GlcN-Ins. A cysteine is added via its carboxyl group to GlcN-Ins by MshC to form Cys-GlcN-Ins. The final step in the biosynthesis of MSH includes acetylation of the amino group of cysteine using acetyl-CoA and MshD.

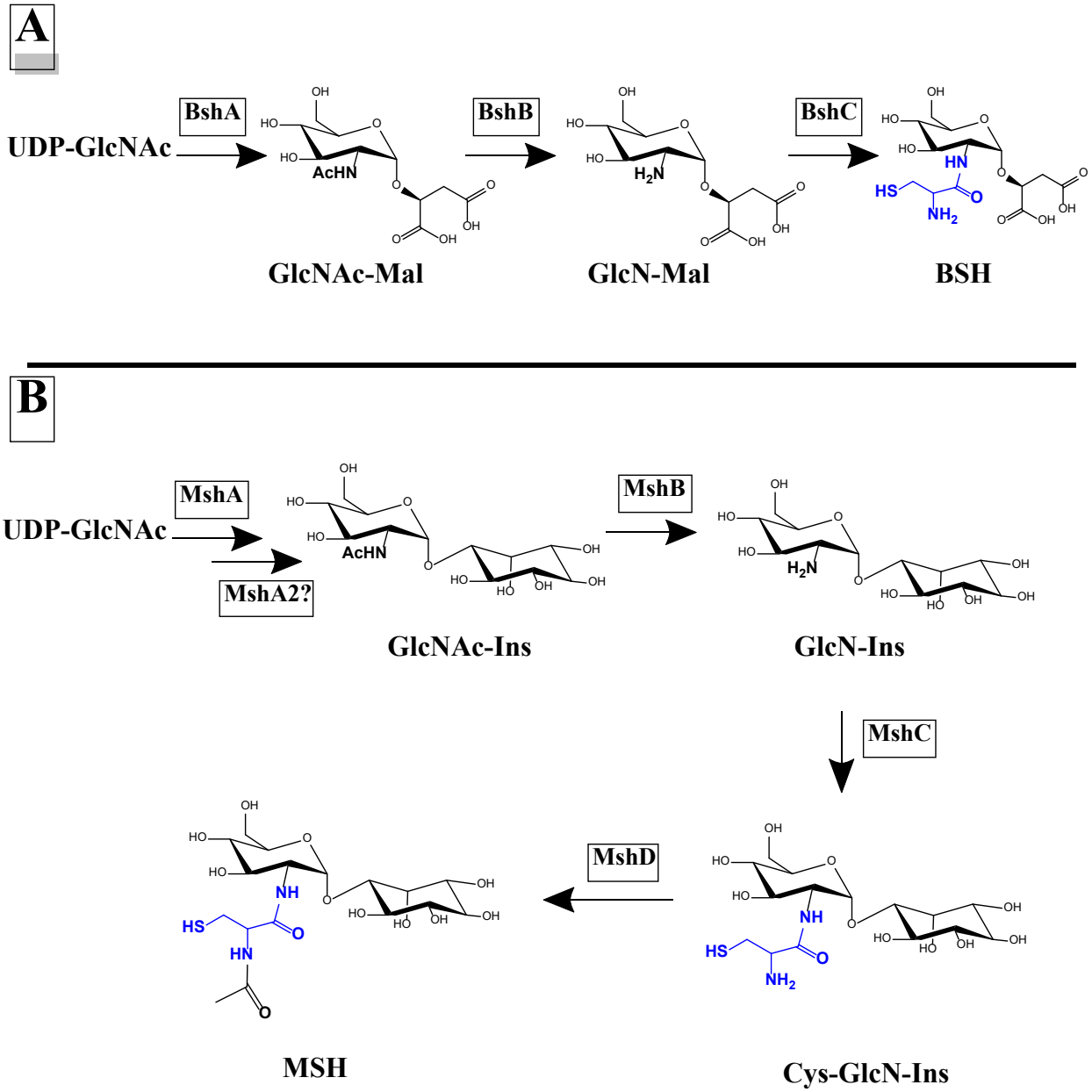


**Figure 4.3 Biosynthetic pathways for BSH and MSH. (A) Biosynthesis of BSH begins with the coupling of L-malic acid to GlcNAc via BshA (L-malic acid glycosyltransferase) to GlcNAc-Mal. Thereafter the GlcNAc-Mal is deacetylated by BshB (an N-acetyl hydrolase) to form GlcN-Mal. The final step involves the addition of a cysteine via BshC (cysteine adding enzyme). (B) The biosynthesis of MSH follows a similar pathway with the exception of two additional steps. A dephosphorylation step occurs after the initial coupling which is hypothesized to be carried out by MshA2. An additional acetylation after the addition of cysteine is carried out by MshD. Redrawn from [7].**

Some of the enzymes involved in the biosynthesis of BSH have already been studied (Figure 4.4). Initially five candidate genes were classified to encode for the glycosyltransferase BshA, which is involved in coupling UDP-GlcNAc and L-malate. However, only one of these genes—*ypjH*—shared some similarity to MshA (~20% identity). The glycosyltransferase activity of the YpjH protein was confirmed using purified enzyme and substrates UDP-

GlcNAc and L-malate [8]. Furthermore, *ypjH* null mutants produced very little GlcNAc-Mal and BSH confirming that *ypjH* indeed encodes for BshA, and that it is essential for BSH biosynthesis [8]. Interestingly, despite BshA and MshA sharing low identity their active site architecture is still conserved. However, their N-terminal regions differ, most likely due to the difference in binding malate versus inositol functional moieties respectively. Upstream of *bshA* are two zinc-dependent deacetylases, *ypjG* (encoding BshB1) and *yojG* (encoding BshB2). A *bshB1* null mutant showed a 2-fold decrease in BSH production; whilst a *bshB2* null mutant showed normal BSH levels. However, in a double *bshB1*/*bshB2* mutant BSH levels were undetectable [8]. The zinc-dependent deacetylase activity has been demonstrated for both BshB1 and BshB2; however, BshB1 appears to play the major role in BSH biosynthesis [8, 9].

The last enzyme in the BSH pathway involves a cysteine-adding enzyme named BshC. The gene encoding for BshC, originally annotated as *yllA*, was identified using the String web-based tool that showed it was co-localized with *bshA* and *bshB* in the majority of BSH producing organisms. The protein sequence of BshC shows no recognizable domains and has no appreciable similarity to MshC, which also performs the ATP-dependent addition of cysteine to GlcN-Ins in MSH biosynthesis [8, 26]. Further confirmation of BshC's involvement in BSH biosynthesis was determined using *bshC* null mutants which showed an accumulation of GlcNAc-Mal and undetectable levels of BSH compared to the wildtype. Complementation of *bshC* restored BSH biosynthesis [8]. Enzyme activity studies using purified BshC under conditions similar to MshC have shown no activity [7, 8, 27-31]. Thus it appears that BshC might function via a different mechanism than that of MshC.

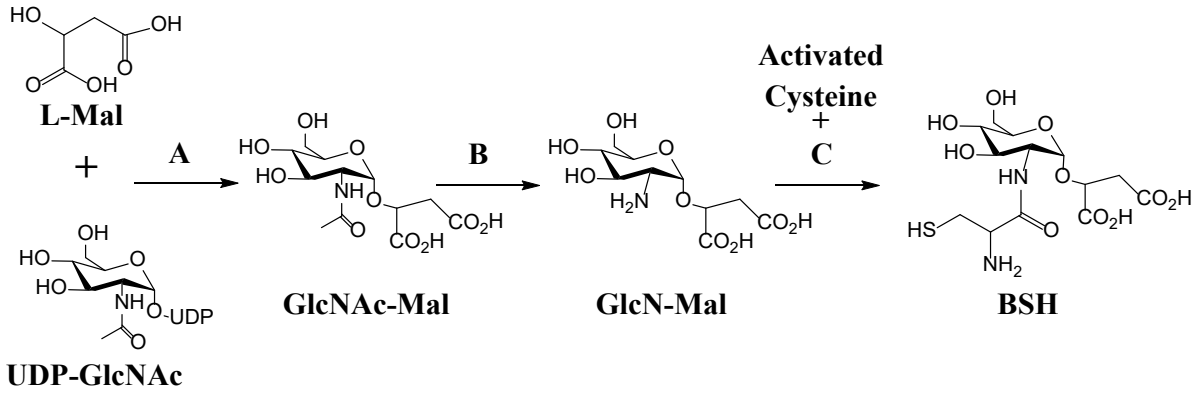


**Figure 4.4 Biosynthesis of bacillithiol (BSH). Enzymes involved in each reaction: (A) Coupling of UDP-GlcNAc to L-malate by glycosyltransferase BshA, (B) *N*-acetyl hydrolase BshB and (C) cysteine adding enzyme BshC.**

To date there are three X-ray crystal structures reported of the enzymes involved in BSH biosynthesis, namely those of *B. subtilis* BshA (PDB: 5D01), *B. cereus* BshB (PDB: 2IXD) and *B. subtilis* BshC (PDB: 4WBD). The structure of BshA shows characteristic features of glycosyltransferases which include the GT-B fold, consisting of two "Rossmann-like" beta/alpha/beta domains separated by a deep inter-domain region with a kinked C-terminal α-helix that crosses over from the C-terminal domain to contact the N-terminal domain [29, 32]. The X-ray crystal structure of BshA also contains the product GlcNAc-Mal bound to the active site. BshB, like other zinc-dependent deacetylases such as MshB and LpxC, form part of the LmbE-like metalloenzyme family that contains a conserved PIG-L (N-acetyl-d-glucosaminylphosphatidylinositol deacetylase) structural domain. These enzymes utilize an essential metal ion/s in the hydrolysis of various substrates that contain an *N*-acetylglucosamine core. The structure of BshB contains an acetate and zinc ion coordinated in the active site [31, 33, 34]. Kinetic studies of BshB show that zinc is essential for the enzyme's activity [8, 31]. The crystal structure of the last enzyme in the BSH biosynthetic pathway BshC contains glycerol and citrate within the active site as well as an ADP moiety bound in a second binding pocket [30]. The structure of BshC (Figure 4.5) provides some clues as to the potential binding mode of the GlcN-Mal, as well as some unexpected results that may provide insight into the lack of activity of BshC. The active site is formed within a Rossman fold where the two carboxylate groups of the bound citrate molecule interact with protein side chains, which might suggest the potential binding of the carboxylates of the malyl moiety of either GlcN-Mal or the BSH product. The remaining carboxylate of the citrate molecule extends into a solvent filled pocket. A glycerol molecule was also found to be bound near the active site citrate in a separate pocket. The active site is also solvent exposed and would appear to accommodate ligands larger than citrate and glycerol (Figure 4.6). Interestingly the two homodimers interact with one another via a 4-helix bundle, with no direct interaction between the domains bearing the active sites.

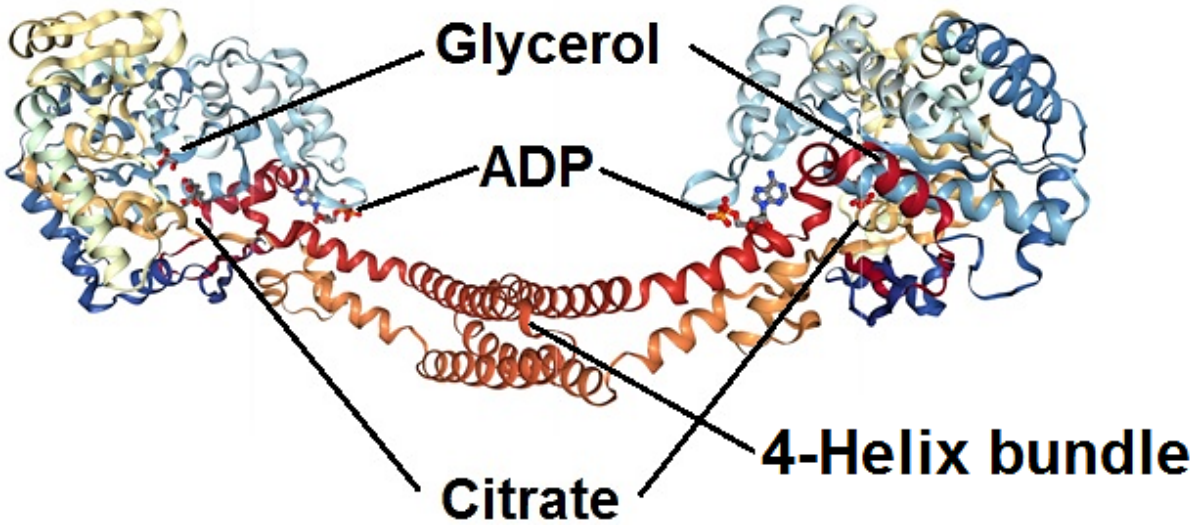


**Figure 4.5 X-ray crystal structure of *Bs*BshC (4WBD) homodimer. Location of glycerol, ADP and citrate are indicated. Red/orange coiled-coils show 4-helix bundle connecting the two homodimers. Light blue/shy blue indicates the core Rossman fold of BshC. Dark blue and light yellow/straw indicate coiled-coiled domains found in a number of BshC orthologs. [30].**

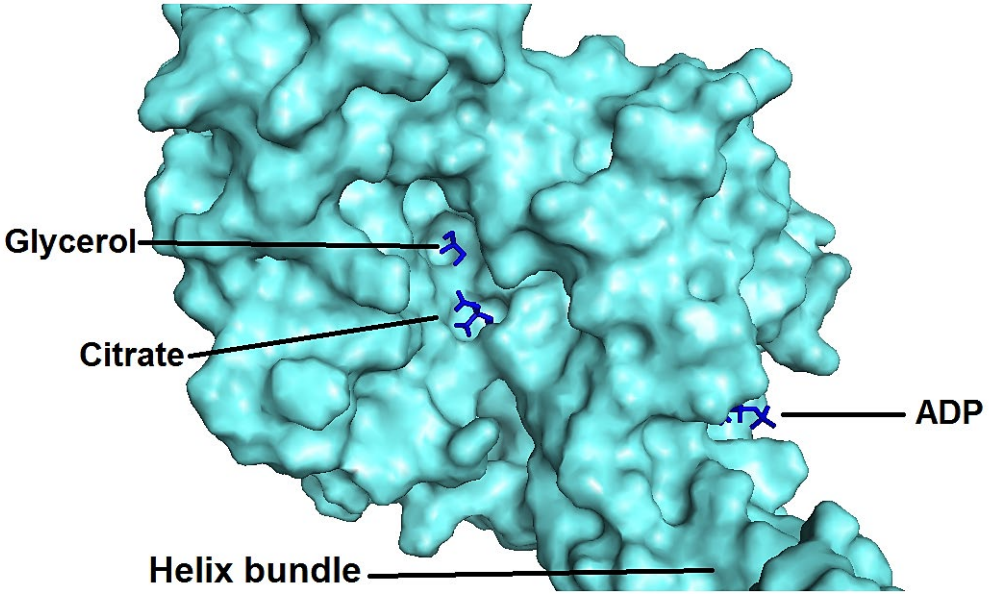


**Figure 4.6 Space filled model of the X-ray crystal structure of *Bs*BshC. The fairly large active site pocket shows both glycerol and citrate bound. An ADP molecule was found to be bound at a separate solvent exposed site on the protein as indicated [30].**

Interestingly, no nucleotides were added in the purification or co-crystallization experiments, suggesting that the ADP was bound during expression of the protein in *E. coli* and remained bound through the purification process. The electron densities for the adenine, ribose, and α-phosphate portions of ADP are well-defined, however the electron density for the β-phosphoryl group is somewhat ambiguous which might suggest a disordered or highly

mobile group, and it is thus possible that a group other than phosphate is present at this position. Other cofactors that contain the adenosine group include NADH and dephospho-CoA. Considering that the synthesis of BSH and CoA might be positively correlated (due to the association of some CoA biosynthetic genes with those of BSH biosynthesis), it is possible that BshC makes use of CoA or de-phospho-CoA as an additional substrate. This would further support the conclusion that BshC is unique in its catalytic mechanism.

Furthermore, the observation that the 4-helix bundle puts the two monomers at a considerable distance from one another suggests a structural arrangement that might facilitate the binding of an extra protein partner that might be required for catalysis. Further studies will be needed in order to confirm these hypotheses.

Studies on the enzymes and processes that produce and rely on BSH—including inhibitor discovery initiatives—require significant amounts of the compound. Due to the failure to date to obtain active BshC, Hamilton and co-workers reported the full chemical synthesis of BSH, as well as a partial chemoenzymatic synthesis that bypasses this step [28]. This has led to BSH becoming commercially available from several sources (such as JEMA Biosciences). However, obtaining BSH in either manner requires a significant investment of time and/or money. Based on the experience of our laboratory with several of the MSH biosynthetic enzymes and in the study of their inhibition, we therefore set out to reconstitute the BSH biosynthetic pathway from *S. aureus* with a dual goal: first, to confirm the activity of the putative enzymes, and second to establish if these enzymes can be used to produce BSH in a biocatalytic fashion. In this chapter our efforts in this regard are described.

## 4.2 Results and discussion

### 4.2.1 Cloning and plasmids used

The genes expressing *bshB* (A0A0E1VJH9_STAA3) and *bshC* (BSHC_STAA8) were amplified from genomic DNA from the *S. aureus* USA 300 strain introducing *NcoI* (5′) and *XhoI* (3′) sites flanking the genes of interest. After digestion with NcoI and XhoI, the gene-containing fragment was successfully inserted into pET28a(+) that was predigested with NcoI and XhoI. The gene encoding BshA (A0A068A5A2_STAAU) was similarly amplified, and it was attempted to clone and insert it in to the BspHI and XhoI sites of the predigested pET28a(+) plasmid. However, after several attempts, we were not successful in being able to amplify the gene of interest. Literature also suggests difficulty in cloning and/or purifying MshC from a number of species [4]. Although not analogous to BshC, our experience highlights a common problem in cloning from GC rich genomes. However, since the BshA

protein is the best characterized of the three biosynthetic enzymes, and shows high levels of structural and mechanistic similarity to its MshA counterpart, we decided to rather focus our efforts on the less studied enzymes in the pathway, namely BshB and BshC.

The identities of all the newly and successfully cloned plasmids were confirmed by DNA sequencing. The plasmids all expressed C-terminal His tagged proteins, which was subsequently exploited for their purification by immobilized-metal affinity chromatography

### 4.2.2 Protein expression and purification

The *Sa*BshB and *Sa*BshC expression plasmids were each separately transformed into *E. coli* BL21* (DE3) cells to be used in heterologous expression. All proteins were expressed by growing the appropriately transformed *E. coli* cell in LB broth at 37°C, with induction of protein expression being achieved using 0.5 mM IPTG. Proteins were obtained from cells after at least 12 hours of expression (i.e. post-induction), by harvesting and lysis followed by purification using immobilized metal affinity chromatography (IMAC) The purified protein was analysed by SDS-PAGE as shown in Figure 4.7. Both proteins expressed well and gave high yields of pure protein.

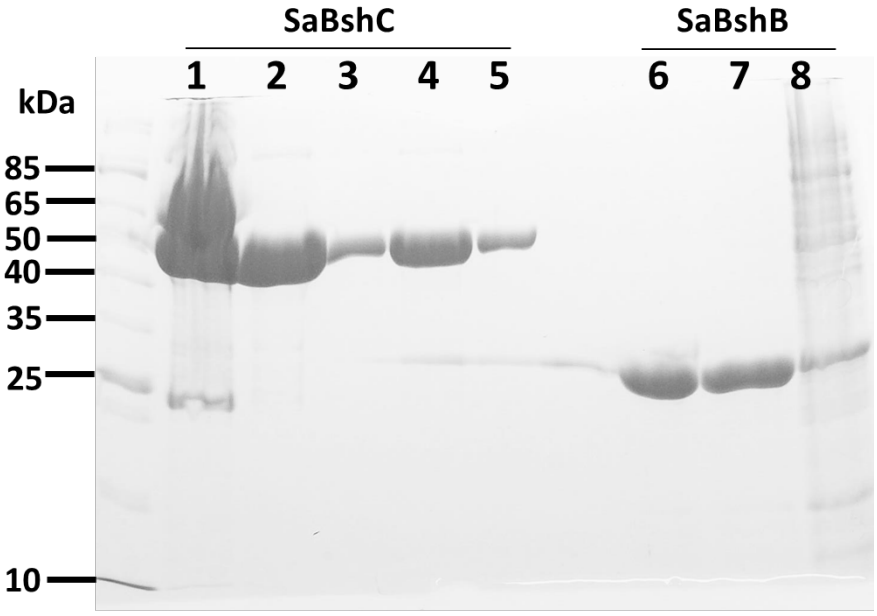


**Figure 4.7 10% SDS-PAGE analysis of the purification procedure of *Sa*BshB and *Sa*BshC. Molecular weight marker shown with respective kDa increments. *Sa*BshB: Lane 8-crude lysate, lane 7-IMAC faction, lane 6-purified protein. *Sa*BshC: Lane 1-crude lysate, Lane 2-IMAC fraction, Lane 3-5-Purified fractions.**

### 4.2.3 Efforts towards enzymatic reconstitution and activity

Reconstitution of the partial pathway was first attempted using *Sa*BshB and either GlcNAc-SMal (the thioglycoside analogue of the native BshB substrate, GlcNAc-OMal) or GlcNAc-OMe as alternative substrates of the enzyme. These substrates were synthesized by a previous member of the group, Dr Ndivhuwo O. Muneri, as part of a different project [35]. Different approaches were attempted in assessing the enzyme's deacetylase activity on these substrates, and the ability of the putative product to be converted by *Sa*BshC. These approaches included first incubating *Sa*BshB with substrate, followed by removal of the protein by precipitation before the supernatant was then analyzed for product formation in the presence of *Sa*BshC, as well as incubating the two enzymes together. The effect of adding a variety of co-substrates were also investigated on the outcome of the reactions. Since the substrates and products do not contain a chromophore, and we did not have access to any HPLC instruments with detectors other than UV-Vis or fluorescence, all reactions were analysed by TLC, and visualized using a variety of staining techniques. The results are summarized in Tables 1–7.

**Table 4. Using various ratios of *Sa*BshB:*Sa*BshC and the substrates GlcNAc-OMe/SMal towards the chemoenzymatic synthesis of BSH.**

| TLC | Spot Number (From left to right) | New spot |
|---|---|---|
| **A** - Ninhydrin Stain 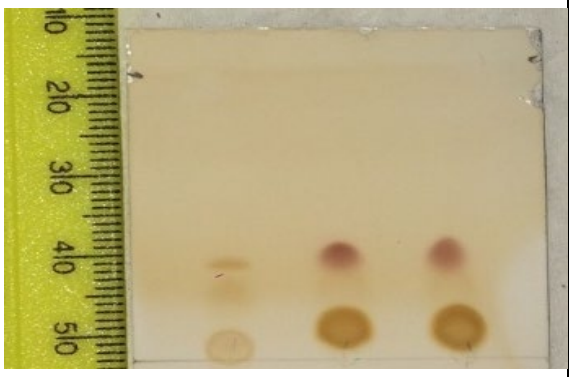 | 1- Authentic BSH (JEMA Biosciences).<br>2- *Sa*BshB, *Sa*BshC (1:1) with GlcNAc-SMal, ATP, Cys.<br>3- *Sa*BshB, *Sa*BshC (1:1) with GlcNAc-OMe, ATP, Cys. | No. |
| **B** - Ninhydrin Stain 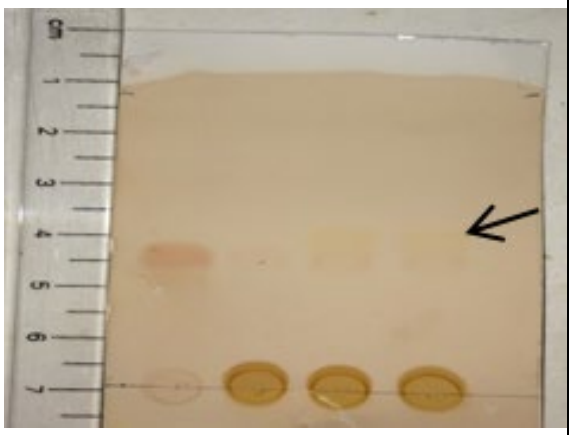 | 1- GlcNAc-OMe.<br>2- *Sa*BshC with lysate of *Sa*BshB reaction and GlcNAc-SMal, ATP, Cys.<br>3- *Sa*BshB with GlcNAc-OMe.<br>4- *Sa*BshB, *Sa*BshC (1:1) with GlcNAc-OMe. | Yes: reaction 3 and 4 indicated by arrow. |
| **C** - Ninhydrin Stain 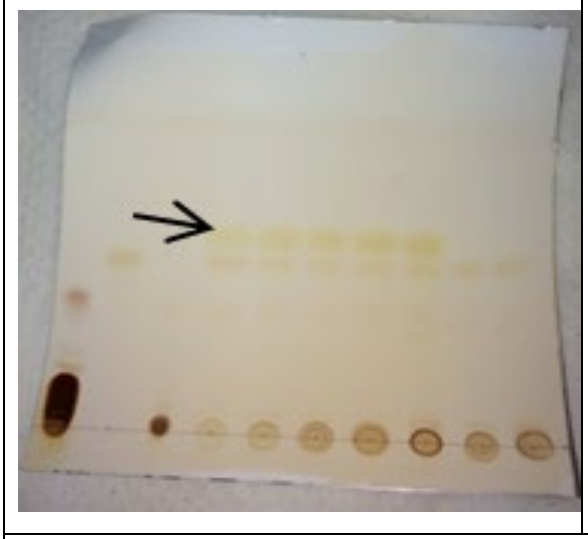 | 1- Cysteine.<br>2- GlcNAc-OMe.<br>3- Glucosamine.<br>4- *Sa*BshB, *Sa*BshC (1:1) with GlcNAc-OMe.<br>5- *Sa*BshB, *Sa*BshC (2:1) with GlcNAc-OMe.<br>6- *Sa*BshB, *Sa*BshC (3:1) with GlcNAc-OMe.<br>7- *Sa*BshB, *Sa*BshC (1:2) with GlcNAc-OMe.<br>8- *Sa*BshB, *Sa*BshC (1:3) with GlcNAc-OMe.<br>9- *Sa*BshC batch 1 with GlcNAc-OMe, ATP, Cys.<br>10- *Sa*BshC batch 2 with GlcNAc-OMe, ATP, Cys. | Yes: reaction 4,5,6,7,8 indicated by arrow. |
| **Conclusion:** *Sa*BshB showed activity towards GlcNAc-OMe, most likely forming GlcN-OMe. Black arrow shows new product from *Sa*BshB reactions. | | |

**Table 5. Evaluating the effect of adding of NADPH, serine and/or glutamate to *Sa*BshB:*Sa*BshC reactions.**

| **TLC** | **Spot Number (From left to right)** | **New spot** |
|---|---|---|
| **D** - UV Light – No staining 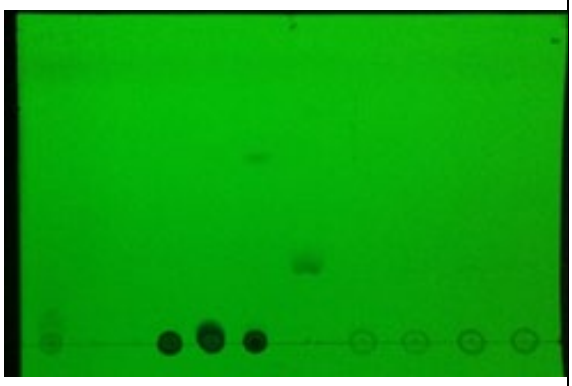 | 1- Cysteine.<br>2- GlcNAc-OMe.<br>3- Glucosamine.<br>4- Glutamate.<br>5- Serine.<br>6- NADPH.<br>7- NADH.<br>8- *Sa*BshB, *Sa*BshC (1:1) with GlcNAc-OMe, serine, ATP.<br>9- *Sa*BshB, *Sa*BshC (1:1) with GlcNAc-OMe, glutamate, ATP.<br>10- *Sa*BshB, *Sa*BshC (1:1) with GlcNAc-OMe, serine, glutamate, NADPH, ATP.<br>11- SaBshB, *Sa*BshC (1:1) with GlcNAc-OMe, serine, glutamate, NADPH, ATP. | No |
| **E** - Ninhydrin Stain 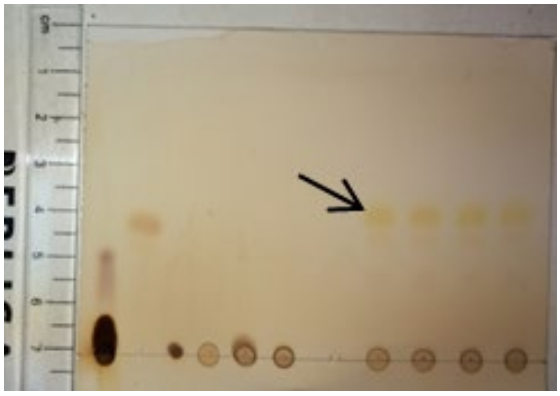 | As for D above.<br>. | Yes: reaction 8,9,10, 11 indicated by arrow. |
| **Conclusion:** The crystal structure of *Bs*BshC showed an unusual surface binding pocket of an ADP moiety. Thus NADPH was added to reactions to determine if this would promote catalysis; however, this was not successful. Other cysteine ligases in the PDB make use of substrates serine/glutamate in their catalytic mechanism; these substrates were also added in the event that *Sa*BshC functioned in a manner similar to other cysteine ligases. However, none of these compounds promoted product formation. Black arrow shows new product from *Sa*BshB reactions. | | |

**Table 6. Assessing the effect of adding the cofactors NADPH or $NAD^+$ in combination with GlcNAc-SMal to *Sa*BshB:*Sa*BshC reactions.**

| TLC | Spot Number (From left to right) | New spot |
|---|---|---|
| **F** - Ninhydrin Stain 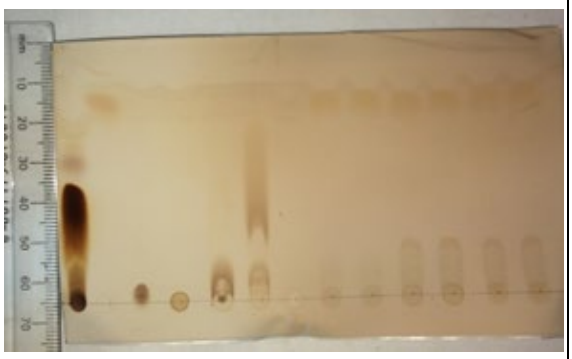 | 1- Cysteine.<br>2- GlcNAc-SMal.<br>3- Glucosamine.<br>4- Glutamate.<br>5- $NAD^+$.<br>6- ATP.<br>7- NADPH.<br>8- *Sa*BshC GlcNAc-SMal, Cysteine, ATP, NAD+.<br>9- *Sa*BshB, *Sa*BshC (1:1) with GlcNAc-SMal, serine, glutamate, NADPH, ATP, cysteine.<br>10- *Sa*BshB, *Sa*BshC (1:1) with GlcNAc-SMal, serine, NADPH, ATP, cysteine.<br>11- *Sa*BshB, *Sa*BshC (1:1) with GlcNAc-SMal, glutamate, NADPH, ATP, cysteine.<br>12- *Sa*BshB, *Sa*BshC (1:1) with GlcNAc-SMal, $NAD^+$, ATP, cysteine.<br>13- *Sa*BshB with GlcNAc-SMal, $NAD^+$, ATP, cysteine. | None |
| **Conclusion:** The results show no new product formation. | | |

**Table 7. Using Ellman's reagent in identifying the formation of thiol-containing products, such as BSH.**

| TLC | Spot Number (From left to right) | New spot |
|---|---|---|
| **G** - Ellman's Reagent stain  | 1- Cysteine.<br>2- GlcNAc-SMal.<br>3- Glucosamine.<br>4- Glutamate.<br>5- NAD+.<br>6- ATP.<br>7- NADPH.<br>8- *Sa*BshC with GlcNAc-SMal, cysteine, ATP, $NAD^+$.<br>9- *Sa*BshB, *Sa*BshC (1:1) with GlcNAc-SMal, serine, glutamine, NADPH, ATP.<br>10- *Sa*BshB, *Sa*BshC (1:1) with GlcNAc-SMal, Serine, NADPH, ATP, Cysteine.<br>11- *Sa*BshB, *Sa*BshC (1:1) with GlcNAc-SMal, glutamate, NADPH, ATP, cysteine.<br>12- *Sa*BshB, *Sa*BshC (1:1) with GlcNAc-SMal, $NAD^+$, ATP, cysteine.<br>13- *Sa*BshB with GlcNAc-SMal, $NAD^+$, ATP, cysteine. | None. |
| **Conclusion:** Ellman's reagent identified unreacted cysteine, but no new product formation. | | |

**Table 8. Evaluating the effect of adding various metals and NADH or $NAD^+$ to *Sa*BshB:*Sa*BshC reactions.**

| TLC | Spot Number (From left to right) | New spot |
|---|---|---|
| **H** - UV Light – No staining 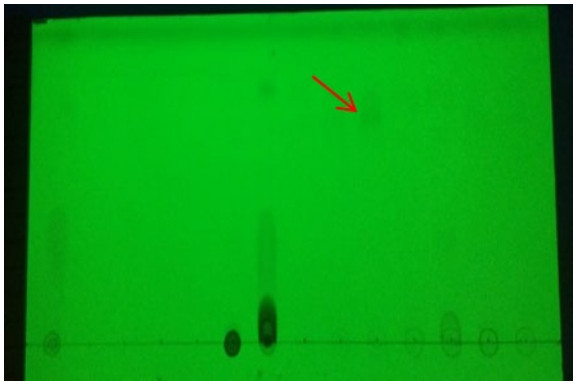 | 1- Cysteine.<br>2- GlcNAc-OMe.<br>3- Glucosamine.<br>4- $ZnCl_2$.<br>5- $MgCl_2$.<br>6- $MnCl_2$.<br>7- $NAD^+$.<br>8- SaBshB co-incubated with GlcNAc-OMe, $MnCl_2$.<br>9- *Sa*BshB, *Sa*BshC (1:1) co-incubated with GlcNAc-OMe, $MnCl_2$, $NAD^+$, ATP, Cysteine.<br>10- *Sa*BshB, *Sa*BshC (1:1) co-incubated with GlcNAc-OMe, NADH, ATP, Cysteine.<br>11- *Sa*BshB, *Sa*BshC (1:1) co-incubated with GlcNAc-OMe, $MnCl_2$, $NAD^+$, ATP, Cysteine.<br>12- *Sa*BshB, *Sa*BshC (1:1) co-incubated with GlcNAc-OMe, $ZnCl_2$, $NAD^+$, Cysteine.<br>13- *Sa*BshB, *Sa*BshC (1:1) co-incubated with GlcNAc-OMe, $NAD^+$, ATP, Cysteine.<br>14- *Sa*BshB, *Sa*BshC (1:1) co-incubated with GlcNAc-OMe, ATP, Cysteine. | Yes, Reaction 10. |
| **I** – Ninhydrin stain 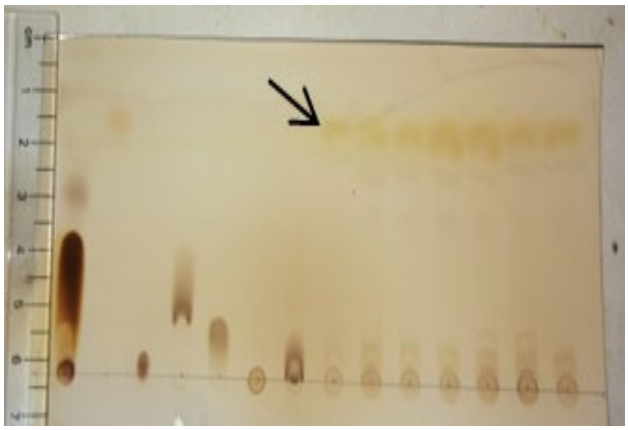 | As for H above | Yes - reactions 8-14 indicated by arrow. |
| **Conclusion:** Black arrow shows product formed from *Sa*BshB reactions. The addition of NADH to *Sa*BshB:*Sa*BshC reaction favors the formation of a new product spot (red arrow). | | |

A number of different conditions were tested towards the chemoenzymatic production of BSH using GlcNAc-OMe and GlcNAc-SMal as starting materials. Thin layer chromatography analysis was carried out on each reaction condition as well as separate reaction components. Different protein ratios of *Sa*BshB to *Sa*BshC were also assessed. There was indeed a new product spot that formed on the TLCs that migrated above the GlcNAc-OMe or GlcNAc-SMal spot as indicated by an arrow in TLC B, C, E and I. This spot only appeared when *Sa*BshB was present with substrate GlcNAc-OMe or GlcNAc-SMal. Moreover, the new product spot had an $R_f$ value that was different to the substrates GlcNAc-OMe/GlcNAc-S-Mal and migrated higher on the TLC. The TLC of authentic BSH analysed using the same solvent conditions and stained with ninhydrin stain (TLC A) gave a light brown spot. When stained with ninhydrin, the new product spot from the *Sa*BshB reactions showed a similar yellow color to that of BSH, in comparison to the substrates GlcNAc-OMe and GlcNAc-SMal that gave in red/orange product spots. This suggests that *Sa*BshB was able to deacetylate both of the alternate substrates.

The second reaction involving the cysteine ligating enzyme *Sa*BshC was tested under several different conditions, including co-incubation of *Sa*BshB and *Sa*BshC in different ratios (1:1, 1:2, 1:3 *Sa*BshB:*Sa*BshC), and using the *Sa*BshB supernatant as starting material for the *Sa*BshC reaction. There are a number of X-ray crystal structures of serine-/glutamate-cysteine ligases (PDB: 3IG5, 3NZT, 1V4G, 2GWC) that are unrelated to *Sa*BshC but that use utilize cysteine and/or glutamate and serine as part of their catalytic cycle. However, the addition of glutamate and serine to reaction conditions of *Sa*BshC did not appear to promote any further product formation. The X-ray crystal structure of BshC contained an ADP moiety bound to the protein in a pocket that is not the active site, and therefore a number of adenosine cofactors such as NAD/NADP, NADH/NADPH were added to the *Sa*BshC reaction. Interestingly a new product did form upon the addition of NADH (red arrow in TLC H, Table 8). The reaction sample analysed in TLC H, as well as starting materials, was therefore analysed separately by HPLC using a C18 column for separation.

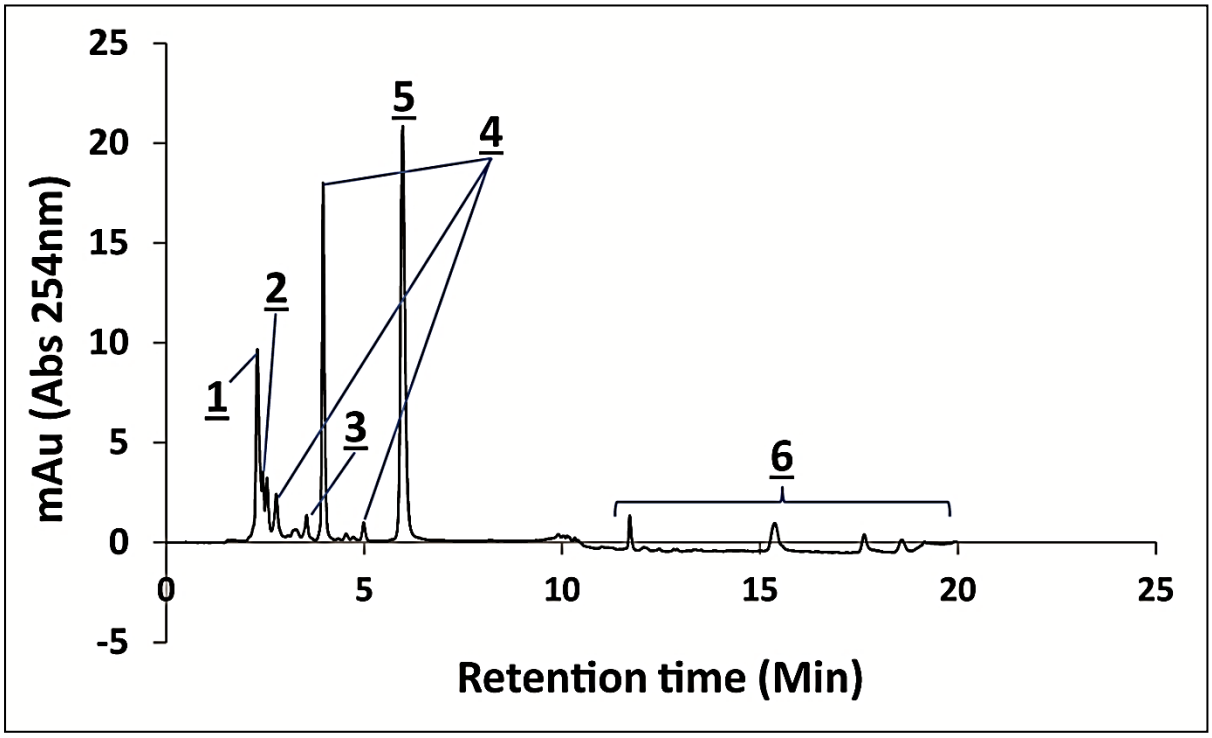


**Figure 4.8 HPLC chromatogram of a reaction mixture containing *Sa*BshB, *Sa*BshC (1:1) co-incubated with GlcNAc-OMe, NADH, ATP, Cysteine. Peak 1: GlcNAc-OMe (2.40 min), Peak 2: ATP/GlcN (2.45 min), Peak 3: NADH (3.6 min), Peak 4: cysteine-related adducts (2.42 min, 3.69 min, 4.75 min), Peak 5: Unknown product (5.98 min), Peaks 6: related to GlcNAc-OMe. Chromatograms of the starting materials analysed separately are shown in materials and methods.**

A new peak indeed appeared at a retention time 5.98 minutes; this peak seemed to be unrelated to any of the substrates used by comparison to known standards. Unfortunately, the identity of this new product is currently stil unknown, as further analysis remains to be performed. Taken together, the actual conditions required for full BshC catalysis still remains elusive.

## 4.3 Conclusion

The results presented in this chapter showed the first successful expression and purification of soluble *S. aureus* BshB and BshC. The activities of both were assessed using various conditions. The *Sa*BshB reaction involves the deacetylation of a GlcNAc substrate. A number of different reaction conditions involving *Sa*BshB and the alternate substrates GlcNAc-OMe or GlcNAc-SMal were assessed. Indeed the formation of new product spots was observed for reactions containing *Sa*BshB and either of the substrates GlcNAc-OMe or GlcNAc-SMal, indicating deacetylation of these substrates. The *Sa*BshC reaction is hypothesized to involve the ATP-dependent addition of cysteine to the amine group of the deacetylated GlcNAc-Mal. The crystal structure of *Bs*BshC suggests that BshC requires an

additional protein partner or an adenosine contains cofactor. However, the unique binding location of the ADP on *Sa*BshC might suggest that this binding pocket is an allosteric site. Further studies will be needed to assess this hypothesis.

The reactions involving *Sa*BshC were performed using a variety of conditions. Considering the active site is formed around a Rossman fold core, different nucleotide cofactors were also added to the reactions. These included NAD+, NADP+, NADH and NADPH. Interestingly the addition of NADH did indeed make a positive difference in promoting the formation of a new product in the *Sa*BshC reaction. The HPLC chromatogram of a sample of the supernatant of the NADH containing reaction showed a new unidentified peak. The apparent further activity in the presence of NADH as well as the information from the *Bs*BshC crystal structure suggests that *Sa*BshC requires an as yet to be determined ADP-containing cofactor for its active conformation which would suggest that its cysteine ligase activity occurs via an unusual mechanism.

The lack of activity of *Sa*BshC thus impedes further studies on the biocatalytic production of BSH. Yet, understanding the biosynthesis of BSH remains an important goal, as it will aid the elucidation of the roles of other enzymes and processes that rely on BSH.

Further investigation should be done in order to assess the possibility of other plausible cofactors that might bind in the Rossman fold of the *Sa*BshC's active site. Furthermore, the hypothesis that *Sa*BshC might require additional protein partners such as *Sa*BshA or a co-incubation of all three enzymes in order to produce BSH will be the focus of future studies.

The work contained in this chapter was not done to address a specific aim, but rather to facilitate the work done towards achieving the other aims contained in this thesis.

## 4.4 Materials and methods

Unless otherwise stated, the majority of all chemicals and compounds were purchased from Sigma-Aldrich. GlcNAc-OMe and GlcNAc-SMal were previously synthesized by Dr Ndivhuwo O. Muneri [35]. Cloning was performed with the help of Dr Andrea Schenkmayerova.

### 4.4.1 Cloning and plasmids used

**SaBshB** – *S. aureus bshB* gene (A0A0E1VJH9_STAA3) was cloned from strain USA300 with *NdeI* and *XhoI* sites flanking the gene. The PCR reaction included 1 µL Kapa Hotstart buffer, 10 µM forward primer, 10 µM reverse primer, 1 ng genomic DNA, 25 µL of 2x Hotstart Ready Mix made up to a final volume of 25 µL with distilled, deionized water. The PCR program involved an initial denaturation step at 95°C for 3 minutes. This was followed by 25 cycles of 98°C for 20 seconds, 55°C for 1 minute 30 seconds, 72°C for 5 minutes. The reaction mixture was subjected to gel electrophoresis on a 1% agarose gel and subsequently visualized through gel staining with NANCY™-520 gel electrophoresis stain and viewed on a UV gel reader. The band corresponding to the *bshB* gene (~660bps) was excised and purified using a Thermo Scientific DNA gel extraction kit. The bshB gene was subsequently used to generate the pET28a-*Sa*BshB plasmid. Briefly the pET28a plasmid as well as the *Sa*BshB-encoding gene was digested separately with NdeI and XhoI (New England Biolabs) for 1 hour at 37°C without shaking. The restriction digestion of pET28a and *bshB* gene was subjected to gel electrophoresis on a 1% agarose gel and subsequently visualized through gel staining with NANCY™-520 gel electrophoresis stain and viewed on a UV gel reader. The *NdeI/XhoI* cut plasmid band and gene band were then excised and purified using a Thermo Scientific DNA gel extraction kit. Ten ng each of NdeI/XhoI cut pET28a and *bshB* were incubated with 1µl of T4 DNA ligase and ligase buffer for 1 hour at 37°C without shaking. Thereafter 1 µL of the plasmid-insert construct was added to 80 µL of chemically-competent Mach 1 cells, and incubated on ice for 30 mins. The cell mixture was heat-shocked at 42°C for 45 seconds, and then cooled on ice for 5 mins. Approximately 900 µL or pr-ewarmed LB broth was added to the transformation mixture and incubated at $37^0$C and shaking for 1 hour. The sample was then centrifuged at 4500 RPM for 10 mins. Half of the supernatant was discarded, with the cell pellet being re-suspended in the remaining supernatant. The resuspended cells were then plated onto LB plates containing 30 mg/L kanamycin and incubated overnight at 37°C. Colonies were then selected and digestion checks done using 1% agarose gels to assess which colony liberated the gene of expected size. The positive colonies were then sent for sequencing for confirmation. The correctly sequenced colonies were grown up overnight at 37°C in 5ml LB containing 30 mg/L kanamycin. Thereafter the pET28a-*Sa*BshB plasmid was isolated and purified using a

Thermo Scientific plasmid extraction kit. The plasmid was then used for transformation into respective cloning/expression cells for further use.

***Sa*BshC**- *S. aureus bshC* gene (BSHC_STAA8) was cloned from strain USA300 with NdeI and XhoI sites flanking the gene. The same procedure described above was used in the generation of the pET28a-*Sa*BshC plasmid. The plasmid was then used for transformation into respective cloning/expression cells for further use.

### 4.4.2 Protein expression and purification

All purified and sequenced plasmids were then transformed into *E. coli* BL21(Star)DE3 for protein overexpression. Overexpression was performed in LB broth supplemented with 30 mg/L kanamycin and grown at 37 °C whilst shaking in non-baffled flasks. Once an $OD_{600nm}$ = 0.5-0.6 was reached the cultures were then induced with IPTG at a final concentration of 0.3 mM. Cultures were then continued overnight at 37 °C. Thereafter the cells were harvested by centrifugation at 8000 rpm.

Each cell pellet was resuspended in approximately 10 mL of sonication buffer (5 mM imidazole, 500 mM NaCl and 20 mM Tris–HCl, pH 7.9; 10 mL/1 g cell paste) and subsequently sonicated to elicit cell lysis. After centrifugation at 15,000 x g for 30 min, the crude extract (supernatant) was applied to a 0.45 µm syringe filter (AMICON) to remove any further debris. The clarified lysate was then applied to a previously prepared ($Ni^{2+}$) 1 mL HisTrapFF metal affinity purification column using an ÅKTAprime purification system. After an initial wash step of 5-10% elution buffer to remove unbound protein, the protein of interest was then eluted by increasing the imidazole concentration to 500 mM. Protein elution was monitored by UV at 280 nm on the ÄKTAPrime. Residual imidazole was then removed from the purified protein fractions and buffer exchanged using a 5ml HiTrap Desalting columns (50 mM HEPES, pH 7.4). Thereafter a 10% SDS-PAGE gel was run for each protein purified. Protein concentration was determined using Bradford reagent (BIO-RAD). Purified proteins were aliquoted and stored at -80°C until further use.

### 4.4.3 Efforts towards enzymatic reconstitution and activity

All enzyme assays were done in reaction buffer: 50 mM HEPES, pH 7.4. Each reaction was done in a total volume of 5 ml reactions. Final concentration of enzyme and substrate used was 500 µM and 1 mM respectively. Each reaction was incubated at 37°C overnight without shaking. A sample of 500 µL of each was aliquoted and enzyme precipitated with 50% acetonitrile and heating at 80°C for 10 minutes. The resultant mixture was centrifuged at 8000 rpm for 30 minutes and the supernatant was spotted on TLC (aluminium-backed Merck

silica gel 60 F254). Solvent system used was n-butanol: acetic acid: $H_2O$ (12:3:5). Spots developed using staining solutions including; ninhydrin stain (0.3 g ninhydrin in 100 mL n-butanol, 3 mL acetic acid), sulfuric acid stain (5% in methanol), permanganate stain (3 g potassium permanganate, 20 g potassium carbonate + 5% aq. NaOH).

### 4.4.4 HPLC chromatography

All enzyme assays were done as described above. Approximately 800 µL of each starting material stock solution and reaction sample were separately aliquoted and precipitated with 50% acetonitrile and heating at 80°C for 10 minutes. The resultant mixture was centrifuged at 8000 rpm for 30 minutes and 500 µL of the supernatant was then subjected to HPLC analysis.

HPLC analysis was performed on an Agilent 1100 instrument using a Luna® 5 µm C18 100 Å column (250 x 4.6 mm). The column was equilibrated with 95% 50 mM CH3COONH4 (pH 5.5) and 5% Acetonitrile. This was followed by elution at a flow rate of 1 mL/min with 95% 50 mM CH3COONH4 (0 – 5 min isocratic), linear gradient increase to 20% Acetonitrile (5 – 6 min), linear gradient increase to 40% Acetonitrile (6 – 10 min), isocratic elution at 40% Acetonitrile (10 – 15 min), linear gradient increase to 60% Acetonitrile (15 – 16 min) and finally isocratic elution at 60% ACN (16 – 20 min). Compounds were detected at 254 nm. HPLC chromatograms of starting materials used are shown below.

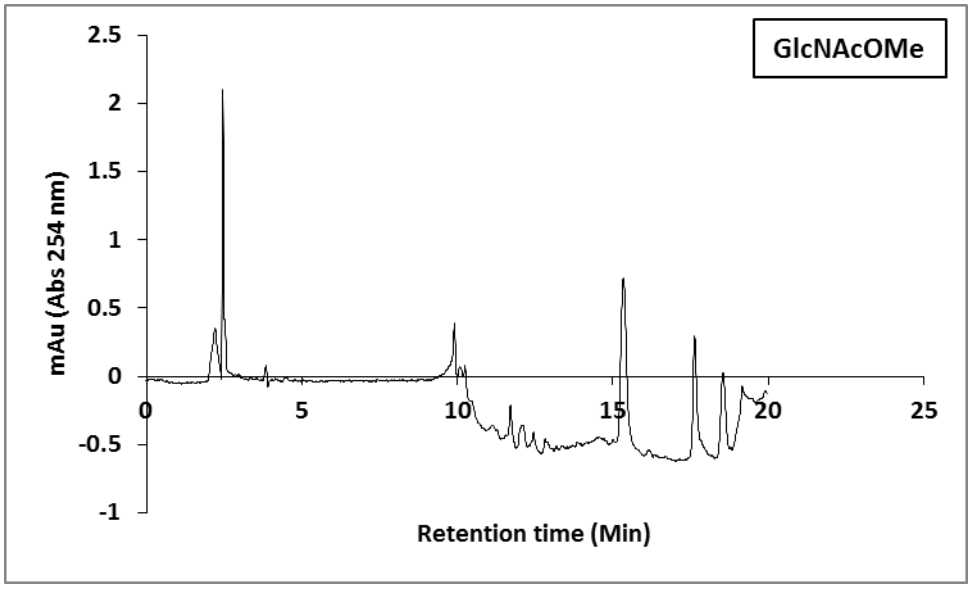


**Figure 4.8.1. HPLC chromatogram of starting material GlcNAc-OMe. GlcNAc-OMe peak retention times: 2.40 min, 9.91 min, 15.35 min, 17.61 min, 18.50 min.**

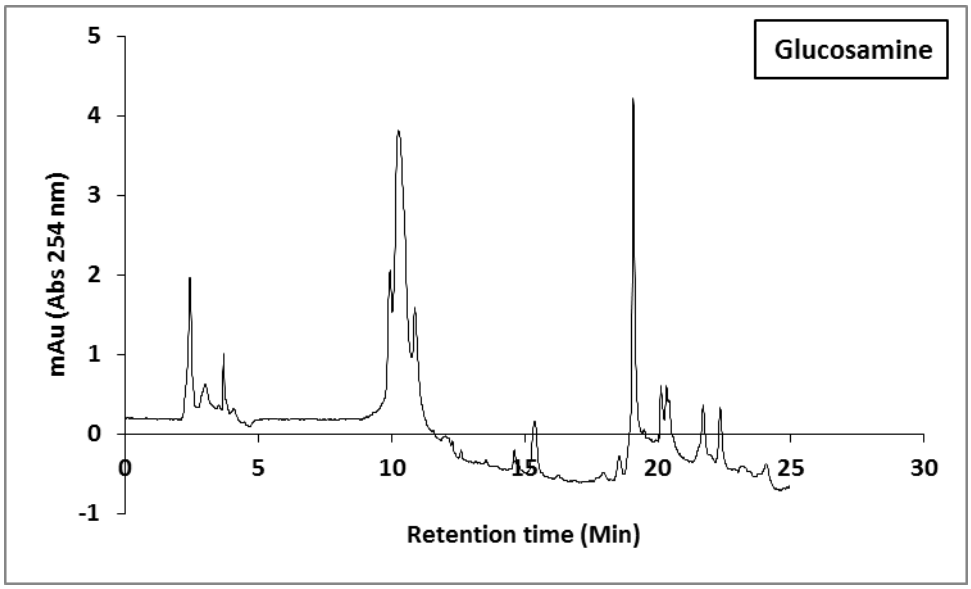


**Figure 4.8.2. HPLC chromatogram of starting material Glucosamine. Glucosamine peak retention times: 2.42 min, 2.92 min, 3.68 min, 10.22 min, 15.40 min, 19.08 min, 21.69 min, 22.35 min.**

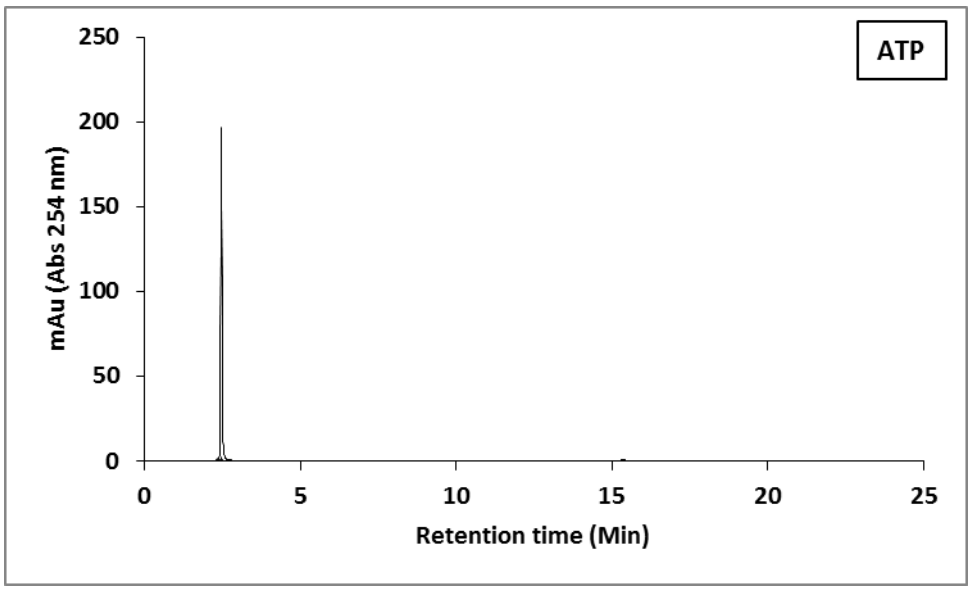


**Figure 4.8.3. HPLC chromatogram of starting material ATP. ATP peak retention time: 2.46 min.**

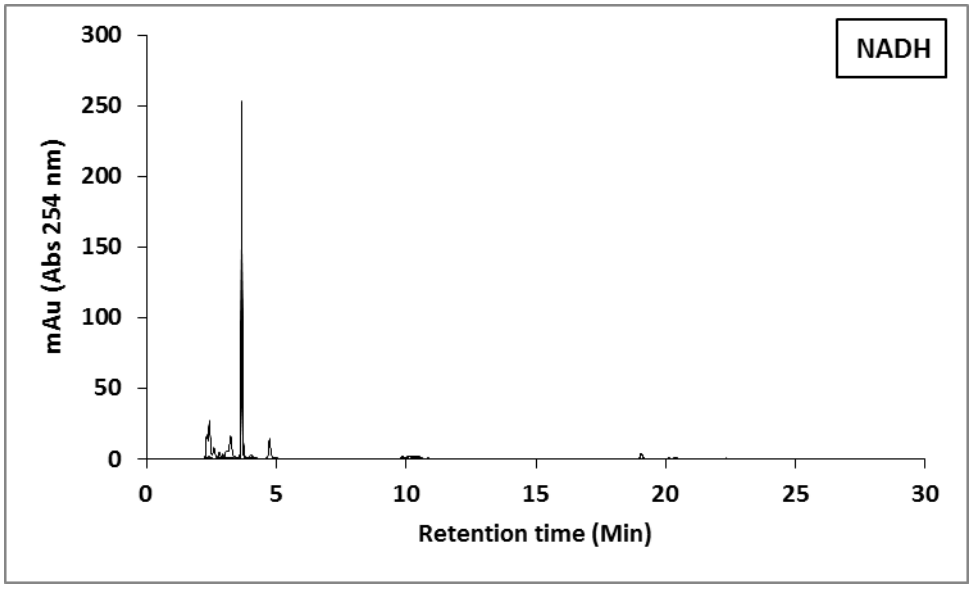


**Figure 4.8.4. HPLC chromatogram of starting material NADH. NADH peak retention time: 3.67 min.**

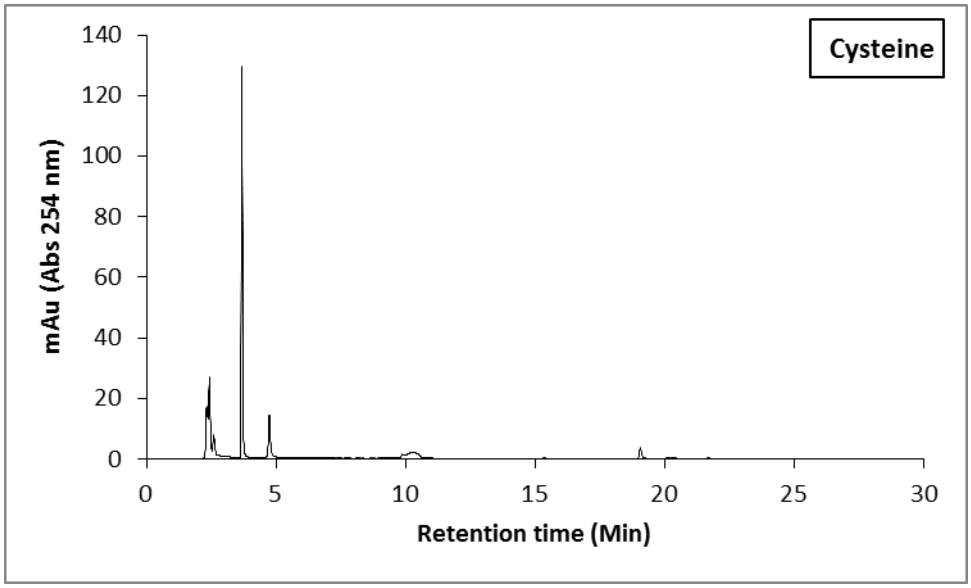


**Figure 4.8.5. HPLC chromatogram of starting material Cysteine. Cysteine peak retention times: 2.42 min, 3.68 min, 4.76 min.**

## 4.5 References

1. Fahey, R.C., *Glutathione analogs in prokaryotes.* Biochim Biophys Acta, 2013. **1830**(5): p. 3182-98.
2. Van Laer, K., C.J. Hamilton, and J. Messens, *Low-molecular-weight thiols in thiol-disulfide exchange.* Antioxid Redox Signal, 2013. **18**(13): p. 1642-53.
3. Rogers, J.M. and E.S. Hunter, 3rd, *Redox redux: a closer look at conceptal low molecular weight thiols.* Toxicol Sci, 2001. **62**(1): p. 1-3.
4. Newton, G.L., N. Buchmeier, and R.C. Fahey, *Biosynthesis and functions of mycothiol, the unique protective thiol of Actinobacteria.* Microbiol Mol Biol Rev, 2008. **72**(3): p. 471-94.
5. Sao Emani, C., et al., *The functional interplay of low molecular weight thiols in Mycobacterium tuberculosis.* J Biomed Sci, 2018. **25**(1): p. 55.
6. Reyes, A.M., et al., *Chemistry and Redox Biology of Mycothiol.* Antioxid Redox Signal, 2018. **28**(6): p. 487-504.
7. Helmann, J.D., *Bacillithiol, a new player in bacterial redox homeostasis.* Antioxid Redox Signal, 2011. **15**(1): p. 123-33.
8. Gaballa, A., et al., *Biosynthesis and functions of bacillithiol, a major low-molecular-weight thiol in Bacilli.* Proc Natl Acad Sci U S A, 2010. **107**(14): p. 6482-6.
9. Newton, G.L., et al., *Bacillithiol is an antioxidant thiol produced in Bacilli.* Nat Chem Biol, 2009. **5**(9): p. 625-7.
10. Fahey, R.C., et al., *Occurrence of glutathione in bacteria.* J Bacteriol, 1978. **133**(3): p. 1126-9.
11. Nicely, N.I., et al., *Structure of the type III pantothenate kinase from Bacillus anthracis at 2.0 A resolution: implications for coenzyme A-dependent redox biology.* Biochemistry, 2007. **46**(11): p. 3234-45.
12. Imber, M., A.J. Pietrzyk-Brzezinska, and H. Antelmann, *Redox regulation by reversible protein S-thiolation in Gram-positive bacteria.* Redox Biol, 2019. **20**: p. 130-145.
13. Chandrangsu, P., et al., *The Role of Bacillithiol in Gram-Positive Firmicutes.* Antioxid Redox Signal, 2018. **28**(6): p. 445-462.
14. Perera, V.R., G.L. Newton, and K. Pogliano, *Bacillithiol: a key protective thiol in Staphylococcus aureus.* Expert Rev Anti Infect Ther, 2015. **13**(9): p. 1089-107.
15. Rosario-Cruz, Z., et al., *Bacillithiol has a role in Fe-S cluster biogenesis in Staphylococcus aureus.* Mol Microbiol, 2015. **98**(2): p. 218-42.
16. Fang, Z. and P.C. Dos Santos, *Protective role of bacillithiol in superoxide stress and Fe-S metabolism in Bacillus subtilis.* Microbiologyopen, 2015. **4**(4): p. 616-31.
17. Posada, A.C., et al., *Importance of bacillithiol in the oxidative stress response of Staphylococcus aureus.* Infect Immun, 2014. **82**(1): p. 316-32.
18. Ma, Z., et al., *Bacillithiol is a major buffer of the labile zinc pool in Bacillus subtilis.* Mol Microbiol, 2014. **94**(4): p. 756-70.
19. Eide, D.J., *Bacillithiol, a new role in buffering intracellular zinc.* Mol Microbiol, 2014. **94**(4): p. 743-6.
20. Rajkarnikar, A., et al., *Analysis of mutants disrupted in bacillithiol metabolism in Staphylococcus aureus.* Biochem Biophys Res Commun, 2013. **436**(2): p. 128-33.

21. Pother, D.C., et al., *Distribution and infection-related functions of bacillithiol in Staphylococcus aureus.* Int J Med Microbiol, 2013. **303**(3): p. 114-23.

22. Lamers, A.P., et al., *Synthesis of bacillithiol and the catalytic selectivity of FosB-type fosfomycin resistance proteins.* Org Lett, 2012. **14**(20): p. 5207-9.

23. Newton, G.L., R.C. Fahey, and M. Rawat, *Detoxification of toxins by bacillithiol in Staphylococcus aureus.* Microbiology, 2012. **158**(Pt 4): p. 1117-26.

24. Chi, B.K., et al., *S-bacillithiolation protects against hypochlorite stress in Bacillus subtilis as revealed by transcriptomics and redox proteomics.* Mol Cell Proteomics, 2011. **10**(11): p. M111 009506.

25. Jensen, L.J., et al., *STRING 8--a global view on proteins and their functional interactions in 630 organisms.* Nucleic Acids Res, 2009. **37**(Database issue): p. D412-6.

26. Sareen, D., et al., *ATP-dependent L-cysteine:1D-myo-inosityl 2-amino-2-deoxy-alpha-D-glucopyranoside ligase, mycothiol biosynthesis enzyme MshC, is related to class I cysteinyl-tRNA synthetases.* Biochemistry, 2002. **41**(22): p. 6885-90.

27. Parsonage, D., et al., *Characterization of the N-acetyl-alpha-D-glucosaminyl l-malate synthase and deacetylase functions for bacillithiol biosynthesis in Bacillus anthracis.* Biochemistry, 2010. **49**(38): p. 8398-414.

28. Sharma, S.V., et al., *Chemical and Chemoenzymatic syntheses of bacillithiol: a unique low-molecular-weight thiol amongst low G + C Gram-positive bacteria.* Angew Chem Int Ed Engl, 2011. **50**(31): p. 7101-4.

29. Winchell, K.R., et al., *A Structural, Functional, and Computational Analysis of BshA, the First Enzyme in the Bacillithiol Biosynthesis Pathway.* Biochemistry, 2016. **55**(33): p. 4654-65.

30. VanDuinen, A.J., et al., *X-ray crystallographic structure of BshC, a unique enzyme involved in bacillithiol biosynthesis.* Biochemistry, 2015. **54**(2): p. 100-3.

31. Fang, Z., et al., *Cross-functionalities of Bacillus deacetylases involved in bacillithiol biosynthesis and bacillithiol-S-conjugate detoxification pathways.* Biochem J, 2013. **454**(2): p. 239-47.

32. Upton, H., et al., *Characterization of BshA, bacillithiol glycosyltransferase from Staphylococcus aureus and Bacillus subtilis.* FEBS Lett, 2012. **586**(7): p. 1004-8.

33. Fadouloglou, V.E., et al., *Crystal structure of the BcZBP, a zinc-binding protein from Bacillus cereus.* FEBS J, 2007. **274**(12): p. 3044-54.

34. Whittington, D.A., et al., *Crystal structure of LpxC, a zinc-dependent deacetylase essential for endotoxin biosynthesis.* Proc Natl Acad Sci U S A, 2003. **100**(14): p. 8146-50.

35. Muneri, N.O., *Engineering and application of glycosidase derived biocatalysts in the study of mycothiol pathway enzymes* in *Department of Biochemistry*. 2017, Stellenbosch University: Stellenbosch.